Targeting viral epigenetics for the control of human adenovirus replication

Morgan Jennings

Thesis submitted to the University of Ottawa
in partial fulfillment of the requirements for the degree of
Doctor of Philosophy in Microbiology and Immunology

Department of Biochemistry, Microbiology, and Immunology
Faculty of Medicine, University of Ottawa

Abstract

Human adenovirus (HAdV) causes minor illness in healthy individuals, but can cause severe disease in at-risk individuals, such as pediatric, geriatric, and especially immunocompromised individuals. This is problematic, as no approved therapeutic exists for treating HAdV infection, worsening the burden these individuals face. During infection, HAdV exploits epigenetic regulation of the host cell by modulating chromatin dynamics, promoting expression of cellular genes productive to infection. Epigenetic regulation of viral DNA is also important, as HAdV DNA is chromatinized during infection. As such, we hypothesized that treatment with compounds capable of regulating viral epigenetics during infection would be an effective strategy in combating HAdV infection. Though treatment with curcumin and CBL0137 have diverse effects within the cell, these compounds are each capable of affecting epigenetic processes, by modulating the expression of epigenetic machinery as well as inhibiting histone chaperones. Thus, we aimed to evaluate the effect of curcumin and CBL0137 treatment, as well as siRNA-mediated depletion of the histone chaperone facilitates chromatin transactions (FACT) complex on HAdV infection. Treatment with curcumin inhibited expression of the viral early 1A (E1A) proteins as well as the late capsid protein hexon. E1A is the first region expressed during infection, and the E1A proteins are vital for modulating cellular gene expression and transactivating other viral genes, and the lack of E1A proteins following curcumin treatment subsequently impacted viral DNA replication and progeny formation. CBL0137 treatment also prevented E1A protein production, which was attributed to CBL0137-induced degradation of the catalytic subunit of RNA polymerase II. However, we noted that other early viral genes contribute to the stabilization of RNA polymerase II

during CBL0137 treatment. Finally, the role of the FACT complex in HAdV infection was explored. Depletion of the FACT complex reduced E1A production by lowering the amount of E1A transcripts within the cell. The FACT complex was also observed co-localizing with viral replication centers, with the FACT complex associating with the viral DNA-binding protein, a key protein in viral replication centers. Taken together, these results indicate targeting E1A production by interfering with viral chromatin is a viable strategy in treating HAdV infection.

Acknowledgements

First, I want to thank my thesis supervisor, Dr. Robin Parks, for his support and guidance throughout my PhD. You provided me with excellent insights in how to conduct research as well as how to communicate my science with others. Thank you as well for the many opportunities you gave me to present at both local and international conferences, giving me the experience to more confidently present my research. I would also like to thank my thesis advisory committee, Dr. Tommy Alain, Dr. Marceline Côté, and Dr. Jeffrey Dilworth, for their excellent advice and constructive criticism during each TAC meeting.

To the past and present members of the Parks lab and my colleagues at the OHRI, you made my time here that much more enjoyable. I appreciate all the assistance with experiments, general scientific discussions, being there for me to vent about my issues (mostly about OC Transpo being late), as well as socializing over coffee. Thank you to Kathy Poulin specifically for all of the valuable training and technical expertise you provided.

Lastly, I want to thank my family and friends for their invaluable support during my studies. To my parents, thank you the strong encouragement and praise you gave me during my time in the Parks lab, you were instrumental in completing my PhD.

Table of Contents

List of Figures

Chapter 1: General Introduction to Adenovirus Biology, the Facilitates Chromatin Transactions Complex, and Curaxins and Curcumin as Therapeutics

Chapter 2: Antiviral Effects of Curcumin on Adenovirus Replication

Chapter 3: Inhibition of Human Adenovirus Replication by the Small Molecule Curaxin

Chapter 4: The FACT Complex is Required for Optimal Human Adenovirus Replication

List of Abbreviations

293: human embryonic kidney cells

A549: human lung adenocarcinoma-derived epithelial cells

AVP: adenoviral protease

c-trapping: chromatin-trapping

CAR: Coxsackie-Adenovirus receptor

CBP: CREB-binding protein

DBP: DNA-binding protein

DDR: DNA-damage response

dsDNA: double-stranded DNA

E1, E2, E3, E4: adenovirus early region 1, 2, 3, and 4

EP300: E1A-association protein p300

FACT: facilitates chromatin transactions

FEAR: FACT-ETS-1 antiviral response

GAPDH: glyceraldehyde-3-phosphate dehydrogenase

GFP: green fluorescent protein

HAdV: human adenovirus

HAT: histone acetyltransferase

HCMV: human cytomegalovirus

HDAC: histone deacetylase

HIV: human immunodeficiency virus

HMGB: high-mobility-group box

hpi: hours post infection

HSV-1, 2: herpes simplex virus types 1 and 2

HTS: high-throughput screens

IAV: influenza A virus

IP: immunoprecipitation

ITR: inverted terminal repeat

KD: Knockdown

KO: Knockout

KSHV: Kaposi's sarcoma-associated herpesvirus

L1, L2, L3, L4, L5: adenovirus late region 1, 2, 3, 4, and 5

MIEP: major immediate early promoter

MLP: major late promoter

MOI: multiplicity of infection

orf: open-reading frame

p300/CBP: EP300 and CBP family of proteins

pIIIa: protein IIIa

pV: protein V

pVI: protein VI

pVII: protein VII

pVIII: protein VIII

pIX: protein IX

PCR: polymerase chain reaction

PFU: plaque-forming unit

Pob3: polymerase one binding protein 3

Pol: adenovirus DNA polymerase

preIIIa: precursor pIIIa

preVI: precursor pVI

preVII: precursor pVII

preTP: precursor terminal protein

PTM: post-translational modification

qPCR: quantitative PCR

RFP: red fluorescent protein

RNAi: RNA interference

RNAP I, II, III: RNA polymerase I, II, and III

rRNA: ribosomal RNA

SARS-CoV-2: severe acute respiratory syndrome coronavirus 2

siRNA: small-interfering RNA

Spt16: suppressor of Ty 16

ssDNA: single-stranded DNA

ssRNA: single-stranded RNA

SSRP1: structure specific recognition protein 1

TP: terminal protein

Virus-associated: VA

ViPR body: virus-induced postreplicative body

VRC: viral replication center

ZIKV: zika virus

Chapter 1:

General Introduction to Adenovirus Biology, the Facilitates Chromatin Transactions Complex, and Curaxins and Curcumin as Therapeutics

Viruses are obligate intracellular parasites, capable of infecting all known forms of life (1). For as long as viruses have existed, viruses have co-evolved with their hosts (2), and this intimate relationship has led to an evolutionary arms race. Various antiviral strategies employed by hosts have evolved, ranging from the restriction enzymes of bacteria (3) to the innate and adaptive immune systems of vertebrates (4, 5). In turn, viruses evolve to both combat cellular attempts to limit their replication as well as exploit cellular machinery to support productive infection (6, 7). Viruses pose a significant threat to humans, directly as human pathogens but also by infecting livestock and crops (8, 9). Preventing virally-induced disease has been a concern even prior to the discovery of viruses as infectious agents in the late 19th century, with many societies employing traditional medicines to combat infection (10-12). Advances in our understanding of both cellular and viral biology has greatly increased our ability to more specifically target and inhibit viral replication (13-15). Despite this, much work is needed to reduce the burden of known virally-induced disease as well as potential emerging pathogens (8, 16, 17).

Human adenovirus (HAdV) is a non-enveloped, double-stranded DNA (dsDNA) virus. There are more than 100 different types of HAdV that are grouped into species A-G (18). Due to variable tissue tropism depending on the type, HAdV is capable of causing respiratory, ocular, and gastrointestinal disease (18). In healthy individuals, HAdV-induced disease is typically self-limiting (19). However, in at-risk populations, such as pediatric, geriatric, and especially immunocompromised individuals, HAdV-induced disease is more severe (20, 21), and can even be fatal, with a mortality rate of as high as 70% in patients with disseminated disease (22). There are currently no approved therapeutics specific for treating HAdV infection (14), and while off-label use of other broad-spectrum antivirals,

such as cidofovir (23), show some success in treating HAdV, these drugs are often associated with secondary toxicity (24). As such, there is a need to discover new compounds or repurpose existing ones for the treatment of HAdV infection in vulnerable patients.

HAdV was first isolated from adenoid tissues in the 1950s (25, 26), which is where HAdV derives its name. Research into HAdV has in turn greatly improved our general understanding of cellular biology, such as gene splicing, which was initially identified due to HAdV gene expression (27, 28), as well as alternative polyadenylation (29, 30). The ability of the early region 1A (E1A) proteins to interact with numerous cellular proteins (31) contributed to identification and characterization of cellular proteins, such as the retinoblastoma protein (32-34) and histone acetyltransferases (HATs) E1A-associated protein p300 (EP300) (35, 36) and related CBP (37) (referred to as the p300/CBP family). Additionally, due to advances in both our understanding of HAdV biology and genome editing techniques such as molecular cloning, HAdV emerged as a promising viral vector for gene therapy, as later generations of helper-dependent HAdV vectors can have most of the viral genome replaced with transgenes, giving a large coding capacity (38). HAdV has also been modified to preferentially replicate within cancer cells as an anticancer strategy (39), with two such oncolytic viruses approved for use in humans (40, 41). Finally, HAdV vectors have been used as vaccine platforms, targeting influenza A virus (IAV) (42), human immunodeficiency virus 1 (HIV-1) (43), tuberculosis (44) or severe acute respiratory syndrome coronavirus 2 (SARS-CoV-2) (45) infection.

1.1 HAdV biology: the viral genome

HAdV contains a linear dsDNA genome of ~30–40 kb (46). HAdV species C types 2 (HAdV-2) and 5 (HAdV-5) are the most extensively characterized types of HAdV, and are very similar in their biology. Unless otherwise noted, the data presented pertains to HAdV-2 and HAdV-5. The HAdV-5 genome is approximately 36 kb, and encodes over 40 proteins, many of which due to alternative splicing of the same transcript (figure 1.1). Adenoviral coding regions are designated early or late if they occur prior to or following viral DNA replication, respectively (47), though some genes are expressed intermediately (48). The ends of HAdV genomes are composed of inverted terminal repeats (ITRs), which act as the origin of DNA replication, with the ~200 bp viral packaging sequence positioned adjacent to the left ITR (49). Bound to the 5' end of each strand is the viral terminal protein (TP), explained in greater detail below.

1.1.1 Early genes

The E1 region encodes the E1A proteins, which are the first viral proteins expressed following entry into the nucleus, and are vital for productive infection. The *E1A* gene is known to produce 5 major isoforms of 289, 243, 217, 171, and 55 amino acids, with the two larger isoforms predominating during early infection (50). The E1A proteins are major transcriptional regulators, but do not bind to DNA directly. Instead, E1A performs this task by interacting directly with at least 32 proteins and indirectly with over 2000 proteins (31), and modulates over 10,000 cellular promoters during infection (51). As the virus tends to naturally infect terminally differentiated epithelial cells, one of the roles of E1A is to induce entry into the S-phase of the cell cycle (52). E1A accomplishes this task by interacting with several proteins, such as the retinoblastoma tumour suppressor protein (35), which frees

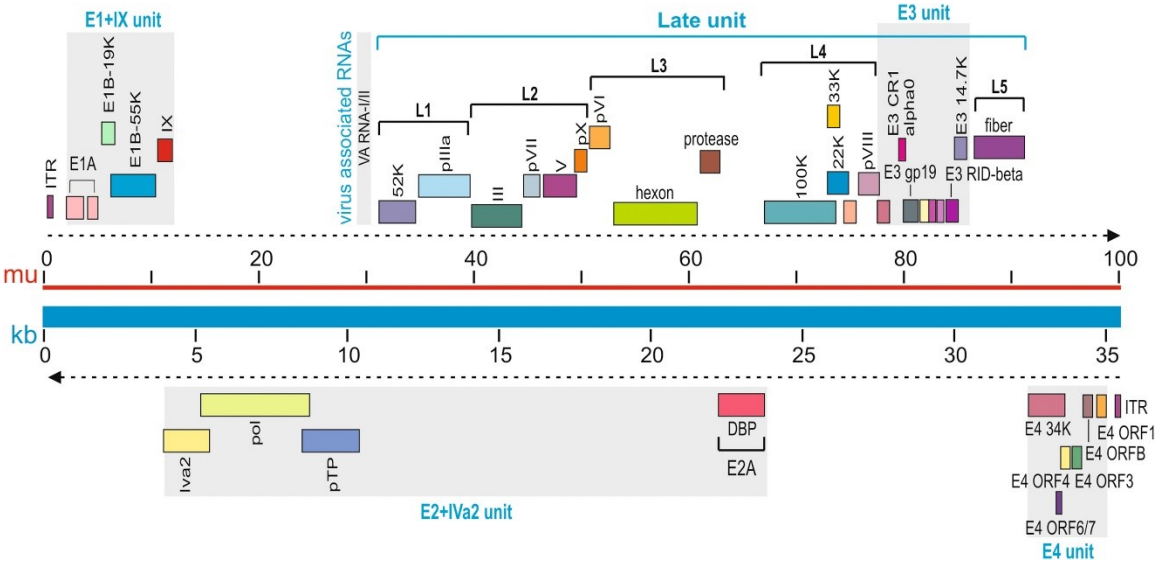

Figure 1.1 Schematic representation of the HAdV-5 genome. Obtained with permission from (53). Relative location of early regions (E1-E4, highlighted in grey), virus associated RNAs, and late regions (L1-L5) are shown. On either end of the genome are the inverted terminal repeats (ITRs). Not shown is the U exon protein.

E2F to promote expression of genes to enter S-phase (54). E1A also binds to p300/CBP in order to redirect H3 lysine 18 acetylation to cellular targets involved in induction of the S-phase while many other genes are inactivated (51, 52). In addition to regulating cellular gene expression, E1A transactivates its own promoter (55, 56), as well as the other early viral promoters (57), allowing expression of the early regions E1B, E2, E3, and E4.

Also encoded by the E1 region are the E1B proteins, E1B-19K, and E1B-55K. In general, the E1B proteins serve to prevent apoptosis induced by the activities of E1A (58-60). However, E1B-55K plays a much larger role in infection. E1B-55K binds to and repurposes p53 as a repressor of p53 activated genes (61). Additionally, E1B-55K itself can target cellular substrates for degradation, such as DAXX (62). E1B-55K can interact with the viral E4 open reading frame (orf) 6 protein and cellular Elongin B/C, Cul5, and RBX1 proteins to form an E3 ligase complex, which targets numerous cellular targets for proteasomal degradation. Examples of targets include p53 to inhibit apoptosis and ensuring the infected cell remains in the s-phase (63), Mre11 of the MRN complex to contribute to inhibition of the DNA-damage response (DDR) (64), or RALY and hnRNP-C to relieve a restriction on viral RNA processing (65). Together, the E1 proteins are crucial for productive viral infection, and are removed to generate replication incompetent viral vectors (also known as helper-dependent HAdV), increasing coding capacity (38, 66).

The E2 region encodes proteins involved in viral DNA replication and is split into two units. *E2A* encodes the DNA-binding protein (DBP), while *E2B* encodes the viral DNA polymerase (Pol) and precursor form of TP, preTP, which is cleaved by the adenoviral protease (AVP) upon maturation of the capsid (67). Though DBP is vital for viral DNA replication, DBP is also involved in regulation of viral gene expression, such as enhancing

E1A and *E2A* expression while partially inhibiting the E4 promoter (68). DBP is also involved in particle assembly by interacting with viral packaging proteins (69, 70), though DBP is typically not present within mature capsids. In addition to the role of the preTP/TP in viral DNA replication, preTP/TP also helps protect viral genomes from being recognized by the DDR, as the ends of viral genomes would otherwise appear like double-stranded breaks (71), as well as prevents nucleases from attacking viral DNA (72). The specifics of HAdV-5 DNA replication are explained in greater detail in section 1.2.4.

The E3 region encodes at least six proteins that have immunomodulatory functions (73, 74). The E3 region is not required for replication in culture, and thus is removed to further increase cloning capacity in gene therapy vectors (66, 75). Finally, the E4 region encodes proteins with numerous functions, such as altering cellular protein stability, reorganization of cellular structures within the nucleus, regulation of late viral RNA splicing, and inhibition of the cellular DNA damage response, with many of these proteins having redundant activity (76). Expression of the E4 region yields a single transcript that is spliced to generate at least seven proteins, E4orf1, E4orf2, E4orf3, E4orf3/4, E4orf4, E4orf6, and E4orf6/7 (74). E4orf6 is the best studied of the E4 proteins, due to its ability to be sufficient for viral replication in the absence of other E4 proteins (76). As outlined above, the E4orf6 protein also associates with E1B-55K and cellular proteins to form an E3 ligase complex to redirect ubiquitin machinery to promote degradation of alternative substrates.

1.1.2 Intermediate genes

Though HAdV infection is typically divided into early and late phases, some

proteins are expressed intermediately. Examples include the structural protein IX (pIX, though expression increases as the late phase progresses) (77), and the U exon protein, which is possibly involved in DNA replication or RNA transcription (78, 79). HAdV also encodes virus-associated (VA) RNAs (VA RNAI and RNAII), which are involved in translation of early and late viral genes, inactivation of the interferon response, contributes to host gene expression modulation, and inhibits the RNA interference (RNAi) pathway during late infection (80-83). IVa2 is expressed following DNA replication (84). To fully activate the major late promoter (MLP), the late region 4 (L4) proteins L4-22K and L4-33K are required. These proteins are regulated by the L4 promoter, which is activated by IVa2 and E4orf3 (48). The discovery of the L4 promoter resolved the paradox of late proteins being required to activate their own promoter.

1.1.3 Late genes

Once activated, transcription from the MLP gives rise to a long transcript (27,000 bp long, or ~75% the total genome length (85)) that is alternatively spliced into the late transcription units, L1–L5 (86). The majority of the proteins produced by the major late transcriptional unit are structural capsid proteins. The L1 region encodes the proteins L1-52/55K, which are involved in virion assembly (87), and precursor protein IIIa (preIIIa), which in its mature, cleaved form (pIIIa), acts as a minor cement protein within the capsid (46). The L2 region encodes the penton base (also known as protein III), one of the major capsid proteins found at each vertex, and inner core precursor protein VII (preVII), protein V (pV), and precursor protein μ (preμ), also known as protein X (46, 88). Both preVII and preμ are cleaved by the AVP during capsid maturation, yielding protein VII (pVII) and μ

(89). The L3 region encodes inner core precursor protein VI (preVI), major capsid protein hexon (also known as protein II), and the AVP (46). The L4 region encodes the mentioned L4-100k and L4-22/33K proteins, as well as protein VIII (pVIII), another cement protein (46). In addition to activating the MLP, L4-33K is also involved in virion assembly (90). Finally, L5 encodes the fiber protein (protein IV), the last major capsid protein, which extends out of each vertex (46), and is used for cell attachment (91).

1.2 HAdV biology: life cycle

1.2.1 The mature virion

The mature HAdV virion is composed of 12 proteins grouped into major, minor/cement, and core proteins, as well as the viral DNA and two copies of TP (figure 1.2). The virion is ~90 nm from vertex to vertex, and in the case of HAdV-5, the fiber protein further extends out ~30 nm. The length of the fiber protein varies depending on the type of HAdV (46). Each vertex is composed of a pentamer of the penton protein surrounded by five trimers of the hexon protein (referred to as the group of six), while each face is composed of nine trimers of hexon (referred to as the group of nine) (92). Each vertex is in turn capped by a trimer of the fiber protein (88). pIX is the only minor protein found on the outside of the capsid, and helps stabilize hexon trimers with one another (93). Within the virion, the minor proteins pIIIa, pVI, and pVIII also assist with stabilizing the capsid (88, 94, 95). The proteins pV, pVII, and protein μ are all inner core proteins (88, 96, 97). Proteins pVII and μ contribute to condensation of viral DNA within the capsid (97), while pV connects the condensed viral DNA with the inner shell of the capsid, by interacting with pVII and pX, as well as the cement proteins pVI and pVIII (46). Virions

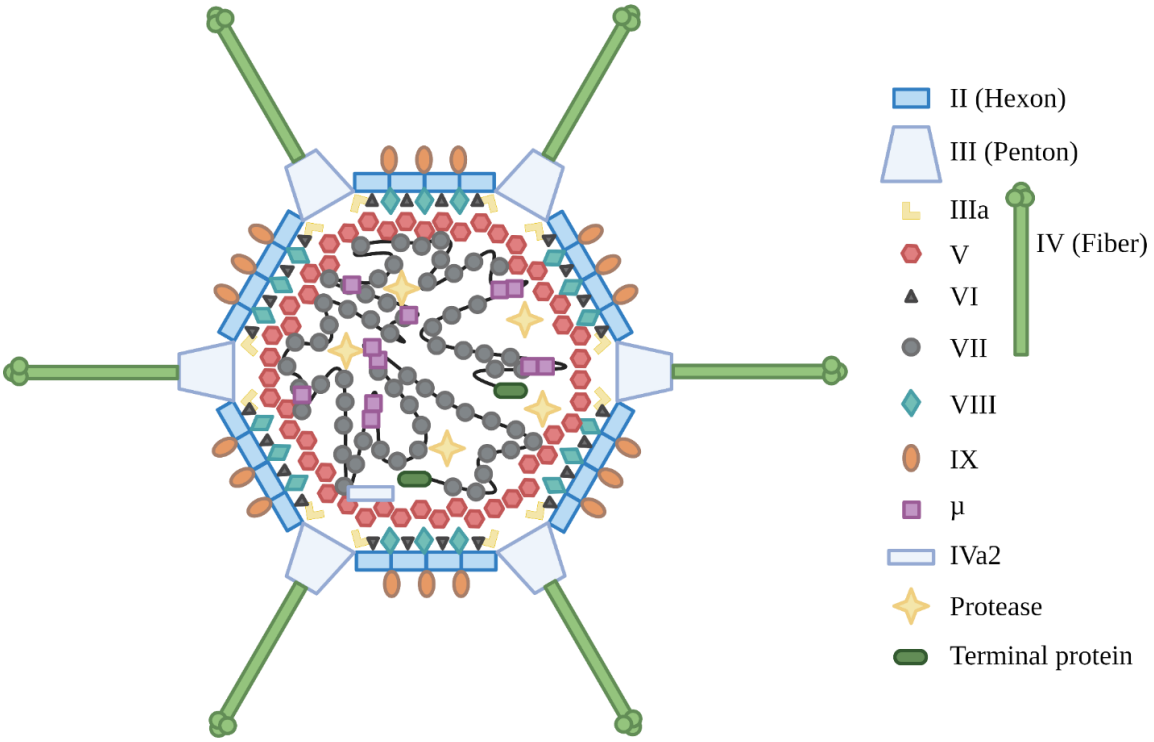

Figure 1.2 Schematic of the HAdV-5 virion. Obtained with permission from (98), depicting approximate locations of viral major, minor, and core proteins.

can be generated in the absence of pVII, suggesting condensation of viral DNA is not necessary for packaging, but these virions are unable to escape the endosome following endocytosis (99). Finally, capsids contain the proteins IVa2, which is found at a single vertex (49) and AVP, which is required for maturation of the virion (88). The exact structure of the viral core has not been elucidated (46).

1.2.2 Cellular uptake to nuclear import

The overall infection cycle takes about 48 h in normal cells (100), while in transformed cells replication is much more rapid, completing a cycle in 24-36 h. At the beginning of HAdV-5 infection, the fiber protein binds to the Coxsackie-Adenovirus receptor (CAR), which is the primary receptor for HAdV-5 and Coxsackie B virus (101, 102), though alternate receptors exist (103). Once the fiber knob binds to CAR, a secondary interaction occurs between the penton protein and αvβ3 or αvβ5 integrins, which triggers internalization of HAdV by clathrin-mediated endocytosis (104). During internalization, difference in mobility between CAR and relatively immobile integrins leads to shearing off the fiber proteins from the capsid (105), allowing for the release of pVI from the inner capsid. pVI possesses membrane lytic activity, and results in rupture of the endosome and subsequent release of the virus into the cytoplasm (106). To reach the nucleus, the capsid travels along microtubules (107), and is progressively dismantled (108-110). Once the partially disassembled capsid reaches a nuclear pore, pVII-bound HAdV DNA is released and subsequently imported into the nucleus (108-114).

The pVII molecules that accompany viral DNA into the nucleus are known to serve a few functions. First, pVII helps protect HAdV DNA from detection by the DDR (115),

as activation of the DDR prior to expression of early viral genes to counter the DDR leads to concatemerization of viral DNA, which prevents productive infection (116, 117). Second, free pVII can associate with host chromatin as well as high-mobility-group B (HMGB) proteins, together suppressing cellular immune danger sensing (118, 119). Third, free pVII also depletes histone H1 isoforms from cellular chromatin, and the combination of sequestering HMGB and H1 depletion inhibits cell cycle progression beyond the S-phase, ensuring efficient viral replication (120). Fourth, small amounts of pVII on viral DNA appears to stimulate transcription of viral DNA (121-123), and pVII can be found bound to the viral DNA up to at least ~10 h post infection (hpi) (121, 122, 124-127). pVII is removed from viral DNA in a transcription-independent manner (127, 128). In cell-free experiments, the proteins SET (129, 130), NAP-1 (131), and nucleophosmin (132) have been identified as potential remodelers of pVII-wrapped viral DNA, though this has not been demonstrated during actual infection.

1.2.3 Epigenetic regulation during HAdV replication

On cellular DNA, two histone H2A–H2B and H3–H4 dimers (forming an octamer) wrapped by ~150 bp of DNA form the basic unit of chromatin, nucleosomes. Post-translational modification (PTM) of the N-terminal "tails" of histones influences the "openness" and "compactness" of chromatin, or regions of active and repressive gene expression, respectively (133, 134). In general, acetylation of histone tails is associated with open chromatin (e.g. acetylation of H3K9, H3K18, H3K56, and H4K16), while methylation is associated with closed chromatin (e.g. trimethylation of H3K9 and H3K27) (133, 135). DNA itself may also be methylated, typically repressing gene expression (though DNA methylation of some loci can promote gene expression) (136, 137). Other

mechanisms utilized by the cell to control gene expression include non-coding RNAs (138), as well as direct accessibility to DNA sequences by remodeling nucleosome position (139). Together, these epigenetic mechanisms grant the cell more control over gene regulation and allow the establishment of cell identity (140).

The dynamics of epigenetic regulation is exploited by HAdV and other nuclear viruses (141-143), allowing modulation of viral gene expression, as well as altering cellular gene expression to support productive infection. HAdV infection induces global changes in the epigenetic landscape, such as reducing global H3K18 acetylation status, while maintaining the marks on promoters for genes involved in the cell cycle (51). Prior to expression of E1A, cellular histones must be deposited on viral DNA (128), suggesting HAdV DNA must also be chromatinized for productive infection. Indeed, all members of the nucleosome can be detected on viral DNA (121, 126, 127, 144). Furthermore, micrococcal nuclease digestion of early HAdV DNA yields a repeating ~200 bp structure, similar to cellular chromatin, suggesting that the histones found on viral DNA are indeed wrapped in physiologically-spaced, nucleosome-like structures (126, 145-149). The histones on HAdV DNA are also modified, as acetylated H3 can be detected at all HAdV promoters tested (121). However, as the infection progresses into the late phase, viral genomes instead show irregularly spaced nucleosome-like structures at approximately one-tenth the density of cellular chromatin (127), though it is not known if this is an intentional strategy employed by HAdV, or rather due a combination of increasing number of viral genomes and reduced histone pools available due to inhibition of cellular mRNA translation (150, 151).

The importance of epigenetic regulation during HAdV infection is underscored by

the fact that several studies have shown that compounds that modulate the activity of cellular epigenetic proteins are capable of inhibiting HAdV replication (14). Compounds such as pan-histone deacetylase (HDAC) inhibitors SAHA (inhibiting HDACs 1-3, 6, 7, and 11), trichostatin A (HDACs 1, 3, 4, 6, and 10) (152), and valproic acid (HDACs 1-5, and 7) (153) have anti-HAdV effects, with many more with potential compounds (154). Histone methyltransferases inhibitors also are capable of inhibiting HAdV replication (154, 155).

Despite forcing cells into the S-phase of the cell cycle, HAdV does not incorporate the histone variant H3.1, which is expressed exclusively during the S-phase (156, 157), onto viral DNA (126, 127, 144). Instead, HAdV DNA incorporates the histone variant H3.3 (121, 127, 144), though the histone chaperone that accomplishes this task has not been identified (98). While knockdown (KD) of histone H3.3 chaperone HIRA did not decrease association of H3.3 on wild type HAdV-5 DNA (127), loss of HIRA did reduce association of H3.3 on a helper-dependent vector (126). KD of CHD1, another H3.3 chaperone, did not lower viral yield in HAdV-5 infected cells (158). While DAXX is known to act as a H3.3 chaperone, it is actively targeted for degradation during HAdV infection, and mutant viruses unable to degrade DAXX actually leads to repression of viral transcription, as these histones were unacetylated (62, 159, 160). The chaperone responsible for H2A-H2B deposition is also unknown. Regardless of the histone chaperone that deposits histones on viral DNA, once chromatinized, *E1A* expression can commence, leading to changes in cellular gene expression to better support productive infection. Expression of E1A also leads to transactivation of the other early viral genes, which all slowly accumulate over time (161). Once sufficient E2 proteins are present, viral DNA replication commences (67).

1.2.4 Viral DNA replication

In HAdV-infected cells, viral DNA replication begins ~30 hpi in normal cells (161), and much more rapidly in cancer cells, between 10-12 hpi (162). As viral DNA replication commences (summarized in figure 1.3), the viral Pol and preTP associate with one another. The Pol/preTP complex then binds to the viral ITR, and along with Oct-1 and NF1, forms the viral DNA replication pre-initiation complex. DBP binding to the pre-initiation complex enhances binding of Pol and NF1 to the origin of replication (163), and aids in unwinding the dsDNA genome (165, 166). This also has the effect of stimulating the elongation phase of DNA replication (163). As Pol progresses along viral DNA, DBP binds to the displaced single-stranded DNA (ssDNA) intermediate, cooperatively binding to other DBP molecules, thereby allowing ATP-independent unwinding of viral DNA. These ssDNA intermediates are additionally protected by DBP to avoid degradation by cellular nucleases (167, 168) as well as recognition by the DDR against naked DNA (167, 169). Once the ssDNA intermediate is fully displaced, by annealing the complementary ITR at the ends of viral DNA, the ssDNA intermediate forms a "pan-handle" structure. This process recapitulates the native ITR, serving as a template for another round of DNA replication, eventually generating another dsDNA molecule (170). DBP-bound viral DNA is not the template for viral gene expression (171), and since histones remain associated with viral DNA at 18 hpi (127), it is likely that some viral genomes remain associated with histones to support viral gene expression. Indeed, viral transcription can be detected on the periphery of both early and late viral replication centers (VRCs) (172, 173). As outlined above, viral DNA replication induces the expression of IVa2 (84). IVa2 and E4orf3 activate expression of L4-22K and L4-33K (48), which in turn activate the MLP and ushers in the

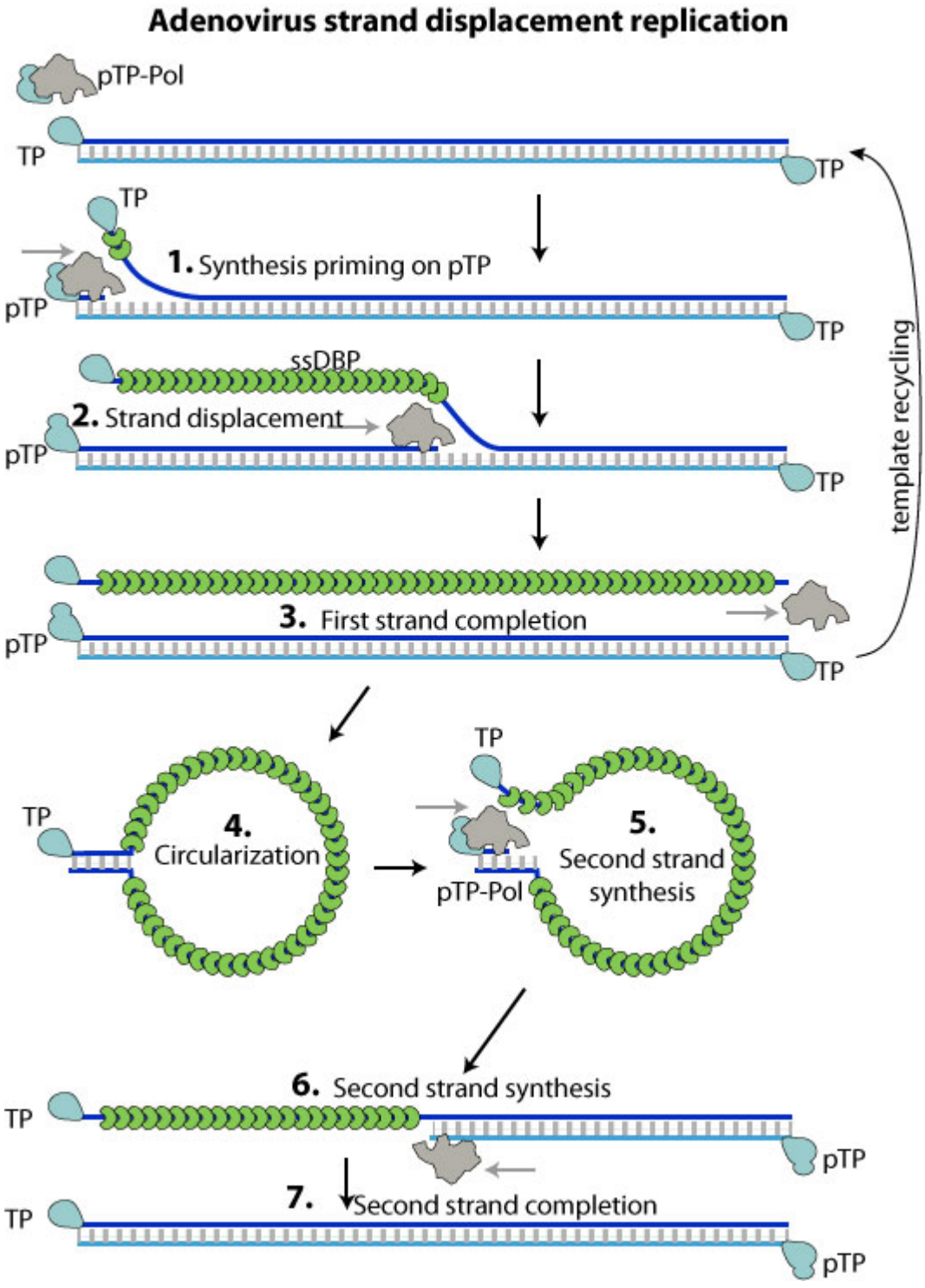
Adenovirus strand displacement replication
pTP-Pol
TP
TP
TP
1. Synthesis priming on pTP
pTP
TP
ssDBP
2. Strand displacement
pTP
TP
template recycling
3. First strand completion
pTP
TP
TP
4.
Circularization
TP
5.
Second strand
synthesis
pTP-Pol
6. Second strand synthesis
TP
pTP
7. Second strand completion
TP
pTP

Figure 1.3 HAdV DNA strand displacement replication. Obtained with permission from the ExPASy Bioinformatics Resource Portal (164). The linear HAdV genome is replicated through protein-primed, strand displacement.

late phase of infection.

1.2.5 Late gene expression to viral egress

Following the activation of the MLP, late viral proteins accumulate within the nucleus, eventually leading to virion formation (69, 173). Historically, it was unknown if HAdV virions were formed by inserting viral DNA into preformed capsids, known as the sequential model, or if capsids formed around viral cores, known as the concerted model. Despite some evidence suggesting virions are formed via the sequential model (174, 175), a larger body of evidence would suggest that virions form via the concerted model (69, 173, 176). Virion assembly is coupled to active viral DNA replication, as inhibition of viral DNA replication after the onset of late gene expression reduced virion formation despite the presence of accumulated viral DNA which could otherwise be packaged into virions (177). DBP-negative viral genomes bubble out of VRCs, acquiring core proteins as the genomes travel to the nuclear periphery where final capsid assembly takes place (69, 173, 178). Eventually, increased expression of the adenoviral death protein induces destabilization of the nuclear envelope, rupturing the nucleus and leading to death of the cell, allowing escape of replicated virions (179), completing the viral lifecycle.

While viral cores during virion formation appear to be devoid of DBP, it is unknown if these viral genomes are still associated with significant amounts of histones, which need to be replaced by preVII. The protein TAF-III has been identified as a potential chaperone for deposition of preVII onto viral DNA, as it has a greater affinity for preVII over pVII, and can transfer preVII onto DNA in cell-free systems (180), which would otherwise form insoluble complexes without TAF-III (181). Depletion of TAF-III causes histones to be

retained on viral DNA (182). PreVII also interacts with chromatin remodeling proteins CHD3 and BAZ1A, potentially contributing to removal of histones from viral DNA (183). In addition, viral DNA may be predisposed to bind to preVII due to reduced cellular protein translation impacting the levels of histones within the nucleus (150, 151). Regardless, viral DNA associated with preVII and other core proteins would then go on to form mature virions, as outlined above.

Taken together, HAdV infection involves many complex processes where a significant disruption can prevent successful generation of progeny. While targeting viral proteins and processes during infection directly reduces the potential for cytotoxicity against the host, such a strategy increases the risk of resistance due to direct evolutionary pressure against the virus (184, 185). An alternative strategy is instead to target the host processes the virus co-opts for productive infection, striking a balance between direct impact on the host and reducing the possibility of the virus developing resistance against a treatment (185, 186). Such strategies may also reveal compounds with broad-spectrum activity against many viruses (187, 188), allowing for repurposing of compounds against viral infection. Thus, identifying host factors vital for productive infection can represent potential targets to inhibit viral infection.

1.3 The Facilitates Chromatin Transactions complex

Among eukaryotes, the facilitates chromatin transactions (FACT) complex is a conserved protein complex involved in numerous cellular processes (189-191). The FACT complex was initially identified as a key factor involved in transcription elongation through nucleosomes (192), which can act as physical obstacles impeding the passage of RNA

polymerase II (RNAP II) (193-195). This led to the complex initially being named the facilitates chromatin transcription complex (192). However, since then, the FACT complex has been shown to be involved in other cellular processes, such as transcription initiation (196, 197), DNA replication (198, 199) and repair (200, 201). The FACT complex is also capable of assembling nucleosomes on naked DNA (202, 203). The role of the FACT complex in diverse chromatin-related processes has led some to instead use the word transactions when referring to the complex (204). In yeast, a common model organism used in studies of eukaryotic processes (205, 206), the complex is composed of three protein subunits, suppressor of Ty 16 (Spt16, also known as Cdc68), polymerase one binding protein 3 (Pob3), and non-histone protein 6 (Nhp6) (189). In humans, the FACT complex is only composed of two proteins, SUPT16H (Spt16 homologue) and structure specific recognition protein 1 (SSRP1, a fusion of Pob3 and Nhp6) (189, 196, 207).

The FACT complex is reported to have an unusual mode of self regulation (208). The mRNA of both SUPT16H and SSRP1 associate with the FACT complex itself, stabilizing the complex. In turn, the loss of mRNA (such as via RNAi) of either subunit destabilizes the entire complex and leads to reduced quantities of both SUPT16H and SSRP1 protein. This indicates only one subunit needs to necessarily be targeted in order lower the quantity of the entire complex.

Within the cell, the FACT complex is distributed throughout the nucleoplasm and associates with genes undergoing active transcription (209-211). The FACT complex is also enriched in nucleoli, where it is involved in RNAP I and III transcription (212). In proliferating cells, transcription of rRNA genes by RNAP I accounts for 60-80% of total RNA transcription (213, 214), which could explain the enrichment of the FACT complex

within nucleoli.

During embryonic development, FACT expression is high and remains high in undifferentiated/proliferating cells, but decreases as cells differentiate (210, 215-217). Owing to the importance of the FACT complex in undifferentiated cells, knockout (KO) of the FACT complex is embryonically lethal (218, 219). In adult mice, differentiated cells are unharmed by the loss of the FACT complex while stem cells in several organs are unable to properly proliferate, which ultimately contributed to lethality (220). In many cancers, the FACT complex is upregulated (217, 221), and the discrepancy between FACT complex expression in differentiated vs cancer cells have led to researchers targeting the FACT complex as an anticancer strategy (221, 222).

Each subunit of the FACT complex functions cooperatively to remodel nucleosomes (figure 1.4). During nucleosome remodeling, the FACT complex can only weakly bind to intact nucleosomes, and requires the DNA to be partially unwound from the nucleosome, such as by the activity of RNA and DNA polymerases (223, 224). Once bound to the nucleosome and DNA, SUPT16H removes one H2A-H2B dimer from the nucleosome, forming a hexasome and leads to unwrapping of DNA from the hexasome, thereby allowing passage of the polymerase (225, 226). After the polymerase has passed, the FACT complex reassembles the nucleosome in order to maintain chromatin stability (190, 200, 225, 227). Depletion of the FACT complex has been associated with increased histone turnover (228), and results in increased transcription from cryptic promoters (229-231), as well as scrambling of histone marks (232).

1.3.1 Role of the FACT complex in gene transcription

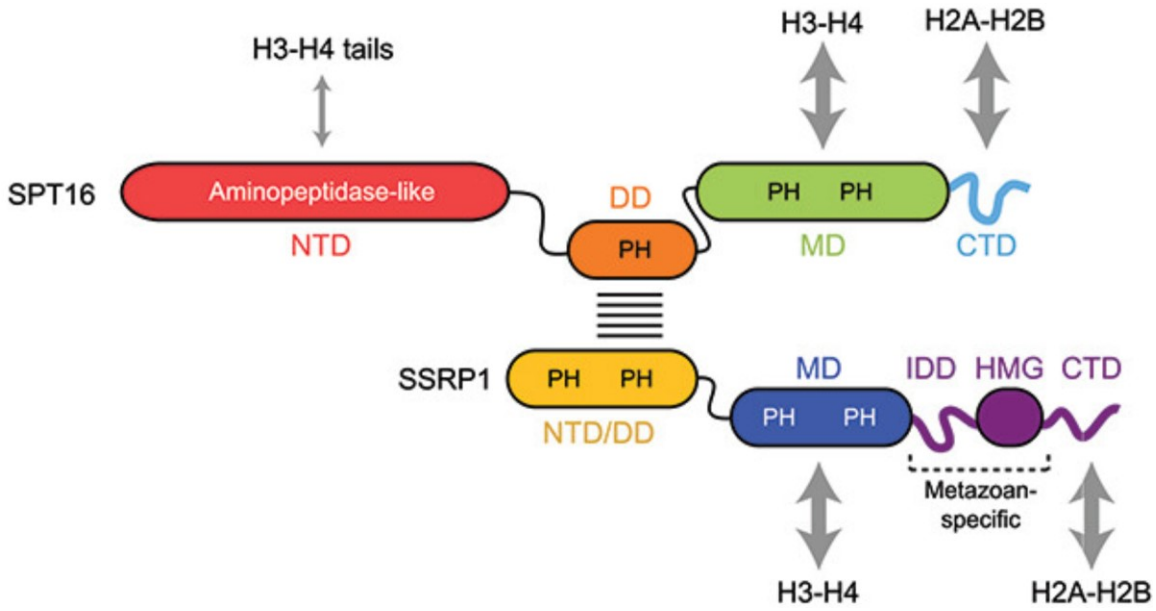

Figure 1.4 Schematic of the FACT complex. Obtained with permission from (204). The gray double arrows indicate known physical interactions of FACT domains with histones. NTD, N-terminal domain; DD, dimerization domain; MD, middle domain; CTD, C-terminal domain; IDD, intrinsically disordered domain; HMG, High mobility group domain; PH, Pleckstrin homology.

As mentioned above, the FACT complex is best known for its role in gene transcription, both in transcription initiation and elongation. During transcription initiation, the RNAP II complex and general transcription factors bind to the core promoter of a given gene, forming the pre-initiation complex (233, 234). Enhancers promote pre-initiation complex assembly at the core promoter as well as contribute to activation of RNAP II (233, 235-237). The FACT complex contributes to transcription initiation. For the pre-initiation complex to form, the promoter of a particular gene needs to be open, and nucleosomes present on the promoter can inhibit the formation of the pre-initiation complex (238). In studies of yeast, the FACT complex is required for disassembly of nucleosomes on several promoters, such as *PHO5* (197), *HO* (239, 240), and *GAL1-GAL10* (241). The FACT complex plays a similar role in mammalian cells. For example, the FACT complex interacts transiently with Oct4 and is recruited to the promoters of Oct4 target genes to deplete nucleosomes (242). Loss of the FACT complex strongly reduced formation of the pre-initiation complex globally (243). Additionally, the FACT complex itself may recruit transcription factors to promoters, as is the case for the *HO* promoter in yeast (239, 240). However, the FACT complex also plays a role in maintaining the silenced state of repressed genes, as mentioned above (228-231).

In *in vitro* studies of transcription, RNAP II transcribes very poorly on chromatin templates (244), while *in vivo*, factors exist that can alleviate the barrier nucleosomes pose to the passage of RNAP II during transcription elongation. Such factors include the FACT complex (190, 192), though other transcription elongation factors exist (245-250). As RNAP II attempts to transcribe through a nucleosome, it encounters regions where there is a strong interaction between nucleosomal DNA and histones at +15 and +45 bp into the

nucleosome (251). The pausing at the +45 position is alleviated by the FACT complex (252), as the nucleosomal DNA is sufficiently peeled off for FACT complex to bind to the nucleosome/nucleosomal DNA (223, 224). Once the FACT complex is recruited to the first nucleosome of a gene (referred to as the +1 nucleosome), work by Jeronimo et al. (211) suggests that Chd1 assists the FACT complex in following RNAP II towards the 3' end of the gene, possibly by "evicting" the FACT complex from post-transcribed nucleosomes. Following passage of RNAP II, the FACT complex reassembles the nucleosome by returning the H2A-H2B dimer to the hexasome (190, 200, 225, 227), which contributes to the maintenance of histone marks patterns on nucleosomes (232). RNAP I (transcribing rRNA, except for 5S rRNA) and III (transcribing tRNA and 5S rRNA)-dependent transcription also appears to require the FACT complex, as the FACT complex is associated with the chromatin of RNAP I and III-transcribed genes, and loss of the FACT complex decreases transcription of these genes (212).

1.3.2 Role of the FACT complex in DNA replication

The ability of the FACT complex to modulate nucleosomes is also utilized by eukaryotic cells during DNA replication. Similar to gene transcription initiation, nucleosomes can influence the ability of the pre-replication complex to form at origins of replication (253), suggesting the FACT complex could be involved in clearing origins of replication of nucleosomes. Additionally, nucleosomes not only need to be disassembled ahead of the replication fork to allow passage of the replisome, but nucleosomes need to be reassembled on both the parental strand and daughter strand. This maintains proper histone marks such that the replicated cell can maintain its epigenetic state (254, 255).

While other histone chaperones can contribute to these processes (256-261), the FACT complex has been shown to be involved in both tasks. The FACT complex interacts with the MCM complex to disassemble nucleosomes ahead of the replication fork (198), and the interaction between the MCM and FACT complexes increases the helicase activity of the MCM complex (262), improving DNA replication efficiency. The FACT complex reassembles parental nucleosomes on replicated DNA (199). Loss of the FACT complex leads to the dissociation of the MCM complex following replication stress (263). The FACT complex also weakly but directly interacts with RPA (264), and since RPA can bind to free H3-H4 (265), this may be another mechanism promoting nucleosome deposition on replicated DNA by the FACT complex.

1.3.3 Role of the FACT complex in DNA damage repair

The FACT complex assists in maintaining chromatin stability as well as reorganizing chromatin to facilitate DNA repair following DNA damage (200, 201), accumulating at sites of DNA damage (266-268). Perhaps unsurprisingly given the role of the FACT complex in transcription, the FACT complex contributes to transcription-coupled nucleotide excision repair, with rapid eviction of H2A-H2B dimers at sites of UV-induced damage, not only allowing repair machinery access to damaged DNA (269), but even recruiting repair factors to the lesion (270). FACT-mediated repair allows transcriptional restart following repair, which does not occur in the absence of the FACT complex, even if the lesion is repaired (269). At least in the context of UV-induced DNA damage, the FACT complex appears to be recruited to sites of damage by the association CK2 with SSRP1, which phosphorylates SSRP1 and switches the specificity of SSRP1 binding to

damaged DNA (266, 271-273). During dsDNA break repair, H2AX can be phosphorylated (known as γH2AX) by the ATM, ATR, and DNA-PK pathways (274, 275). The FACT complex is implicated specifically with the DNA-PK-mediated pathway, as cisplatin-induced DNA damage caused relocalization of FACT proteins from the nucleolus to the site of DNA damage that appeared to be dependent on DNA-PK (276). At the site of damage, γH2AX is exchanged onto nucleosomes by the FACT complex, and this process is reversed by ADP-Ribosylation of SUPT16H by PARP1 (277), while KD of RNF40 inhibited recruitment of the FACT complex to sites of DNA damage (278). The FACT complex associates with APE1 during base excision repair (279), XRCC1 and PARP1 during ssDNA break repair (280), and Rad54 during homologous recombination (281).

1.3.4 Role of the FACT complex in viral infection

Though it depends on the virus and context of infection, the FACT complex has been shown to be either a pro or antiviral factor during viral infection. Recently, a major antiviral pathway involving the FACT complex was identified, termed the FACT-ETS-1 Antiviral Response (FEAR) pathway (282). Early viral gene expression induces the SUMOylation of SUPT16H, and the resulting accumulation of SUMOylated SUPT16H activates the FEAR pathway. Activation of the FEAR pathway induces expression of ETS-1, and ETS-1 in turn increases the expression of genes involved in the antiviral response. Activation of the FEAR pathway is independent of the interferon response, and may have evolved prior to the interferon response itself. The pathway was identified due to cytoplasmic retention of SUMOylated SUPT16H by the vaccinia virus A51R protein (which itself is conserved among poxviruses). KD of SUPT16H was sufficient to increase

viral titers of vesicular stomatitis virus, IAV, and yellow fever virus (but not of herpes simplex virus type 1 (HSV-1)), suggesting the FEAR pathway may inhibit infection of diverse viruses (282).

Despite the FEAR pathway, the FACT complex is exploited by both RNA and DNA viruses to promote infection. Consistent with the role of the FACT complex in maintaining the silenced state on cryptic promoters (229-231), the FACT complex can suppress viral transcription from integrated viral DNA in HIV-1 and human T-lymphotropic virus type 1 infection, likely acting as a pro-latency factor (283). Paradoxically, the FACT complex is required for expression driven by the long terminal repeat of HIV-1 (284), despite earlier work indicating the FACT complex is a pro-latency factor, suggesting different cellular cues may influence FACT complex activity during HIV-1 infection. Avian leukosis virus requires the FACT complex for integration of viral DNA (285), but appears not to be involved in integration of HIV (284). Loss of the FACT complex or inhibition by the curaxin CBL0137, a DNA intercalating agent with pleiotropic effects (286, 287) (discussed in greater detail in section 1.4), increased interferon activity and inhibited replication of zika virus (ZIKV), IAV, and SARS-CoV-2 (288). In the case of IAV, inhibition of replication was due to CBL0137 treatment, suggesting the additional effects of CBL0137-treatment were responsible for the anti-IAV effects observed, as KD of SUPT16H alone improved IAV replication (282). CBL0137-treatment during human cytomegalovirus (HCMV) infection indicated that the FACT complex is required for viral reactivation, as the FACT complex was prevented from binding to the major immediate early promoter (MIEP) (289). The FACT complex is required for Kaposi's sarcoma-associated herpesvirus (KSHV) latency-associated nuclear antigen-dependent DNA replication (290). The FACT

complex has been shown to interact with the viral ICP22 protein during HSV-1 infection (291, 292), a requirement for efficient transcription elongation of viral genes. Finally, the FACT complex has been observed co-localizing with HAdV VRCs (293), though the role of the FACT complex in HAdV infection was not determined. Efforts to inhibit the FACT complex via curaxins have indicated that curaxins may be potent, broad-spectrum antiviral compounds. The ability of CBL0137 to inhibit HSV-1 and HCMV, both dsDNA viruses, suggests it may be able to inhibit HAdV replication as well.

1.4 Curaxins as therapeutics

Curaxins are small, carbazole-like DNA intercalating molecules (286, 287). Without causing DNA damage (294), curaxin-treatment leads to nucleosome unfolding and subsequently affects chromatin organization (295). As curaxin molecules intercalate DNA, they induce a conformational change that causes DNA to be partially unwound from nucleosomes, mimicking the effect induced by RNAP II and replisome complexes as they attempt to pass through the nucleosome (296). As binding of the FACT complex to nucleosomes requires partial unwinding of nucleosomal DNA (223, 224), curaxin-treatment causes the FACT complex to become associated with nucleosomes globally and essentially sequestered, a process referred to as chromatin-trapping (c-trapping) (296, 297). Curaxin treatment ultimately has pleiotropic effects on the cell, such as suppression of NF-κB signaling, activation of NOTCH1 signaling, suppression of MYCN expression, stabilization of p53, formation of Z-DNA, and in sufficiently high concentrations (10 μM), eviction of histones from chromatin (287, 296, 298, 299). A recent study also demonstrated that curaxin-treatment induces the degradation of the catalytic subunit of the RNAP I and

II complexes, as these complexes become stalled and are targeted by the ubiquitin-proteosome system (299). It is unclear if curaxin-induced stalling of RNAP II complexes is due to the inability to transcribe past the unfolded nucleosome or, more likely, if curaxin treatment induces a DNA lesion originating from torsional stress, possibly by accumulation of Z-DNA.

The original curaxin molecule, CBLC000, was initially identified during a drug screen against the renal carcinoma RCC45 cell line for compounds that stabilize p53 without causing genotoxicity (286). Subsequent molecular optimization studies of CBLC000 yielded several derivative molecules with enhanced biological potency, including CBL0137 (figure 1.5), which has improved stability and water-solubility. Due to these favourable properties, CBL0137 is the primary curaxin molecule used in research, including numerous preclinical cancer models demonstrating antineoplastic efficacy (286, 300-307), which ultimately led to a phase I/II clinical trial investigating CBL0137 treatment for various solid tumours (NCT04870944).

As alluded to above, curaxin treatment is also capable of inhibiting both RNA and DNA virus replication. The FACT complex, in conjunction with BRD4, appears to control the induction of interferon signaling via epigenetic suppression, and CBL0137 treatment induced an interferon response, which ultimately inhibited ZIKV, IAV, and SARS-CoV-2 replication (288). HIV-1 replication is inhibited both by CBL0137 and CBL0100 (308, 309). CBL0137 is not only capable of inhibiting replication of HSV-1 (292) and HCMV (289), but also increased survival in a lethal mouse model of HSV-1 infection (292). Should CBL0137 be approved for use in treating cancer in humans, the broad antiviral properties of CBL0137 suggest it could easily be repurposed to treat viral infection as well.

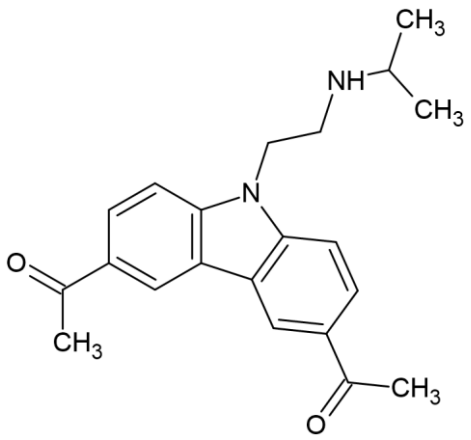

Figure 1.5 Chemical structure of CBL0137. Chemical structure of the curaxin CBL0137.

The antiviral properties of CBL0137 are in part due to CBL0137 interfering with proper gene regulation/expression of either viral or cellular genes (288, 289, 292, 308). As epigenetic modulating compounds can have anti-HAdV properties (152-155), discovering additional compounds capable of interfering with HAdV infection via epigenetic modulation could prove useful. One promising source of such modulators are natural compounds (310, 311), such as curcumin (312).

1.5 Curcumin as a therapeutic

Curcumin (diferuloylmethane) is a natural compound derived from the rhizome of *Curcuma longa* plant (313, 314). Curcumin along with desmethoxycurcumin, and bisdemethoxycurcumin, form the curcuminoids (figure 1.6), representing approximately 3-5% of ground and dried turmeric (315). While used as a strong food dye and consumed as a spice (via turmeric) (313), curcumin is perhaps known best for its use in traditional medicine, due to anti-inflammatory and wound-healing properties (316, 317). As a natural compound that is easily sourced, these properties have made curcumin an attractive potential therapeutic, and much research has gone into the feasibility of using curcumin to treat various diseases. Such research has demonstrated that curcumin has anticancer, antioxidant, and antimicrobial (including antifungal, antibacterial, and importantly, antiviral) properties, at least *in vitro* (12, 316, 318, 319). However, hampering the translation from *in vitro* to successful *in vivo* studies and clinical trials is the poor water-solubility and bioavailability of curcumin. Due to its poor solubility, as little as 1% of administered curcumin is actually absorbed by the body, and is undetectable in target tissues (320, 321). Additionally, what little curcumin that is actually absorbed is unstable

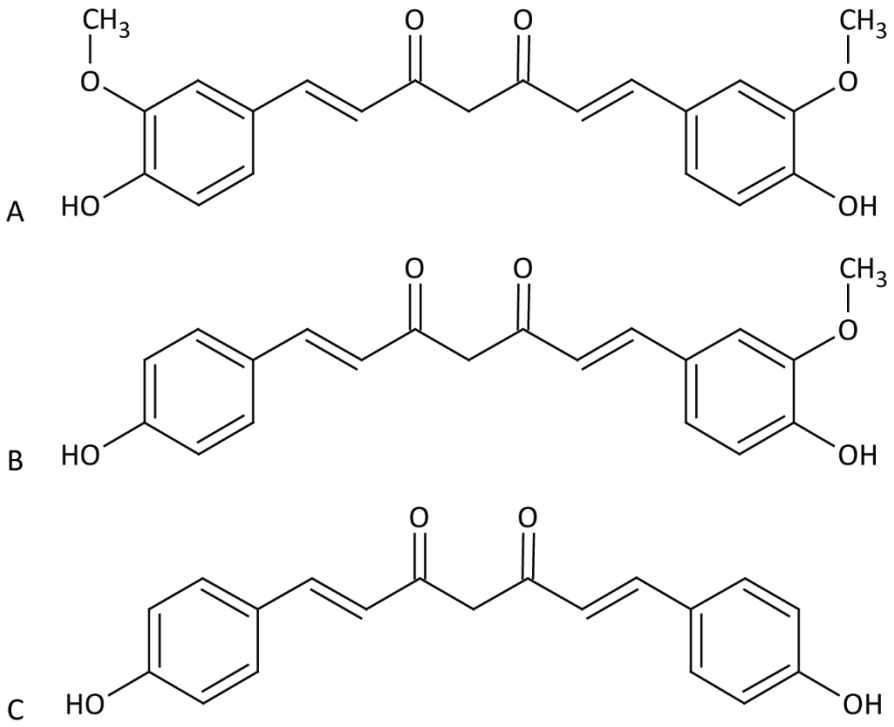

Figure 1.6 Chemical structure of curcuminoids. Obtained with permission from (12). Chemical structure of curcumin (A), demethoxycurcumin (B), and bisdemethoxycurcumin (C).

at physiological pH, and rapidly degrades into ineffective products (313). As a result, many groups have performed studies into alternative formulations and analogues of curcumin in attempts to improve bioavailability and stability to increase the effectiveness of curcumin in potential clinical trials (322-327).

Similar to curaxins, curcumin treatment has pleiotropic effects on cellular processes (328-330). For example, research into the anticancer properties of curcumin demonstrated that curcumin can downregulate the PI3K–AKT–mTOR pathway (331, 332), suppress NF-κB signaling (333-335), inhibit cell cycle progression through upregulation of p53, p21, and p27 (331, 336-339), among many other pathways (328). Curcumin also interferes with epigenetic regulation (312, 340). Curcumin treatment modulates HDAC activity, downregulating HDACs 1-4, 6, and 8 (341-350). However, other groups reported upregulation of HDACs 1, 2, 4, 5, and 8 (346, 351, 352), and this discrepancy between upregulating and downregulating specific HDACs may be due to lower doses of curcumin used (<12.5 μM), as well as a cell type-specific effect. The HAT p300/CBP is also inhibited by curcumin (353-355).

Thanks to the pleiotropic effect of treatment with curcumin and derivatives, curcumin can inhibit both RNA and DNA viruses via diverse mechanisms (12, 356, 357). The first evidence of the antiviral properties of curcumin was inhibition of the HIV-1 viral protease (358), with subsequent research also demonstrating inhibition of reverse transcription (325), replication (359), and degradation of the viral TAT protein (360). Direct incubation of IAV with curcumin inhibits viral entry (361), and suppression of NF-κB and PI3K/AKT signaling pathways also inhibit viral replication and egress, respectively (334, 362). Curcumin and analogues can weakly inhibit the dengue virus protease, while

alterations in cellular lipogenesis and actin filament organization interfere with productive replication (363). Curcumin inhibits SARS-CoV-2 by interfering with the binding of the viral spike protein with ACE2 (364-366), and was able to inhibit viral replication as well (367-370). Many studies have performed molecular-docking simulations suggesting curcumin can also inhibit the SARS-CoV-2 protease (368, 371-373), though to date no studies have verified this *in vitro*. Curcumin prevents hepatitis B virus entry by downregulation of the NTCP receptor (374). Both HSV-1 and 2 are inhibited by curcumin by preventing VP16-mediated recruitment of RNAP II to viral promoters (359, 375, 376), while KSHV is inhibited due to inhibition of APE1-mediated redox function (377). Against HCMV, curcumin reduces the expression of viral IEA proteins (378), and downregulates Hsp90 (379). Taken together, should a reliable solution to the poor bioavailability, solubility, and stability of curcumin be found, curcumin could act as a potent broad-spectrum antiviral compound.

HAdV, though self-limiting in healthy individuals, can induce severe disease at-risk populations (20-22). However, there is no approved therapeutic for treating HAdV infection (14). As HAdV exploits cellular epigenetic machinery for productive infection, interfering with HAdV infection by targeting such processes represents a promising strategy (14). Direct targeting of the FACT complex, should it be required during HAdV infection, could potentially impact HAdV gene expression, as is the case with HSV-1 (291). Treatment with the compounds CBL0137 or curcumin, each having broad-spectrum antiviral properties (12, 289, 292, 309), could also potentially inhibit HAdV infection by interfering with proper epigenetic regulation (295, 299, 341, 343, 344, 346, 350, 353).

1.6 Rationale, hypothesis and objectives

As is the case with the host cell, proper maintenance of chromatin is important for regulation of viral gene expression during productive HAdV infection, and represents a target for controlling HAdV disease in at-risk individuals. The overarching **hypothesis** of this thesis is that treatment with compounds capable of regulating viral epigenetics can interfere with HAdV infection. This includes evaluating siRNA-mediated depletion of the FACT complex, as well as treatment with the pleiotropic drugs CBL0137 and curcumin. Thus, the **objective** is to evaluate compounds capable of interfering with chromatin dynamics in the context of HAdV infection. The **specific aims** include:

(a) Evaluate curcumin as an anti-HAdV compound.

   i. Determine if curcumin-treatment can inhibit HAdV replication.

(b) Evaluate curaxin as an anti-HAdV compound.

   i. Determine if curaxin-treatment can inhibit HAdV replication.

   ii. Elucidate the mechanism of action of any anti-HAdV effect.

(c) Evaluate the role of the FACT complex in HAdV infection.

   i. Determine if the FACT complex is required for HAdV replication.

   ii. Elucidate the mechanism of action of any anti-HAdV effect.

Chapter 2:

Antiviral Effects of Curcumin on Adenovirus Replication

Morgan R. Jennings[1,2] and Robin J. Parks[1-4,*]

[1]Regenerative Medicine Program, Ottawa Hospital Research Institute, Ottawa, K1H 8L6 ON, Canada

[2]Department of Biochemistry, Microbiology and Immunology, University of Ottawa, Ottawa, K1N 6N5 ON, Canada

[3]Centre for Neuromuscular Disease, University of Ottawa, Ottawa, K1N 6N5 ON, Canada

[4]Department of Medicine, The Ottawa Hospital, Ottawa, K1H 8L6 ON, Canada

*Corresponding author

Note: This chapter appears as published in Microorganisms.

Jennings MR, Parks RJ. Antiviral Effects of Curcumin on Adenovirus Replication. Microorganisms. 2020;8(10):1524-40.

2.1 Abstract

Human adenovirus (HAdV) is a common pathogen that can cause severe morbidity and mortality in certain populations, including pediatric, geriatric, and immunocompromised patients. Unfortunately, there are no approved therapeutics to combat HAdV infections. Curcumin, the primary curcuminoid compound found in turmeric spice, has shown broad activity as an antimicrobial agent, limiting the replication of many different bacteria and viruses. In this study, we evaluated curcumin as an anti-HAdV agent. Treatment of cells in culture with curcumin reduced HAdV replication, gene expression, and virus yield, at concentrations of curcumin that had little effect on cell viability. Thus, curcumin represents a promising class of compounds for further study as potential therapeutics to combat HAdV infection.

2.2 Introduction

Human adenovirus (HAdV) is a non-enveloped, icosahedral, double-stranded DNA (dsDNA) virus, capable of infecting ocular (380), respiratory (381), or gastrointestinal tissues (382). HAdV is grouped into 7 species (A to G), and further sub-grouped into over 90 different types (381). In healthy individuals, HAdV infection is typically self-limiting (19). However, HAdV infection can cause severe morbidity and mortality in certain populations, including pediatric, geriatric, and immunocompromised patients (20). Currently, there is no therapy specific to HAdV available to the general public, and infections are usually treated with common antiviral drugs, such as cidofovir (14). Cidofovir, a cytidine analog, inhibits HAdV DNA replication by inhibiting HAdV DNA polymerase, as well as preventing chain elongation when incorporated into the viral DNA (23). However, cidofovir is often associated with high levels of nephrotoxicity (24, 383, 384). Brincidofovir (CMX001, Chimerix Inc., Durham, NC, USA), a lipid conjugate of cidofovir, has improved oral bioavailability and reduced nephrotoxicity (385, 386), but has been associated with gastrointestinal toxicity (386). Immunotherapy using anti-HAdV T-cells has shown some early success in bone marrow transplant patients, but studies are still ongoing and there is a lack of data on the effectiveness of this therapy in solid organ transplant patients (20, 386, 387). Additionally, the time-intensive nature of producing anti-HAdV T-cells severely limits the wider adoptability of this therapy (386).

An effective method used to discover novel antiviral compounds is to screen libraries of small molecules to assess their effect on viral replication. Several groups have performed such high throughput screens (HTS) to identify compounds affecting HAdV (14, 154, 388-390). Using reporter viruses derived from several HAdV types and

expressing green fluorescent protein (GFP), Sanchez-Cespedes et al. (388) identified the piperazinone derivative 15D8 as an effective inhibitor of HAdV replication. Using an assay based on inhibition of cytopathic effect in cells, Hartline et al. (389) performed a screen of 16 compounds for efficacy against several different DNA viruses, including HAdV, and identified filociclovir, a nucleoside analogue (391), as effective against HAdV and several other viruses.

Our research group developed an HTS protocol to identify compounds that inhibit HAdV replication (390). We utilized a HAdV type 5-based construct that expressed red fluorescent protein (RFP) as part of the late transcription unit, such that RFP is only expressed at appreciable levels following viral DNA replication (152). As such, the degree to which a test compound affects viral gene expression and replication inversely correlates with quantity of RFP present in the treated cells (390). Using this HTS strategy, we tested the Prestwick library (~1200 compounds, most of which are FDA-approved) for compounds affecting HAdV infection and identified 11 compounds with anti-HAdV activity (390). Follow-up studies on three cardiotonic steroids (digoxin, digitoxigenin, and lanatoside C) identified in this screen showed that these compounds primarily affected early 1 A (E1A) expression, and ultimately all reduced virus yield from treated cells (390). We also screened the Cayman Epigenetic Screening library, containing 150 small molecules that modulate the activity of epigenetic regulatory proteins, including methyltransferases, demethylases, histone acetyltransferases and deacetylases, and acetylated lysine readers, and identified 19 compounds exhibiting anti-HAdV activity (154). Finally, we showed that suberoylanilide hydroxamic acid (SAHA), a histone deacetylase (HDAC) inhibitor, effectively inhibits HAdV replication at several stages in

the HAdV lifecycle, including gene expression and DNA replication (152). The effect of SAHA was attributed to inhibition of Class I HDAC, primarily HDAC2, showing that HDAC activity is required for normal HAdV replication. Thus, compounds identified in these screens may act as effective anti-HAdV therapeutics in addition to providing insight into basic virus biology.

A promising class of compounds that show broad antimicrobial activity are the curcuminoids. Curcumin (diferuloylmethane) is a polyphenolic chemical naturally produced by the turmeric plant (*Curcuma longa*), and is the primary curcuminoid compound found in turmeric spice (314). Curcumin has a variety of biological activities, impacting many different cellular pathways (315, 392). Curcumin has shown efficacy in a variety of model systems, including models of cancer (393-395), inflammation (318) and wound healing (317). Curcumin also exhibits anti-bacterial (396) and anti-viral properties (reviewed in Reference (397)). Indeed, curcumin has shown wide-ranging antiviral activity against many diverse viral species, including single-stranded RNA (ssRNA) and dsDNA viruses (397). Mechanistically, curcumin can exert antiviral effects either directly on virus-encoded factors (360, 362, 398), or through affecting cellular processes or pathways crucial for normal virus function (334, 363). In this study, we investigated the efficacy of curcumin as an anti-HAdV compound.

2.3 Materials and Methods

2.3.1 Cell lines, Viruses and Reagents

Experiments were conducted in the human lung adenocarcinoma-derived A549 cell line (CCL-185, American Type Culture Collection (ATCC), Manassas, VA, USA), unless stated otherwise. Cells were cultured in Minimum Essential Medium (MEM, Sigma Aldrich, St. Louis, MO, USA) containing 10% (v/v) Fetal Bovine Serum (FBS, Sigma Aldrich), 2 mM GlutaMAX (Invitrogen, Carlsbad, CA, USA), and 1x antibiotic-antimycotic (Invitrogen). HAdV-4 (VR-4), and HAdV-7 (VR-7) were obtained from the ATCC, and stocks were propagated and titered on A549 cells. HAdV-5 was obtained from Dr. John Bell (Ottawa Hospital Research Institute, Ottawa, Canada), and it was grown and titered on 293 cells.

The curcumin used in the experiments described in figures 2.1–6 was obtained from Sigma Aldrich (≥65% purity, C1386), while the curcumin used in the experiments described in figure 2.7 was obtained from Cayman Chemical (≥90% purity, 81025, Ann Arbor, MI, USA). Curcumin was freshly dissolved in dimethyl sulfoxide (DMSO, BP231-1, Thermo Fisher Scientific, Waltham, MA, USA) to prepare a stock solution before each experiment. The stock solution of curcumin was diluted to the desired concentration in cell medium with a final DMSO concentration of 0.25% for each treatment.

2.3.2 Infection and Drug Treatments

Medium was removed from confluent monolayers of A549 cells prior to infection with HAdV in a minimum volume. The multiplicity of infection (MOI) was calculated as plaque-forming units (PFU) per cell, and an MOI of 10 was used for all experiments, unless

specified otherwise. Virus inoculums were diluted in phosphate-buffered saline (PBS, Sigma Aldrich), and added to the cells for 1 hour (h) at 37 °C with periodic rocking. Medium containing either vehicle or curcumin was then added to the cells, followed by incubation in a humidified CO2 incubator at 37 °C until the indicated time points. Unless otherwise noted, the indicated hours post-infection (hpi) are from the initiation of infection. Thus, for example, at 8 hpi, the infected cells would have been exposed to curcumin for 7 h.

2.3.3 Immunoblot analysis

At the indicated timepoints, medium was removed, and the cells were lysed in 2x Laemmli buffer (62.5 mM Tris-HCl pH 6.8, 25% w/v glycerol, 2% w/v sodium dodecyl sulphate (SDS), 0.01% w/v bromophenol blue) containing 5% v/v β-mercaptoethanol, and stored at −20 °C. Samples were boiled for 5 min prior to protein separation by sodium dodecyl sulphate-polyacrylamide gel electrophoresis (SDS-PAGE). Separated proteins were transferred to an Immobilon-P polyvinylidene difluoride (PVDF) membrane (Millipore, Burlington, MA, USA). The membrane was blocked with 5% w/v skim milk powder dissolved in Tris-buffered saline (20 mM Tris-HCl pH 7.6, 135 mM NaCl) containing 0.2% Tween 20 (Thermo Fisher Scientific) (TBST) and probed with antibodies diluted in the 5% milk solution. The following primary antibodies were used: anti-HAdV-5 E1A (1/5000 typically incubated overnight; MA5-13643, Invitrogen), mouse anti-tubulin (1/10,000 for 1 h incubation; CP06, Millipore), rabbit anti-tubulin (1/10,000 for 1 h incubation; ab59680, Abcam, Cambridge, UK), anti-Adenovirus Type 5 (α-HAdV-5, 1/10,000 for 1 h incubation; ab6982, Abcam). The membranes were then washed three

times in TBST and incubated with the appropriate secondary antibodies conjugated to horseradish peroxidase (HRP, BioRad, Hercules, CA, USA). Blots were developed using the Immobilon Classico Western HRP Substrate (Millipore) and visualized by standard autoradiography. All immunoblot data are representative of three or more independent experiments.

To more accurately quantify protein band intensities, immunoblots were processed for and analyzed using an Odyssey CLx imaging system (Li-Cor Biosciences, Lincoln, NE, USA). Separated proteins were transferred to an Immobilon-FL PVDF membrane (Millipore), and the membrane was blocked with Intercept Blocking Buffer (Li-Cor Biosciences). The following primary antibodies were used: anti-HAdV-5 E1A (1/5000 incubated overnight), mouse anti-tubulin (1/10,000 for 1 h incubation), rabbit anti-tubulin (1/10,000 for 1 h incubation), and α-HAdV-5 (1/10,000 for 1 h incubation), which were diluted in Intercept Blocking Buffer solution containing 0.2% Tween 20. The membrane was then washed three times in PBS containing 0.2% Tween (PBST) and incubated with the appropriate IRDye secondary antibodies (680RD and 800CW, Li-Cor Biosciences), diluted in Intercept Blocking Buffer solution containing 0.2% Tween 20 and 0.01% SDS and protected from light. The membrane was washed three times in PBST while still protected from light, followed by a final rinse with PBS. Membranes were then scanned using an Odyssey CLx system (Li-Cor Biosciences) and analyzed using Image Studio Lite (version 5, Li-Cor Biosciences). All protein quantification data are representative of three or more independent experiments.

2.3.4 Quantitative real-time PCR (qPCR)

A549 cells were infected and incubated in medium containing curcumin as described above. At the indicated time points, medium was removed, and the cells were harvested using SDS-proteinase K (10 mM Tris-HCl pH 7.4, 10 mM EDTA, 1% w/v SDS, 1 mg/mL proteinase K) and incubated overnight at 37 °C. DNA was extracted from the cell lysates using a standard phenol-chloroform method, precipitated with ethanol and NaCl, and the resulting DNA pellet was dissolved in 1x Tris-EDTA (TE). qPCR was performed using 200 ng of genomic DNA per reaction. The following primers were used: 5'-CTC CCC ACA CAC ATG CAC TTA and 5'-CCT AGT CCC AGG GCT TTG ATT for human glyceraldehyde-3-phosphate dehydrogenase (GAPDH); 5'-CCA TTA AAC CAG TTG CCG TGA GAG and 5'-GGC GTT TAC AGC TCA AGT CCA AAG for HAdV E1A. Viral genome copy numbers were calculated from the Ct values using a standard curve obtained using serial dilutions of pCB6, a bacterial plasmid containing the entire HAdV-5 genome. Values were normalized using GAPDH copy numbers, calculated from a standard curve obtained using serial dilutions of a bacterial plasmid containing a cloned fragment of the human *GAPDH* gene, designated pMJ100. To generate pMJ100, a 99 bp fragment of the human *GAPDH* gene (generated using PCR primers 5'-CTC CCC ACA CAC ATG CAC TTA and 5'-CCT AGT CCC AGG GCT TTG ATT) was cloned into SmaI-digested pBlueScript II KS(+), verified by sequencing, and purified by cesium chloride buoyant density centrifugation.

2.3.5 Plaque Assay for Virus Yield

To determine the effect of curcumin on virus yield, we performed a plaque assay of virus recovered from curcumin-treated cells. Briefly, monolayers of A549 cells were

infected with HAdV-5 at an MOI of 10. The virus inoculum was removed after one h of infection, cells were washed with PBS to remove unbound virus, and fresh medium containing vehicle or curcumin was added. After 24 h of infection, the cells were collected by scraping into the medium, 40% w/v sucrose (diluted in 10 mM Tris pH 8.0) was added to a final concentration of 4% w/v, and the samples lysed by three freeze/thaw cycles. For the plaque assay, monolayers of A549 cells were infected with dilutions of the cell lysates. After 1 h of infection, the cells were overlaid with medium containing agarose (50% v/v of a 1% w/v agarose solution, 43% clear 2x MEM, 5% FBS, 1% GlutaMAX, and 1% antibiotic-antimycotic). Plaques were counted 10 days later.

2.3.6 MTS Metabolic Activity Assays

Next, 96-well plates were seeded with 5000 A549 cells per well and incubated overnight. The next day, the medium was removed from the wells and fresh medium containing either vehicle or curcumin was added, and incubated for the required time. Metabolic activity was determined using the CellTiter 96 Aqueous Non-Radioactive Cell Proliferation Assay (Promega, Madison, WI, USA) according to the manufacturer's instructions. Briefly, cells were incubated for 1 h at 37 °C with 20 µL of the 3-(4,5-dimethylthiazol-2-yl)-5-(3-carboxymethoxyphenyl)-2-(4-sulfophenyl)-2H-tetrazolium (MTS) substrate, and absorbance readings were obtained at 490 nm using the SpectraMax 190 plate spectrophotometer (Molecular Devices, San Jose, CA, USA). As curcumin can alter the color of the medium, all absorbances were corrected using wells containing curcumin-treated medium but lacking cells.

2.3.7 Statistical Analysis

Statistical analysis was performed by using GraphPad Prism8 software (version 8, GraphPad Software Inc., San Diego, CA, USA). A two-tailed unpaired t-test with Welch's correction was used for comparing treatment to mock or vehicle. Differences with $p \leq 0.05$ were considered significant.

2.4 Results

2.4.1 Treatment with Curcumin Reduces HAdV-5 Protein Expression

Curcumin has broad anti-viral activity and can inhibit replication of a diverse group of viruses (397). To investigate whether curcumin can inhibit HAdV replication, we first examined early and late protein expression from the virus in cells treated with varying concentrations of curcumin. A549 cells were infected with HAdV-5 at an MOI of 10 and, 1 hpi, medium containing curcumin (0, 25, 50, and 100 μM) was added. An MOI of 10 was chosen to ensure sufficient E1A production for detection by immunoblot analysis. At 8 and 24 hpi, medium was removed and the cells were collected in 2x Laemmli buffer. For the samples collected at the early 8hpi time point, we examined the quantity of E1A protein within the cells, as the *E1A* region is the first region to be transcribed following entry of viral DNA into the nucleus, and the E1A species of proteins are vital for stimulating subsequent aspects of the viral replicative cycle (399). Treatment with curcumin caused a dose-dependent decrease in the quantity of E1A protein in the HAdV-infected cells. At 8 hpi, a trend appeared toward lower E1A protein in cells treated with 25 μM curcumin, which reached significance at 50 μM, and was below the level of detection at 100 μM (figure 2.1A). E1A expression was quantified using the Odyssey CLx imaging system, with E1A levels reduced to 75%, 30%, and 0% of vehicle with 25, 50, and 100 μM of curcumin, respectively (figure 2.1B). Samples harvested 24 hpi were also analyzed by immunoblot using the Odyssey imaging system, using an α-HAdV-5 antibody capable of binding to several late HAdV-5 proteins, such as the capsid proteins hexon, penton, and fiber. As observed for E1A protein, there appeared a dose-dependent decrease in the quantity of late proteins present in the curcumin-treated cells (figure 2.1C). The decrease in late proteins

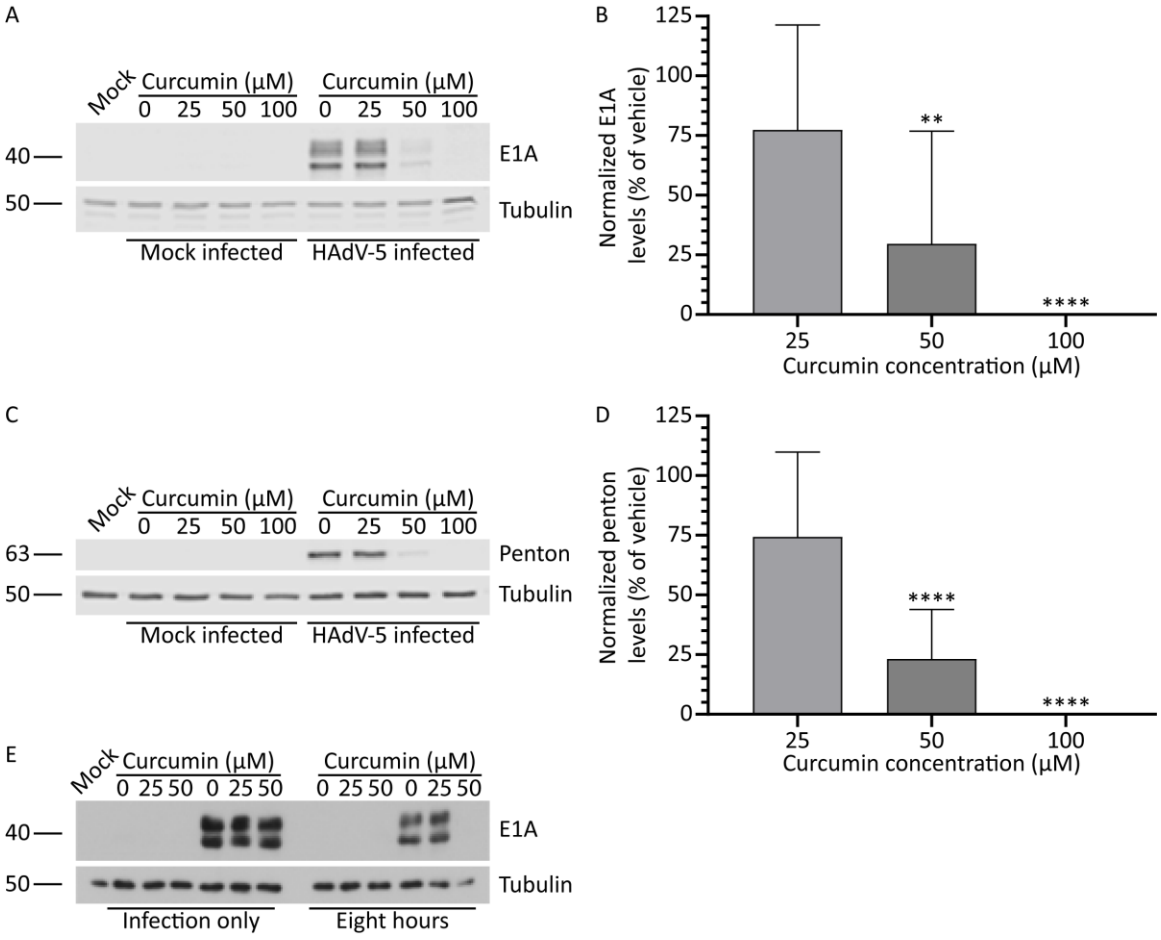
A
Mock
Curcumin (μM)
0 25 50 100
Curcumin (μM)
0 25 50 100
40
50
E1A
Tubulin
Mock infected
HAdV-5 infected
B
Normalized E1A levels (% of vehicle)
125
100
75
50
25
0
**
****
25
50
100
Curcumin concentration (μM)
C
Mock
Curcumin (μM)
0 25 50 100
Curcumin (μM)
0 25 50 100
63
50
Penton
Tubulin
Mock infected
HAdV-5 infected
D
Normalized penton levels (% of vehicle)
125
100
75
50
25
0
****
****
25
50
100
Curcumin concentration (μM)
E
Mock
Curcumin (μM)
0 25 50 0 25 50
Curcumin (μM)
0 25 50 0 25 50
40
50
E1A
Tubulin
Infection only
Eight hours

Figure 2.1. Treatment with curcumin reduces human adenovirus (HAdV)-5 protein levels. A549 cells were infected with HAdV-5 at a multiplicity of infection (MOI) of 10 for 1 h, and overlaid with medium containing curcumin (0, 25, 50, and 100 μM). At 8 and 24 hours post-infection (hpi), crude cell protein extracts were collected for immunoblot analysis. (A), (B) Samples prepared at 8 hpi were analyzed for quantity of the early 1 A (E1A) protein. (C), (D) Samples harvested 24 hpi were probed with antibody to HAdV-5 capsids proteins. Images and quantification for penton protein are shown. Signal intensities were quantified using Odyssey CLx imaging system, with each sample normalized to the tubulin loading control. Values are plotted relative to vehicle-treated cells. The mean of nine experiments are shown and the error bars represent standard deviation (SD) of the mean. (E) A549 cells were infected with HAdV-5 at an MOI of 10 for 1 h in the presence of 0, 25, and 50 μM of curcumin. One hpi, one group received medium containing no curcumin, while the other received medium containing the indicated concentrations of curcumin. At 8 hpi, crude cell protein extracts were prepared and analyzed by immunoblot for E1A, with tubulin as a loading control. ** $p \leq 0.01$, **** $p \leq 0.0001$.

reached significance at concentrations 50 μM and above, as shown by quantification of penton protein levels within the infected cells (figure 2.1D). Of note, treatment with 50 μM of curcumin led to an identical level of inhibition of late gene expression when the experiment was repeated with HAdV at an MOI of 1, 5, or 10. Thus, treatment with curcumin reduced the quantity of both early and late viral proteins in HAdV-5-infected cells.

Curcumin can exert its anti-viral effects through multiple mechanisms, including preventing the virus from entering the cell. Curcumin can directly inactivate the virion prior to infection (400), sterically interfere with cellular receptor engagement (401), or inhibit cellular pathways necessary for internalization (363). Indeed, curcumin was shown to suppress PI3K/Akt signalling (402), which is required for HAdV internalization (403). Thus, the curcumin-induced reduction in HAdV gene expression may be due to reduced virus entry. To test this possibility, A549 cells were infected with HAdV-5 at an MOI of 10 in the presence of curcumin (0, 25, and 50 μM), and 1 hpi, one group received medium lacking curcumin, while the other received medium containing curcumin (0, 25, and 50 μM). At 8 hpi, medium was removed and the cells were collected in 2x Laemmli buffer. Exposure of the infected cells to 50 μM curcumin for the entire 8 h of infection prevented detectable expression of E1A (figure 2.1E). However, treatment with curcumin during only the 1 h of infection did not lower E1A levels, indicating curcumin does not inhibit HAdV inactivate the virus or prevent internalization, at least at the concentrations tested.

2.4.2 Treatment with Curcumin Causes a Dose-Dependent Decrease in A549 Cellular Metabolic Activity

The effect of curcumin on HAdV protein expression could be due to a direct effect of the drug on the virus, or indirect due to the effect of the drug on host cell health. We thus examined the effect of curcumin on A549 cell metabolic activity. Briefly, A549 cells in a 96-well plate were treated with medium containing 0–100 μM curcumin and, 8 and 24 h later, assayed for cellular metabolic activity using the CellTiter 96 Aqueous Non-Radioactive Cell Proliferation assay. After 8 h of incubation with curcumin, concentrations of 50 μM and below showed no significant difference in metabolic activity relative to vehicle, although higher concentrations of curcumin adversely affected cell metabolism (figure 2.2A). Thus, at 8 hpi, the 75% reduction in E1A protein we observed in HAdV-infected cells treated with 50 μM curcumin (figure 2.1A, B) is likely due to direct effects of the drug on the virus and not due to indirect effects on host cell health. Conversely, the complete loss of E1A protein levels we observe at 100 μM of curcumin is due to adverse effects on host cell health. At the 24 h timepoint, cells treated with 50 μM of curcumin showed a significant ~30% reduction in metabolic activity, suggesting that reduced penton levels observed in treated cells (figure 2.1C, D) may be due, at least in part, to effects on host cell health rather than solely due to direct effects of curcumin on HAdV function.

2.4.3 Treatment with Curcumin Reduces HAdV-5 Genome Copy Number within Cells

Given that treatment with curcumin can reduce the quantity of both viral early and late proteins within cells, we next examined whether genome copy number of the virus was also reduced. A549 cells were infected with HAdV-5 at an MOI of 10 for 1 h, and incubated in curcumin-containing medium until 8 or 24 hpi. DNA isolated from the infected cells was subjected to qPCR with primers to an amplicon located within the viral *E1A* region and

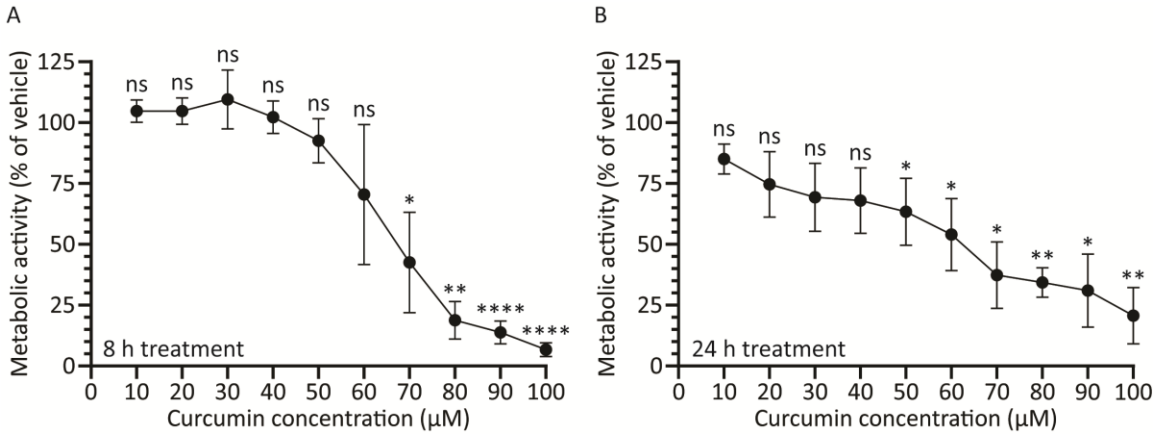

Figure 2.2. Treatment with curcumin causes a dose-depended decrease in cellular metabolic activity. A549 cells in 96-well plates were incubated with medium containing curcumin from 0–100 µM. Cellular metabolic activity was determined 8 (A) or 24 (B) h later. The mean of three experiments are shown and the error bars represent standard deviation (SD) of the mean. * $p \leq 0.05$, ** $p \leq 0.01$, **** $p \leq 0.0001$, ns $p > 0.05$.

also the cellular gene *GAPDH*. All cells showed a similar viral genome copy number at 8 hpi (figure 2.3A). At 24 hpi, we observed a ~2-fold and ~5-fold decline in genome copy number in cells treated with 25 and 50 μM of curcumin, respectively, although these differences did not reach significance. However, cells treated with 100 μM exhibited almost a 3-log reduction in viral genome copy number, as expected based on the significant effect curcumin has on cell health at this concentration (figure 2.2B). Indeed, the quantity of viral genome present in cells treated with 100 μM of curcumin was not significantly different from samples analyzed at 8 h.

We also examined the kinetics of viral DNA replication in the presence of 50 μM of curcumin. A549 cells were infected with HAdV-5 at an MOI of 10 for 1 h, and incubated in curcumin-containing medium. DNA was isolated from infected cells at 8 hpi, and then every subsequent 4 h until 24 hpi. Isolated DNA was subjected to qPCR using the same primers as above. Treatment of cells with curcumin appeared to delay the onset of viral DNA replication by 4 h (figure 2.3B). However, once viral DNA replication had initiated, the rate of replication appeared similar between curcumin- and vehicle-treated cells, although the peak quantity of viral DNA at 24 hpi was reduced by ~5-fold in the curcumin treated cells, similar to the previous experiment (figure 2.3A). Therefore, treatment with curcumin causes a delay in the onset of HAdV DNA replication.

2.4.4 Treatment with Curcumin Reduces Viral Yield

Next, we examined the effect of curcumin on virus yield. A549 cells were infected with HAdV-5 at an MOI of 10, and 1 hpi, the cells were washed extensively to remove unattached virus, and medium containing curcumin (0, 25, 50, and 100 μM) was added. At

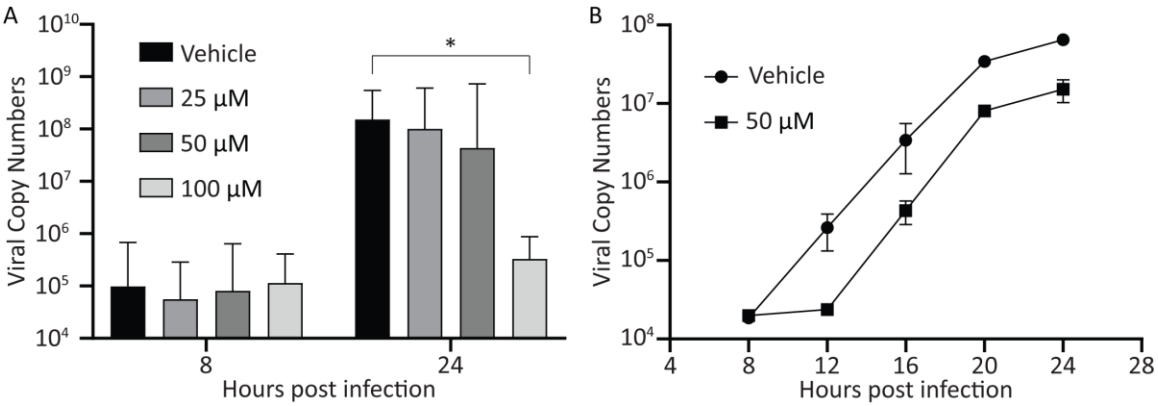

Figure 2.3. Treatment with curcumin reduces HAdV-5 genome copy number within cells. (A) A549 cells were infected with HAdV-5 at an MOI of 10 and overlaid with medium containing curcumin (0, 25, 50, and 100 µM). At 8 and 24 hpi, total DNA was isolated from the cells by sodium dodecyl sulphate (SDS)-proteinase K digestion and phenol/chloroform extraction. The resulting DNA was subjected to qPCR to determine the average genome copy number per 200 ng DNA, normalized to the average copy number of human GAPDH. The mean of three experiments are shown and the error bars represent standard deviation (SD) of the mean. (B) A549 cells were infected with HAdV-5 at an MOI of 10 and overlaid with medium containing curcumin (0 and 50 µM). Eight hpi and every 4 h until 24 hpi, total DNA was isolated from the cells by SDS-proteinase K digestion and phenol/chloroform extraction. The resulting DNA was subjected to qPCR to determine the average genome copy number per 200 ng DNA, normalized by average copy number of human GAPDH. Data represents a single experiment analyzed in duplicate, with error bars representing standard deviation (SD) of the mean. * $p \leq 0.05$.

24 hpi, the infected cells were collected into the medium, and the recovered virus was analyzed by plaque assay. While 50 μM of curcumin lowered virus yield by approximately one log, this was not statistically significant (figure 2.4). However, 100 μM of curcumin significantly reduced viral yield by approximately 3.5 log. Since there are no detectable early or late viral proteins in HAdV-infected cells treated with 100 μM curcumin (figure 2.1), and no significant increase in viral genome copy number within the cell (figure 2.3A), the virus present at 24 hpi in 100 μM curcumin-treated cells likely represents residual virus from the infecting inoculum, as we have observed previously (404). Indeed, there was no difference in virus recovery when comparing the titer of virus recovered at 4 hpi (before virus DNA replication) for vehicle or 100 μM of curcumin treated cells with that of virus recovered at 24 hpi in the cells treated with 100 μM curcumin. Thus, treatment of cells with curcumin causes a reduction in early and late proteins within the HAdV-infected cell, ultimately reducing virus yield.

2.4.5 Continued Exposure to Curcumin is Required to Inhibit HAdV Protein Expression

Our data indicates that the concentrations of curcumin that abrogate HAdV infection are in the range that can have significant adverse effects on cell function. Given this narrow therapeutic window, we asked whether transient exposure to curcumin could inhibit HAdV replication while preserving cell function. We first examined cell metabolic activity in cells exposed to either 50 or 100 μM of curcumin for different periods of time. Briefly, A549 cells in a 96-well plate were treated with medium containing 0, 50, or 100 μM of curcumin for either 1, 2, or 4 h, at which point the cells were washed and fresh medium without curcumin was replaced, or the cells were exposed to curcumin for the

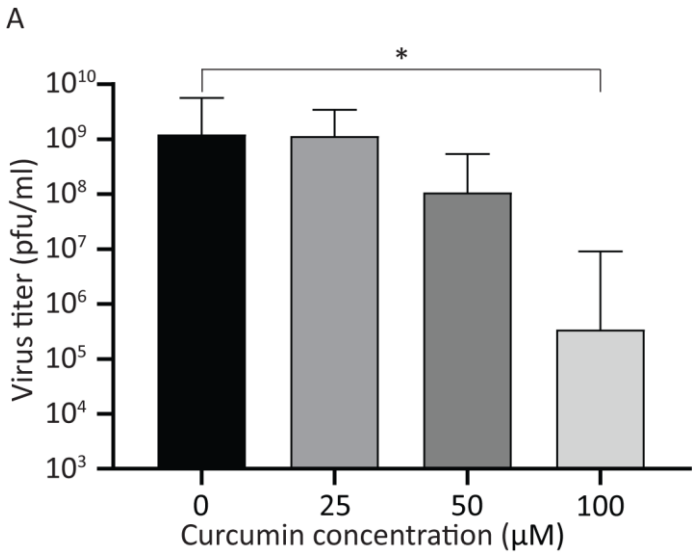

Figure 2.4. Treatment with curcumin reduces viral yield. A549 cells were infected with HAdV-5 at an MOI of 10 for 1 h and overlaid with medium containing curcumin (0, 25, 50, and 100 μM). Twenty-four hpi, the cells were harvested into the medium, and the titer of recovered viruses was analyzed by plaque assay. The mean of three experiments are shown, and the error bars represent standard deviation (SD) of the mean. * $p \leq 0.05$.

entire 24-h period. Metabolic activity in all cells was examined after 24 h. As shown in figure 2.5A, incubation of cells with 50 μM curcumin for all time periods caused a similar minor reduction in metabolic activity which was not significantly different from cells treated with vehicle. For cells treated with 100 μM curcumin, exposure to the drug for the entire 24 h period caused a significant ~90% reduction in metabolic activity. However, treatment with 100 μM curcumin for 1, 2, or 4 h preserved metabolic activity, although there was still a trend toward reduced activity relative to cells treated with vehicle. Thus, there are conditions under which cells can be treated with higher doses of curcumin, and metabolic activity can be preserved.

We next asked whether transient treatment with curcumin was sufficient to abrogate HAdV replication. A549 cells were infected with HAdV-5 at an MOI of 10 for 1 h, at which point medium containing 50 μM of curcumin was added. The cells were incubated in the presence of the drug for 2, 4, 7, and 23 h (i.e., equivalent to 3, 5, 8, and 24 hpi, respectively), washed with PBS and fresh medium with no curcumin replaced. In addition, a control plate of HAdV-infected cells received medium supplemented with vehicle for the entire 8 or 24 h period. At 8 and 24 hpi, crude protein lysates were collected and analyzed by immunoblot for early and late proteins. Treatment with 50 μM of curcumin prevented expression of E1A protein at the 8 hpi when the cells were exposed to drug for the first 4 or more h of infection; however, removal of the drug after 2 h led to detectable levels of E1A protein at the 8 h time point (figure 2.5B). This observation suggests that continued exposure to curcumin is required for anti-HAdV efficacy. Indeed, for late protein expression, we observed an inverse correlation between time of exposure to drug and quantity of penton present within the infected cells (figure 2.5C). Thus, removal of curcumin allows the virus

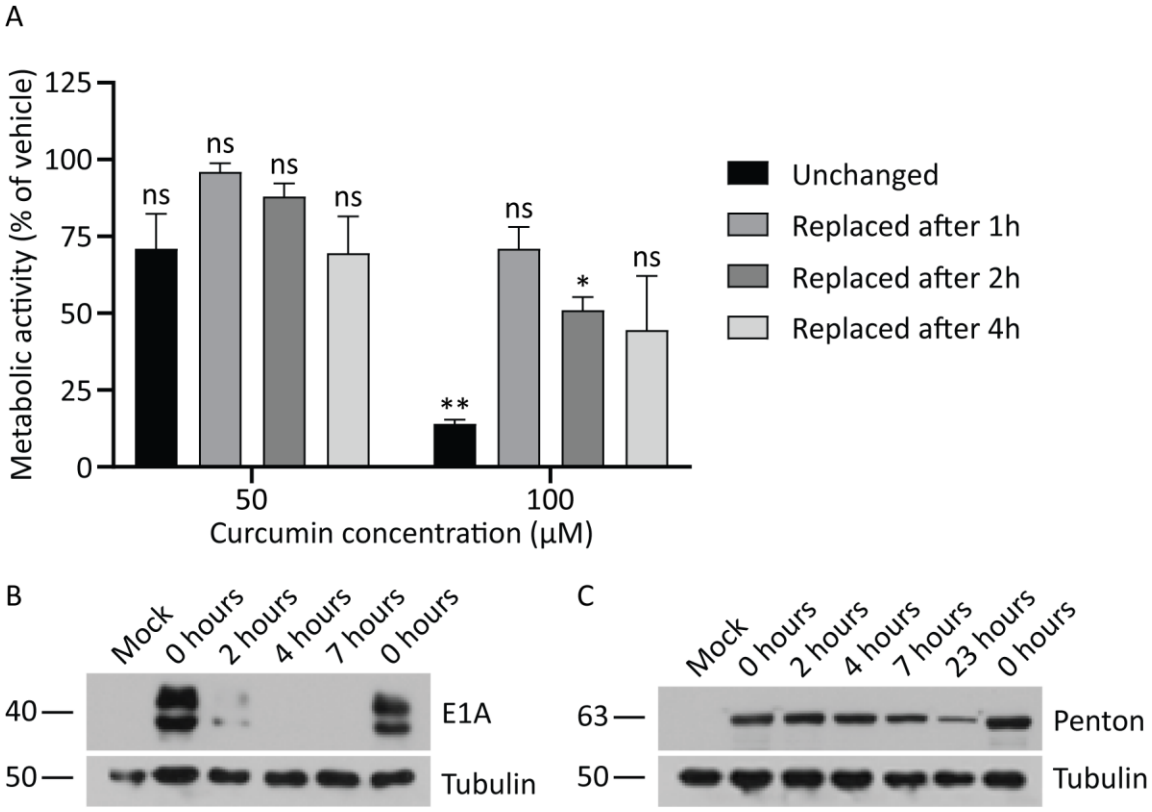
A
Metabolic activity (% of vehicle)
125
100
75
50
25
0
ns
ns
ns
ns
**
ns
*
ns
50
100
Curcumin concentration (μM)
Unchanged
Replaced after 1h
Replaced after 2h
Replaced after 4h
B
Mock
0 hours
2 hours
4 hours
7 hours
0 hours
40
50
E1A
Tubulin
C
Mock
0 hours
2 hours
4 hours
7 hours
23 hours
0 hours
63
50
Penton
Tubulin

Figure 2.5. Continued exposure to curcumin is required to inhibit HAdV replication. (A) A549 cells were treated with medium containing 0, 50, or 100 μM of curcumin. Medium was removed from the plates after 1, 2, or 4 h and replaced with fresh medium for the remainder of the 24-h time course. As a control, a series of plates were incubated in the presence of curcumin for the entire 24 h. Cellular metabolic activity was determined at the 24-h timepoint by MTS assay. The mean of two experiments are shown and the error bars represent standard deviation (SD) of the mean. (B), (C) A549 cells were infected with HAdV-5 at an MOI of 10 for 1 h and overlaid with medium containing curcumin (50 μM) or vehicle. After 2, 4, 7, and 23 h incubation in the presence of curcumin, the medium was replaced with fresh medium lacking curcumin. Eight and 24 hpi, crude cell protein extracts were prepared and analyzed by immunoblot for E1A and late protein levels, with tubulin as a loading control. * $p \leq 0.05$, ** $p \leq 0.01$, ns $p > 0.05$.

to initiate gene expression, albeit with delayed kinetics that is dependent on the length of exposure, indicating that the cells need constant exposure to curcumin in order to effectively limit HAdV protein expression.

2.4.6 Treatment with Curcumin Reduces HAdV Types 4 and 7 Protein Levels

Our study shows that curcumin can limit HAdV-5 gene expression and replication. However, HAdV-5 is not the most prevalent serotype associated with human disease and accounted for only less than 4% of all HAdV infection cases reported in the USA (405). HAdV-4 and HAdV-7 are typically associated with more severe disease, accounting for 12.4 and 8.5%, respectively, of all reported cases in patients (406). Therefore, we next examined whether curcumin could be used to control infection by other, more clinically relevant HAdV types. A549 cells were infected with either HAdV-4 or HAdV-7, treated with medium containing curcumin (0, 25, 50, and 100 μM), and the cells were harvested 24 hpi in 2x Laemmli buffer. We examined late protein expression for these viruses using the α-HAdV-5 antibody, as several of the HAdV-4 and HAdV-7 capsid proteins cross-react with these antibodies (390). Similar to HAdV-5, we observed a dose-dependent reduction in late proteins in samples infected with HAdV-4 and HAdV-7 and treated with 50 and 100 μM of curcumin (figure 2.6A, C). The quantity of penton capsid protein (~65 kDa major band) within the infected cells was significantly reduced for HAdV-4 at concentrations of curcumin 50 μM and above, while HAdV-7 showed a statistically significant reduction in late protein levels only at 100 μM of curcumin (figure 2.6B, D). Thus, curcumin is capable of reducing HAdV protein expression in all three types of HAdV tested.

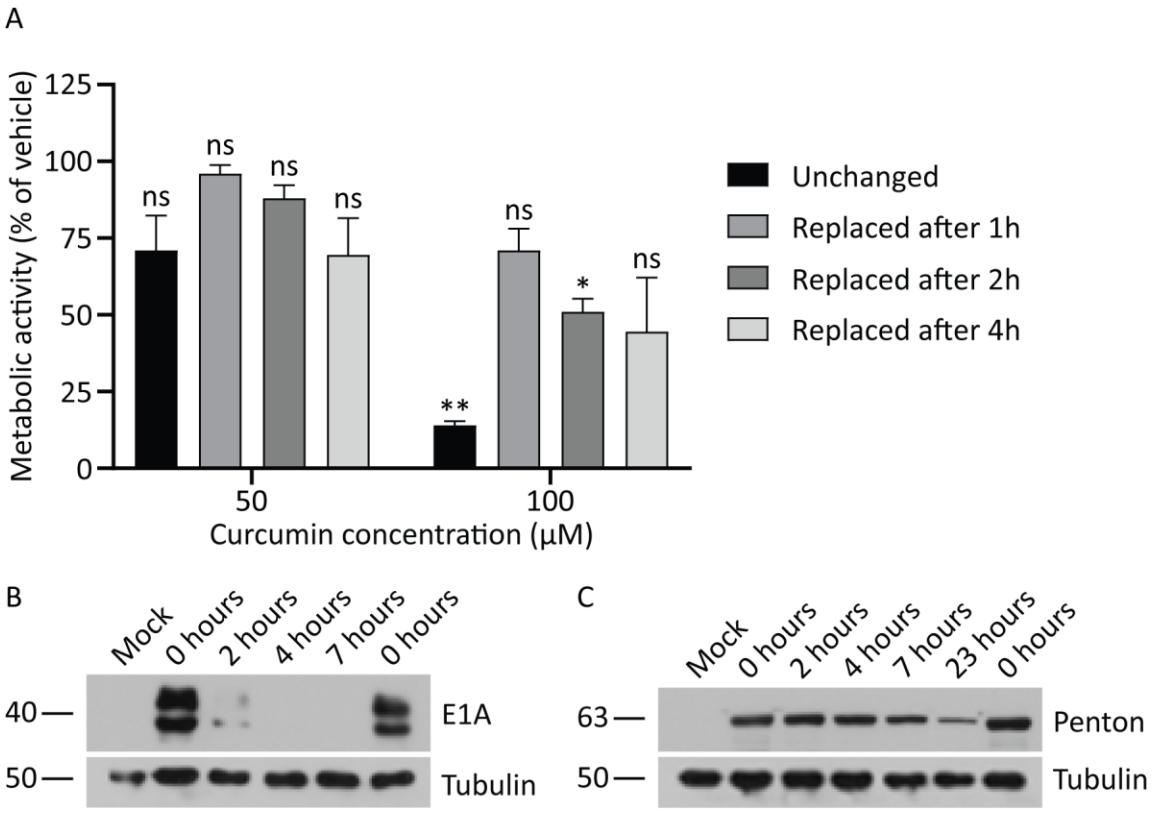

Figure 2.6. Treatment with curcumin reduces HAdV types 4 and 7 protein levels. A549 cells were infected with HAdV-4 or -7 at an MOI of 10 for 1 h, and overlaid with medium containing curcumin (0, 25, 50, and 100 μM). Twenty-four hpi, crude cell protein extracts were prepared and analyzed by immunoblot for late protein levels. (A) Samples infected with HAdV-4 were analyzed for expression of several late HAdV proteins by immunoblot using an α-HAdV-5 antibody. (B) Quantification of penton protein from HAdV-4 (~63 kDa major band) normalized to tubulin. Values are presented relative to vehicle-treated cells. (C) Samples infected with HAdV-7 were analyzed for expression of several late HAdV proteins by immunoblot using an α-HAdV-5 antibody. (D) Quantification of penton protein from HAdV-7 (~63 kDa major band) normalized to tubulin. Values are presented relative to vehicle-treated cells. The mean of three experiments are shown, and the error bars represent standard deviation (SD) of the mean. * $p \leq 0.05$, **** $p \leq 0.0001$.

2.4.7 Treatment with Curcumin of Higher Purity Improves Efficacy and Selectivity against HAdV

The curcumin used in our study to this point was reported ≥65% pure. Thus, there may be a significant level of impurities in our curcumin preparations which may affect efficacy of the test compound. We obtained curcumin of greater purity (≥90% pure) and examined its effect on HAdV gene expression and cell health. Briefly, A549 cells were infected with HAdV-5 at an MOI of 10 and, 1 hpi, medium containing the higher purity curcumin (0, 25, 50, and 100 μM) was added. Samples were harvested 8 and 24 hpi for immunoblot analysis. Similar to our previous results, treatment with curcumin caused a dose-dependent decrease in the quantity of E1A protein in the HAdV-infected cells (figure 2.7). However, perhaps unsurprisingly, treatment with curcumin of higher purity appeared to have a greater effect on viral gene expression compared to curcumin of lower purity: less E1A protein was present within the infected cells at 25 μM for the higher-purity curcumin relative to less pure curcumin (figure 2.1A, B). E1A protein was undetectable in cells treated with 50 μM of the high purity curcumin (figure 2.7A). Quantification of signal intensities showed that E1A protein levels were reduced to 53%, 1%, and 1% of vehicle with 25, 50, and 100 μM of curcumin, respectively (figure 2.7B). As observed for E1A protein, a dose-dependent decrease appeared in the quantity of late proteins present in the curcumin-treated cells. Indeed, treatment with 50 μM of above of the higher-purity curcumin resulted in undetectable levels of penton (figure 2.7C, D).

We additionally analyzed the effect of the higher-purity curcumin on cell health. Briefly, A549 cells were treated with medium containing 0–100 μM higher-purity curcumin and, 8 and 24 h later, assayed for cellular metabolic activity. Compared to the lower purity

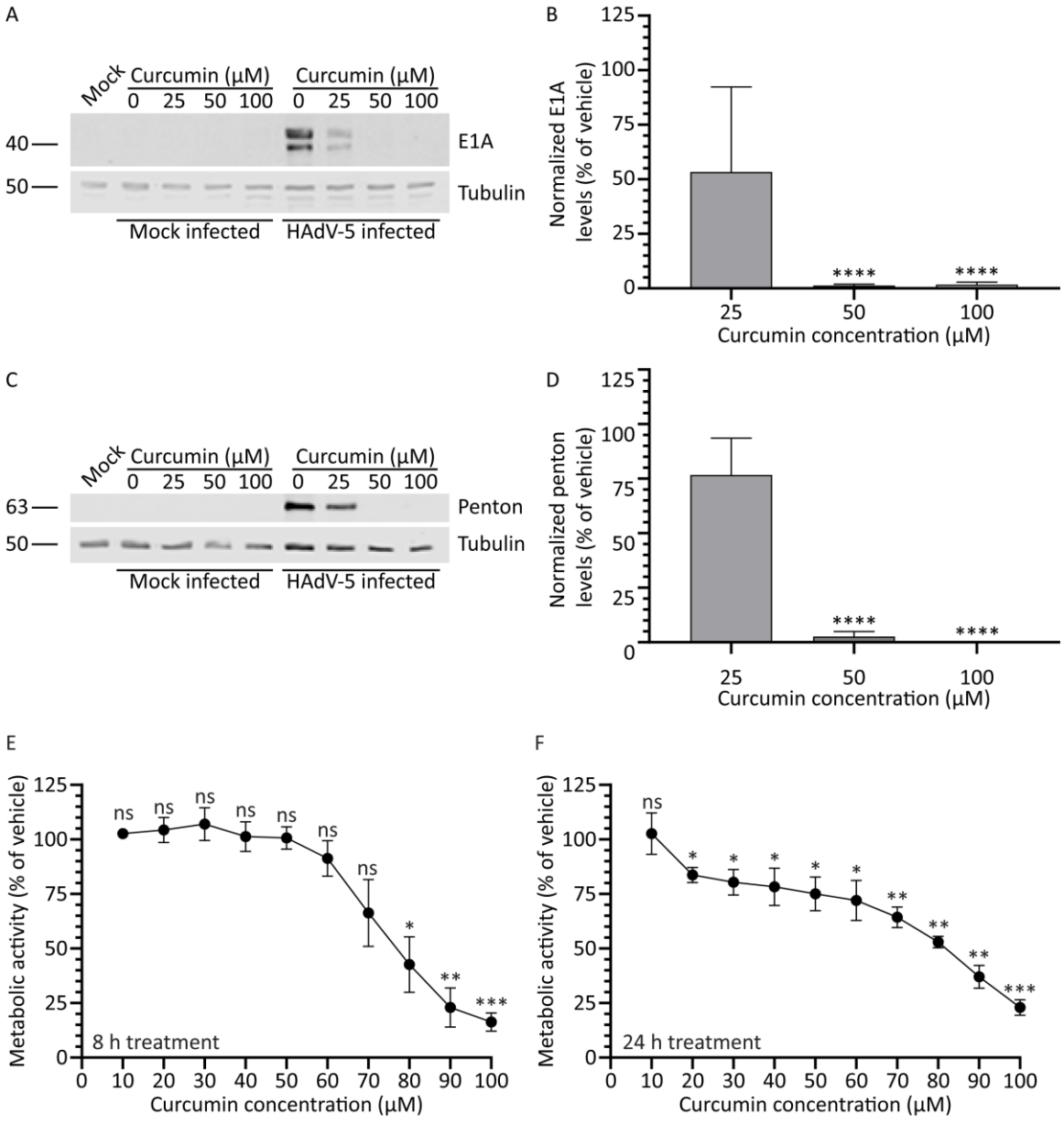
A
Mock
Curcumin (μM)
0 25 50 100
Curcumin (μM)
0 25 50 100
40
50
E1A
Tubulin
Mock infected
HAdV-5 infected
B
Normalized E1A levels (% of vehicle)
125
100
75
50
25
0
****
****
25
50
100
Curcumin concentration (μM)
C
Mock
Curcumin (μM)
0 25 50 100
Curcumin (μM)
0 25 50 100
63
50
Penton
Tubulin
Mock infected
HAdV-5 infected
D
Normalized penton levels (% of vehicle)
125
100
75
50
25
0
****
****
25
50
100
Curcumin concentration (μM)
E
Metabolic activity (% of vehicle)
125
100
75
50
25
0
ns ns ns ns ns ns ns * ** ***
8 h treatment
0 10 20 30 40 50 60 70 80 90 100
Curcumin concentration (μM)
F
Metabolic activity (% of vehicle)
125
100
75
50
25
0
ns * * * * * ** ** ** ***
24 h treatment
0 10 20 30 40 50 60 70 80 90 100
Curcumin concentration (μM)

Figure 2.7. Treatment with higher purity curcumin improves efficacy against HAdV. A549 cells were infected with HAdV-5 at an MOI of 10 for 1 h and overlaid with medium containing curcumin of higher purity (0, 25, 50, and 100 μM). (A), (B) Samples prepared at 8 hpi were analyzed for the quantity of the early protein E1A. (C), (D): Samples harvested 24 hpi were probed with antibody to HAdV-5 capsid proteins. Images and quantification for penton protein are shown. Signal intensities were quantified using Odyssey CLx imaging system, with each sample normalized to the tubulin loading control. (E), (F) A549 cells in 96-well plates were incubated with medium containing higher-purity curcumin from 0–100 μM. Cellular metabolic activity was determined 8 (E) or 24 (F) h later. Values are plotted relative to vehicle-treated cells. The mean of three experiments are shown, and the error bars represent standard deviation (SD) of the mean. * $p \leq 0.05$, ** $p \leq 0.01$, *** $p \leq 0.001$, **** $p \leq 0.0001$, ns $p > 0.05$.

curcumin, the higher purity curcumin was slightly less toxic to the cells. After 8 h treatment, treatment with the higher-purity curcumin had no effect on cellular metabolic activity until concentrations exceeded approximately 70 μM (figure 2.7E). Treatment of cells with the higher-purity curcumin resulted in no greater than a ~25% reduction in cellular metabolic activity up to a concentration of 60 μM (figure 2.7E, F); however, concentrations above this had a greater deleterious effect on cell health. Thus, treatment of cells with higher-purity curcumin appears to improve the efficacy of the compound against HAdV with no additional increase in cellular toxicity.

2.5 Discussion

HAdV infection continues to be a serious cause of morbidity and mortality in populations at risk (20, 382, 386). Though drugs capable of inhibiting HAdV replication are available, these are off-label uses and can result in significant toxicity to the patient (382, 386). Thus, there is a need for identification of compounds that can effectively and safely inhibit HAdV replication to treat infection.

Our results show that treatment with curcumin reduces both early and late gene expression (figure 2.1), genome accumulation (figure 2.3) and, ultimately, virus yield (figure 2.4) for HAdV-5. Using late gene expression as a surrogate read-out for virus replicative capacity, we show that curcumin also inhibits HAdV-4 and HAdV-7 (figure 2.6). The effects on early gene expression appear to be direct, as at 50 μM curcumin there was a significant reduction in E1A protein levels within treated cells (figure 2.1B, 2.7B) with no effect on cell health (figure 2.2A, 2.7E). However, extended exposure to 50 μM curcumin did reduce cellular metabolic activity by ~30% (figure 2.2B, 2.7F), suggesting at least part of the effect on late HAdV protein levels may be due to effects on cell health. In addition, E1A proteins are critically required for virus gene expression and replication (399), so it is possible that the later effects on virus function may also be due to an inability to generate sufficient quantities of E1A proteins. If the efficacy of curcumin is solely due to inhibition of E1A protein expression, forced expression of E1A should rescue the ability of HAdV to replicate in curcumin-treated cells. We previously described an HAdV vector in which high-level *E1A* expression is driven by the human cytomegalovirus (HCMV) immediate early enhancer/promoter (152), and attempted to circumvent the curcumin-induced block in HAdV replication. Treatment with curcumin dramatically lowered the

levels of E1A produced from this virus and, as a result, HAdV replication was not rescued. However, since the HCMV immediate early enhancer/promoter is the first promoter activated during native HCMV infection and drives expression of proteins crucial for efficient initiation of the HCMV lifecycle (406), our observation suggests that curcumin could also be an effective treatment for HCMV.

There are a number of potential mechanisms by which curcumin may inhibit HAdV gene expression and replication. First, curcumin upregulates expression of the death-domain-associated protein (Daxx) (407), a protein found in promyelocytic leukemia protein (PML) nuclear bodies (PML-NB) that are involved in an interferon (IFN)-induced antiviral response against HAdV (159). During infection, the HAdV proteins E4 ORF3 and E1B-55k normally antagonize this response (62, 159). Ineffective expression of early viral proteins caused by curcumin may prevent HAdV from shutting down this anti-viral pathway. Second, as previously reported by our research group, HDAC activity is required for HAdV replication (152), and curcumin has been reported to lower HDAC activity (350). Finally, curcumin can inhibit the activity of p300/CREB-binding protein (p300/CBP) (353), a key cellular protein that interact with E1A and mediates global changes in gene expression within the cell to modify the microenvironment for optimal viral replication (51). Any or all these mechanisms may be involved in the anti-HAdV effects of curcumin.

Our studies revealed that, although showing some efficacy against HAdV, curcumin displays a very narrow therapeutic window. Similar to our observations, previous work using curcumin against A549 cells as an in vitro cancer model showed that curcumin can cause apoptosis in A549 cells (408). Thus, a balance must be reached between efficacy

against HAdV and maintaining health of the cell. Curcumin may show greater efficacy as an anti-HAdV agent in non-transformed cell lines or patients. Curcumin also naturally shows poor bioavailability and stability at physiological pH (409), which would limit its distribution to infected tissues in vivo. However, many research groups have synthesized and evaluated curcumin derivatives that show enhanced bioavailability, stability, and/or anti-viral activity (325, 362, 363). The use of nanoparticles and other formulations and carriers can enhance curcumin solubility and bioactivity (315), which can improve antiviral activity (410-412). Such approaches may enhance efficacy of curcumin against HAdV.

In summary, our work shows that curcumin can reduce HAdV early and late gene expression, as well as virus yield, in vitro. Our work extends previous observations that curcumin is capable of inhibiting other viruses, including zika virus, human immunodeficiency virus, and influenza A virus, among many others (397). Thus, curcumin-derivative compounds or formulations that reduce toxicity while increasing efficacy may find use as effective broad-spectrum antiviral therapeutics.

2.6 Author contributions

A more detailed description of contributions of collaborators can be found at the end of the thesis.

Author contributions: M.R.J.: Conceptualization; Data curation; Formal analysis; Investigation; Methodology; Visualization; Writing—original draft; Writing—review & editing. R.J.P.: Conceptualization; Formal analysis; Funding acquisition; Project administration; Resources; Supervision; Visualization; Writing—review & editing.

Funding: This research was supported by grants to Robin J. Parks from the Canadian Institutes of Health Research (MOP-136898, MOP-142316) and the Natural Sciences and Engineering Research Council (RGPIN-2014-04810, RGPIN-2019-04786).

Conflicts of interest: The authors declare no conflict of interest.

2.7 Acknowledgements

We would like to thank Kathy Poulin and Bratati Saha for their assistance and guidance throughout this study.

Chapter 3:

Inhibition of Human Adenovirus Replication by the Small Molecule Curaxin

Morgan R. Jennings[1,2] and Robin J. Parks[1-4, *]

[1]Regenerative Medicine Program, Ottawa Hospital Research Institute, Ottawa, Ontario, Canada

[2]Department of Biochemistry, Microbiology and Immunology, University of Ottawa, Ottawa, Ontario, Canada

[3]Centre for Neuromuscular Disease, University of Ottawa, Ottawa, Ontario, Canada

[4]Department of Medicine, The Ottawa Hospital, Ottawa, Ontario, Canada

[*]Corresponding Author

3.1 Abstract

Human adenovirus (HAdV) is a common cold virus, which can cause severe disease in at-risk populations. No therapeutic has been approved to treat HAdV infections. Curaxins are a family of DNA intercalating agents that induce chromatin damage, ultimately altering cellular gene regulation and expression, and are currently in human clinical trial as anticancer agents. Many of the pathways that are aberrant in cancer are also co-opted by viruses, suggesting curaxins could also act as broad anti-viral agents. Treatment of cells with the curaxin CBL0137 significantly decreased HAdV protein levels, inhibited viral DNA replication, and lowered viral yield at concentrations well tolerated by the cell. Mechanistically, CBL0137 induced degradation of the catalytic subunit of cellular RNA polymerase II, which reduced transcription of the viral early region 1A (*E1A*). *E1A* is the first region expressed from the virus and encodes key proteins vital for transactivating other viral genes and subverting many cellular pathways within the infected cell. Time of addition experiments showed that CBL0137 was less effective at inhibiting HAdV replication when administered after the onset of early gene expression. We show that co-expression of the HAdV early proteins E1 and E4orf6 prevent CBL0137-mediated RNAP II degradation, thus allowing progression of the viral lifecycle even in the presence of the drug. Thus, CBL0137 is effective at preventing initiation of viral gene expression, but less effective at combating an established infection. Taken together, our results suggest that CBL0137 may be an effective therapeutic to treat HAdV in patients with refractory disease.

3.2 Introduction

Human Adenovirus (HAdV) is a common cold virus, accounting for approximately 5-10% of all respiratory tract infections in children under 5 years of age (22, 413), with a hospitalization rate of 18.9 per 10,000 discharges in the US for children under the age of 18 (414). In addition to respiratory disease, HAdV can also cause conjunctivitis and gastrointestinal disease, depending on the viral type and infected tissue, and over 100 different types have been identified that are grouped into 7 species (18). HAdV infections are typically benign in healthy individuals (19), but can cause severe morbidity and mortality in pediatric, geriatric, and especially immunocompromised patients (20, 21), with a mortality rate as high as ~70% in patients with disseminated disease (22). There are currently no FDA-approved therapies specific to HAdV (14), despite many drug-screening efforts to discover inhibitory compounds (152, 154, 388-390) (reviewed in (14, 415)). Certain broad-spectrum antivirals have shown some success in treating HAdV infection, however these drugs are often associated with unwanted side-effects, such as hepatotoxicity in the case of cidofovir (24). As such, discovery of new compounds capable of safely inhibiting HAdV replication is needed to lessen the burden of HAdV infection in at-risk populations.

During a screen against the RCC45 renal cell carcinoma cell line to identify non-genotoxic compounds capable of activating/stabilizing p53 in cancer cells, Gasparian et al. (286) identified a carbazole-like molecule, CBLC000, that induced cell-death in cancer cells but spared normal cells. Molecular optimization studies of CBLC000 yielded several derivative molecules with enhanced biological potency, which collectively are referred to as curaxins (286). One such compound, CBL0137, showed superior stability and water-

solubility relative to the parent compound. CBL0137 has shown anti-neoplastic efficacy in numerous preclinical cancer models, including renal cell carcinoma (286), glioblastoma (301, 303), neuroblastoma (300), small-cell lung cancer (304), melanoma (302), ovarian cancer (305), leukemia (306), and myeloproliferative neoplasm (MPN) (307). These promising results in preclinical studies has led to a phase I/II clinical trial investigating CBL0137 treatment for relapsed or refractory glioma, malignant central nervous system neoplasm, lymphoma, malignant solid neoplasm, and osteosarcoma solid tumours (NCT04870944).

CBL0137 is a DNA intercalating agent that does not induce DNA damage (294). Instead, CBL0137 causes nucleosome unfolding and impacts chromatin organization (295). This process has pleiotropic effects, including inducing stabilization of p53, suppression of NF-κB signaling, activation of NOTCH1 signaling, suppression of MYCN expression and trapping of the facilitates chromatin transactions (FACT) complex on the unfolded nucleosomes (referred to as chromatin-trapping, or c-trapping) (287, 296). CBL0137 was recently reported to induce stalling of RNA polymerase II (RNAP II) and subsequent degradation of the protein by the ubiquitin-proteosome system (299).

While much of the focus on CBL0137 is due to its anti-cancer properties, others have reported that CBL0137 treatment of infected cells can inhibit viral replication. Treatment of cells with CBL0137 led to induction of the interferon response and activation of interferon-stimulated genes, which resulted in an intracellular environment that was refractory to replication of zika virus (ZIKV), influenza A virus (IAV), and severe acute respiratory syndrome coronavirus 2 (SARS-CoV-2) (288). CBL0100 (a more potent, but less soluble and stable curaxin) and CBL0137 were each capable of inhibiting acute human

immunodeficiency virus 1 (HIV-1) replication (308, 309). CBL0137 was also effective against the nuclear dsDNA viruses human cytomegalovirus (HCMV) and herpes simplex virus type 1 (HSV-1). In the case of HCMV, CBL0137 prevented the FACT complex from binding to and transactivating the major immediate early promoter (MIEP), which subsequently inhibited viral reactivation (289), while CBL0137-treatment in HSV-1 infection inhibited the interaction of the FACT complex with the viral protein ICP22, which normally acts to recruit the FACT complex to the viral genome to promote expression of the viral immediate early genes necessary for productive infection (292). In short, curaxins appear to have broad anti-viral activity. In this study, we show that CBL0137 inhibits HAdV-5 replication.

3.3 Materials and Methods

3.3.1 Cell lines, Viruses, Transfections, and Reagents

Experiments were conducted in the human lung adenocarcinoma-derived A549 cell line (CCL-185, American Type Culture Collection (ATCC), Manassas, VA, USA) or 293 cells (a kind gift from Dr. Frank Graham, Professor Emeritus, McMaster University) (416). Cells were cultured in Minimum Essential Medium (MEM, M2279-500ML, Sigma Aldrich, Oakville, ON, Canada) containing 10% (v/v) Fetal Bovine Serum (FBS, Sigma Aldrich), 2 mM GlutaMAX (35050061, Gibco, Ottawa, ON, Canada), and 1x antibiotic-antimycotic (15240062, Gibco).

HAdV-5 was obtained from Dr. John Bell (Ottawa Hospital Research Institute, Ottawa, Canada), and was grown in 293N3S cells (a gift from Dr. Frank Graham) (417) and titered on 293 cells. HAdV-5 was purified by cesium chloride buoyant density centrifugation, as previously described (418). For infections, medium was removed from confluent monolayers of cells prior to infection with HAdV in a minimum volume. The multiplicity of infection (MOI) was calculated as plaque-forming units (PFU) per cell. Virus inoculums were diluted in phosphate-buffered saline (PBS, D8537-500ML, Sigma Aldrich), and incubated with the cells for 1 hour (h) at 37 °C with periodic rocking. Medium containing vehicle (0.1% dimethyl sulfoxide (DMSO)) or CBL0137 (19110, Cayman Chemical, Burlington, ON, Canada) was then added to the cells, followed by incubation in a humidified CO_2 incubator at 37 °C until the indicated time points. All time points are relative to the initial addition of the virus inoculum to the cells, which is considered t=0 h post infection (hpi).

For transfections, 293 cells were seeded onto 35 mm plates ($3.0x10^5$ cells/plate).

The next day, when cells were ~80% confluent, 1 μg of either pEGFP-C3, pRP3512 (GFP-tagged E4orf6 regulated by the CMV promoter), or pRP3516 (FLAG-tagged E4orf6 regulated by the CMV promoter) was transfected into cells using Lipofectamine 2000 (11668019, Invitrogen, Ottawa, ON, Canada), according to manufacturer's instructions. To generate pRP3512, an 896 bp HindIII/BamHI fragment from pRP1068 (419) containing the E4orf6 gene was cloned into HindIII/BamHI-digested pEGFP-C3. To generate pRP3516, pRP3512 was first digested with NheI/XhoI to remove GFP, the DNA ends repaired with T4 DNA polymerase, and recircularized generating pRP3515. Complementary 54 bp oligonucleotides encoding a FLAG-tag sequence and HindIII compatible ends were cloned into HindIII-digested pRP3515, generating pRP3516. Plasmids were verified by sequencing, and purified by cesium chloride buoyant density centrifugation using standard methods.

3.3.2 Immunoblot Analysis

Immunoblots were processed for and analyzed using a ChemiDoc MP imaging system (Bio-Rad, Mississauga, ON, Canada). At the indicated timepoints, medium was removed, and the cells were lysed directly on the plates in 2x Laemmli buffer (referred to as protein loading buffer (PLB), 62.5 mM Tris-HCl pH 6.8, 25% *w/v* glycerol, 2% *w/v* sodium dodecyl sulphate (SDS), 0.01% *w/v* bromophenol blue, 5% v/v β-mercaptoethanol (added immediately prior to use)), and stored at −20 °C. Samples were boiled for 5 min prior to protein separation by sodium dodecyl sulphate-polyacrylamide gel electrophoresis (SDS-PAGE). Separated proteins were transferred to an Immobilon-FL PVDF membrane (IPFL00010, Sigma Aldrich), and the membrane was blocked with Intercept Blocking

Buffer (927-70001, Li-Cor Biosciences). The following primary antibodies were used: anti-Adenovirus Type 5 (M58) (E1A, 1/5,000 for overnight incubation; MA513643, Invitrogen), Anti-Adenovirus Type 5 (recognizes all capsid proteins including hexon, 1/10,000 for 1h incubation; ab6982, Abcam, Toronto, ON, Canada), mouse anti-Tubulin (1/10,000 for 1 h incubation; CP06, Sigma Aldrich), rabbit anti-Tubulin (1/10,000 for 1 h incubation; ab59680, Abcam), anti-Rpb1 NTD (D8L4Y) (POLR2A, 1/2,000 for overnight incubation; 14958S, Cell Signaling Technology, Canada, Whitby, ON, Canada), anti-GFP (1/5,000 for overnight incubation; A-11122, Invitrogen), and anti-FLAG (1/5,000 for overnight incubation; F1804, Sigma Aldrich), which were diluted in Intercept Blocking Buffer containing 0.2% Tween 20 (BP337500, Thermo Fisher Scientific, Ottawa, ON, Canada). The membrane was then washed three times in phosphate-buffered saline (10 mM Na_2HPO_4, 1.8 mM KH_2PO_4, 2.7 mM KCl, 137 mM NaCl, pH 7.4) containing 0.1% Tween 20 (PBST) and incubated with the appropriate IRDye secondary antibodies (680RD and 800CW, Li-Cor Biosciences), diluted in Intercept Blocking Buffer containing 0.2% Tween 20 and 0.01% SDS and protected from light. The membrane was washed three times in PBST while still protected from light, followed by a final rinse with PBS. Membranes were scanned and analyzed using Image Lab (version 6.1, Bio-Rad). All immunoblot data are representative of three or more independent experiments.

3.3.3 MTS Metabolic Activity Assay

96-well plates were seeded with 5,000 A549 cells per well and incubated overnight. The next day, the medium was removed from the wells and fresh medium containing either vehicle or CBL0137 was added, and incubated for 24h. Metabolic activity was determined

using the CellTiter 96 Aqueous Non-Radioactive Cell Proliferation Assay (Promega, Madison, WI, USA) according to the manufacturer's instructions. Briefly, cells were incubated for 1 h at 37 °C with 20 µL of the 3-(4,5-dimethylthiazol-2-yl)-5-(3-carboxymethoxyphenyl)-2-(4-sulfophenyl)-2H-tetrazolium (MTS) substrate, and absorbance readings were obtained at 490 nm using the SpectraMax 190 plate spectrophotometer (Molecular Devices, San Jose, CA, USA). Wells containing no cells were used as a negative control.

3.3.4 Quantitative PCR (qPCR) and Reverse Transcription qPCR (RT-qPCR)

To examine whether CBL0137 affected HAdV-5 DNA replication, we determined the viral genome copy number in infected cells. A549 cells were infected and incubated in medium containing CBL0137 as described above. At the indicated time points, medium was removed, and the cells were harvested using SDS-proteinase K (10 mM Tris-HCl pH 7.4, 10 mM EDTA, 1% *w/v* SDS, 1 mg/mL proteinase K (P8044-5G, Sigma Aldrich)) and incubated overnight at 37 °C. DNA was extracted from the cell lysates using a standard phenol-chloroform method, precipitated with isopropanol and NaCl, and the resulting DNA pellet was dissolved in TE (10 mM Tris-HCl pH 8.0, 1 mM EDTA). qPCR was performed using 200 ng of genomic DNA per reaction. The following primers were used: 5'-CTC CCC ACA CAC ATG CAC TTA and 5'-CCT AGT CCC AGG GCT TTG ATT for human glyceraldehyde-3-phosphate dehydrogenase (*GAPDH*); 5'-CCA TTA AAC CAG TTG CCG TGA GAG and 5'-GGC GTT TAC AGC TCA AGT CCA AAG for HAdV *E1A*. Viral genome copy number were calculated from the Ct values using a standard curve obtained using serial dilutions of pCB6, a plasmid containing the entire

HAdV-5 genome. Values were normalized using *GAPDH* copy number, calculated from a standard curve obtained using serial dilutions of a plasmid containing a cloned fragment of the human *GAPDH* gene, pMJ100, as described previously (162).

To determine if CBL0137 affected viral *E1A* transcription, we determined *E1A* mRNA copy number from infected cells. A549 cells were infected and incubated in medium containing CBL0137 as described above. At the indicated time points, medium was removed, and the cells were harvested using TRIzol (15596026, Invitrogen). Total RNA was extracted from the cell lysates using the PureLink RNA Mini Kit (12183018A, Invitrogen), according to the manufacturer's instructions, and then treated with the DNA-*free* DNA removal kit (AM1906, Invitrogen). The resulting RNA was reverse transcribed into complementary DNA (cDNA) using the High Capacity cDNA Reverse Transcription kit (4368814, Applied Biosciences, Ottawa, ON, Canada). qPCR was performed using 1 µL of the cDNA reaction. The following primers were used: 5'-ACA ACT TTG GTA TCG TGG AAG G and 5'- GCC ATC ACG CCA CAG TTT C for human *GAPDH*; 5'- TCC GGT CCT TCT AAC ACA CC and 5'-GGC GTT TAC AGC TCA AGT CC for HAdV *E1A*. *E1A* mRNA copy number were calculated from the Ct values using a standard curve obtained using serial dilutions of pCB6. Values were normalized using *GAPDH* mRNA copy number, calculated from a standard curve obtained using serial dilutions of a bacterial plasmid containing a cloned fragment of human *GAPDH* cDNA, pMJ111. To generate pMJ111, a 105 bp fragment of the human *GAPDH* cDNA (generated using PCR primers 5'-ACA ACT TTG GTA TCG TGG AAG G and 5'- GCC ATC ACG CCA CAG TTT C) was cloned into SmaI-digested pBlueScript II KS (+), verified by sequencing, and purified by cesium chloride buoyant density centrifugation using standard methods.

3.3.5 Plaque Assay for Virus Yield

To determine the effect of CBL0137 on virus yield, we performed a plaque assay of virus recovered from CBL0137-treated cells. Briefly, monolayers of A549 cells were infected with HAdV-5 at an MOI of 10. The virus inoculum was removed after one h of infection, cells were washed with PBS to remove unbound virus, and fresh medium containing vehicle or CBL0137 was added. After 4 or 24 h of infection, the cells were collected by scraping into the medium, 40% *w/v* sucrose (diluted in 10 mM Tris pH 8.0) was added to a final concentration of 4% *w/v*, and the samples were lysed by three freeze/thaw cycles. For the plaque assay, monolayers of A549 cells were infected with dilutions of the cell lysates. After 1 h of infection, the cells were overlaid with medium containing agarose (50% *v/v* of a 1% *w/v* agarose solution, 43% clear 2x MEM (11935046, Gibco), 5% FBS, 1% GlutaMAX, and 1% antibiotic-antimycotic). Plaques were counted 10 days later.

3.3.6 Immunofluorescence Microscopy

To confirm transfection efficiency of GFP-tagged constructs, 293 cells were seeded onto 35 mm plates ($3.0x10^5$ cells/plate), and the next day, transfected with pEGFP-C3 or pRP3512, as described above. The following day, fluorescent images of live cells were obtained with a Plan-APOCHROMAT 20x/0.75 NA Infinity objective on a Zeiss Axiovert 200m microscope equipped with an Axiocam 506 mono camera and captured using ZEN 2 (version 2.0.0.0, Carl Zeiss Microscopy LLC, White Plains, NY, USA), and images were processed using FIJI (version 2.14.0 (419)).

3.3.7 Statistical Analysis

Statistical analysis was performed using GraphPad Prism8 software (version 8, GraphPad Software Inc., San Diego, CA, USA). To calculate significance, a one-way ANOVA or T-test was performed, as indicated. Differences with $p \leq 0.05$ were considered significant.

3.4 Results

3.4.1 Treatment with CBL0137 inhibits HAdV early and late protein production

We first assessed the effect of varying concentrations of CBL0137 on cellular metabolic activity of A549 cells at 24 h post-treatment by MTS assay. Treatment of cells with CBL0137 at 0.1 μM or lower did not affect cellular metabolic activity relative to vehicle-treated cells, whereas doses of 0.5 μM or above had a modest effect on metabolic activity of A549 cells (figure 3.1A). Although we did not test higher doses of CBL0137, extrapolation of the data shown in figure 3.1A suggests a 50% cytotoxic concentration (CC50) of approximately 100 μM. Treatment with 0.5 or 3.0 μM CBL0137 both caused a ~20% reduction in cellular metabolic activity. In general, a decrease in cellular metabolic activity of less than 30% is considered non-cytotoxic (421), and therefore we limited our testing of CBL0137 to concentrations 3 μM or lower.

We next evaluated the effect of CBL0137 treatment on the quantity of HAdV-5 early and late proteins produced during infection. A549 cells were infected with HAdV-5 at an MOI of 10, and 1 hpi, medium containing varying concentrations of CBL0137 was added. Infection was then allowed to progress for 8 and 24 hpi, indicative of the early and late phases of infection, respectively, before the cells were harvested. The quantity of E1A (early) and hexon (late) protein was examined by immunoblot. *E1A* is the first region to be expressed from the HAdV genome, and encodes proteins that are vital for hijacking cellular gene expression to support productive infection, and also transactivating expression from several other HAdV promoters (31, 422). Hexon protein is a component of the viral capsid, and is only expressed at appreciable levels after the induction of viral DNA replication and onset of the late phase of infection (161, 423). Treatment with 3.0 μM of CBL0137 caused

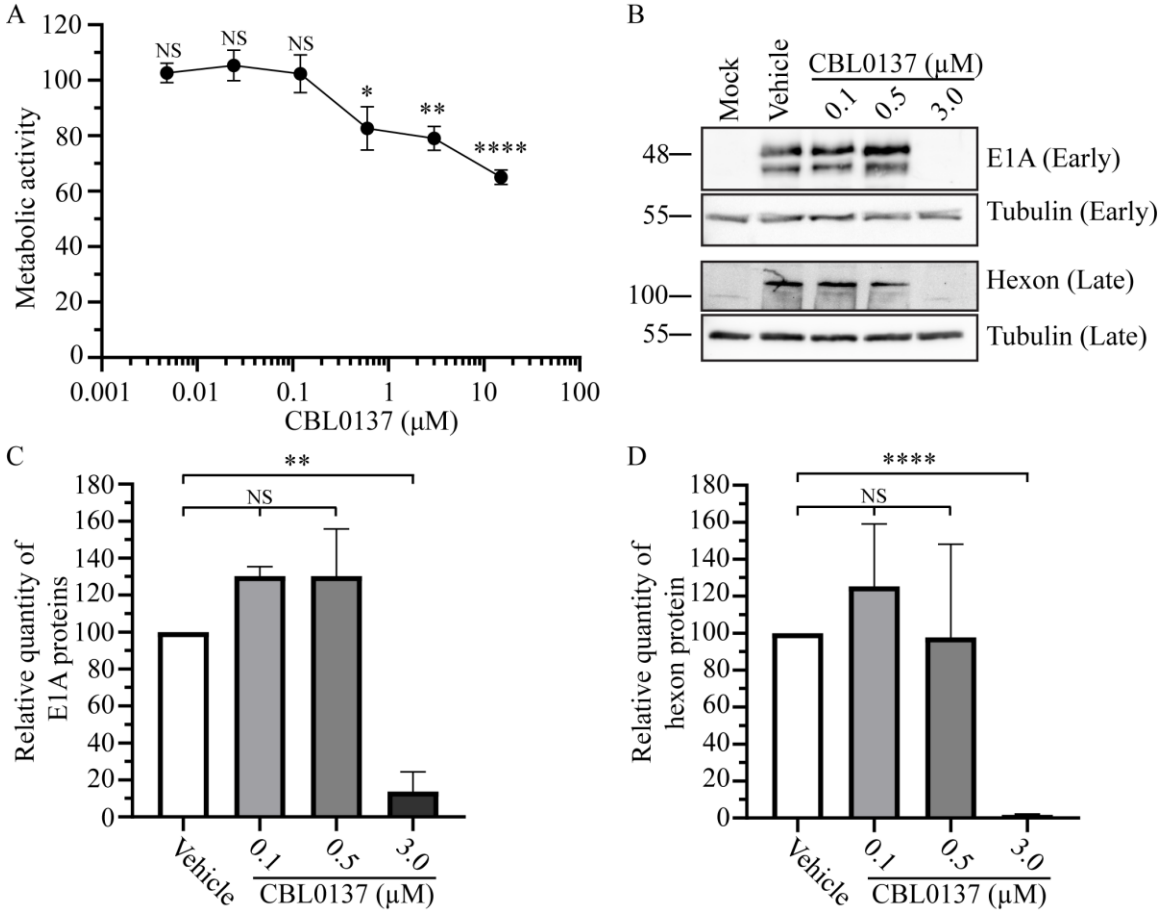
A
Metabolic activity
CBL0137 (μM)
NS
NS
NS
*
**
****
B
Mock
Vehicle
CBL0137 (μM)
0.1
0.5
3.0
48—
55—
100—
55—
E1A (Early)
Tubulin (Early)
Hexon (Late)
Tubulin (Late)
C
Relative quantity of E1A proteins
**
NS
Vehicle
CBL0137 (μM)
D
Relative quantity of hexon protein
****
NS
Vehicle
CBL0137 (μM)

Figure 3.1. Treatment with CBL0137 inhibits HAdV early and late protein production. Panel A: A549 cells were treated with varying concentrations of CBL0137 and, after 24 h of treatment, metabolic activity was assessed by MTS assay. Panel B-D: A549 cells were infected with HAdV-5 at an MOI of 10. One hpi, medium containing varying concentrations of CBL0137 was added. At 8 and 24 hpi (early and late, respectively), medium was removed and the cells were harvested into protein loading buffer (PLB), and the quantity of E1A (early) and hexon (late) was analyzed by immunoblot analysis. The signal intensity of E1A (Panel C) and hexon (Panel D) was quantified and normalized to the quantity of tubulin. The mean of three experiments is shown, and the error bars represent standard deviation (SD) of the mean. Significance was calculated using a one-way ANOVA. NS – not significant, * – $p < 0.05$, ** – $p < 0.01$, **** – $p < 0.0001$.

a significant reduction in both E1A and hexon proteins, producing only ~15% and ~1%, respectively, of these proteins relative to vehicle treatment (figure 3.1B-D). Since HAdV gene expression was unaffected in cells treated with 0.5 μM but inhibited at 3.0 μM, despite both concentrations reducing metabolic activity to a similar extent (figure 3.1A), this suggests the effect of CBL0137 treatment is not due to general cytotoxic effects of the drug on cell health but, rather, due to more specific effects on virus function. Thus, these results show that CBL0137 is capable of significantly attenuating HAdV protein production at concentrations that are tolerated by the host cell.

3.4.2 Treatment with CBL0137 inhibits viral DNA replication and lowers viral yield

Given the key role of E1A proteins in promoting all subsequent aspects of HAdV gene expression and replication, the ability of CBL0137 to abrogate E1A protein expression suggests that genome replication is likely also affected by the drug. Therefore, we next assessed viral genome copy number within CBL0137-treated A549 cells. A549 cells were infected with HAdV-5 and, 1 hpi, treated with 3.0 μM of CBL0137. Total cellular DNA was isolated 8 and 24 hpi, with the 8 hpi timepoint representing a time prior to viral DNA replication in these cells, thus acting as a control to verify similar viral input. To assess viral genome copy number, quantitative PCR (qPCR) was performed using primers recognizing the *E1A* gene which was then normalized to cellular *GAPDH*. Treatment with CBL0137 had no effect on viral genome copy number at 8 hpi, indicating identical association or uptake of virus in vehicle- and CBL0137-treated cells (figure 3.2A). In vehicle-treated cells, we observed an ~460-fold increase in viral genome copy number between 8 and 24 hpi. In CBL0137-treated cells, we observed only an ~10-fold increase in

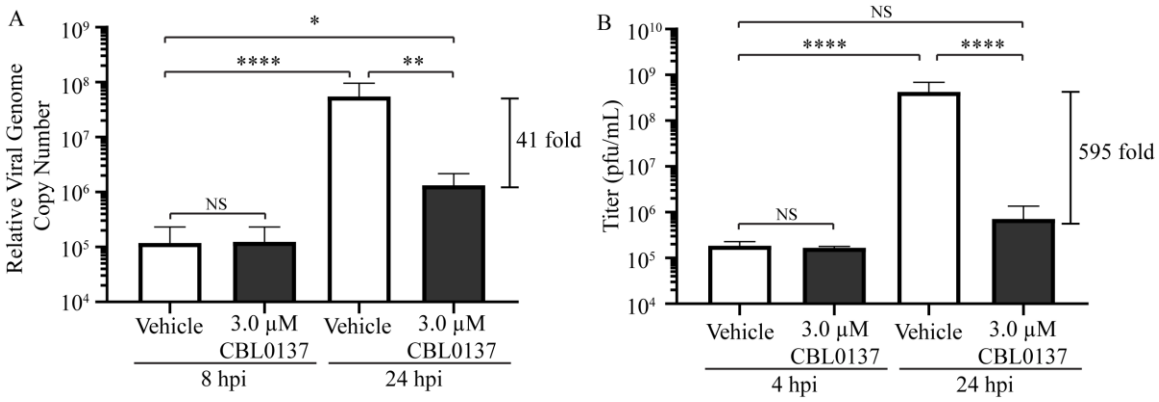

Figure 3.2. Treatment with CBL0137 inhibits viral DNA replication and lowers viral yield. Panel A: A549 cells were infected with HAdV-5 at an MOI 10, and 1 hpi, medium containing vehicle or 3 µM CBL0137 was added. Total DNA was isolated from the cells at 8 and 24 hpi by sodium dodecyl sulphate (SDS)-proteinase K digestion and phenol/chloroform extraction. The resulting DNA (200 ng) was subjected to qPCR to determine the relative average viral genome copy number, normalized to the average copy number of human *GAPDH*. Panel B: A549 cells were infected with HAdV-5 at an MOI of 10 for 1 h and overlaid with medium containing either vehicle or 3 µM CBL0137. The cells were harvested into the medium at 4 and 24 hpi, and the titer of recovered viruses was analyzed by plaque assay. For both panels, the mean of three experiments is shown, and the error bars represent standard deviation (SD) of the mean. Significance was calculated using a one-way ANOVA. NS – not significant, * – $p < 0.05$, ** – $p < 0.01$, **** – $p < 0.0001$.

genome copy number between 8 and 24 hpi, or 40-fold less viral genomes relative to vehicle treatment, indicating that treatment with CBL0137 significantly reduced HAdV genome accumulation within the cells. As expected, treatment of A549 cells with CBL0137 also reduced viral yield, as assessed by plaque assay (figure 3.2B). Indeed, virus recovery from CBL0137-treated cells was reduced ~600-fold relative to vehicle-treated cells, and was not significantly different from samples isolated at 4 hpi, suggesting that virus recovered at the 24 hpi time point may simply reflect residual virus from the applied inoculum. Taken together, these results indicate that treatment with CBL0137 reduced HAdV early gene expression, resulting in reduced viral DNA replication and late gene expression, ultimately preventing production of progeny virions.

3.4.3 CBL0137 inhibits E1A transcription through induction of degradation of the catalytic subunit of RNA polymerase II

Recently, Espinoza et al. (299) demonstrated that select DNA intercalating agents, including CBL0137, induce degradation of RNAP II, which suggests a mechanism by which CBL0137 may affect HAdV early gene expression. These DNA intercalators induce torsional stress in the DNA that impacts nuclear chromatin structure, resulting in a stalling of RNA transcription. The stalled RNA polymerase is then ubiquitinated, removed from the DNA, and degraded by the proteasome (299, 424-426). HAdV does not encode a viral RNA polymerase and relies on host RNAP II (427). We first determined whether treatment with 3.0 μM of CBL0137 induced degradation of RNAP II in uninfected A549 cells. A549 cells were treated with either vehicle or 3.0 μM of CBL0137, and protein lysates were harvested 0.5, 1, 2, 4, and 8 h post treatment, and we assessed the effect on RNAP II by

immunoblot. We used an antibody which recognizes both the unphosphorylated (IIa) and hyperphosphorylated (IIo) forms of POLR2A, the catalytic subunit of RNAP II. The IIa form of POLR2A provides a measure of free RNAP II, while the IIo form provides a measure of RNAP II that is bound to DNA (299, 428). CBL0137 treatment caused a time-dependent reduction of the total cellular level of POLR2A (figure 3.3A), with an initial half-life of approximately 1.25 h, though the rate of degradation slowed with the quantity of total POLR2A plateauing at ~15-20% between 4 and 8 h (figure 3.3B), consistent with observations in other cell types (299). Next, we assessed POLR2A protein levels following treatment with 3.0 μM of CBL0137 in both mock- and HAdV-5-infected cells that were harvested 8 and 24 hpi. For the 8 h timepoint, CBL0137 caused a reduction in both forms of POLR2A in both uninfected and infected cells (figure 3.3C). As we observed previously, there was reduced levels of E1A proteins in infected cells treated with CBL0137, relative to untreated or vehicle-treated cells. At 24 hpi, infection with HAdV-5 caused a modest accumulation of POLR2A form IIo in untreated and vehicle treated cells (figure 3.3D). As the POLR2A form IIo represents RNAP II bound to DNA, this suggests that transcription was more active in the infected cells relative to uninfected cells. Treatment of infected cells with CBL0137 caused a loss of form IIo, and a modest enrichment of POLR2A form IIa. As we observed previously, the quantity of hexon protein within the CBL0137-treated cells was greatly reduced relative to vehicle-treated cells. Interestingly, E1A proteins could be detected in CBL0137-treated cells at 24 hpi, although at a significantly reduced level compared to that observed in vehicle-treated cells (figure 3.3D). The presence of low quantities of E1A proteins at late times of infection in CBL0137-treated cells could reflect incomplete inhibition of HAdV gene expression by the drug or loss of efficacy of the drug

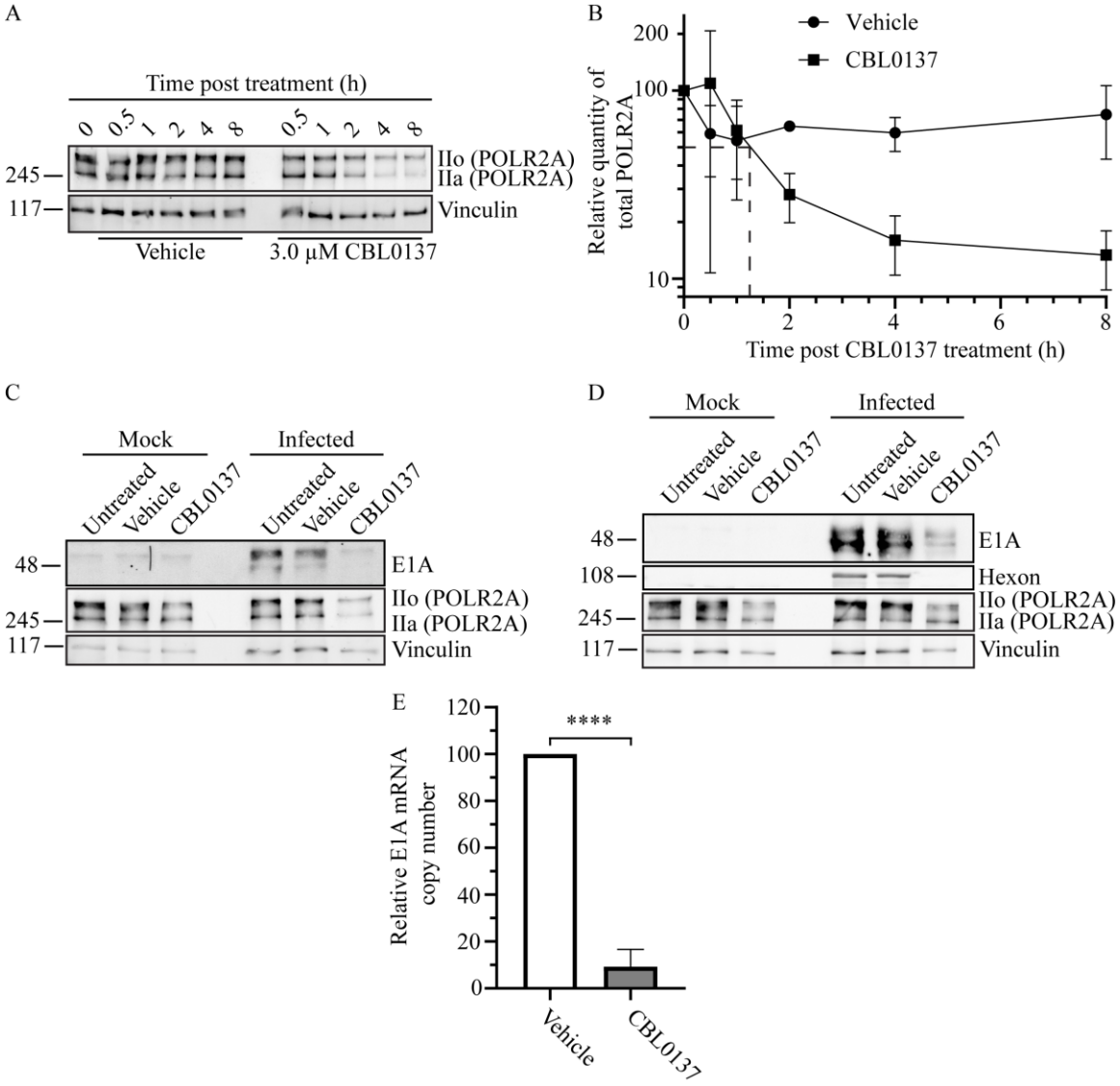
A
Time post treatment (h)
0
0.5
1
2
4
8
0.5
1
2
4
8
245
117
IIo (POLR2A)
IIa (POLR2A)
Vinculin
Vehicle
3.0 µM CBL0137
B
Vehicle
CBL0137
Relative quantity of total POLR2A
200
100
10
0
2
4
6
8
Time post CBL0137 treatment (h)
C
Mock
Infected
Untreated
Vehicle
CBL0137
Untreated
Vehicle
CBL0137
48
245
117
E1A
IIo (POLR2A)
IIa (POLR2A)
Vinculin
D
Mock
Infected
Untreated
Vehicle
CBL0137
Untreated
Vehicle
CBL0137
48
108
245
117
E1A
Hexon
IIo (POLR2A)
IIa (POLR2A)
Vinculin
E
Relative E1A mRNA copy number
120
100
80
60
40
20
0
****
Vehicle
CBL0137

Figure 3.3. CBL0137 inhibits *E1A* transcription through induction of degradation of the catalytic subunit of RNA polymerase II. Panel A: A549 cells were treated with vehicle or 3.0 μM CBL0137, and at 0.5, 1, 2, 4, and 8 h post treatment, medium was removed and the cells were harvested into PLB, and the quantity of POLR2A was determined by immunoblot analysis. Panel B: The signal intensity of total POLR2A from Panel A was quantified and normalized to the quantity of tubulin, and plotted relative to t = 0 h. Panel C and D: A549 cells were mock infected or infected with HAdV-5 at an MOI of 10, and medium containing varying concentrations of CBL0137 was added at 1 hpi. At 8 (Panel C) and 24 (Panel D) hpi, medium was removed and cells were harvested into PLB and the quantity of E1A, hexon, and POLR2A protein were determined by immunoblot analysis. Panel E: A549 cells were infected with HAdV-5 at an MOI of 10, and 1 hpi, medium containing 3.0 μM of CBL0137 was added. Total RNA was isolated at 8 hpi, and analyzed by qRT-PCR for relative *E1A* mRNA copy number, normalized to cellular *GAPDH*. For panels B and E, the mean of three experiments is shown, and the error bars represent standard deviation (SD) of the mean. Significance was calculated using a T-test. **** – $p < 0.0001$.

over time, possibly due to the natural half-life of the drug. CBL0137 is reported to have a half-life of ~6-24 h in plasma of pediatric and adult patients (429, 430). We also evaluated *E1A* mRNA copy number at 8 hpi following treatment with CBL1037. Consistent with a loss of RNAP II, treatment of cells with 3.0 μM CBL0137 reduced the quantity of *E1A* transcripts to ~10% of that observed in vehicle-treated cells (figure 3.3E). Thus, CBL0137 treatment induces an early loss of RNAP II, which prevents efficient expression of E1A, and likely other early proteins, ultimately compromising initiation of a productive infection.

3.4.4 CBL0137 treatment is required early in infection to inhibit HAdV replication

Since HAdV is reliant on cellular RNAP II for transcription of both early and late viral genes, we would predict that CBL0137 should directly inhibit late gene expression if the drug is applied solely during the late phase of the virus lifecycle. This would be a direct effect on late gene expression, rather than a ripple effect caused by lack of early gene expression. We therefore performed a time of addition experiment to evaluate the effect of CBL0137 on accumulation of early and late proteins within the cell. For the early time points, CBL0137 was added to medium at 1, 4 or 6 hpi, and samples were harvested and analyzed at 8 hpi (figure 3.4A). For the late time points, CBL0137 was added at varying time points between 1 and 12 hpi, and protein samples were harvested at 24 hpi (figure 3.4B). For samples harvested at 8 hpi, the quantity of E1A protein within the cells correlated with the time of drug addition, suggesting that CBL0137 was fairly effective at blocking early viral gene expression at the time that it was applied to the cells (figure 3.4A). Thus, no E1A proteins are present within the cells treated at 1 hpi, with progressively more

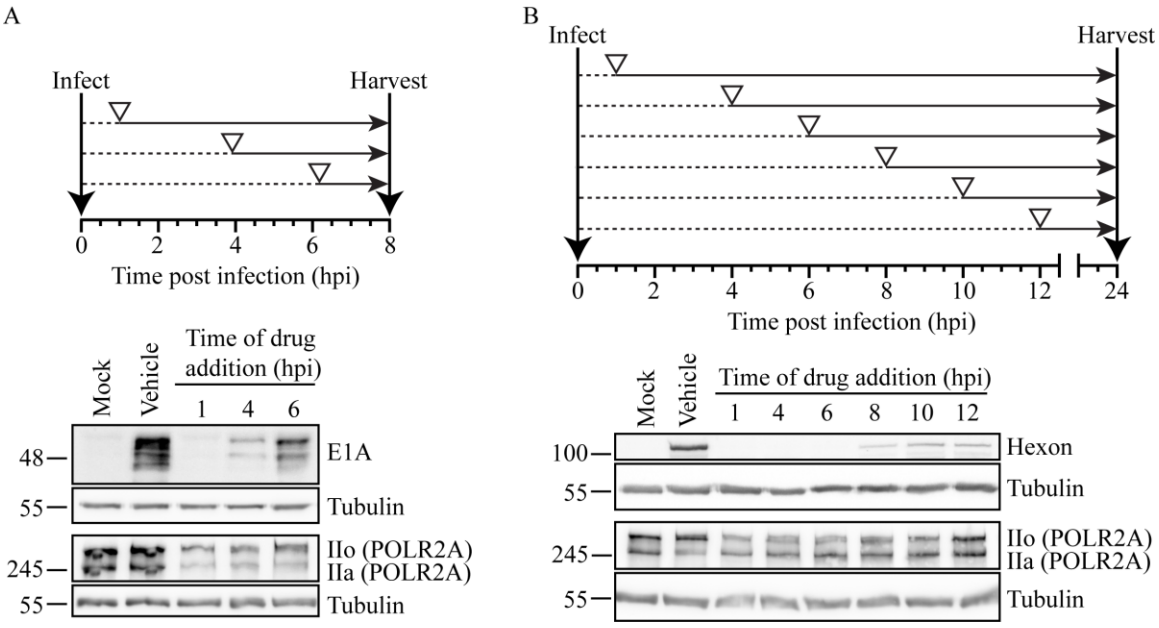

Figure 3.4. CBL0137 treatment is required early in infection to inhibit HAdV replication. A549 cells were infected with HAdV-5 at an MOI of 10 for 1 h, and medium containing 3.0 μM of CBL0137 was added at the indicated timepoints (open triangles). At 8 (Panel A) and 24 (Panel B) hpi, the cells were harvested into PLB, and the quantity of E1A (Panel A), hexon (Panel B), POLR2A and tubulin (Panels A and B) were analyzed by immunoblot assay.

E1A proteins present within the cells if infection is allowed to proceed for 4 or 6 h before drug is added, but all time points showed reduced levels of E1A proteins relative to vehicle-treated cells harvested at 8 hpi. We also observed a progressively increased quantity of POLR2A within the cells when the drug was added at 4 or 6 hpi, with more POLR2A present if the drug was added later. In A549 cells, HAdV late gene expression typically begins at 12 hpi (152, 390, 431). If CBL0137 was applied to the infected cells at 6 hpi or earlier, we did not observe any hexon protein at the 24 hpi time point (figure 3.4B), indicating a complete block of late gene expression. However, treatment of infected cells with CBL0137 at 8 hpi or later allowed for some expression of hexon protein at the 24 hpi time point. Thus, sufficient POLR2A activity was retained in cells treated with CBL0137 at 8 hpi or later to mediate hexon expression. Curiously, analysis of POLR2A protein levels within the treated cells showed that application of CBL0137 no longer induced degradation of the protein when applied at later time points, most notably at 12 hpi where the protein levels of POLR2A appeared identical to mock-treated cells. This was somewhat surprising, as we previously determined the half-life of POLR2A in CBL0137-treated cells was only 1.25 h (figure 3.3B). These data indicate that CBL0137 treatment is required during the early phase of infection to successfully inhibit HAdV replication, and also suggests that early viral gene expression may promote at least partial stabilization of POLR2A within the cells.

3.4.5 HAdV-5 early genes inhibit CBL0137-induced degradation of POLR2A protein

Chromatin damage caused by the DNA intercalator BMH-21 leads to degradation of POLR2A that is dependent on the activity of the ubiquitin-dependent protein segregase

p97, a Cullin-RING ubiquitin ligase and the proteasome (299). The specific Cullin-RING ubiquitin ligase family member involved in this process has not been determined. In response to DNA damage-dependent stalling, POLR2A is initially monoubiquitinated by NEDD4 and subsequently polyubiquitinated by Elongin A/B/C–CUL5–RBX2 or pVHL–Elongin B/C–CUL2–RBX1 E3 ligase complexes (424-426). For DNA damage-independent RNAP II stalling, POLR2A is instead polyubiquitinated solely by NEDD4 (432). In HAdV-infected cells, the viral proteins E1B-55K and E4orf6 are known to integrate with Elongin B/C, CUL5, and RBX1 to form an E3 ligase complex, which redirects the ubiquitin machinery to alternative substrates, ultimately degrading a selection of cellular proteins that would be refractory to the progression of infection, such as p53, Mre11, and RAD50 (63-65). The ability of E1B-55K/E4orf6 to alter ubiquitin-dependent protein degradation within the cell could be responsible for the observed RNAP II stabilization, or rather lack of degradation, in CBL0137-treated cells. As such, we examined whether expression of E1B-55K and E4orf6 were sufficient to block CBL0137-mediated RNAP II degradation. We transfected 293 cells (which endogenously express HAdV-5 E1A and E1B, including E1B-55K (416, 433)) with an expression plasmid encoding GFP-tagged E4orf6 (or GFP alone as a control) and, 24 h post transfection, the cells were treated with CBL0137, and harvested 8 h post drug treatment. We confirmed expression of both control GFP and our GFP-E4orf6 proteins in the transfected cells by immunofluorescence and immunoblot. Although a similar transfection efficiency was achieved (figure 3.5A), the quantity of GFP-E4orf6 was significantly reduced relative to GFP alone (figure 3.5B). We also observed a high molecular weight GFP-positive smear

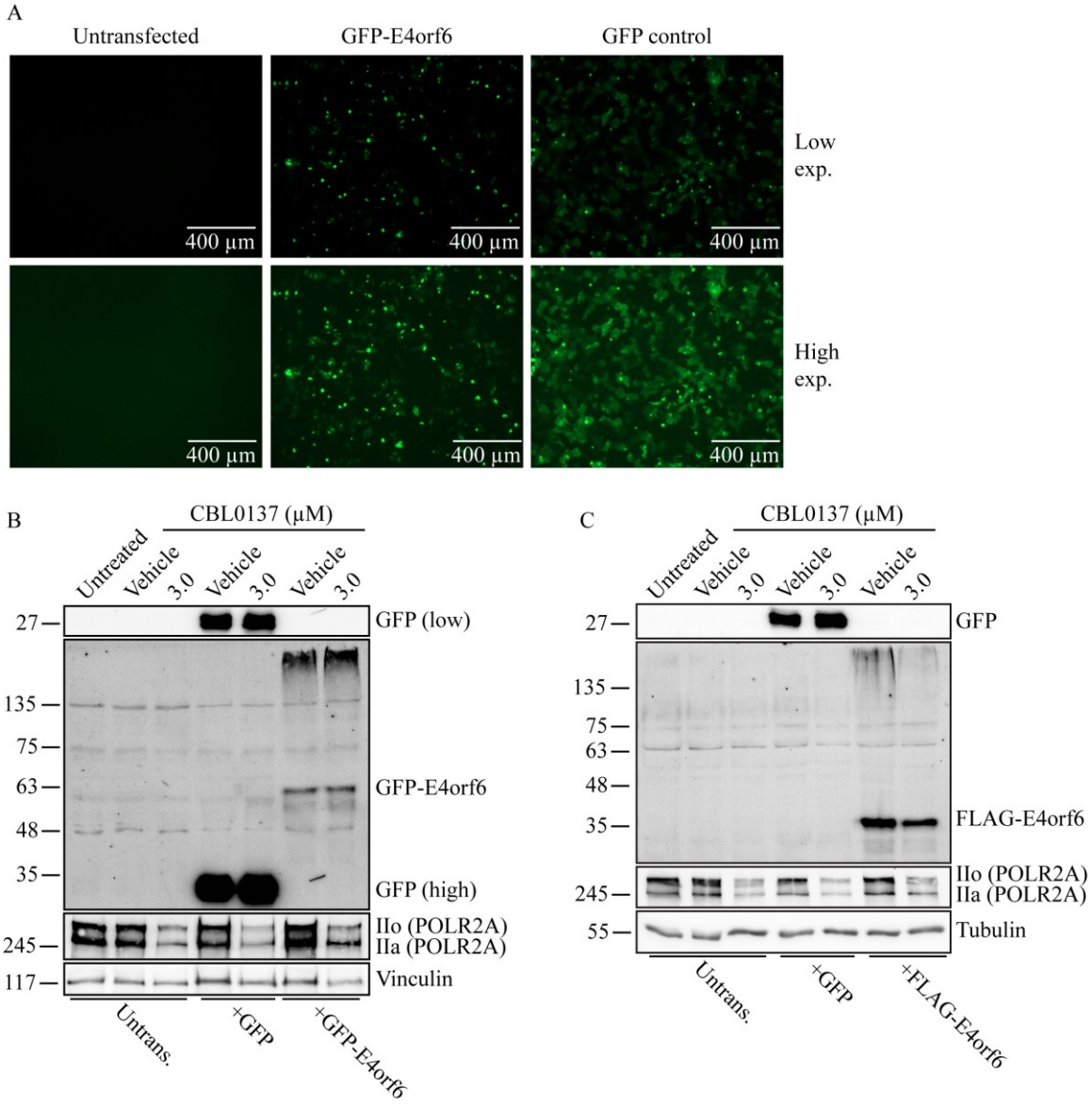
A
Untransfected
GFP-E4orf6
GFP control
Low exp.
High exp.
400 µm
B
CBL0137 (µM)
Untreated
Vehicle
3.0
Vehicle
3.0
Vehicle
3.0
27
135
75
63
48
35
245
117
GFP (low)
GFP-E4orf6
GFP (high)
IIo (POLR2A)
IIa (POLR2A)
Vinculin
Untrans.
+GFP
+GFP-E4orf6
C
CBL0137 (µM)
Untreated
Vehicle
3.0
Vehicle
3.0
Vehicle
3.0
27
135
75
63
48
35
245
55
GFP
FLAG-E4orf6
IIo (POLR2A)
IIa (POLR2A)
Tubulin
Untrans.
+GFP
+FLAG-E4orf6

Figure 3.5. HAdV-5 early genes inhibit CBL0137-induced degradation of POLR2A protein. 293 cells were transfected with pEGFP-C3 (GFP), pRP3512 (GFP-E4orf6) (Panels A and B), or pRP3516 (FLAG-E4orf6) (Panel C). Immunofluorescent microscopy of GFP signal was performed 24 h post-transfection to ensure similar transfection efficiency (Panel A). The cells were treated with CBL0137 at 24 h post transfection and protein samples collected after 8 h of treatment. Samples were analyzed by immunoblot assay for GFP (Panels B and C), FLAG (Panel C), and POLR2A (Panels B and C), with tubulin as a loading control.

from ~135 to 245 kDa only in GFP-E4orf6-transfected lanes (figure 3.5B), suggesting that the GFP-E4orf6 protein itself may be subjected to post-translational modification. This high molecular species was also observed for FLAG-tagged E4orf6 which lacks the GFP protein fusion (figure 3.5C), indicating that E4orf6 protein is indeed post-translationally modified when expressed in 293 cells. In untransfected and GFP-transfected cells, addition of 3.0 μM CBL0137 induced degradation of RNAP II (figure 3.5B, C). Expression of GFP-E4orf6 or FLAG-E4orf6 within the CBL0137-treated 293 cells partially rescued the cellular levels of POLR2A IIa, suggesting that E4orf6 may influence the stability/degradation of RNAP II in the CBL0137-treated cells. Thus, in our time of addition experiment, allowing early gene expression to proceed, before applying CBL0137, likely actively prevented CBL0137-induced degradation of RNAP II (figure 3.4D). Taken together, these results suggest that early expression of E1B-55K and E4orf6 from the viral genome may redirect ubiquitin/proteosome protein(s) to prevent CBL0137-induced degradation of RNAP II. Thus, these studies have identified the curaxin family of compounds as an effective class of anti-HAdV agents, but also highlight that HAdV encodes proteins that may impact the efficacy of the drug.

3.5 Discussion

While HAdV causes only minor illness in otherwise healthy patients, HAdV can cause significant morbidity and mortality in at-risk populations, such as the pediatric, geriatric, or immunocompromised individuals (20, 21, 434, 435). There are currently no approved therapeutics to safely treat HAdV infection (14). Our lab conducted previous studies to identify and evaluate compounds that can potentially be used to treat HAdV infection (152, 154, 162, 390). Repurposing drugs represents a very attractive avenue for treating viruses, as it has the potential to decrease the time needed from a discovery at the bench to an approved treatment. CBL0137 is currently under evaluation as an anti-cancer therapeutic (286, 287, 436), with data supporting *in vivo* use (286, 292, 300-307, 437). The promising results observed in preclinical models of cancer have led to a clinical trial evaluating the use of CBL0137 against several different cancer types in humans (NCT04870944). Furthermore, curaxins have already shown efficacy against several DNA and RNA viruses (288, 289, 292, 308, 309), and *in vivo* CBL0137 treatment protected mice against lethal HSV-1 infection (292). Thus, CBL0137 and other curaxins could show therapeutic efficacy against HAdV and be easily adopted for human use.

CBL0137 is a DNA intercalating agent that induces nucleosome unfolding thus causing chromatin damage (295). CBL0137-mediated alteration of chromatin has pleiotropic effects within the cell, including stabilization of p53, suppression of MYCN expression, suppression of NF-κB signaling, activation of NOTCH1 signaling, and trapping of the FACT complex on the unfolded nucleosomes (287, 296), as well as the downstream consequences of these effects. CBL0137 treatment also induces degradation of RNAP II and Z-DNA formation (299). We confirmed that RNAP II is degraded upon

treatment with 3.0 μM of CBL0137 in A549 cells (figure 3.3), which reduced *E1A* transcription and subsequently prevented progression of infection (figures 3.2-4). Interestingly, CBL0137-mediated degradation of RNAP II may have been counteracted by HAdV early gene expression, likely through action of E1B-55K and E4orf6 proteins (figure 3.5). E1B-55K and E4orf6 naturally function in concert with several cellular Cullin-RING E3 ligase complexes to promote degradation of several cellular proteins that would naturally be refractory to efficient virus replication (63-65). These viral proteins may function to redirect normal E3 ligase activity away from RNAP II. Alternatively, if CBL0137 is inducing RNAP II degradation using the DNA damage-independent NEDD4 polyubiquitination pathway (432), NEDD4 itself may be targeted for degradation by the viral E3 ligase, again leading to RNAP II stabilization. As such, CBL0137 may be expected to have reduced efficacy against a virus already undergoing replication, but would effectively block initiation of subsequent rounds of infection/replication, thus preventing spread of the virus within the host.

For both HSV-1 and HCMV, CBL0137 is believed to exert its antiviral effects through inhibition of the FACT complex. While CBL0137 does not directly bind to the FACT complex, CBL0137 establishes a chromatin state in which the FACT complex becomes trapped on destabilized nucleosomes (c-trapping), though the process is reversible following removal of CBL0137 from DNA (296, 297). For HSV-1 infection, the viral ICP22 protein interacts with the FACT complex to promote efficient transcription elongation of viral genes (291, 292), while the FACT complex is required by HCMV for transactivation of the viral MIEP (289). The FACT complex could also be required for efficient expression of HAdV early genes, but CBL0137-induced degradation of RNAP II

is a major insult within the cell, and precludes analysis of any specific role of FACT in modulating HAdV gene expression. Indeed, given the pleiotropic effects of CBL0137 treatment, it is possible that other cellular processes vital for productive infection may be negatively impacted by the drug, thus contributing to inhibition of infection of these viruses.

The ability of CBL0137 to stabilize p53 (286) could potentially explain our results, as HAdV normally antagonizes p53 to prevent cell cycle arrest and induction of apoptosis (52, 63). While we did observe stabilization of p53 following CBL0137 treatment in infected A549 cells, KD of the cell cycle inhibitor p21 did not rescue HAdV-5 replication following CBL0137 treatment (data not shown). We also examined CBL0137 treatment in HAdV-5 infected the p53-null H1299 cell line. Though CBL0137 treatment still inhibited HAdV-5 infection in H1299 cells, we later determined that CBL0137 was cytotoxic (data not shown), confounding our results. Though not definitive, our results therefore suggest that the effect of CBL0137 on HAdV-5 replication is independent of p53.

CBL0137 treatment has also been shown to induce an interferon response, restricting replication of ZIKV, IAV, and SARS-CoV-2 (288). However, when we examined the expression of IFNβ in CBL0137-treated, HAdV-5 infected-A549 cells, we observed that at CBL0137 concentrations capable of inhibiting HAdV-5, there was no corresponding increase in IFNβ expression (data not shown). This suggests, at least in A549 cells, that CBL0137-mediated induction of the interferon response does not contribute to the anti-HAdV-5 effect of CBL0137 treatment.

Our results also suggest that targeting RNAP II, at least transiently, could be an effective approach to treat HAdV infection. Other DNA intercalating agents, such as BMH-

21, aclarubicin, and actinomycin D, also induce degradation of RNAP II (299), suggesting these compounds may also impact HAdV infection. Actinomycin D is already approved for use in treating human cancer (438). Future studies will need to address the efficacy of these compounds in appropriate tissue culture and animal models of HAdV infection (439, 440).

In summary, we have shown that treatment with CBL0137 inhibits HAdV infection. Our work extends the observation that CBL0137 treatment can be used to inhibit infection of several dsDNA (289, 292) and RNA (288, 309) viruses. Given the success of CBL0137 in preclinical *in vivo* cancer (286, 437) and viral infection (292) models, CBL0137 could easily be repurposed to treat HAdV infection in at-risk individuals, thereby reducing the burden of disease in these patients.

3.6 Author contributions

A more detailed description of contributions of collaborators can be found at the end of the thesis.

Author contributions: Morgan R. Jennings: Conceptualization; Data curation; Formal analysis; Investigation; Methodology; Visualization; Funding acquisition; Writing - original draft; Writing - review & editing.

Robin J. Parks: Conceptualization; Formal analysis; Funding acquisition; Project administration; Resources; Supervision; Visualization; Writing - review & editing.

Funding: The research was supported by research funds R.J.P from the Canadian Institutes of Health Research (MOP-142316, PJT-178120) and the Natural Sciences and Engineering Research Council (RGPIN-2019-04786). M.R.J was supported by a Queen Elizabeth II Graduate Scholarship in Science and Technology from the Ontario Provincial Government (Canada). The funders had no role in study design, data collection and interpretation, or the decision to submit the work for publication.

Conflicts of Interest: The authors declare no conflict of interest.

3.7 Acknowledgements

We would like to thank Kathy Poulin for excellent technical assistance and guidance throughout this study. We also thank Drs. Heather Greenstone (NIH/NIAID) and Karoly Toth (Saint Louis University) for valuable discussion.

Chapter 4:

The FACT complex is Required for Optimal Human Adenoviral Replication

Morgan R. Jennings[1,2], Panayiotis O. Vacratsis[3] and Robin J. Parks[1,2,4,5,*]

[1]Regenerative Medicine Program, Ottawa Hospital Research Institute, Ottawa, Ontario, Canada,

[2]Department of Biochemistry, Microbiology and Immunology, University of Ottawa, Ottawa, Ontario, Canada

[3]Department of Chemistry and Biochemistry, University of Windsor, Windsor, Ontario, Canada, N9B 3P4

[4]Centre for Neuromuscular Disease, University of Ottawa, Ottawa, Ontario, Canada

[5]Department of Medicine, The Ottawa Hospital, Ottawa, Ontario, Canada

*Corresponding Author

4.1 Abstract

The facilitates chromatin transactions (FACT) complex, a heterodimer of SSRP1 and SUPT16H proteins, is a key cellular complex involved in cellular gene transcription initiation and elongation, DNA replication and DNA repair, due to its histone chaperone activity. The FACT complex has also been shown to have both pro- and anti-viral properties, depending on the virus. We therefore investigated whether the FACT complex was required for human adenovirus (HAdV) type 5 replication. Small interfering RNA-mediated knockdown of SSRP1 or SUPT16H reduced expression of early region 1A (E1A) proteins, due to a reduction of *E1A* transcripts within cells. Although E1A proteins and the FACT complex proteins showed partial overlap in the infected cell nucleus, as assessed by immunofluorescence analysis, the two proteins do not associate. We show that late in HAdV-5 infected cells, the FACT complex relocalizes from the nucleolus to viral replication centers, where the FACT complex proteins interact with the HAdV-encoded DNA-binding protein. Knockdown of the FACT complex also led to reduced accumulation of newly replicated genomes within infected cells, a subsequent reduction in late protein expression and reduced production of progeny virions. Taken together, these results indicate that the FACT complex is required for optimal HAdV-5 replication.

4.2 Introduction

Within the nucleus, cellular DNA is organized into chromatin, with nucleosomes serving as its fundamental unit. Nucleosomes consist of an octamer of histones (H2A, H2B, H3, and H4), around which DNA is wrapped. Post-translational modifications of the N-terminal of histones tails play a vital role in gene expression and regulation, helping determine the "openness" and "compactness" of chromatin, or regions of active and repressive gene expression, respectively (133, 134). Indeed, epigenetic regulation is vital in establishing global gene regulation within the cell and, consequently, determining cell identity (140). Epigenetic regulation is also important for many nuclear viruses (reviewed in (141-143)), which frequently exploit the cellular epigenetic machinery to regulate expression of viral genes, as well as to modulate host cellular gene expression to promote expression of genes that support productive infection and inhibit genes that are refractory to viral replication. For human adenovirus (HAdV), the viral DNA is dynamically remodeled throughout the course of infection (98), and becomes associated with histones and wrapped in repeating nucleosome-like structures early in infection, prior to initiation of expression of early viral genes (128). Thus, HAdV likely utilizes cellular epigenetic regulatory proteins to support viral gene expression and replication. Indeed, work by our lab and others has demonstrated that compounds that modulate the activity of epigenetic regulatory proteins can impact HAdV infection (152-155, 441), suggesting that epigenetic regulation is critical during HAdV infection.

While nucleosomes are vital for epigenetic regulation of genes, nucleosomes can also represent a physical obstacle for gene transcription initiation and transcription elongation (194). Additional chromatin remodeling proteins are typically required to

modify, shift or evict nucleosomes from promoter regions to provide access for transcription factors to bind to the DNA, as well as to allow the passage of RNA polymerase II (RNAP II) through the nucleosome-bound DNA. One such factor is the facilitates chromatin transactions (FACT) complex which, in humans, is composed of two proteins, SUPT16H and SSRP1 (208). The FACT complex is perhaps best known for its role in transcription elongation (200), and is thought to destabilize the nucleosomal structure through removal of one H2A/H2B dimer from the nucleosome during passage of the RNAP II enzyme and replacing the dimer after the polymerase has passed (202, 225, 226). However, the FACT complex has also been implicated in several other processes within the cell, including transcription initiation (227), DNA replication (198, 199), and DNA repair (200, 201). Homozygous knockout of SUPT16H (219) or SSRP1 (218) is lethal to early mouse embryos, clearly indicating that the FACT complex has a crucial role(s) within the cell.

Previous studies have shown that the FACT complex can be either a pro-viral or an anti-viral factor of both RNA and DNA viruses, depending on the virus and specific context. Work by Rex et. al. (282) demonstrated that the FACT complex is involved in an antiviral response that appears to have evolved prior to the interferon response. Termed the FACT-ETS-1 Antiviral Response (FEAR) pathway, activation of this pathway results in enhanced expression of the ETS-1 transcription factor, which ultimately induces virus restriction programs within the cell. Although the FEAR pathway is induced by vaccinia virus, the virus-encoded A51R protein antagonizes the response and blocks FACT-mediated expression of ETS-1. The FEAR pathway also inhibits vesicular stomatitis virus, influenza A virus (IAV), and yellow fever virus replication, as knockdown (KD) of

SUPT16H was sufficient to increase the quantity of virus produced in the cell (282). For human immunodeficiency virus 1 (HIV-1) and human T-lymphotropic virus type 1 infections, the FACT complex suppressed viral transcription, possibly acting as a pro-latency factor (283) and, consistent with this, the FACT complex also repressed murine endogenous retrovirus-L (MERVL) gene expression (231). However, paradoxically, Lopez et. al. (284) found that the FACT complex is required for expression driven by the long terminal repeat during HIV-1 infection, but is not required for integration of the reverse transcribed viral DNA, suggesting the FACT complex may have a dual role during HIV-1 infection. By contrast, the avian leukosis virus, another retrovirus, required the FACT complex for integration of viral DNA (285). The FACT complex also appears to regulate the interferon response, through interaction with BRD4, a regulator of interferon signaling (442). KD of SUPT16H or treatment with the curaxin CBL0137, a drug that can inhibit the FACT complex (286, 287), increased interferon activity, which ultimately inhibited replication of zika virus, IAV, and severe acute respiratory syndrome coronavirus 2 (288). However, it should be noted that IAV replication was inhibited specifically by CBL0137 treatment, suggesting that additional effects of CBL0137-treatment may contribute to the observed antiviral effect, since KD of SUPT16H actually promoted IAV replication (282). Kaposi's sarcoma-associated herpesvirus requires the FACT complex for latency-associated nuclear antigen dependent DNA replication (290). During herpes simplex virus 1 (HSV-1) infection, the viral ICP22 protein recruits the FACT complex to the viral genome to promote efficient transcription elongation of viral genes (282, 291). Infection with an ICP22 mutant unable to bind FACT led to stalling of RNAP II near the transcription start sites on the viral genome, suggesting inefficient transcription elongation. Human

cytomegalovirus (HCMV) also requires the FACT complex for viral reactivation, as treatment with CBL0137 prevented the FACT complex from binding to and transactivating the major immediate early promoter, thereby inhibiting viral reactivation (289).

Unpublished work by our lab also demonstrated that treatment with CBL0137 is capable of inhibiting HAdV-5 infection, but this effect was attributed to CBL0137-induced degradation of RNA polymerase II (RNAP II) (299), which precluded us from determining any specific role for the FACT complex in HAdV-5 infection. In this study, we evaluated the role of the FACT complex in HAdV-5 infection directly using small interfering RNA (siRNA)-mediated KD of SUPT16H and/or SSRP1, and show that the FACT complex is required for optimal HAdV-5 replication.

4.3 Materials and Methods

4.3.1 Cell lines, Viruses, Transfections and Reagents

Experiments were conducted in the human lung adenocarcinoma-derived A549 cell line (CCL-185, American Type Culture Collection (ATCC), Manassas, VA, USA). Cells were cultured in Minimum Essential Medium (MEM, Sigma Aldrich, Oakville, ON, Canada) containing 10% (v/v) Fetal Bovine Serum (FBS, Sigma Aldrich), 2 mM GlutaMAX (35050061, Gibco, Ottawa, ON, Canada), and 1x antibiotic-antimycotic (15240062, Gibco).

HAdV-5 was obtained from Dr. John Bell (Ottawa Hospital Research Institute, Ottawa, Canada). AdDBP^{FLAG} (lab designation AdRP3122) has been described previously (404), and is an E1+ and E3-deleted virus encoding a FLAG-tagged DNA-binding protein (DBP). AdPVII^{FLAG} (AdCC100) is an E1+ and E3-deleted virus encoding a FLAG-tagged protein VII, and was constructed in a similar manner as previously described (126, 127). All viruses were grown in 293N3S cells (417) and titered on 293 cells (416), both a kind gift from Dr. Frank Graham (Professor Emeritus, McMaster University). All viruses were purified by cesium chloride buoyant density centrifugation, as described previously (418). For viral infections, medium was removed from confluent monolayers of cells prior to infection with HAdV in a minimum volume. The multiplicity of infection (MOI) was calculated as plaque-forming units (PFU) per cell. Unless noted otherwise, infections were performed at an MOI of 10. Virus inoculums were diluted in phosphate-buffered saline (PBS, D8537-500ML, Sigma Aldrich), and added to the cells for 1 hour (h) at 37 °C with periodic rocking. The cells were subsequently washed with PBS to remove unbound virus and fresh medium was added to the cells. The infected cells were incubated in a humidified

CO_2 incubator at 37 °C until the indicated time points. All time points are relative to the initial addition of the virus inoculum to the cells, which is considered t=0 h post infection (hpi).

To generate pMJ102, which encodes FLAG-tagged DBP driven by the human cytomegalovirus (HCMV) immediate early enhancer/promoter and contains ampicillin and neomycin resistance genes, viral DNA obtained from $AdDBP^{FLAG}$ was PCR amplified using the following primers: 5'- ATA GAA TTC GCC ACC ATG GCC AGT CG and 5' – ATA GCG GCC GCG CCG TTT AA. The resulting DNA product was digested with EcoRI and NotI, and cloned into EcoRI and NotI digested pcDNA3.1. The plasmid integrity was verified by sequencing, and the plasmid was purified by cesium chloride buoyant density centrifugation using standard methods.

Pooled small interfering RNA (siRNA) targeting human SUPT16H (M-009517-00-0005) and SSRP1 (M-011783-01-0005), and siGenome non-targeting control siRNA (D-001206-13-05) were obtained from Horizon Discovery (Lafayette, CO, USA). A549 cells were seeded in 12-well ($0.5x10^5$ cells/well) or 6-well ($3.2x10^5$ cells/well) plates and transfected with 100 nM total siRNA using Lipofectamine 2000 (11668019, Invitrogen, Ottawa, ON, CA) according to the manufacturer's instructions for A549 cells. Single KDs were performed using 50 nM siRNA targeting SUPT16H or SSRP1 along with 50 nM non-targeting control siRNA to a final concentration of 100 nM, while double KDs targeting both SUPT16H and SSRP1 used 50 nM siRNA each for a final concentration of 100 nM. The transfection medium was removed after 4 h, the cells were rinsed with PBS, and complete medium was added. KD was confirmed at 72 h post-transfection by immunoblot analysis, and the cells were infected at this point, as described above.

4.3.2 Immunoblot Analysis

At the indicated timepoints, medium was removed, and the cells were lysed in 2x Laemmli buffer (62.5 mM Tris-HCl pH 6.8, 25% *w/v* glycerol, 2% *w/v* sodium dodecyl sulphate (SDS), 0.01% *w/v* bromophenol blue, 5% v/v β-mercaptoethanol (added immediately prior to use)), and stored at −20 °C. The samples were boiled for 5 min prior to protein separation by sodium dodecyl sulphate-polyacrylamide gel electrophoresis (SDS-PAGE). Separated proteins were transferred to an Immobilon-FL PVDF membrane (IPFL00010, Sigma Aldrich), and the membrane was blocked with Intercept Blocking Buffer (927-70001, Li-Cor Biosciences, Lincoln, NE, USA). The following primary antibodies were used: anti-Adenovirus Type 5 (M58) (E1A, 1/5,000 for overnight (O/N) incubation; MA513643, Thermo Fisher Scientific), Anti-Adenovirus Type 5 E1A (1/2,000 for O/N incubation; 554155, BD Biosciences, Mississauga, CA), Anti-Adenovirus Type 5 (recognizes all capsid proteins, including hexon, 1/10,000 for 1 h incubation; ab6982, Abcam, Toronto, ON, Canada), anti-SUPT16H (1/5,000 for O/N incubation; ab204343, Abcam), anti-SSRP1 (1/5,000 for O/N incubation; 15696-1-AP, Proteintech, Rosemont, IL, USA), mouse anti-tubulin (1/10,000 for 1 h incubation; CP06, Sigma Aldrich), rabbit anti-tubulin (1/10,000 for 1 h incubation; ab59680, Abcam). The primary antibodies were diluted in Intercept Blocking Buffer containing 0.2% Tween 20. The membrane was then washed three times in PBS (10 mM Na_2HPO_4, 1.8 mM KH_2PO_4, 2.7 mM KCl, 137 mM NaCl, pH 7.4) containing 0.1% Tween 20 (PBST) and incubated with the appropriate IRDye secondary antibodies (680RD and 800CW, Li-Cor Biosciences), diluted in Intercept Blocking Buffer containing 0.2% Tween 20 and 0.01% SDS, again protected from light. The membrane was washed three times in PBST, followed by a final rinse with PBS.

Membranes were scanned using a ChemiDoc MP imaging system (Bio-Rad, Mississauga, ON, Canada), and the resulting signal analyzed using Image Lab (version 6.1, Bio-Rad). All immunoblot data are representative of three or more independent experiments.

4.3.3 MTS Metabolic Activity Assay

96-well plates were seeded with 5,000 A549 cells per well and incubated O/N. The next day, the cells were transfected with siRNA targeting SSRP1 or non-targeting control, as described above. The cells were incubated in medium without serum, containing 2mM GlutaMAX and 1x antibiotic-antimycotic. Three days later, the medium was removed from the wells and fresh medium containing serum was added, and incubated for 24 h. Metabolic activity was determined using the CellTiter 96 Aqueous Non-Radioactive Cell Proliferation Assay (Promega, Madison, WI, USA) according to the manufacturer's instructions. Briefly, cells were incubated for 1 h at 37 °C with 20 µL of the 3-(4,5-dimethylthiazol-2-yl)-5-(3-carboxymethoxyphenyl)-2-(4-sulfophenyl)-2H-tetrazolium (MTS) substrate, and absorbance readings were obtained at 490 nm using the SpectraMax 190 plate spectrophotometer (Molecular Devices, San Jose, CA, USA). Wells containing no cells were used as a negative control.

4.3.4 Polymerase Chain Reaction

To determine if KD of SUPT16H or SSRP1 affected HAdV-5 DNA replication, we determined the viral genome copy number in infected cells by quantitative PCR. Three days post KD, A549 cells were infected as described above. At the indicated time points, medium was removed, and the cells were harvested using SDS-proteinase K (10 mM Tris-

HCl pH 7.4, 10 mM EDTA, 1% *w/v* SDS, 1 mg/mL proteinase K (P8044-5G, Sigma Aldrich)) and incubated O/N at 37°C. DNA was extracted from the cell lysates using a standard phenol-chloroform method, precipitated with isopropanol and NaCl, and the resulting DNA pellet was dissolved in TE (10 mM Tris-HCl pH 8.0, 1 mM EDTA). qPCR was performed using 200 ng of genomic DNA per reaction. The following primers were used: 5'-CTC CCC ACA CAC ATG CAC TTA and 5'-CCT AGT CCC AGG GCT TTG ATT for human glyceraldehyde-3-phosphate dehydrogenase (*GAPDH*); 5'-CCA TTA AAC CAG TTG CCG TGA GAG and 5'-GGC GTT TAC AGC TCA AGT CCA AAG for HAdV *E1A*. Viral genome copy number were calculated from the Ct values using a standard curve obtained from serial dilutions of pCB6, a plasmid containing the entire HAdV-5 genome. Values were normalized using *GAPDH* copy number, calculated from a standard curve obtained using serial dilutions of a plasmid containing a cloned fragment of the human *GAPDH* gene, pMJ100, as described previously (162).

To determine whether FACT KD affected production and accumulation of viral *E1A* transcripts, we determined *E1A* mRNA copy number from infected cells. Three days after KD, A549 cells were infected as described above and, at the indicated time points, medium was removed, and cell lysates were obtained using TRIzol (15596026, Invitrogen). Total RNA was extracted from the cell lysates using the PureLink RNA Mini Kit columns (12183018A, Invitrogen), according to the manufacturer's instructions. The isolated RNA was then treated with the DNA-*free* DNA removal kit (AM1906, Invitrogen). The resulting RNA was reverse transcribed into complementary DNA (cDNA) using the High Capacity cDNA Reverse Transcription kit (4368814, Invitrogen). qPCR was performed using 1 μL of the cDNA per reaction. The following primers were used: 5'-ACA ACT TTG GTA TCG

TGG AAG G and 5’- GCC ATC ACG CCA CAG TTT C for human *GAPDH*; 5’- TCC GGT CCT TCT AAC ACA CC and 5’-GGC GTT TAC AGC TCA AGT CC for HAdV-5 *E1A*. *E1A* mRNA copy number were calculated from the Ct values using a standard curve obtained using serial dilutions of pCB6. Values were normalized using *GAPDH* mRNA copy number, calculated from a standard curve obtained using serial dilutions of a bacterial plasmid containing a cloned fragment of human *GAPDH* cDNA, pMJ111. To generate pMJ111, a 105 bp fragment of the human *GAPDH* cDNA (generated using PCR primers 5’-ACA ACT TTG GTA TCG TGG AAG G and 5’- GCC ATC ACG CCA CAG TTT C) was cloned into SmaI-digested pBlueScript II KS (+), verified by sequencing, and purified by cesium chloride buoyant density centrifugation using standard methods. To quantify the relative abundance of each *E1A* isoform following FACT KD, we performed PCR using the following primers: 5’-ATT ATC TGC CAC GGA GGT GT-3’ and 5’-GGA TAG CAG GCG CCA TTT TA-3’ (443). Amplicons were resolved on 2% agarose gels and the image was captured using the ChemiDoc imaging system.

4.3.5 Plaque Assay for Virus Yield

To examine the effect of FACT KD on virus yield, we performed a plaque assay of virus recovered from treated A549 cells. Briefly, 3 days after KD, monolayers of A549 cells were infected with HAdV-5 at an MOI of 10. After 1 h of infection, the virus inoculum was removed, the cells were washed once with PBS to remove unbound virus, and fresh medium was added. At 4, 18, 21, and 24 hpi, the cells were collected by scraping into the medium, 40% *w/v* sucrose (prepared in 10 mM Tris pH 8.0) was added to a final concentration of 4% *w/v*, and the samples were lysed by three freeze/thaw cycles. For the

plaque assay, monolayers of A549 cells were infected with dilutions of the cell lysates. After 1 h of infection, the cells were overlaid with medium containing agarose (50% *v/v* of a 1% *w/v* agarose solution, 43% clear 2x MEM (11935046, Gibco), 5% FBS, 1% GlutaMAX, and 1% antibiotic-antimycotic). Plaques were counted 10 days later.

4.3.6 Immunofluorescence

A549 cells ($4x10^4$ cells) were seeded onto 1 cm round coverslips in 12-well tissue-culture plates and, the next day, infected with $AdDBP^{FLAG}$. At the indicated timepoints, medium was removed and the cells were rinsed with cold PBS. Cells were fixed using 4% paraformaldehyde (pH 7.0) in PBS for 10 minutes (min), then rinsed 3 times with cold PBS. Cells were permeabilized using 0.25% Triton X-100 (X100-100ML, Sigma Aldrich) in PBS for 10 min, followed by 3 rinses in PBS, 5 min each. Coverslips were incubated in 5% donkey serum (DS, S30-100ML, Sigma Aldrich) in PBS for 30 min to block nonspecific antibody binding. Coverslips were incubated in 5% DS in PBS containing the following primary antibodies: anti-SUPT16H (1/1,500, 28598-1-AP, Proteintech), anti-SSRP1 (1/1,000), anti-FLAG (1/1,000, F1804, Sigma Aldrich) O/N at 4°C, or for 1 h at 21°C with anti-nucleolin (1/1,000, MAB1277-I-25UG, Sigma Aldrich). The coverslips were then rinsed 3 times with PBS. Coverslips were incubated 1 h protected from light in 5% DS in PBS containing the following secondary antibodies: Alexa Fluor 594 anti-rabbit IgG (1/1,000; A21207, Invitrogen), Alexa Fluor 488 anti-rabbit IgG (1/1,000; A21206, Invitrogen), Alexa Fluor 594 anti-mouse IgG (1/1,000; A21203, Invitrogen), and Alexa Fluor 488 anti-mouse IgG (1/1,000; A21202, Invitrogen). After secondary antibody removal and 6 washes in PBS, 5 min each, the coverslips were incubated with Hoechst

3342 (1 µg/ml in PBS, H3570, Life Technologies, Burlington, ON, CA) for 1 min. Lastly, the coverslips were rinsed with PBS and placed on glass slides using Dako Fluorescent Mounting Medium (Agilent Technologies, Santa Clara, CA, USA). Fluorescent images were obtained with a Plan-APOCHROMAT 63x/1.4 oil-immersion Ph3 objective on a Zeiss Axio Imager.M1 microscope equipped with an AxioCam HRm camera and captured using AxioVision software (version 4.9.1, Carl Zeiss Microscopy LLC, White Plains, NY, USA), and images were processed using FIJI (version 2.14.0 (419)).

4.3.7 Nuclear Fractionation and Co-immunoprecipitation

To evaluate protein associations, A549 cells were seeded onto 10-cm dishes ($4.0x10^6$ cells). The next day, the cells were infected with appropriate virus, as described above. At the indicated timepoints, medium was removed, and the cells were rinsed in cold PBS. The cells were scraped from the plate and transferred to a new tube. The cells were rinsed 3-times with cold PBS, with cells pelleted between washes by centrifugation at 3000xg for 5 min at 4°C. All subsequent steps were performed on ice using cold reagents. The PBS was discarded, the cells were resuspended in 500 µL hypotonic buffer (20 mM Tris pH 7.4, 10 mM NaCl, 3 mM $MgCl_2$), and incubated for 15 min. Next, 25 µL of 10% Nonidet P40 substitute (Biolynx, Brockville, ON, CA) was added, and the tube was vortexed for 10 seconds (s) at maximum speed to lyse the cells, and the nuclei were pelleted by centrifugation (845xg for 10 min at 4°C). The supernatant (cytoplasmic fraction) was discarded, while the nuclei were resuspended in a volume equivalent to the packed nuclei (approximately 50 µL) with nuclear resuspension buffer (50 mM HEPES pH 7.6, 300 mM NaCl, 1 mM EDTA, 0.5 mM dithiothreitol (DTT), with 1x protease inhibitor tablet, 10 mM

β-glycerophosphate (BGP), and 200 μM phenylmethylsulfonylfluoride (PMSF) added prior to use). Nuclei were flash frozen, and thawed on ice to lyse the nuclei. Once thawed, the solution was clarified by centrifugation (15,000xg for 20 min at 4°C), and the resulting supernatant (nuclear lysate) was transferred to a new tube and brought up to 200 μL with pulldown buffer (PD buffer, 50 mM HEPES pH 7.6, 150 nM NaCl, 1mM EDTA, 0.5mM DTT, with 1x protease inhibitor tablet, 10 mM BGP, and 200 μM PMSF added prior to use).

A bead slurry was prepared by washing 300 μL of unconjugated protein G Dynabeads (10004D, Invitrogen) in 1 mL PD buffer 3 times, and resuspended in 300 μL of PD buffer. An aliquot (40 μL) of the nuclear lysate was reserved as input. The remaining nuclear lysate was brought up to 400 μL with PD buffer, and 40 μL of the bead slurry was added to the tube, which was then placed on a rotating platform for 1.5 h at 4°C, to eliminate proteins that non-specifically bound to the beads. After preclearing, the supernatant was divided into 5 tubes, each of which was brought to 400 μL with PD buffer. Each tube received 10 μg of antibody targeting mouse FLAG (F1804, Millipore, Burlington, MA, USA), SUPT16H (20551-1-AP), or SSRP1 (15696-1-AP) as indicated, while the remaining tubes received 10 μg of IgG of the appropriate species. The tubes were incubated on a rotating platform at 4°C O/N.

The next day, 40 μL of the prepared bead slurry was added to each tube and placed back on the rotating platform for 2 h at 4°C to conjugate the antibody complexes to the beads. The supernatant, containing the unbound, flowthrough proteins, was transferred to a new tube and combined with 5x Laemmli buffer (156.25 mM Tris-HCl pH 6.8, 62.5% v/v glycerol, 5% w/v sodium dodecyl sulphate (SDS), 0.01% w/v bromophenol blue,

12.5% v/v β-mercaptoethanol). The beads were washed 3 times in pulldown wash buffer (50 mM HEPES pH 7.6, 150 nM NaCl, 1mM EDTA, 0.5mM DTT, 0.1% Nonidet P40 substitute, with 1x protease inhibitor tablet, 10 mM BGP, and 200 μM PMSF added prior to use), before being resuspended in 40 μL of 2x Laemmli buffer (62.5 mM Tris-HCl pH 6.8, 25% v/v glycerol, 2% w/v sodium dodecyl sulphate (SDS), 0.01% w/v bromophenol blue, 5% v/v β-mercaptoethanol). After processing, all samples were stored at -20°C.

To confirm that the protein associations were due to direct binding, and not due to independent binding of the two proteins to the same DNA molecule, the nuclear lysates were pretreated with DNase I prior to incubation with antibody. $MgCl_2$ (final 5 mM) and $CaCl_2$ (final 0.5 mM) were added to the nuclear lysates, and 1 μL of DNase I (10 mg/mL) was added, and incubated O/N at 4°C. The next day, appropriate antibody was added and the lysates were processed for co-immunoprecipitation (co-IP) as described above.

4.3.8 Statistical Analysis

Statistical analysis was performed by using GraphPad Prism8 software (version 8, GraphPad Software Inc., San Diego, CA, USA). Statistical significance was determined using one-way ANOVA or multiple T-tests, as indicated in each figure legend. Differences with $p \leq 0.05$ were considered significant.

4.4 Results

4.4.1 Knockdown of SUPT16H and SSRP1 lowers expression of E1A proteins in infected cells

We first assessed whether the FACT complex was required for expression of HAdV early genes, focusing on early region 1A (*E1A*), the first region expressed from the viral genome and which encodes proteins crucial for regulating many aspects of the virus lifecycle (55, 444, 445). A549 cells were transfected with siRNA targeting SUPT16H and/or SSRP1, or non-targeting control. Seventy-two hours (h) post-transfection, the cells were infected with HAdV-5, and protein lysates were harvested at 8 hpi, indicative of the early phase of infection. The FACT complex has an unusual mode of self-regulation whereby SUPT16H and SSRP1 mRNA associate with the FACT complex itself. This interaction is required not only for stability of the FACT complex proteins but, in the absence of this interaction, SUPT16H and SSRP1 mRNA becomes unstable and are less efficiently translated (208). As a consequence, KD of one member of the FACT complex directly impacts the protein levels of the other member of the complex (208). We confirmed KD of SUPT16H and SSRP1 and, as anticipated, KD of one protein was sufficient to lower the quantity of the other protein (figure 4.1A). Treatment of infected cells with non-targeting siRNA had no effect on the levels of E1A proteins, whereas siRNA-mediated KD of SUPT16H, SSRP1, or both reduced the quantity of E1A proteins present within the cells (figure 4.1B, C), suggesting that the FACT complex is required for optimal *E1A* expression. We confirmed that treatment of the cells with siRNA to the SUPT16H, SSRP1, or both, did not significantly impact cell metabolic activity (figure 4.1D), indicating that reduced expression of E1A was not simply due to reduced cell bioenergetics. Taken

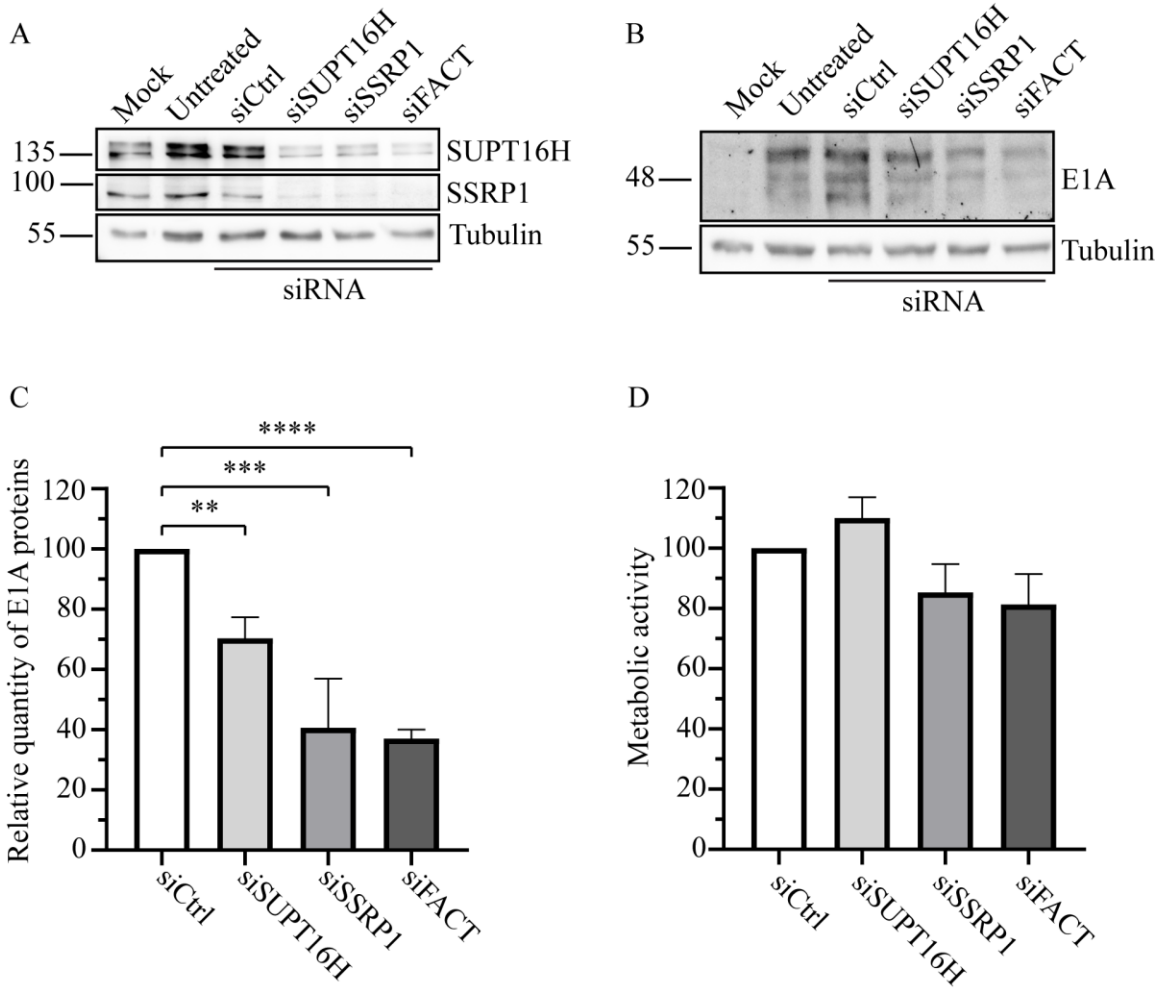
A
Mock
Untreated
siCtrl
siSUPT16H
siSSRP1
siFACT
135
100
55
SUPT16H
SSRP1
Tubulin
siRNA
B
Mock
Untreated
siCtrl
siSUPT16H
siSSRP1
siFACT
48
55
E1A
Tubulin
siRNA
C
Relative quantity of E1A proteins
****
***
**
120
100
80
60
40
20
0
siCtrl
siSUPT16H
siSSRP1
siFACT
D
Metabolic activity
120
100
80
60
40
20
0
siCtrl
siSUPT16H
siSSRP1
siFACT

Figure 4.1. Knockdown of SUPT16H and SSRP1 lowers expression of E1A proteins in infected cells. Panels A-C: A549 cells were transfected with siRNA targeting SUPT16H, and/or SSRP1, or non-targeting control. Seventy-two hours post-transfection, the cells were infected with HAdV-5 at an MOI of 10. At 8 hpi, medium was removed and cells were harvested using protein loading buffer. The quantity of SUPT16H and SSRP1 (A), and E1A (B) were analyzed by immunoblot using the ChemiDoc MP imaging system, and the relative quantity of E1A proteins, normalized to tubulin protein signal, was calculated (C). Panel D: A549 cells were transfected with siRNA targeting SUPT16H, and/or SSRP1, or non-targeting control. Seventy-two hours post-transfection, fresh medium was added, and 24 h later, the MTS solution was added to each well, and placed in the incubator for 1 h. The absorbance of each well was measured, and metabolic activity was calculated, relative to non-targeting control. The mean of three independent experiments is shown, and the error bars represent standard deviation (SD) of the mean. Significance was calculated by one-way ANOVA. ** – $p < 0.01$, *** – $p < 0.001$, **** – $p < 0.0001$.

together, these results indicate that the FACT complex is required for optimal *E1A* expression. Since KD of one member of the FACT complex was sufficient to reduce both proteins, for subsequent experiments we only performed KD of SSRP1 alone.

4.4.2 Knockdown of SSRP1 reduces E1A transcript accumulation

The FACT complex is well known for its role in transcription initiation and elongation (200, 227). Thus, the reduction in the quantity of E1A protein following FACT complex KD could be due to less efficient *E1A* transcription, resulting in fewer *E1A* mRNA transcripts. As such, we next examined the effect of SSRP1 KD on *E1A* mRNA copy number within infected cells. Briefly, SSRP1 was subjected to KD in A549 cells and, 72 h later, cells were infected with HAdV-5, and total RNA was isolated each hour from 3 to 7 hpi, converted to cDNA, and then analyzed by qPCR using primers that target *E1A* within exon 2 (common to all *E1A* mRNA isoforms). Under our qPCR conditions, *E1A* mRNA could not be detected prior to 3 hpi. KD of SSRP1 did not affect the quantity of *GAPDH* mRNA (figure 4.2A), indicating *GAPDH* could be used to normalize our results. KD of SSRP1 caused a modest delay in the appearance of *E1A* mRNA transcripts, by about 30 min, but the overall rate of mRNA expression was unchanged, as shown by the identical slope of *E1A* transcript accumulation in siSSRP1- and siCtrl-treated cells (figure 4.2B). We also assessed the relative abundance of each *E1A* RNA isoform. During infection, HAdV expresses 5 isoforms of E1A, termed 13, 12, 11, 10, and 9 S, with isoforms 13 and 12 S being more abundant during early infection (50). SSRP1 KD caused a very modest decrease in both the 13 and 12 S isoforms, while 11, 10 and 9 S appeared modestly increased in abundance, but these differences were not statistically significant (unpublished

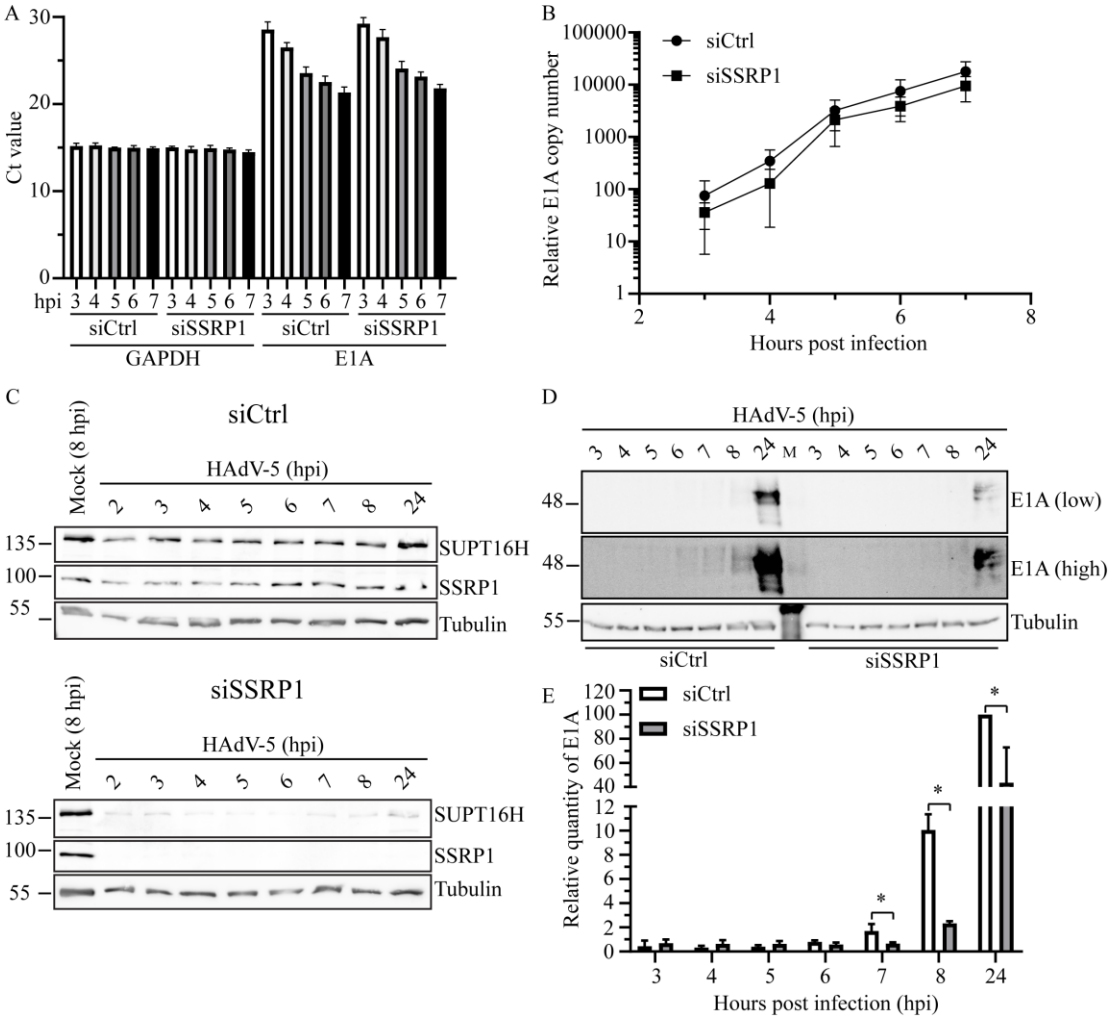
A
Ct value
hpi 3 4 5 6 7 3 4 5 6 7 3 4 5 6 7 3 4 5 6 7
siCtrl
siSSRP1
siCtrl
siSSRP1
GAPDH
E1A
B
siCtrl
siSSRP1
Relative E1A copy number
Hours post infection
C
siCtrl
Mock (8 hpi)
HAdV-5 (hpi)
SUPT16H
SSRP1
Tubulin
siSSRP1
D
HAdV-5 (hpi)
E1A (low)
E1A (high)
Tubulin
siCtrl
siSSRP1
E
siCtrl
siSSRP1
Relative quantity of E1A
Hours post infection (hpi)

Figure 4.2. Knockdown of SSRP1 reduces *E1A* transcript accumulation. Panels A-B: A549 cells were transfected with siRNA targeting SSRP1 or non-targeting control and, 72 h later, the cells were infected with HAdV-5 at an MOI of 10. At the indicated timepoints, total RNA was isolated, and converted to cDNA. The resulting cDNA was analyzed by qPCR for *E1A* and *GAPDH*. (A) Raw Ct values are reported. Note: A higher Ct value is indicative of less DNA in the sample. (B) Relative *E1A* mRNA copy number, normalized to cellular *GAPDH*. Panels C-E: A549 cells were transfected with siRNA targeting SSRP1 or non-targeting control and, 72 h post-transfection, the cells were infected with HAdV-5 at an MOI of 10. At the indicated timepoints, cells were harvested using reporter loading buffer. The quantity of SUPT16H, SSRP1 (C), E1A (D), and tubulin proteins were analyzed by immunoblot and relative quantity of E1A proteins calculated (E). The mean of three independent experiments is shown, and the error bars represent SD of the mean. Significance was calculated by one-way ANOVA (B) and multiple T-tests (E). * – $p < 0.05$.

data, MRJ and RJP).

The modest delay in *E1A* mRNA accumulation within HAdV-infected cells treated with siRNA to SSRP1 suggests that there may also be a delay in initiation of expression and accumulation of E1A proteins. We therefore examined the kinetics of E1A protein accumulation in infected cells treated with siRNA targeting SSRP1 or a non-targeting control, to get a more comprehensive view for *E1A* expression. Protein lysates from the cells were harvested every hour from 2-8 hpi and at 24 hpi. KD of SSPR1 was confirmed, and led to a reduction in levels of both SSRP1 and SUPT16H within the cells at all time points (figure 4.2C). In cells treated with non-targeting control siRNA, E1A was detectable by immunoblot at approximately 6-7 hpi, and increased approximately 10-fold between 6 and 8 hpi (figure 4.2D, E). In contrast, in cells treated with siRNA to SSRP1, E1A protein was first detected at 8 hpi at a level that was ~5-fold lower than that observed in controls, and reached only ~40% of control levels at 24 hpi. Taken together, KD of SSRP1 reduces production of E1A proteins within HAdV-infected cells.

4.4.3 E1A proteins do not associate with the FACT complex

E1A proteins have many different binding partners within the cell (31, 444), and can indirectly control the epigenetic status of the chromatin. For example, HAdV E1A proteins bind to and redirect the cellular p300/CBP histone acetyltransferase to epigenetically reprogram cellular chromatin thus conferring a global change in cellular gene expression (51, 446). As E1A proteins stimulate the activity of the *E1A* promoter (55, 56), we examined whether E1A proteins associate with the FACT complex to perhaps redirect its activity and enhance expression of E1A, similar to as reported for the HSV-1

ICP22 protein (291). We first performed immunofluorescence (IF) analysis of infected cells to determine if E1A proteins co-localized with or re-localized FACT complex proteins. A549 cells were seeded onto sterilized coverslips, and infected with AdPVII^{FLAG} at a multiplicity of infection (MOI) of 100 to ensure sufficient E1A protein for visualization by IF. Cells were fixed 8 hpi, and probed with antibodies to E1A and SUPT16H proteins, while nuclei were stained with Hoechst. In uninfected cells, SUPT16H was localized primarily to the nucleolus, as has been described previously (212). We also observed diffuse staining of SUPT16H throughout the nucleoplasm (Figure 4.3A). In HAdV-infected cells, E1A was found throughout the nucleoplasm but specifically excluded from the nucleolus. SUPT16H in HAdV-infected cells showed a similar distribution pattern as in uninfected cells at this 8 hpi time point, with no obvious relocalization away from the nucleolus. Thus, E1A and the FACT complex share a diffuse expression pattern within the nucleoplasm, with the exclusion of the nucleolus, suggesting that the two proteins could associate. To more directly address whether the two proteins are associated, we performed a co-immunoprecipitation (co-IP) experiment. Nuclear lysates were prepared at 8 hpi from HAdV-5 infected cells and subjected to IP with antibodies to E1A, SUPT16H, and SSRP1 proteins, or isotype control. Pulldown with antibody to E1A proteins efficiently enriched for E1A proteins, but failed to co-immunoprecipitate either SUPT16H or SSRP1 (figure 4.3B). Similarly, pulldown of SUPT16H or SSRP1 did not co-immunoprecipitate E1A (figures 4.3C, D). Taken together, these results suggest under our immunoprecipitation (IP) conditions, the FACT complex and HAdV E1A proteins do not associate with one another.

4.4.4 SSRP1 and SUPT16H co-localize with viral replication centers late in infection

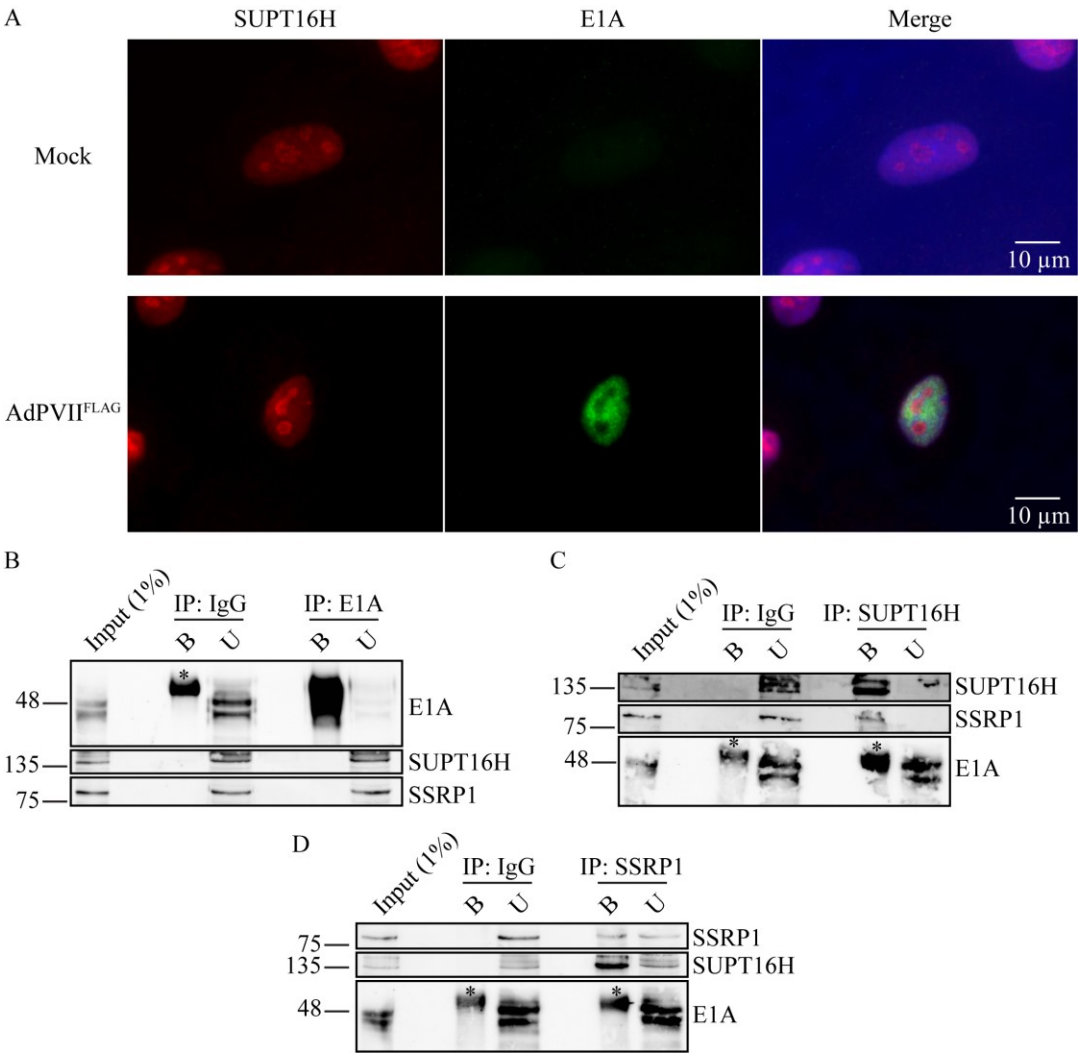

Figure 4.3. E1A proteins do not associate with the FACT complex. Panel A: A549 cells on sterilized coverslips were infected with AdPVII^{FLAG} (encoding FLAG-tagged viral protein VII) at an MOI of 100, and 8 hpi, the cells were analyzed by immunofluorescence for E1A, and SUPT16H proteins. Panels B-D: A549 cells were infected with HAdV-5 at an MOI of 10 and 8 h later, nuclei were fractionated and the resulting nuclear lysates were subjected to immunoprecipitation using antibodies to E1A (B), SUPT16H (C), and SSRP1 (D) or IgG as a negative control. E1A, SUPT16H, and SSRP1 in the resulting samples were analyzed by immunoblot. B - bound fraction, U - unbound fraction, * - antibody heavy chain.

Although FACT complex proteins in the nucleus of infected cells did not re-localize early during HAdV infection, we did observe the proteins re-localizing from the nucleolus to viral replication centers (VRCs) at late times of infection, as has been recently reported (293). Other nucleolar proteins, such as upstream binding factor (UBF) and B23 (also known as nucleophosmin or NPM1) have also been observed to relocalize to VRCs (178, 447). To effectively mark the VRCs, we utilized an HAdV-5 vector containing a FLAG tag on the viral DNA-binding protein (DBP), termed AdDBP^{FLAG} (404). DBP is a key protein involved in viral DNA replication (67, 448) and, as VRCs are the site of viral DNA replication, DBP is an excellent marker of these structures in infected cells. A549 cells were seeded onto sterilized coverslips, and infected with AdPVII^{FLAG} (to compare FACT complex localization relative to figure 4.3) or AdDBP^{FLAG}. Cells were fixed 18 hpi, and probed with antibodies targeting FLAG, SSRP1, SUPT16H, and nucleolin, while nuclei were stained with Hoechst. In mock-infected cells, SSRP1 and SUPT16H were present throughout the nucleus, but with a clear concentration of the proteins within the nucleolus, as marked by nucleolin (figure 4.4A, B). In infected cells, the two proteins no longer localize to the nucleolus, but instead formed district regions reminiscent of VRC (figure 4.4A, B). Indeed, the two proteins localize with DBP in infected cells (figure 4.4C) and, as expected (449), the DBP does not localize to the nucleolus (figure 4.4D). Nucleolin has been reported to translocate from the nucleolus to the cytoplasm when HAdV protein V is expressed from a plasmid (450), and to VRCs during infection. This appears to occur as the VRCs mature into structures containing virus-induced post replication bodies (451), which themselves are surrounded by a shell of protein V (173). We did not observe re-localization of nucleolin during the time frame used in our studies. These results show

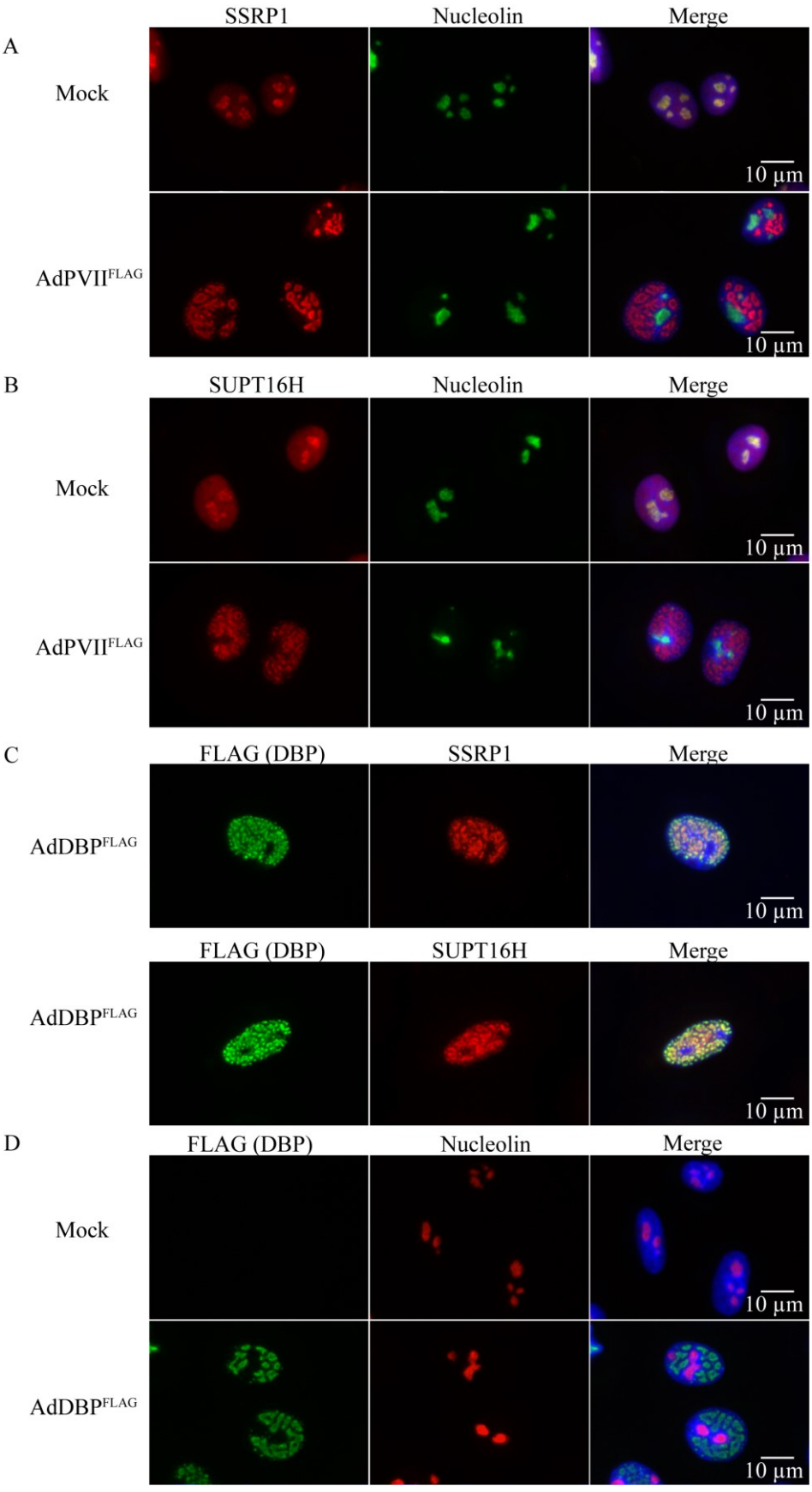
A
SSRP1
Nucleolin
Merge
Mock
AdPVII^FLAG
10 µm
B
SUPT16H
Nucleolin
Merge
Mock
AdPVII^FLAG
10 µm
C
FLAG (DBP)
SSRP1
Merge
AdDBP^FLAG
FLAG (DBP)
SUPT16H
Merge
AdDBP^FLAG
10 µm
D
FLAG (DBP)
Nucleolin
Merge
Mock
AdDBP^FLAG
10 µm

Figure 4.4. SSRP1 and SUPT16H co-localize with viral replication centers late in infection. A549 cells on sterilized coverslips were infected with AdPVII^{FLAG} (encoding FLAG-tagged viral protein VII) or AdDBP^{FLAG} (encoding FLAG-tagged viral DNA-binding protein (DBP)) at an MOI of 10 and, 18 hpi, the cells were analyzed by immunofluorescence microscopy for DBP-FLAG, SSRP1, SUPT16H or nucleolin.

that the FACT complex co-localizes with VRCs that form late in infection.

4.4.5 SSRP1 and SUPT16H associate with DBP

The FACT complex proteins SUPT16H and SSRP1 appeared to strongly co-localize with DBP within the VRC (figure 4.4). We therefore investigated whether the FACT proteins associate with DBP through a co-IP assay. Briefly, A549 cells were infected with AdDBP^{FLAG} and, 24 hpi, nuclear lysates were prepared from infected cells and incubated overnight (O/N) with antibodies targeting FLAG, SUPT16H, or SSRP1, as well as isotype control. FLAG IP of DBP^{FLAG} resulted in co-IP of both SUPT16H and SSRP1 (figure 4.5A). These results were confirmed using reciprocal co-IP, whereby IP of SSRP1 (figure 4.5B) or SUPT16H (figure 4.5C) resulted in co-IP of DBP^{FLAG}. These results suggest that FACT can associate with HAdV-5 DBP.

The association of FACT and DBP could be due to direct interaction of the proteins or mediated indirectly simply through both proteins being bound to the same DNA fragment. We therefore repeated our co-IP experiment in the presence of DNase I. We first confirmed the conditions for DNase I treatment. One µg of the pcDNA3.1 was resuspended in pulldown (PD) buffer alone or supplemented with 5.0 mM $MgCl_2$ and 0.5 mM $CaCl_2$, treated with DNase I, and incubated O/N at 4°C. We observed complete digestion of pcDNA3.1, but only when PD buffer was supplemented with $MgCl_2$, $CaCl_2$ and DNase I (figure 4.5D). We repeated the FLAG IP experiment using nuclear lysates which had been supplemented with $MgCl_2$ and $CaCl_2$, and treated with DNase I O/N at 4°C. The next day, antibodies targeting FLAG or IgG isotype control were added, and IP was performed as described above. Treating the nuclear lysates with DNase I prior to IP did not impact the

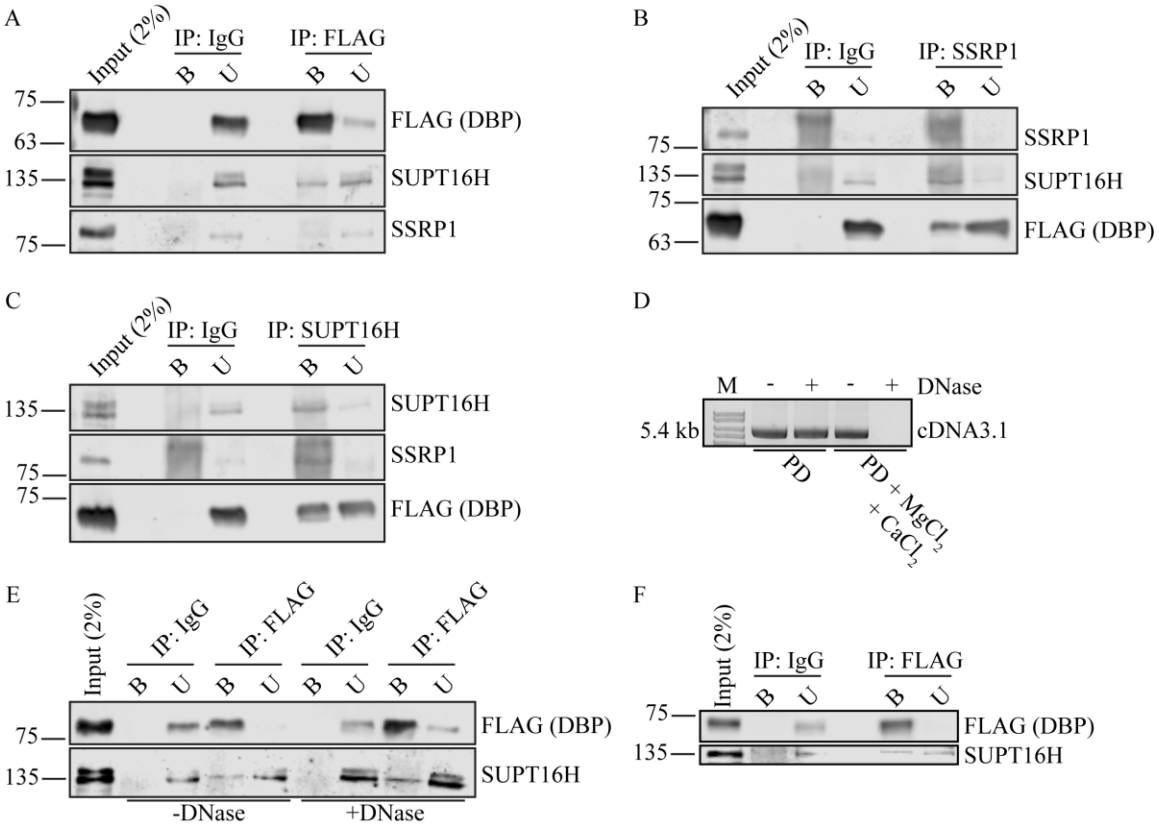
A
Input (2%)
IP: IgG
IP: FLAG
B
U
B
U
75
63
135
75
FLAG (DBP)
SUPT16H
SSRP1
B
Input (2%)
IP: IgG
IP: SSRP1
B
U
B
U
75
135
75
63
SSRP1
SUPT16H
FLAG (DBP)
C
Input (2%)
IP: IgG
IP: SUPT16H
B
U
B
U
135
75
75
SUPT16H
SSRP1
FLAG (DBP)
D
M
-
+
-
+
DNase
5.4 kb
cDNA3.1
PD
PD + MgCl2 + CaCl2
E
Input (2%)
IP: IgG
IP: FLAG
IP: IgG
IP: FLAG
B
U
B
U
B
U
B
U
75
135
FLAG (DBP)
SUPT16H
-DNase
+DNase
F
Input (2%)
IP: IgG
IP: FLAG
B
U
B
U
75
135
FLAG (DBP)
SUPT16H

Figure 4.5. SSRP1 and SUPT16H associate with DBP. Panels A-C: A549 cells were infected with AdDBP^{FLAG} at an MOI of 10. Twenty-four hpi, nuclei were fractionated and the resulting nuclear lysates were subjected to immunoprecipitation using antibodies to FLAG (A), SSRP1 (B), and SUPT16H (C). Panel D: To confirm DNase activity under our conditions, 1 µg of pcDNA3 was resuspended in pulldown (PD) buffer alone or supplemented with 5.0 mM $MgCl_2$ and 0.5 mM $CaCl_2$, and incubated with or without DNase at 4°C overnight. The resulting samples were subjected to agarose gel electrophoresis. Panel E: A549 cells were infected with AdDBP^{FLAG} at an MOI of 10. Twenty-four hpi, nuclei were fractionated and the resulting nuclear lysates was supplemented with 5.0 mM $MgCl_2$ and 0.5 mM $CaCl_2$, and incubated overnight at 4°C with and without DNase. The following day, the nuclear lysate was subjected to immunoprecipitation using antibody to FLAG. Panel F: A549 cells were transfected with an expression plasmid encoding FLAG-tagged DBP, and 24 h post transfection, nuclei were fractionated, and the resulting nuclear protein lysate was subjected to immunoprecipitation using antibody to FLAG. The resulting samples were analyzed for SSRP1, SUPT16H, DBP-FLAG by immunoblot. B - bound fraction, U - unbound fraction.

ability of SUPT16H to co-IP with DBP (figure 4.5E). These results indicate that the association of the FACT complex and DBP was due to protein-protein interactions and not due to the proteins binding to the same DNA molecule.

Finally, to determine whether other viral accessory proteins were required for the DBP-FACT complex interaction, we performed plasmid-based overexpression of DBP within A549 cells. Briefly, A549 cells were transfected with an expression plasmid encoding FLAG-tagged DBP, and 24 h post-transfection, nuclear lysates were obtained and subjected to IP using anti-FLAG antibody. Similar to AdDBP^{FLAG} infected cells, SUPT16H protein co-immunoprecipitated following IP of DBP (figure 4.5F), indicating DBP and the FACT complex can associate in the absence of viral infection or other viral proteins. Taken together, these results indicate DBP and the FACT complex proteins are associated with one another.

4.4.6 Knockdown of FACT proteins inhibits viral DNA replication and late protein production

As E1A proteins are vital for productive infection (31, 422), the lag in accumulation of *E1A* transcripts and proteins within cells subjected to KD for FACT proteins suggests subsequent stages of the viral life cycle will likely be similarly impacted. Thus, we next evaluated the effect of SSRP1 KD on viral genome copy number with the cells. A549 cells were treated with siRNA to SSRP1 (or non-targeting control), and 72 h later the cells were infected with HAdV-5, and total DNA isolated at 8 hpi (before onset of viral DNA replication) and 24 hpi. As shown in figure 4.6A, although similar genome copy numbers were present within the cells at 8 hpi, indicating similar input of virus, KD of SSRP1

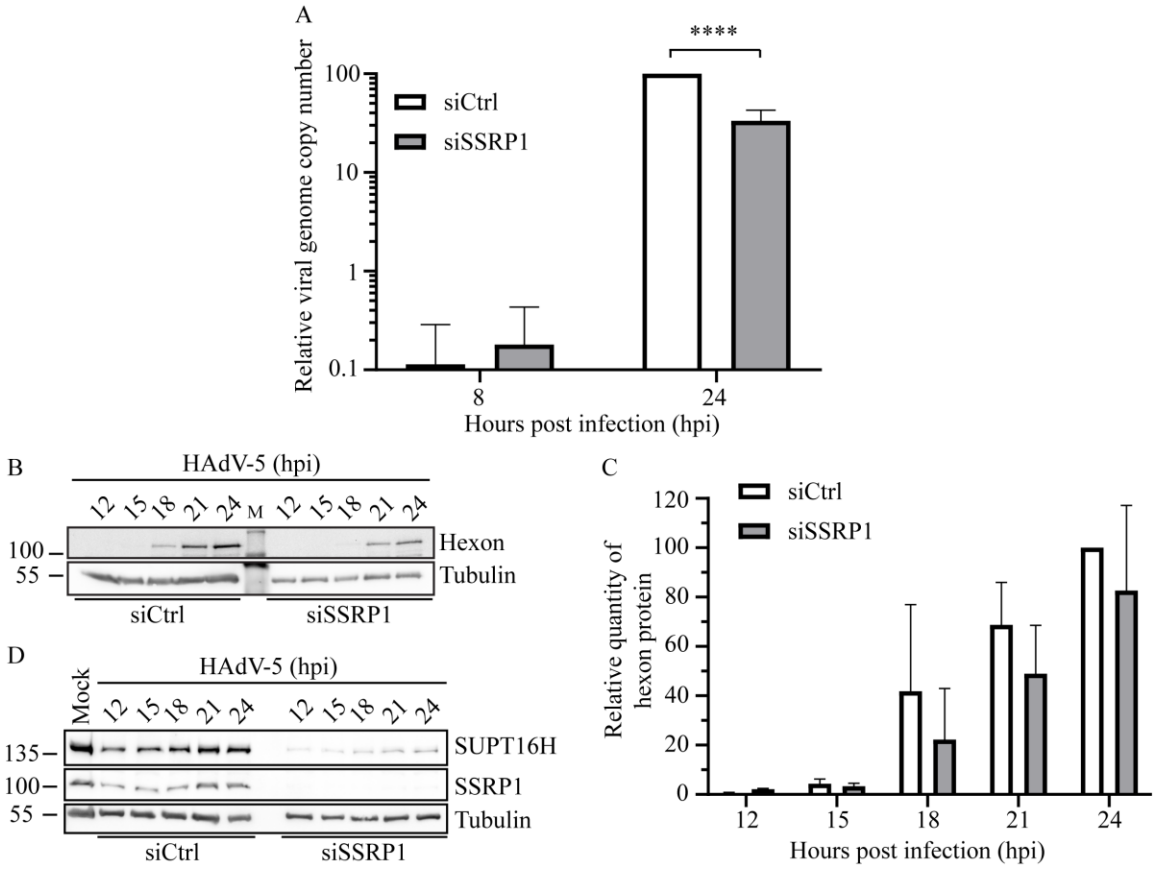

Figure 4.6. Knockdown of SSRP1 inhibits viral DNA replication and late protein production. Panel A: A549 cells were transfected with siRNA targeting SSRP1 or non-targeting control. Seventy-two h post-transfection, the cells were infected with HAdV-5 at an MOI of 10. Total DNA was isolated at 8, 18, 21, and 24 hpi and subjected to qPCR to determine the genome copy number per 200 ng DNA, normalized to the copy number of human *GAPDH*. Panels B-D: A549 cells were transfected with siRNA targeting SSRP1 or non-targeting control, infected 72 h later with HAdV-5 at an MOI of 10, and protein samples collected from 12-24 hpi. The quantity of hexon (B, C), SUPT16H, and SSRP1 (D) was analyzed by immunoblot and, where appropriate, normalized to tubulin signal. The mean of three independent experiments is shown, and the error bars represent SD of the mean. Significance was calculated by multiple T-tests. **** – $p < 0.05$.

resulted in a reduction of viral genomes at 24 hpi to approximately 35% of that observed in cells treated with non-targeting control siRNA. Thus, KD of SSRP1 adversely affected the accumulation of viral genomes within the cells.

In part, the newly replicated viral DNA serves as the template for late gene expression (173, 423), suggesting that reduced accumulation of genomes within cells subjected to KD for FACT complex proteins may also lead to reduced accumulation of late proteins. To directly examine this, we determined the levels of the late protein hexon in cells KD for SSRP1. A549 cells were transfected with siRNA targeting SSRP1, or non-targeting control, and 3 days post-transfection, were infected with HAdV-5. Protein lysates were harvested every 3 h from 12-24 hpi, and analyzed by immunoblot for hexon, SUPT16H, and SSRP1 proteins, with tubulin as a loading control. In siCtrl-treated cells hexon protein was first detectable by immunoblot at 18 hpi (figure 4.6B); however, the quantity of hexon protein present in cells treated with siRNA targeting SSRP1 was reduced by ~20% relative to cells treated with non-targeted control siRNA at 18 hpi and all subsequent time points (figure 4.6B, C). KD of SSRP1 and SUPT16H was confirmed (figure 4.6D). Although the differences in hexon protein levels were not statistically significant, these results suggest that there is a delay in initiation of expression or accumulation of late proteins in cells depleted of the FACT complex. Taken together, these results indicate that KD of FACT complex proteins leads to decreased viral DNA replication and a concomitant reduction in late protein synthesis during infection.

4.4.7 Knockdown of FACT complex proteins reduces progeny virion production

Our results indicate that KD of SSRP1 delays both early and late gene expression, as well as genome replication, suggesting that viral yield will ultimately be reduced. To examine virus recovery in cells following KD of SSRP1, we harvested virus from cells at 4, 18, 21, and 24 hpi, and performed a plaque assay. The 4 hpi is before production of progeny virions, thus acting as a control to confirm similar input of virus. At 4 hpi, there was no difference in titer between cells treated with non-targeting control siRNA or SSRP1 siRNA (figure 4.7). However, as infection progressed, KD of SSRP1 led to reduced virion recovery relative to the non-targeting control, which was statistically significant by the 21 hpi timepoint. At 21 hpi, the titer recovered from cells treated with siRNA targeting SSRP1 was ~18% of control levels, while the titer at 24 hpi was ~24% of control. Thus, KD of SSRP1 reduces progeny virus production. Taken together, our results indicate that the FACT complex is required for optimal HAdV-5 replication.

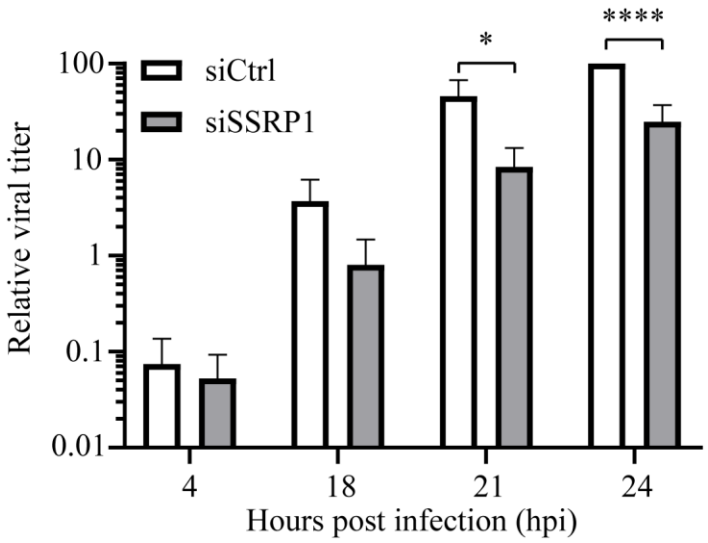

Figure 4.7. Knockdown of SSRP1 reduces progeny virus production. A549 cells were transfected with siRNA to SSRP1 or non-targeting control and, 72 h later, infected with HAdV-5 at an MOI of 10 ($4x10^6$ PFU/well). The cells were harvested into the medium at the indicated times post infection and the titer of recovered virus was analyzed by plaque assay. The mean of three independent experiments is shown, and the error bars represent standard deviation (SD) of the mean. Significance was calculated by multiple T-tests. * – $p < 0.05$, **** – $p < 0.05$.

4.5 Discussion

Eukaryotic genomic DNA is packaged into chromatin, a highly organized complex of DNA and proteins that encodes epigenetic information governing gene expression and cell identity (134, 452, 453). The histones contained in nucleosomes play an active role in gene regulation through post-translational modification of their N-termini and by serving as docking and recognition sites for regulatory proteins required to promote gene expression (134, 454). However, these same nucleosomes can present as physical obstacles during transcription initiation and elongation, impeding binding of transcription factors to promoters and stalling the passage of RNAP II, respectively (194). Thus, additional factors, such as the FACT complex, are required for efficient gene transcription (194, 200, 227). During early HAdV infection, the protein VII-bound viral DNA that enters the nucleus is quickly remodeled and becomes associated with cellular histones that form nucleosome-like structures (98), and this event occurs prior to the onset of early viral gene expression (128). HAdV utilizes many host proteins to facilitate viral gene expression and has evolved to manipulate cellular epigenetic pathways to effectively accomplish this task. The FACT complex appears to be crucial for gene expression of a number of RNA and DNA viruses (284, 289, 291, 292), suggesting HAdV may also require this complex.

Our results show that KD of the FACT complex led to reduced transcription of the *E1A* gene (figures 4.2A, B) leading to reduced production of E1A proteins within infected cells (figures 4.1, 4.2E, F). E1A proteins are crucial for transactivation of other HAdV promoters, thus ensuring efficient expression of other viral genes (455), and also in altering the cellular microenvironment to promote viral replication (31). Thus, it is perhaps unsurprising that KD of the FACT complex also lowered viral DNA replication (figure

4.6A), late gene expression (figure 4.6B, C) and viral yield (figure 4.7) relative to the non-targeting control siRNA, which are likely all due to ripple effects caused by poor *E1A* expression.

The FACT complex could be involved in promoting *E1A* transcription at several different stages of the process. As mentioned, incoming viral genomes are associated with the virus-encoded protein VII, which is a histone/protamine-like protein (456) responsible for condensing the viral DNA in the virion (although virions can still be generated that lack protein VII (99)). Protein VII is removed from the viral DNA before transcription begins (128). The FACT complex can act as a histone chaperone (202, 203), and could be involved in removal or displacement of protein VII from the incoming DNA. We did not detect an interaction of the FACT complex and protein VII by co-IP (MRJ and RJP, unpublished results), indicating that removal of protein VII is likely not accomplished by the FACT complex. The incoming HAdV genome is more accessible to micrococcal nuclease digestion at early gene loci (128), relative to late coding regions, suggesting that the E1 region is already relatively devoid of protein VII and perhaps already accessible for binding to cellular factors. Deposition of histones on viral DNA occurs as early as 0.5 hpi, but the chaperone(s) responsible for this event has not been identified (98). We and others have shown that HAdV-5 DNA associates with nucleosomes containing exclusively the histone variant H3.3 and not H3.1 (126-128, 144). For vectors based on HAdV-5, our studies implicated the histone chaperone HIRA as mediating deposition of H3.3 on the viral DNA (126). However, HIRA appeared not to be involved in H3.3 deposition during infection of wildtype HAdV-5 (127). The FACT complex is capable of assembling nucleosomes on naked DNA (202, 203), thus HAdV could utilize the FACT complex as a histone chaperone

in the early deposition of nucleosome-like structures on the viral DNA. In the absence of this histone chaperoning function of the FACT complex in the KD cells, the viral genome template would not be efficiently transitioned to the nucleosome-bound, transcriptionally-competent form.

The FACT complex is also involved in transcription initiation (200, 227). Nucleosomes need to be in the correct position for transcription factors to bind (238), and the FACT complex can shift nucleosome positioning on certain promoters (197). Thus, the FACT complex could be involved in shifting the location of newly-deposited nucleosomes on the *E1A* promoter, thus providing access for binding of transcription factors or RNA pol II. In yeast, the FACT complex has been shown to be directly involved in recruitment of transcription factors to the promoter region of certain genes, such as the *HO* promoter (239, 240), though this process has not been reported in mammalian cells. ChIP-seq of SSRP1 binding sites in HT1080 human cancer cells showed enrichment for several transcription factor binding sites, including Sp1 (221), a key transcription factor involved in *E1A* promoter activation (457). The FACT complex could be required by HAdV to either shift nucleosomes to allow binding of Sp1 or directly recruit Sp1 to the viral DNA. Lastly, the FACT complex is well known for a role in loosening the DNA-nucleosome structure to aid passage of RNA pol II during transcription elongation (192, 202). The FACT complex removes one histone H2A-H2B dimer from the nucleosome, thus increasing DNA accessibility while still preserving the sub-nucleosome structure, and reassembles the nucleosome after passage of the RNA polymerase (225, 226). However, KD of the FACT complex appeared to delay the temporal expression of *E1A* transcripts but not the rate of *E1A* transcript accumulation (Figure 4.2B), indicating that FACT is likely not required or

is not crucial for elongation of *E1A* transcripts.

During HSV-1 infection, the viral ICP22 protein recruits the FACT complex to the viral genome to aid in transcription elongation of viral genes (291). HAdV E1A proteins have been shown to interact directly with several chromatin modulating proteins, such as EP300/CBP (458), EP400 (459), and PCAF (460), to alter their specificity and/or function to promote viral infection. We did not detect interaction of E1A proteins with the FACT complex by co-IP analysis (Figure 4.3), indicating that the ability of E1A proteins to activate the *E1A* promoter (55, 56) is likely not through E1A-mediated modulation of FACT activity directed towards the *E1A* promoter.

Although our data indicates the FACT complex is required for optimal *E1A* expression, we also observed that the FACT complex co-localized (figure 4.4) and co-immunoprecipitated (figure 4.5) with the viral DBP in VRCs at late time of infection. The FACT complex was recently reported to co-localize with VRCs in HAdV-infected cells (293), confirming our results. In cells subjected to FACT KD, we observed reduced accumulation of viral genomes (Figure 4.6), which could have been due to ripple effects caused by reduced expression of HAdV early genes. However, the association of FACT complex proteins and DBP suggests an additional, more direct role for the complex during the late phase of infection. DBP is encoded by the viral *E2A* transcription unit and is involved in promoting replication elongation by the HAdV-encoded DNA polymerase (67, 448) as well as coating and protecting the ssDNA viral replication intermediate from degradation by cellular nucleases (167, 168). DBP is also involved in regulation of viral gene expression and particle assembly (reviewed in (70)). During replication of cellular DNA, the FACT complex interacts with the MCM complex in order to disassemble

nucleosomes ahead of the replication fork (198) and reassemble the parental nucleosomes on the newly-replicated DNA (199). The FACT complex could be involved in modulating the viral nucleoprotein structure during DNA replication, displacing and replacing histones or DBP to facilitate passage of the viral DNA polymerase. However, treatment of cells with CBL0137 at 8 hpi, a time after early gene expression but before viral DNA replication, had no effect on accumulation of late proteins, suggesting that DNA replication was also unaffected (MRJ and RJP, unpublished results). This indirect evidence suggests that the FACT complex may not play a crucial role in promoting viral DNA replication.

The FACT complex has also been implicated in the DNA damage response (DDR) (reviewed in (200, 201)), and accumulates at sites of DNA damage to modulate the local chromatin to facilitate DNA repair (266-268). This could suggest that the FACT complex is recruited to VRCs by detecting viral genomes simply as broken or damaged DNA. HAdV replication does activate the ATM and ATR pathways (117), or the DNA-PK (461) pathway. Interestingly, cisplatin-induced re-localization of FACT proteins from the nucleolus to the site of DNA damage has been reported to be dependent on DNA-PK (276). However, the downstream consequences of FACT localization in the context of HAdV replication and the DDR are unclear, as HAdV is known to promote degradation (116) or mislocalization (462) of many components of the MRN complex necessary for DNA repair (reviewed in (71)), to prevent repair-mediated concatemerization of the HAdV genome.

Recently, the FACT complex was shown to be involved in an evolutionarily conserved antiviral pathway termed FEAR (FACT-ETS-1 Antiviral Response) (282). Early gene expression of some viruses triggers nuclear accumulation of SUMOylated SUPT16H and activation of expression of E26 transformation-specific sequence-1 (ETS-1), a

transcription factor that regulates cellular virus restriction programs. The poxvirus A51R protein antagonizes this pathway by tethering the SUMOlyated SPT16H in the cytoplasm (282). DBP could be acting in a similar manner to sequester the FACT complex and prevent activation of the FEAR pathway. DBP appeared to interact equally well with both species of SUPT16H present in infected cells, as presumably the upper band of SUPT16H observed in our immunoblots is the SUMOlyated form of SUPT16H. Identification of the specific residues of DBP that bind to FACT may allow for the development of a virus encoding mutant DBP that can no longer bind the protein, allowing for investigation of FEAR pathway attenuation.

Our results also provide an additional mechanism behind the anti-HAdV-5 effects of CBL0137 (MRJ and RJP, unpublished results). CBL0137 is a water-soluble DNA intercalating agent initially evaluated for its anti-cancer properties (286, 287, 436), but it has also shown efficacy as an antiviral agent against a number of RNA and DNA viruses (288, 289, 291, 292, 309). The anti-HAdV properties of CBL0137-treatment was attributed to degradation of the cellular RNA polymerase II, which HAdV uses to transcribe early genes necessary to kick-start the virus replicative cycle. However, CBL0137 induces pleiotropic effects on the cell (reviewed in (287)), including induction of chromatin damage which results in trapping of the FACT complex onto unfolded nucleosomes (200, 296, 297). As KD of the FACT complex alone was sufficient to lower E1A proteins (Figure 4.1), our results indicate that in addition to RNAP II degradation, trapping of the FACT complex may also contribute to the anti-HAdV effects of CBL0137.

In summary, this report shows that the FACT complex is required for optimal HAdV infection. Our work extends the observation that the FACT complex is important

for productive infection in both RNA and DNA viruses. These findings provide a greater understanding of HAdV biology, representing another potential target for anti-HAdV therapeutics.

4.6 Author contributions

A more detailed description of contributions of collaborators can be found at the end of the thesis.

Author contributions: Morgan R. Jennings**:** Conceptualization, Data curation, Formal analysis, Investigation, Methodology, Funding acquisition, Visualization, Writing - original draft, Writing - review & editing.

Panayiotis O. Vacratsis: Data curation, Formal analysis, Funding acquisition, Methodology, Writing - review & editing.

Robin J. Parks: Conceptualization, Formal analysis, Funding acquisition, Project administration, Resources, Supervision, Visualization, Writing - review & editing.

Funding: The research was supported by research funds R.J.P from the Canadian Institutes of Health Research (MOP-142316, PJT-178120) and the Natural Sciences and Engineering Research Council (RGPIN-2019-04786). P.O.V was supported by research funds from the Natural Sciences and Engineering Research Council (Discovery Grant 298468). M.R.J was supported by a Queen Elizabeth II Graduate Scholarship in Science and Technology from the Ontario Provincial Government (Canada). The funders had no role in study design, data collection and interpretation, or the decision to submit the work for publication.

Conflicts of interest: The authors declare no conflict of interest.

4.7 Acknowledgements

We would like to thank Kathy Poulin for excellent technical assistance and guidance throughout this study.

Chapter 5:

General Discussion and Conclusions

HAdV causes respiratory, gastrointestinal, and ocular disease (18) that in healthy individuals is often self-limiting (19). However, in pediatric, geriatric, and immunocompromised individuals, HAdV-induced disease is much more severe (20-22). There is no therapeutic approved for use in treating HAdV infection (14). Targeting host processes represents a promising avenue for treating viral infections due to decreased direct evolutionary pressure on the virus (185, 186). Viruses have minimized genomes, dispensed with many crucial functions and thus are reliant on host processes. Given the crucial role of epigenetic regulation in modulating expression of host genes, it is not surprising that nuclear viruses, such as HAdV, have evolved to exploit cellular machinery involved in epigenetic regulation (142). Indeed, compounds that can modulate epigenetic regulatory proteins are capable of inhibiting HAdV infection (152-155). Thus, the overall objective of this work was to evaluate additional compounds capable of regulating viral epigenetics in the context of HAdV infection, such as treatment with siRNA targeting the FACT complex and CBL0137. Curcumin treatment has also been shown to interfere with epigenetic regulation (312, 340), providing a potential mechanism behind the anti-HAdV effect observed. The results obtained and their significance are discussed below.

5.1 The FACT complex is required for optimal human adenoviral replication

In chapter 4, the role of the FACT complex in HAdV-5 infection was examined. KD of the FACT complex or SSRP1 alone was sufficient to decrease the relative quantity of E1A proteins, while simultaneously not significantly impacting cell health (figure 4.1, 4.2E, F). Examination of the relative quantity of *E1A* mRNA transcripts showed that KD of SSRP1 delayed the timing of appearance of *E1A* transcripts but not the overall kinetics

of *E1A* transcript accumulation (figure 4.2A, B). Though E1A and SSRP1 were present throughout the nucleoplasm, E1A does not associate with the FACT complex (figure 4.3). However, as infection progressed, it was observed that the FACT complex co-localizes with VRCs (figure 4.4), and co-IP analysis indicated that the FACT complex associates with the viral DBP (figure 4.5). SSRP1 KD reduced viral DNA replication, and also reduced the relative quantity of hexon protein, though this did not reach significance (figure 4.6). Finally, depletion of the FACT complex significantly reduced the formation of progeny virions (figure 4.7).

The FACT complex is best known as a transcription elongation factor (192, 200, 202), with the precedent of another dsDNA virus, HSV-1, exploiting this property for transcription elongation of viral genes (291). However, our results suggest that HAdV does not require the FACT complex for transcription elongation of viral genes, as the overall rate of *E1A* transcription was not affected by SSRP1 KD (figure 4.2). Instead, our results are more consistent with the FACT complex initially preparing viral genomes for *E1A* transcription. In this context, the histone chaperone activity of the FACT complex (202, 203) suggests the FACT complex could be depositing histones onto viral DNA, a requirement for *E1A* transcription (128). The chaperone that accomplishes this task has not been identified (98). This could be tested by performing ChIP-seq targeting H3.3 on siSRRP1 and siCtrl treated samples, and evaluating histone association on the *E1A* gene. Should the FACT complex be the histone chaperone that chromatinizes viral DNA, KD of the FACT complex should reduce histone association on the *E1A* gene.

Alternatively, the FACT complex may instead be supporting transcription initiation of *E1A* by ensuring the *E1A* promoter is free of nucleosomes to allow binding of

transcription factors. The FACT complex can shift nucleosomes off promoters (197, 239-242), and at least in yeast, the FACT complex can also recruit transcription factors themselves to certain promoters (239, 240). The FACT complex is recruited to various transcription factor binding sites, including SP1 (221), a transcription factor involved in *E1A* activation (457). This suggests the FACT complex may be recruited to the *E1A* promoter, and may even recruit SP1 itself to the *E1A* promoter, to ensure efficient binding of *E1A* transcription factors by shifting deposited nucleosomes. Similar to above, this possibility could be tested by performing ChIP-seq analysis targeting H3.3, examining the positioning of deposited histones on the *E1A* promoter, as well as evaluating SP1 association with the *E1A* promoter in the context of SSRP1 KD. Regardless of how the FACT complex is required in preparing the *E1A* promoter, once E1A is successfully produced, the ability of E1A to transactivate its own promoter (55, 56) could compensate for FACT complex depletion and may explain our *E1A* mRNA transcript results.

Our results also indicate that the FACT complex associates and colocalizes with the viral DBP, a finding that was recently confirmed by Hidalgo et al. (293). We did not explore the significance of this observation in the context of HAdV infection. However, given that c-trapping induced by CBL0137 treatment when added between 8-10 hpi did not prevent production of the hexon protein, and thus viral DNA replication (figure 3.4), this implies the FACT complex within VRCs is not involved with viral DNA replication. Instead, it is possible that the FACT complex is sequestered into VRCs in order to inhibit normal activity, possibly due to the role of the FACT complex in the DDR (via DNA-PK-mediated phosphorylation of H2AX) or in the FEAR pathway (282). Assuming the FACT complex interacts directly with DBP, generation of a cell line expressing mutant FACT complex

proteins unable to bind to DBP would allow evaluation of FACT association with DNA-PK or expression of ETS-1-associated genes during HAdV infection. If the association between the FACT complex and DBP is due to anchoring by an additional protein(s), then the above experiment would require identifying the anchoring protein, and evaluating infection following depletion of said protein. These experiments would also allow verification if productive infection can still proceed despite preventing FACT complex localization to VRCs. Ultimately, our results suggest the FACT complex may play a positive role during early HAdV infection, but as infection transitions to the late phase, the FACT complex is instead neutral or even refractory to HAdV infection, as has been observed with DNA-PK during HAdV infection (71).

5.2 Inhibition of human adenovirus replication by the small molecule curaxin

In chapter 3, the effect of the curaxin molecule CBL0137 on HAdV-5 replication was examined. We initially evaluated CBL0137 treatment in HAdV-5 infection as an inhibitor of the FACT complex, however CBL0137-induced RNAP II degradation precluded us from attributing the effects of CBL0137 treatment on HAdV-5 replication on c-trapping. Treatment with CBL0137 significantly reduced both the relative quantity of E1A and hexon proteins, at concentrations tolerated by the cell (figure 3.1). The loss of E1A proteins, which was attributed to degradation of RNAP II (figure 3.3), impacted later stages of infection, reducing viral DNA replication and lowering progeny formation (figure 3.2). However, we also observed that at the late timepoint in infected cells, RNAP II appeared to be partially stabilized, as well as there being evidence of early viral gene expression (figure 3.3D). Indeed, during a time of addition analysis, treating infected cells

with CBL0137 at later times resulted in a greater preservation of POLR2A, and hexon became detectable once treated sufficiently late in infection (figure 3.4). These observations led us to speculate that early viral genes redirect E3 ligase activity away from POLR2A following CBL0137 treatment. Transfection of 293 cells with plasmids that encodes tagged E4orf6 proteins partially stabilized POLR2A following CBL0137 treatment, suggesting that early viral proteins do indeed contribute to stabilization of RNAP II (figure 3.5).

CBL0137, a DNA intercalating agent, has pleiotropic effects on the cell (286, 287, 299). Without inducing direct DNA damage (294), CBL0137 nonetheless appears to cause a DNA lesion which leads to stalling of the RNAP II complex and eventual targeting and degradation of POLR2A by the proteasome system (299). CBL0137-induced degradation of RNAP II inhibited *E1A* transcription. However, as discussed in chapter 4, the FACT complex itself is required for optimal viral replication. Thus, c-trapping of the FACT complex onto nucleosomes by CBL0137 may also contribute to the anti-HAdV-5 effect of CBL0137 treatment.

CBL0137 has been shown to lead to stabilization of p53 (286). Indeed, in HAdV-infected, we observed stabilization of p53 following CBL0137 treatment (data not shown). During infection, HAdV normally antagonizes p53 to prevent cell cycle arrest and induction of apoptosis (52, 63), suggesting another mechanism behind the anti-HAdV effects of CBL0137 treatment. Furthermore, the reduction in *E1A* transcription also implies a reduction in *E1B* transcription, indicating that the virus would also be unable to repurpose and degrade p53. However, KD of p21, a cell cycle inhibitor activated by p53 (463), did not rescue HAdV-5 replication following CBL0137 treatment (data not shown). We also

examined CBL0137 treatment in HAdV-5 infected H1299 cells, a cancer cell line that does not express p53. We initially found that CBL0137 treatment still inhibited HAdV-5 infection despite the lack of p53, though it was later determined that CBL0137 was cytotoxic to H1299 cells, potentially explaining the lack of viral replication (data not shown). Additionally, CBL0137 treatment can inhibit ZIKV, IAV, and SARS-CoV-2 replication by inducing an interferon response normally negatively regulated by the FACT complex (287). However, at least in HAdV-5-infected A549 cells, treatment with CBL0137 did not appear to induce IFNβ expression (data not shown). These results ultimately suggest that the effect of CBL0137 on HAdV-5 replication is independent of p53 and the interferon response.

Due to interest as an anti-cancer compound, CBL0137 has been extensively studied in *in vivo* models of cancer (286, 300-307). Success in these models has led to a phase I/II clinical trial investigating CBL0137 treatment in solid tumours (NCT04870944), which is still recruiting. CBL0137 has also successfully been used in a lethal *in vivo* model of HSV-1 infection (292). Should CBL0137 be approved for use in humans to treat cancer, our results indicate it could very easily be repurposed to treat HAdV infection.

5.3 Antiviral effects of curcumin on adenovirus replication

In chapter 2, the antiviral properties of curcumin on HAdV infection were evaluated. Treatment with curcumin in HAdV-5 infected cells was sufficient to significantly reduce the relative quantity of both the early E1A proteins and late penton protein (figure 2.1), but only at concentrations that appeared to reduce cell health, suggesting curcumin has a narrow therapeutic window (figure 2.2). Due to the effect of

curcumin on E1A, treatment with curcumin reduced both viral DNA replication (figure 2.3) and progeny formation (figure 2.4). Transient treatment with curcumin was sufficient to increase metabolic activity, and was still effective at reducing the relative quantity of early E1A proteins, but was less effective at reducing the relative quantity of late penton (figure 2.5). Curcumin treatment was slightly less effective against the more pathogenic types HAdV-4 and 7 infection (figure 2.6). Finally, the effect of the purity of curcumin was evaluated, and indicated higher purity curcumin was more effective at reducing the relative quantities of E1A and penton, while also lowering cellular metabolic activity to a lesser extent relative to less pure curcumin (figure 2.7).

Curcumin treatment has diverse effects within the cell (328-330). The ability of curcumin to modulate epigenetic regulation (312, 340) may contribute to the anti-HAdV effects observed. Curcumin treatment downregulates expression of HDACs 1-4, 6, and 8 (341-350). Work by Saha et al. (152) indicated that between HDACs 1-3, it was loss of HDAC2 that inhibited late viral expression. The effect of HDAC6 (inhibited by SAHA and trichostatin A treatment) KD on HAdV-5 infection was not evaluated. Though we did not evaluate the effect of curcumin treatment on HDAC2 or 6 in HAdV-5 infected cells, this suggests that curcumin treatment could be inhibiting HAdV replication by downregulating HDAC2, and possibly HDAC6. The relative quantity of E1A proteins during wild type HAdV-5 infection was reduced following SAHA treatment (152), in agreement with the effect of curcumin treatment on E1A.

As discussed in chapter 2, curcumin treatment also increases DAXX expression (407). DAXX is normally targeted for degradation by HAdV-5 (62), and preventing DAXX degradation causes deposition of unacetylated histones on viral DNA, which leads to

repression of viral gene expression (160). Increased DAXX expression due to curcumin treatment therefore may be contributing to repression of *E1A* expression.

Inhibition of p300/CBP by curcumin may also contribute to HAdV inhibition. While p300/CBP is important for induction of the S-phase in HAdV-infected terminally differentiated cells (51, 52), this process may not be as required in proliferating cells, such as the A549 cells used in our study. Currently, no evidence exists directly linking p300/CBP activity to *E1A* expression itself, suggesting that if initial *E1A* expression requires p300/CBP, inhibition of p300/CBP by curcumin could potentially contribute to the reduction in the quantity of E1A observed. Additionally, work by Pelka et al. (455) indicated that KD of p300/CBP reduced transactivation of the E4 promoter by E1A. Deletion of the E4 proteins leads to severe defects in viral DNA replication and late gene expression (76). This suggests that even if p300/CBP inhibition does not contribute to the effect of curcumin on E1A in HAdV-infected cells, these may have reduced expression of E4 proteins, which could contribute to inhibition of late viral gene expression.

Though curcumin has potent epigenetic modulating properties (312, 340), curcumin could be inhibiting E1A production by alternate means. Though curcumin-induced upregulation of DAXX expression may contribute to repression of viral genes, DAXX is also a component of the anti-HAdV interferon response that is normally countered by early HAdV proteins (159). Increased quantities of DAXX may leave the cell in an antiviral state unable to be countered by early viral proteins, inhibiting infection, which could be tested by evaluating induction of the interferon response in curcumin-treated, infected cells. Curcumin may have a more direct effect on E1A proteins by inhibiting Hsp90 (379, 464), which chaperones newly synthesized E1A proteins (465). If

this is the case and is the primary mechanism behind the effect of curcumin on E1A, then in theory *E1A* mRNA transcripts would be similar between treated and untreated, HAdV-infected cells.

While curcumin has shown much promise *in vitro*, the poor solubility, bioavailability, and stability (313, 320, 321) of curcumin significantly hampers translation to use in human therapies. Attempts to solve this issue by various groups involves generating alternative formulations or analogues of curcumin, which have shown some success (322-327), including improving the efficacy of curcumin against viruses (12). Strategies that can successfully bypass the limitations of curcumin could potentially lead to approval of curcumin as a therapeutic in humans.

5.4 Concluding remarks

In at-risk individuals, HAdV infection represents a significant burden (20-22). The lack of safe and efficacious treatment for HAdV infection contributes a great deal to the suffering of these individuals (14), highlighting the need to discover compounds that can treat HAdV infection. We have shown treatment with curcumin, CBL0137, and siRNA targeting the FACT complex, compounds that regulate viral epigenetics, can interfere with HAdV replication. Though the mechanism of action varies, all three compounds primarily control HAdV infection by interfering with production of the viral E1A proteins. The lack of E1A proteins negatively impacts all subsequent aspects of HAdV infection (31, 55-57), representing an excellent target to combat HAdV. While more work is needed before these compounds can be translated to human use, they nonetheless constitute promising treatments for HAdV infection.

References

1. Summers WC. Virus Infection. In: Schaechter M, editor. Encyclopedia of Microbiology (Third Edition). Oxford: Academic Press; 2009. p. 546-52.

2. Nasir A, Romero-Severson E, Claverie JM. Investigating the Concept and Origin of Viruses. Trends in Microbiology. 2020;28(12):959-67.

3. Rostøl JT, Marraffini L. (Ph)ighting Phages: How Bacteria Resist Their Parasites. Cell Host Microbe. 2019;25(2):184-94.

4. Riera Romo M, Pérez-Martínez D, Castillo Ferrer C. Innate immunity in vertebrates: an overview. Immunology. 2016;148(2):125-39.

5. Boehm T, Swann JB. Origin and Evolution of Adaptive Immunity. Annu Rev Anim Biosci. 2014;2:259-83.

6. Gao Z, Feng Y. Bacteriophage strategies for overcoming host antiviral imm unity. Front Microbiol. 2023;14:1211793.

7. Naz SS, Aslam A, Malik T. An Overview of Immune Evasion Strategies of DNA and RNA Viruses. Infect Disord Drug Targets. 2021;21(7):e300821192322.

8. Nathanson N. Chapter 1 - The Human Toll of Viral Diseases: Past Plagues and Pending Pandemics. In: Katze MG, Korth MJ, Law GL, Nathanson N, editors. Viral Pathogenesis (Third Edition). Boston: Academic Press; 2016. p. 3-16.

9. Sankaran N, Weiss RA. Viruses: Impact on Science and Society. In: Bamford DH, Zuckerman M, editors. Encyclopedia of Virology (Fourth Edition). Oxford: Academic Press; 2021. p. 671-80.

10. Dvorkin-Camiel L, Whelan JS. Tropical American Plants in the Treatment of Infectious Diseases. J Diet Suppl. 2008;5(4):349-72.

11. Li T, Peng T. Traditional Chinese herbal medicine as a source of molecules with antiviral activity. Antivir Res. 2013;97(1):1-9.

12. Jennings MR, Parks RJ. Curcumin as an Antiviral Agent. Viruses. 2020;12(11):1242.

13. Pollard AJ, Bijker EM. A guide to vaccinology: from basic principles to new developments. Nat Rev Immunol. 2021;21(2):83-100.

14. Saha B, Parks RJ. Recent Advances in Novel Antiviral Therapies against Human Adenovirus. Microorganisms. 2020;8(9):1284-04.

15. Xu S, Ding D, Zhang X, Sun L, Kang D, Huang B, et al. Newly Emerging Strategies in Antiviral Drug Discovery: Dedicated to Prof. Dr. Erik De Clercq on Occasion of His 80th Anniversary. Molecules. 2022;27(3):850.

16. Savedchuk S, Raslan R, Nystrom S, Sparks MA. Emerging Viral Infections and the Potential Impact on Hypertension, Cardiovascular Disease, and Kidney Disease. Circ Res. 2022;130(10):1618-41.

17. Gogoi D, Baruah PJ, Narain K. Immunopathology of emerging and re-emerging viral infections: an updated overview. Acta Virol. 2024;68.

18. Greber UF. Adenoviruses - Infection, pathogenesis and therapy. FEBS Lett. 2020;594(12):1818-27.

19. Lichtenstein DL, Wold WSM. Experimental infections of humans with wild-type adenoviruses and with replication-competent adenovirus vectors: replication, safety, and transmission. Cancer Gene Ther. 2004;11(12):819-29.

20. Lion T. Adenovirus infections in immunocompetent and immunocompromised patients. Clin Microbiol Rev. 2014;27(3):441-62.

21. Bhatti Z, Dhamoon A. Fatal adenovirus infection in an immunocompetent host. Am J Emerg Med. 2017;35(7):1034.e1-.e2.

22. Lynch JP, 3rd, Kajon AE. Adenovirus: Epidemiology, Global Spread of Novel Serotypes, and Advances in Treatment and Prevention. Semin Respir Crit Care Med. 2016;37(4):586-602.

23. Chamberlain JM, Sortino K, Sethna P, Bae A, Lanier R, Bambara RA, et al. Cidofovir Diphosphate Inhibits Adenovirus 5 DNA Polymerase via both Nonobligate Chain Termination and Direct Inhibition, and Polymerase Mutations Confer Cidofovir Resistance on Intact Virus. Antimicrob Agents Chemother. 2018;63(1):e01925-18.

24. Takamatsu A, Tagashira Y, Hasegawa S, Honda H. Disseminated adenovirus infection in a patient with a hematologic malignancy: a case report and literature review. Future Sci OA. 2019;5(8):FSO412.

25. Rowe WP, Huebner RJ, Gilmore LK, Parrott RH, Ward TG. Isolation of a Cytopathogenic Agent from Human Adenoids Undergoing Spontaneous Degeneration in Tissue Culture. Proc Soc Exp Biol Med. 1953;84(3):570-3.

26. Hilleman MR, Werner JH. Recovery of new agent from patients with acute respiratory illness. Proc Soc Exp Biol Med. 1954;85(1):183-8.

27. Berget SM, Moore C, Sharp PA. Spliced segments at the 5' terminus of adenovirus 2 late mRNA. Proc Natl Acad Sci USA. 1977;74(8):3171-5.

28. Chow LT, Gelinas RE, Broker TR, Roberts RJ. An amazing sequence arrangement at the 5' ends of adenovirus 2 messenger RNA. Cell. 1977;12(1):1-8.

29. Nevins JR, Darnell JE. Groups of adenovirus type 2 mRNA's derived from a large primary transcript: probable nuclear origin and possible common 3' ends. J Virol.

1978;25(3):811-23.

30. Nevins JR, Darnell JE, Jr. Steps in the processing of Ad2 mRNA: poly(A)+ nuclear sequences are conserved and poly(A) addition precedes splicing. Cell. 1978;15(4):1477-93.

31. King CR, Zhang A, Tessier TM, Gameiro SF, Mymryk JS. Hacking the Cell: Network Intrusion and Exploitation by Adenovirus E1A. MBio. 2018;9(3):e00390-18.

32. Whyte P, Buchkovich KJ, Horowitz JM, Friend SH, Raybuck M, Weinberg RA, et al. Association between an oncogene and an anti-oncogene: the adenovirus E1A proteins bind to the retinoblastoma gene product. Nature. 1988;334(6178):124-9.

33. Li Y, Graham C, Lacy S, Duncan AM, Whyte P. The adenovirus E1A-associated 130-kD protein is encoded by a member of the retinoblastoma gene family and physically interacts with cyclins A and E. Genes Dev. 1993;7(12a):2366-77.

34. Ewen ME, Xing YG, Lawrence JB, Livingston DM. Molecular cloning, chromosomal mapping, and expression of the cDNA for p107, a retinoblastoma gene product-related protein. Cell. 1991;66(6):1155-64.

35. Whyte P, Williamson NM, Harlow E. Cellular targets for transformation by the adenovirus E1A proteins. Cell. 1989;56(1):67-75.

36. Eckner R, Arany Z, Ewen M, Sellers W, Livingston DM. The adenovirus E1A-associated 300-kD protein exhibits properties of a transcriptional coactivator and belongs to an evolutionarily conserved family. Cold Spring Harb Symp Quant Biol. 1994;59:85-95.

37. Arany Z, Newsome D, Oldread E, Livingston DM, Eckner R. A family of transcriptional adaptor proteins targeted by the E1A oncoprotein. Nature.

1995;374(6517):81-4.

38. Sayedahmed EE, Kumari R, Mittal SK. Current Use of Adenovirus Vectors and Their Production Methods. Methods Mol Bio. 2019;1937:155-75.

39. Matsunaga W, Gotoh A. Adenovirus as a Vector and Oncolytic Virus. Curr Issues Mol Biol. 2023;45(6):4826-40.

40. Yi L, Ning Z, Xu L, Shen Y, Zhu X, Yu W, et al. The combination treatment of oncolytic adenovirus H101 with nivolumab for refractory advanced hepatocellular carcinoma: an open-label, single-arm, pilot study. ESMO Open. 2024;9(2):102239.

41. Lee A. Nadofaragene Firadenovec: First Approval. Drugs. 2023;83(4):353-7.

42. Kim J, Chang J. Cross-protective efficacy and safety of an adenovirus-based universal influenza vaccine expressing nucleoprotein, hemagglutinin, and the ectodomain of matrix protein 2. Vaccine. 2024;42(15):3505-13.

43. Harro C, Sun X, Stek JE, Leavitt RY, Mehrotra DV, Wang F, et al. Safety and immunogenicity of the Merck adenovirus serotype 5 (MRKAd5) and MRKAd6 human immunodeficiency virus type 1 trigene vaccines alone and in combination in healthy adults. Clin Vaccine Immunol. 2009;16(9):1285-92.

44. Radosevic K, Wieland CW, Rodriguez A, Weverling GJ, Mintardjo R, Gillissen G, et al. Protective immune responses to a recombinant adenovirus type 35 tuberculosis vaccine in two mouse strains: CD4 and CD8 T-cell epitope mapping and role of gamma interferon. Infection and Immunity. 2007;75(8):4105-15.

45. Chavda VP, Bezbaruah R, Valu D, Patel B, Kumar A, Prasad S, et al. Adenoviral Vector-Based Vaccine Platform for COVID-19: Current Status. Vaccines. 2023;11(2):432.

46. Gallardo J, Pérez-Illana M, Martín-González N, San Martín C. Adenovirus

Structure: What Is New? Int J Mol Sci. 2021;22(10):5240-56.

47. Davison AJ, Benkő M, Harrach B. Genetic content and evolution of adenoviruses. J Gen Virol. 2003;84(Pt 11):2895-908.

48. Morris SJ, Scott GE, Leppard KN. Adenovirus late-phase infection is controlled by a novel L4 promoter. J Virol. 2010;84(14):7096-104.

49. Christensen JB, Byrd SA, Walker AK, Strahler JR, Andrews PC, Imperiale MJ. Presence of the adenovirus IVa2 protein at a single vertex of the mature virion. J Virol. 2008;82(18):9086-93.

50. Radko S, Jung R, Olanubi O, Pelka P. Effects of Adenovirus Type 5 E1A Isoforms on Viral Replication in Arrested Human Cells. PLoS One. 2015;10(10):e0140124-e.

51. Ferrari R, Pellegrini M, Horwitz GA, Xie W, Berk AJ, Kurdistani SK. Epigenetic reprogramming by adenovirus e1a. Science. 2008;321(5892):1086-8.

52. Ben-Israel H, Kleinberger T. Adenovirus and Cell-Cycle Control. Front Biosci. 2002;7(4):1369-95.

53. Lee CS, Bishop ES, Zhang R, Yu X, Farina EM, Yan S, et al. Adenovirus-mediated gene delivery: Potential applications for gene and cell-based therapies in the new era of personalized medicine. Genes Dis. 2017;4(2):43-63.

54. Zheng L, Lee WH. The retinoblastoma gene: a prototypic and multifunctional tumor suppressor. Exp Cell Res. 2001;264(1):2-18.

55. Jones N, Shenk T. An adenovirus type 5 early gene function regulates expression of other early viral genes. Proc Natl Acad Sci USA. 1979;76(8):3665-9.

56. Leong K, Berk AJ. Adenovirus early region 1A protein increases the number of template molecules transcribed in cell-free extracts. Proc Natl Acad Sci USA.

1986;83(16):5844-8.

57. Berk AJ. Adenovirus promoters and E1A transactivation. Annu Rev Genet. 1986;20(1):45-77.

58. Han J, Sabbatini P, Perez D, Rao L, Modha D, White E. The E1B 19K protein blocks apoptosis by interacting with and inhibiting the p53-inducible and death-promoting Bax protein. Genes Dev. 1996;10(4):461-77.

59. Tarakanova VL, Wold WS. Adenovirus E1A and E1B-19K proteins protect human hepatoma cells from transforming growth factor beta1-induced apoptosis. Virus Research. 2010;147(1):67-76.

60. Hidalgo P, Ip WH, Dobner T, Gonzalez RA. The biology of the adenovirus E1B 55K protein. FEBS Lett. 2019;593(24):3504-17.

61. Martin MED, Berk AJ. Adenovirus E1B 55K Represses p53 Activation In Vitro. J Virol. 1998;72(4):3146-54.

62. Schreiner S, Wimmer P, Sirma H, Everett RD, Blanchette P, Groitl P, et al. Proteasome-dependent degradation of Daxx by the viral E1B-55K protein in human adenovirus-infected cells. J Virol. 2010;84(14):7029-38.

63. Querido E, Blanchette P, Yan Q, Kamura T, Morrison M, Boivin D, et al. Degradation of p53 by adenovirus E4orf6 and E1B55K proteins occurs via a novel mechanism involving a Cullin-containing complex. Genes Dev. 2001;15(23):3104-17.

64. Blanchette P, Cheng CY, Yan Q, Ketner G, Ornelles DA, Dobner T, et al. Both BC-box motifs of adenovirus protein E4orf6 are required to efficiently assemble an E3 ligase complex that degrades p53. Mol Cell Biol. 2004;24(21):9619-29.

65. Herrmann C, Dybas JM, Liddle JC, Price AM, Hayer KE, Lauman R, et al.

Adenovirus-mediated ubiquitination alters protein-RNA binding and aids viral RNA processing. Nat Microbiol. 2020;5(10):1217-31.

66. Wold WS, Toth K. Adenovirus vectors for gene therapy, vaccination and cancer gene therapy. Curr Gene Ther. 2013;13(6):421-33.

67. van der Vliet PC. Adenovirus DNA Replication. In: Doerfler W, Böhm P, editors. The Molecular Repertoire of Adenoviruses II: Molecular Biology of Virus-Cell Interactions. Berlin, Heidelberg: Springer Berlin Heidelberg; 1995. p. 1-30.

68. Chang LS, Shenk T. The adenovirus DNA-binding protein stimulates the rate of transcription directed by adenovirus and adeno-associated virus promoters. J Virol. 1990;64(5):2103-9.

69. Condezo GN, San Martín C. Localization of adenovirus morphogenesis players, together with visualization of assembly intermediates and failed products, favor a model where assembly and packaging occur concurrently at the periphery of the replication center. PLoS Pathog. 2017;13(4):e1006320.

70. Bertzbach LD, Seddar L, von Stromberg K, Ip WH, Dobner T, Hidalgo P. The adenovirus DNA-binding protein DBP. J Virol. 2024;98(2):e0188523.

71. Kleinberger T. En Guard! The Interactions between Adenoviruses and the DNA Damage Response. Viruses. 2020;12(9):996.

72. Pronk R, Stuiver MH, van der Vliet PC. Adenovirus DNA replication: the function of the covalently bound terminal protein. Chromosoma. 1992;102:S39-45.

73. Windheim M, Hilgendorf A, Burgert HG. Immune evasion by adenovirus E3 proteins: exploitation of intracellular trafficking pathways. In: Doerfler W, Böhm P, editors. Adenoviruses: Model and Vectors in Virus-Host Interactions: Immune System,

Oncogenesis, Gene Therapy. Berlin, Heidelberg: Springer Berlin Heidelberg; 2004. p. 29-85.

74. Donovan-Banfield Ia, Turnell AS, Hiscox JA, Leppard KN, Matthews DA. Deep splicing plasticity of the human adenovirus type 5 transcriptome drives virus evolution. Commun Biol. 2020;3(1):1-14.

75. Uchitel J, Kantor B, Smith EC, Mikati MA. Viral-Mediated Gene Replacement Therapy in the Developing Central Nervous System: Current Status and Future Directions. Pediatr Neurol. 2020;110:5-19.

76. Weitzman MD. Functions of the adenovirus E4 proteins and their impact on viral vectors. Front Biosci. 2005;10:1106-17.

77. Boulanger P, Lemay P, Blair GE, Russell WC. Characterization of Adenovirus Protein IX. J Gen Virol. 1979;44(3):783-800.

78. Tollefson AE, Ying B, Doronin K, Sidor PD, Wold WS. Identification of a new human adenovirus protein encoded by a novel late l-strand transcription unit. J Virol. 2007;81(23):12918-26.

79. Ying B, Tollefson AE, Wold WS. Identification of a previously unrecognized promoter that drives expression of the UXP transcription unit in the human adenovirus type 5 genome. J Virol. 2010;84(21):11470-8.

80. Svensson C, Akusjärvi G. Adenovirus VA RNAI: a positive regulator of mRNA translation. Mol Cell Biol. 1984;4(4):736-42.

81. O'Malley RP, Mariano TM, Siekierka J, Mathews MB. A mechanism for the control of protein synthesis by adenovirus VA RNAI. Cell. 1986;44(3):391-400.

82. Andersson MG, Haasnoot PC, Xu N, Berenjian S, Berkhout B, Akusjärvi G.

Suppression of RNA interference by adenovirus virus-associated RNA. J Virol. 2005;79(15):9556-65.

83. Aparicio O, Razquin N, Zaratiegui M, Narvaiza I, Fortes P. Adenovirus virus-associated RNA is processed to functional interfering RNAs involved in virus production. J Virol. 2006;80(3):1376-84.

84. Winter N, D'Halluin JC. Regulation of the biosynthesis of subgroup C adenovirus protein IVa2. J Virol. 1991;65(10):5250-9.

85. Hajikhezri Z, Kaira Y, Schubert E, Darweesh M, Svensson C, Akusjärvi G, et al. Fragile X-Related Protein FXR1 Controls Human Adenovirus Capsid mRNA Metabolism. J Virol. 2023;97(2):e0153922.

86. Shaw AR, Ziff EB. Transcripts from the adenovirus-2 major late promoter yield a single early family of 3' coterminal mRNAs and five late families. Cell. 1980;22(3):905-16.

87. Hasson TB, Soloway PD, Ornelles DA, Doerfler W, Shenk T. Adenovirus L1 52- and 55-kilodalton proteins are required for assembly of virions. J Virol. 1989;63(9):3612-21.

88. Benevento M, Di Palma S, Snijder J, Moyer CL, Reddy VS, Nemerow GR, et al. Adenovirus Composition, Proteolysis, and Disassembly Studied by In-depth Qualitative and Quantitative Proteomics. J Biol Chem. 2014;289(16):11421-30.

89. Mangel WF, San Martín C. Structure, function and dynamics in adenovirus maturation. Viruses. 2014;6(11):4536-70.

90. Wu K, Guimet D, Hearing P. The adenovirus L4-33K protein regulates both late gene expression patterns and viral DNA packaging. J Virol. 2013;87(12):6739-47.

91. Henry LJ, Xia D, Wilke ME, Deisenhofer J, Gerard RD. Characterization of the knob domain of the adenovirus type 5 fiber protein expressed in Escherichia coli. J Virol. 1994;68(8):5239-46.

92. San Martín C. Latest insights on adenovirus structure and assembly. Viruses. 2012;4(5):847-77.

93. Reddy VS. The Role of Hexon Protein as a Molecular Mold in Patterning the Protein IX Organization in Human Adenoviruses. J Mol Biol. 2017;429(18):2747-51.

94. Crosby CM, Barry MA. IIIa deleted adenovirus as a single-cycle genome replicating vector. Virology. 2014;462-463:158-65.

95. Reddy VS, Nemerow GR. Structures and organization of adenovirus cement proteins provide insights into the role of capsid maturation in virus entry and infection. Proc Natl Acad Sci USA. 2014;111(32):11715-20.

96. Pérez-Berná AJ, Marion S, Chichón FJ, Fernández JJ, Winkler DC, Carrascosa JL, et al. Distribution of DNA-condensing protein complexes in the adenovirus core. Nucleic Acids Res. 2015;43(8):4274-83.

97. Kulanayake S, Tikoo SK. Adenovirus Core Proteins: Structure and Function. Viruses. 2021;13(3):388.

98. Jennings MR, Parks RJ. Human Adenovirus Gene Expression and Replication Is Regulated through Dynamic Changes in Nucleoprotein Structure throughout Infection. Viruses. 2023;15(1):161.

99. Ostapchuk P, Suomalainen M, Zheng Y, Boucke K, Greber UF, Hearing P. The adenovirus major core protein VII is dispensable for virion assembly but is essential for lytic infection. PLoS Pathog. 2017;13(6):e1006455.

100. Zhao H, Dahlö M, Isaksson A, Syvänen A-C, Pettersson U. The transcriptome of the adenovirus infected cell. Virology. 2012;424(2):115-28.

101. Bergelson JM, Cunningham JA, Droguett G, Kurt-Jones EA, Krithivas A, Hong JS, et al. Isolation of a common receptor for Coxsackie B viruses and adenoviruses 2 and 5. Science. 1997;275(5304):1320-3.

102. Tomko RP, Xu R, Philipson L. HCAR and MCAR: the human and mouse cellular receptors for subgroup C adenoviruses and group B coxsackieviruses. Proc Natl Acad Sci USA. 1997;94(7):3352-6.

103. Zhang Y, Bergelson JM. Adenovirus receptors. J Virol. 2005;79(19):12125-31.

104. Wickham TJ, Mathias P, Cheresh DA, Nemerow GR. Integrins alpha v beta 3 and alpha v beta 5 promote adenovirus internalization but not virus attachment. Cell. 1993;73(2):309-19.

105. Burckhardt CJ, Suomalainen M, Schoenenberger P, Boucke K, Hemmi S, Greber UF. Drifting motions of the adenovirus receptor CAR and immobile integrins initiate virus uncoating and membrane lytic protein exposure. Cell Host Microbe. 2011;10(2):105-17.

106. Wiethoff CM, Nemerow GR. Adenovirus membrane penetration: Tickling the tail of a sleeping dragon. Virology. 2015;479-480:591-9.

107. Leopold PL, Ferris B, Grinberg I, Worgall S, Hackett NR, Crystal RG. Fluorescent virions: dynamic tracking of the pathway of adenoviral gene transfer vectors in living cells. Hum Gene Ther. 1998;9(3):367-78.

108. Greber UF, Willetts M, Webster P, Helenius A. Stepwise dismantling of adenovirus 2 during entry into cells. Cell. 1993;75(3):477-86.

109. Bauer M, Flatt JW, Seiler D, Cardel B, Emmenlauer M, Boucke K, et al. The

E3 Ubiquitin Ligase Mind Bomb 1 Controls Adenovirus Genome Release at the Nuclear Pore Complex. Cell Rep. 2019;29(12):3785-95.e8.

110. Greber UF, Suomalainen M. Adenovirus entry: Stability, uncoating, and nuclear import. Mol Microbiol. 2022;118(4):309-20.

111. Chatterjee PK, Vayda ME, Flint SJ. Identification of proteins and protein domains that contact DNA within adenovirus nucleoprotein cores by ultraviolet light crosslinking of oligonucleotides 32P-labelled in vivo. J Mol Biol. 1986;188(1):23-37.

112. Strunze S, Engelke Martin F, Wang IH, Puntener D, Boucke K, Schleich S, et al. Kinesin-1-Mediated Capsid Disassembly and Disruption of the Nuclear Pore Complex Promote Virus Infection. Cell Host Microbe. 2011;10(3):210-23.

113. Cassany A, Ragues J, Guan T, Bégu D, Wodrich H, Kann M, et al. Nuclear Import of Adenovirus DNA Involves Direct Interaction of Hexon with an N-Terminal Domain of the Nucleoporin Nup214. J Virol. 2015;89(3):1719-30.

114. Bauer M, Gomez-Gonzalez A, Suomalainen M, Schilling N, Hemmi S, Greber UF. A viral ubiquitination switch attenuates innate immunity and triggers nuclear import of virion DNA and infection. Sci Adv. 2021;7(51):eabl7150.

115. Avgousti DC, Della Fera AN, Otter CJ, Herrmann C, Pancholi NJ, Weitzman MD. Adenovirus Core Protein VII Downregulates the DNA Damage Response on the Host Genome. J Virol. 2017;91(20):e01089-17.

116. Stracker TH, Carson CT, Weitzman MD. Adenovirus oncoproteins inactivate the Mre11-Rad50-NBS1 DNA repair complex. Nature. 2002;418(6895):348-52.

117. Carson CT, Schwartz RA, Stracker TH, Lilley CE, Lee DV, Weitzman MD. The Mre11 complex is required for ATM activation and the G2/M checkpoint. EMBO J.

2003;22(24):6610-20.

118. Lotze MT, Tracey KJ. High-mobility group box 1 protein (HMGB1): nuclear weapon in the immune arsenal. Nat Rev Immunol. 2005;5(4):331-42.

119. Avgousti DC, Herrmann C, Kulej K, Pancholi NJ, Sekulic N, Petrescu J, et al. A core viral protein binds host nucleosomes to sequester immune danger signals. Nature. 2016;535(7610):173-7.

120. Lynch KL, Dillon MR, Bat-Erdene M, Lewis HC, Kaai RJ, Arnold EA, et al. A viral histone-like protein exploits antagonism between linker histones and HMGB proteins to obstruct the cell cycle. Curr Biol. 2021;31(23):5227-37.e7.

121. Komatsu T, Haruki H, Nagata K. Cellular and viral chromatin proteins are positive factors in the regulation of adenovirus gene expression. Nucleic Acids Res. 2011;39(3):889-901.

122. Johnson JS, Osheim YN, Xue Y, Emanuel MR, Lewis PW, Bankovich A, et al. Adenovirus protein VII condenses DNA, represses transcription, and associates with transcriptional activator E1A. J Virol. 2004;78(12):6459-68.

123. Chen J, Morral N, Engel DA. Transcription releases protein VII from adenovirus chromatin. Virology. 2007;369(2):411-22.

124. Haruki H, Gyurcsik B, Okuwaki M, Nagata K. Ternary complex formation between DNA-adenovirus core protein VII and TAF-Ibeta/SET, an acidic molecular chaperone. FEBS Lett. 2003;555(3):521-7.

125. Xue Y, Johnson JS, Ornelles DA, Lieberman J, Engel DA. Adenovirus protein VII functions throughout early phase and interacts with cellular proteins SET and pp32. J Virol. 2005;79(4):2474-83.

126. Ross PJ, Kennedy MA, Christou C, Risco Quiroz M, Poulin KL, Parks RJ. Assembly of helper-dependent adenovirus DNA into chromatin promotes efficient gene expression. J Virol. 2011;85(8):3950-8.

127. Giberson AN, Saha B, Campbell K, Christou C, Poulin KL, Parks RJ. Human adenoviral DNA association with nucleosomes containing histone variant H3.3 during the early phase of infection is not dependent on viral transcription or replication. Biochem Cell Biol. 2018;96(6):797-807.

128. Schwartz U, Komatsu T, Huber C, Lagadec F, Baumgartl C, Silberhorn E, et al. Changes in adenoviral chromatin organization precede early gene activation upon infection. EMBO J. 2023;42(19):e114162.

129. Matsumoto K, Nagata K, Ui M, Hanaoka F. Template activating factor I, a novel host factor required to stimulate the adenovirus core DNA replication. J Biol Chem. 1993;268(14):10582-7.

130. Komatsu T, Dacheux D, Kreppel F, Nagata K, Wodrich H. A Method for Visualization of Incoming Adenovirus Chromatin Complexes in Fixed and Living Cells. PLoS One. 2015;10(9):e0137102.

131. Kawase H, Okuwaki M, Miyaji M, Ohba R, Handa H, Ishimi Y, et al. NAP-I is a functional homologue of TAF-I that is required for replication and transcription of the adenovirus genome in a chromatin-like structure. Genes Cells. 1996;1(12):1045-56.

132. Okuwaki M, Iwamatsu A, Tsujimoto M, Nagata K. Identification of nucleophosmin/B23, an acidic nucleolar protein, as a stimulatory factor for in vitro replication of adenovirus DNA complexed with viral basic core proteins. J Mol Biol. 2001;311(1):41-55.

133. Bannister AJ, Kouzarides T. Regulation of chromatin by histone modifications. Cell Res. 2011;21(3):381-95.

134. Allis CD, Jenuwein T. The molecular hallmarks of epigenetic control. Nat Rev Genet. 2016;17(8):487-500.

135. Cavalieri V. The Expanding Constellation of Histone Post-Translational Modifications in the Epigenetic Landscape. Genes. 2021;12(10).

136. Moore LD, Le T, Fan G. DNA Methylation and Its Basic Function. Neuropsychopharmacol. 2013;38(1):23-38.

137. Greenberg MVC, Bourc'his D. The diverse roles of DNA methylation in mammalian development and disease. Nat Rev Mol Cell Biol. 2019;20(10):590-607.

138. Wei J-W, Huang K, Yang C, Kang C-S. Non-coding RNAs as regulators in epigenetics (Review). Oncol Rep. 2017;37(1):3-9.

139. Wu Y-L, Lin Z-J, Li C-C, Lin X, Shan S-K, Guo B, et al. Epigenetic regulation in metabolic diseases: mechanisms and advances in clinical study. Signal Transduct Target Ther. 2023;8(1):98.

140. Lawrence M, Daujat S, Schneider R. Lateral Thinking: How Histone Modifications Regulate Gene Expression. Trends Genet. 2016;32(1):42-56.

141. Knipe DM, Lieberman PM, Jung JU, McBride AA, Morris KV, Ott M, et al. Snapshots: chromatin control of viral infection. Virology. 2013;435(1):141-56.

142. Milavetz BI, Balakrishnan L. Viral epigenetics. Methods Mol Bio. 2015;1238:569-96.

143. Rehman UU, Ghafoor D, Ullah A, Ahmad R, Hanif S. Epigenetics regulation during virus-host interaction and their effects on the virus and host cell. Microb Pathog.

2023;182:106271.

144. Komatsu T, Nagata K. Replication-uncoupled histone deposition during adenovirus DNA replication. J Virol. 2012;86(12):6701-11.

145. Sergeant A, Tigges MA, Raskas HJ. Nucleosome-like structural subunits of intranuclear parental adenovirus type 2 DNA. J Virol. 1979;29(3):888-98.

146. Daniell E, Groff DE, Fedor MJ. Adenovirus chromatin structure at different stages of infection. Mol Cell Biol. 1981;1(12):1094-105.

147. Beyer AL, Bouton AH, Hodge LD, Miller OL, Jr. Visualization of the major late R strand transcription unit of adenovirus serotype 2. J Mol Biol. 1981;147(2):269-95.

148. Déry CV, Toth M, Brown M, Horvath J, Allaire S, Weber JM. The structure of adenovirus chromatin in infected cells. J Gen Virol. 1985;66(12):2671-84.

149. Tate VE, Philipson L. Parental adenovirus DNA accumulates in nucleosome-like structures in infected cells. Nucleic Acids Res. 1979;6(8):2769-85.

150. Hodge LD, Scharff MD. Effect of adenovirus on host cell DNA synthesis in synchronized cells. Virology. 1969;37(4):554-64.

151. Tallman G, Akers JE, Burlingham BT, Reeck GR. Histone synthesis is not coupled to the replication of adenovirus DNA. Biochem Biophys Res Commun. 1977;79(3):815-22.

152. Saha B, Parks RJ. Histone Deacetylase Inhibitor Suberoylanilide Hydroxamic Acid Suppresses Human Adenovirus Gene Expression and Replication. J Virol. 2019;93(12):e00088-19.

153. Höti N, Chowdhury W, Hsieh J-T, Sachs MD, Lupold SE, Rodriguez R. Valproic Acid, a Histone Deacetylase Inhibitor, Is an Antagonist for Oncolytic Adenoviral Gene

Therapy. Mol Ther. 2006;14(6):768-78.

154. Saha B, Parks RJ. Identification of human adenovirus replication inhibitors from a library of small molecules targeting cellular epigenetic regulators. Virology. 2021;555:102-10.

155. Arbuckle JH, Gardina PJ, Gordon DN, Hickman HD, Yewdell JW, Pierson TC, et al. Inhibitors of the Histone Methyltransferases EZH2/1 Induce a Potent Antiviral State and Suppress Infection by Diverse Viral Pathogens. MBio. 2017;8(4):e01141-17.

156. Smith S, Stillman B. Purification and characterization of CAF-I, a human cell factor required for chromatin assembly during DNA replication in vitro. Cell. 1989;58(1):15-25.

157. Talbert PB, Henikoff S. Histone variants at a glance. J Cell Sci. 2021;134(6):jcs244749.

158. Marcos-Villar L, Pazo A, Nieto A. Influenza Virus and Chromatin: Role of the CHD1 Chromatin Remodeler in the Virus Life Cycle. J Virol. 2016;90(7):3694-707.

159. Ullman AJ, Hearing P. Cellular proteins PML and Daxx mediate an innate antiviral defense antagonized by the adenovirus E4 ORF3 protein. J Virol. 2008;82(15):7325-35.

160. Schreiner S, Bürck C, Glass M, Groitl P, Wimmer P, Kinkley S, et al. Control of human adenovirus type 5 gene expression by cellular Daxx/ATRX chromatin-associated complexes. Nucleic Acids Res. 2013;41(6):3532-50.

161. Crisostomo L, Soriano AM, Mendez M, Graves D, Pelka P. Temporal dynamics of adenovirus 5 gene expression in normal human cells. PLoS One. 2019;14(1):e0211192.

162. Jennings MR, Parks RJ. Antiviral Effects of Curcumin on Adenovirus Replication. Microorganisms. 2020;8(10):1524-40.

163. Stuiver MH, Bergsma WG, Arnberg AC, van Amerongen H, van Grondelle R, van

der Vliet PC. Structural alterations of double-stranded DNA in complex with the adenovirus DNA-binding protein. Implications for its function in DNA replication. J Mol Biol. 1992;225(4):999-1011.

164. Bioinformatics SSIo DNA Strand Displacement Replication. https://viralzone.expasy.org/1940: ViralZone.

165. Zijderveld DC, van der Vliet PC. Helix-destabilizing properties of the adenovirus DNA-binding protein. J Virol. 1994;68(2):1158-64.

166. Dekker J, Kanellopoulos PN, Loonstra AK, van Oosterhout JA, Leonard K, Tucker PA, et al. Multimerization of the adenovirus DNA-binding protein is the driving force for ATP-independent DNA unwinding during strand displacement synthesis. EMBO J. 1997;16(6):1455-63.

167. van der Vliet PC, Keegstra W, Jansz HS. Complex Formation between the Adenovirus Type 5 DNA-Binding Protein and Single-Stranded DNA. Eur J Biochem. 1978;86(2):389-98.

168. Nass K, Frenkel GD. Adenovirus-specific DNA-binding protein inhibits the hydrolysis of DNA by DNase in vitro. J Virol. 1980;35(2):314-9.

169. Nagata K, Guggenheimer RA, Hurwitz J. Adenovirus DNA replication in vitro: synthesis of full-length DNA with purified proteins. Proc Natl Acad Sci USA. 1983;80(14):4266-70.

170. Leegwater PAJ, Rombouts RFA, van der Vliet PC. Adenovirus DNA replication in vitro: Duplication of single-stranded DNA containing a panhandle structure. Biochim Biophys Acta, Gene Struct Expression. 1988;951(2):403-10.

171. Brison O, Kédinger C, Chambon P. Adenovirus DNA template for late transcription

is not a replicative intermediate. J Virol. 1979;32(1):91-7.

172. Pombo A, Ferreira J, Bridge E, Carmo-Fonseca M. Adenovirus replication and transcription sites are spatially separated in the nucleus of infected cells. EMBO J. 1994;13(21):5075-85.

173. Gomez-Gonzalez A, Burkhardt P, Bauer M, Suomalainen M, Mateos JM, Loehr MO, et al. Stepwise virus assembly in the cell nucleus revealed by spatiotemporal click chemistry of DNA replication. Sci Adv. 2024;10(43):eadq7483.

174. Sundquist B, Everitt E, Philipson L, Hoglund S. Assembly of adenoviruses. J Virol. 1973;11(3):449-59.

175. Ishibashi M, Maizel JV, Jr. The polypeptides of adenovirus. V. Young virions, structural intermediate between top components and aged virions. Virology. 1974;57(2):409-24.

176. Khittoo G, Weber J. Genetic analysis of adenovirus type 2. VI. A temperature-sensitive mutant defective for DNA encapsidation. Virology. 1977;81(1):126-37.

177. Weber JM, Déry CV, Mirza MA, Horvath J. Adenovirus DNA synthesis is coupled to virus assembly. Virology. 1985;140(2):351-9.

178. Genoveso MJ, Hisaoka M, Komatsu T, Wodrich H, Nagata K, Okuwaki M. Formation of adenovirus DNA replication compartments and viral DNA accumulation sites by host chromatin regulatory proteins including NPM1. FEBS J. 2020;287(1):205-17.

179. Georgi F, Greber UF. The Adenovirus Death Protein - A small membrane protein controls cell lysis and disease. FEBS Lett. 2020;594(12):1861-78.

180. Samad MA, Okuwaki M, Haruki H, Nagata K. Physical and functional interaction between a nucleolar protein nucleophosmin/B23 and adenovirus basic core proteins. FEBS

Lett. 2007;581(17):3283-8.

181. Burg JL, Schweitzer J, Daniell E. Introduction of superhelical turns into DNA by adenoviral core proteins and chromatin assembly factors. J Virol. 1983;46(3):749-55.

182. Samad MA, Komatsu T, Okuwaki M, Nagata K. B23/nucleophosmin is involved in regulation of adenovirus chromatin structure at late infection stages, but not in virus replication and transcription. J Gen Virol. 2012;93(6):1328-38.

183. Inturi R, Mun K, Singethan K, Schreiner S, Punga T. Human Adenovirus Infection Causes Cellular E3 Ubiquitin Ligase MKRN1 Degradation Involving the Viral Core Protein pVII. J Virol. 2018;92(3):e01154-17.

184. Kwong AD, Rao BG, Jeang KT. Viral and cellular RNA helicases as antiviral targets. Nat Rev Drug Discov. 2005;4(10):845-53.

185. Hajjo R, Sabbah DA, Abusara OH, Kharmah R, Bardaweel S. Targeting Human Proteins for Antiviral Drug Discovery and Repurposing Efforts: A Focus on Protein Kinases. Viruses. 2023;15(2):568.

186. Kaufmann SHE, Dorhoi A, Hotchkiss RS, Bartenschlager R. Host-directed therapies for bacterial and viral infections. Nat Rev Drug Discov. 2018;17(1):35-56.

187. Mahajan S, Choudhary S, Kumar P, Tomar S. Antiviral strategies targeting host factors and mechanisms obliging +ssRNA viral pathogens. Bioorg Med Chem. 2021;46:116356.

188. Roa-Linares VC, Escudero-Flórez M, Vicente-Manzanares M, Gallego-Gómez JC. Host Cell Targets for Unconventional Antivirals against RNA Viruses. Viruses. 2023;15(3):776.

189. Brewster NK, Johnston GC, Singer RA. A bipartite yeast SSRP1 analog comprised

of Pob3 and Nhp6 proteins modulates transcription. Mol Cell Biol. 2001;21(10):3491-502.

190. Formosa T. The role of FACT in making and breaking nucleosomes. Biochim Biophys Acta. 2012;1819(3-4):247-55.

191. Grasser KD. The FACT Histone Chaperone: Tuning Gene Transcription in the Chromatin Context to Modulate Plant Growth and Development. Front Plant Sci. 2020;11:85.

192. Orphanides G, LeRoy G, Chang C-H, Luse DS, Reinberg D. FACT, a Factor that Facilitates Transcript Elongation through Nucleosomes. Cell. 1998;92(1):105-16.

193. Palangat M, Larson DR. Complexity of RNA polymerase II elongation dynamics. Biochim Biophys Acta. 2012;1819(7):667-72.

194. Kujirai T, Kurumizaka H. Transcription through the nucleosome. Curr Opin Struct Biol. 2020;61:42-9.

195. Žumer K, Ochmann M, Aljahani A, Zheenbekova A, Devadas A, Maier KC, et al. FACT maintains chromatin architecture and thereby stimulates RNA polymerase II pausing during transcription in vivo. Mol Cell. 2024;84(11):2053-69.e9.

196. Biswas D, Yu Y, Prall M, Formosa T, Stillman DJ. The yeast FACT complex has a role in transcriptional initiation. Mol Cell Biol. 2005;25(14):5812-22.

197. Ransom M, Williams SK, Dechassa ML, Das C, Linger J, Adkins M, et al. FACT and the proteasome promote promoter chromatin disassembly and transcriptional initiation. J Biol Chem. 2009;284(35):23461-71.

198. Tan BC, Chien CT, Hirose S, Lee SC. Functional cooperation between FACT and MCM helicase facilitates initiation of chromatin DNA replication. EMBO J. 2006;25(17):3975-85.

199. Yang J, Zhang X, Feng J, Leng H, Li S, Xiao J, et al. The Histone Chaperone FACT Contributes to DNA Replication-Coupled Nucleosome Assembly. Cell Rep. 2016;14(5):1128-41.

200. Gurova K, Chang HW, Valieva ME, Sandlesh P, Studitsky VM. Structure and function of the histone chaperone FACT - Resolving FACTual issues. Biochim Biophys Acta - Gene Regul Mech. 2018;1861(9):892-904.

201. Bhakat KK, Ray S. The FAcilitates Chromatin Transcription (FACT) complex: Its roles in DNA repair and implications for cancer therapy. DNA Repair. 2022;109:103246.

202. Belotserkovskaya R, Oh S, Bondarenko VA, Orphanides G, Studitsky VM, Reinberg D. FACT facilitates transcription-dependent nucleosome alteration. Science. 2003;301(5636):1090-3.

203. Wang T, Liu Y, Edwards G, Krzizike D, Scherman H, Luger K. The histone chaperone FACT modulates nucleosome structure by tethering its components. Life Sci Alliance. 2018;1(4):e201800107.

204. Jeronimo C, Robert F. The histone chaperone FACT: a guardian of chromatin structure integrity. Transcription. 2022;13(1-3):16-38.

205. Botstein D, Chervitz SA, Cherry JM. Yeast as a model organism. Science. 1997;277(5330):1259-60.

206. Vanderwaeren L, Dok R, Voordeckers K, Nuyts S, Verstrepen KJ. Saccharomyces cerevisiae as a Model System for Eukaryotic Cell Biology, from Cell Cycle Control to DNA Damage Response. Int J Mol Sci. 2022;23(19):11665.

207. Orphanides G, Wu W-H, Lane WS, Hampsey M, Reinberg D. The chromatin-specific transcription elongation factor FACT comprises human SPT16 and SSRP1

proteins. Nature. 1999;400(6741):284-8.

208. Safina A, Garcia H, Commane M, Guryanova O, Degan S, Kolesnikova K, et al. Complex mutual regulation of facilitates chromatin transcription (FACT) subunits on both mRNA and protein levels in human cells. Cell Cycle. 2013;12(15):2423-34.

209. Saunders A, Werner J, Andrulis ED, Nakayama T, Hirose S, Reinberg D, et al. Tracking FACT and the RNA polymerase II elongation complex through chromatin in vivo. Science. 2003;301(5636):1094-6.

210. Duroux M, Houben A, Růžička K, Friml J, Grasser KD. The chromatin remodelling complex FACT associates with actively transcribed regions of the Arabidopsis genome. Plant J. 2004;40(5):660-71.

211. Jeronimo C, Angel A, Nguyen VQ, Kim JM, Poitras C, Lambert E, et al. FACT is recruited to the +1 nucleosome of transcribed genes and spreads in a Chd1-dependent manner. Mol Cell. 2021;81(17):3542-59.e11.

212. Birch JL, Tan BC, Panov KI, Panova TB, Andersen JS, Owen-Hughes TA, et al. FACT facilitates chromatin transcription by RNA polymerases I and III. EMBO J. 2009;28(7):854-65.

213. Woolford JL, Jr., Baserga SJ. Ribosome biogenesis in the yeast Saccharomyces cerevisiae. Genetics. 2013;195(3):643-81.

214. Lopez FB, Fort A, Tadini L, Probst AV, McHale M, Friel J, et al. Gene dosage compensation of rRNA transcript levels in Arabidopsis thaliana lines with reduced ribosomal gene copy number. Plant cell. 2021;33(4):1135-50.

215. Xiang Y-Y, Wang D-Y, Tanaka M, Igarashi H, Naito Y, Ohtawara Y, et al. Expression of structure-specific recognition protein mRNA in fetal kidney and Fe-

nitrilotriacetate-induced renal carcinoma in the rat. Cancer Lett. 1996;106(2):271-8.

216. Hertel L, De Andrea M, Bellomo G, Santoro P, Landolfo S, Gariglio M. The HMG Protein T160 Colocalizes with DNA Replication Foci and Is Down-regulated during Cell Differentiation. Exp Cell Res. 1999;250(2):313-28.

217. Garcia H, Fleyshman D, Kolesnikova K, Safina A, Commane M, Paszkiewicz G, et al. Expression of FACT in mammalian tissues suggests its role in maintaining of undifferentiated state of cells. Oncotarget. 2011;2(10):783–96.

218. Cao S, Bendall H, Hicks GG, Nashabi A, Sakano H, Shinkai Y, et al. The high-mobility-group box protein SSRP1/T160 is essential for cell viability in day 3.5 mouse embryos. Mol Cell Biol. 2003;23(15):5301-7.

219. Wang J, Zhu X, Dai L, Wang Z, Guan X, Tan X, et al. Supt16 haploinsufficiency causes neurodevelopment disorder by disrupting MAPK pathway in neural stem cells. Hum Mol Genet. 2023;32(5):860-72.

220. Goswami I, Sandlesh P, Stablewski A, Toshkov I, Safina AF, Magnitov M, et al. FACT maintains nucleosomes during transcription and stem cell viability in adult mice. EMBO Rep. 2022;23(4):e53684.

221. Garcia H, Miecznikowski JC, Safina A, Commane M, Ruusulehto A, Kilpinen S, et al. Facilitates chromatin transcription complex is an "accelerator" of tumor transformation and potential marker and target of aggressive cancers. Cell Rep. 2013;4(1):159-73.

222. Shen J, Chen M, Lee D, Law C-T, Wei L, Tsang FH-C, et al. Histone chaperone FACT complex mediates oxidative stress response to promote liver cancer progression. Gut. 2020;69(2):329-42.

223. Martin BJE, Chruscicki AT, Howe LJ. Transcription Promotes the Interaction of the

FAcilitates Chromatin Transactions (FACT) Complex with Nucleosomes in Saccharomyces cerevisiae. Genetics. 2018;210(3):869-81.

224. Liu Y, Zhou K, Zhang N, Wei H, Tan YZ, Zhang Z, et al. FACT caught in the act of manipulating the nucleosome. Nature. 2020;577(7790):426-31.

225. Hsieh F-K, Kulaeva OI, Patel SS, Dyer PN, Luger K, Reinberg D, et al. Histone chaperone FACT action during transcription through chromatin by RNA polymerase II. Proc Natl Acad Sci USA. 2013;110(19):7654-9.

226. Chen P, Dong L, Hu M, Wang Y-Z, Xiao X, Zhao Z, et al. Functions of FACT in Breaking the Nucleosome and Maintaining Its Integrity at the Single-Nucleosome Level. Mol Cell. 2018;71(2):284-93.e4.

227. Formosa T, Winston F. The role of FACT in managing chromatin: disruption, assembly, or repair? Nucleic Acids Res. 2020;48(21):11929-41.

228. Jamai A, Puglisi A, Strubin M. Histone Chaperone Spt16 Promotes Redeposition of the Original H3-H4 Histones Evicted by Elongating RNA Polymerase. Mol Cell. 2009;35(3):377-83.

229. Kaplan CD, Laprade L, Winston F. Transcription elongation factors repress transcription initiation from cryptic sites. Science. 2003;301(5636):1096-9.

230. Mason PB, Struhl K. The FACT complex travels with elongating RNA polymerase II and is important for the fidelity of transcriptional initiation in vivo. Mol Cell Biol. 2003;23(22):8323-33.

231. Chen F, Zhang W, Xie D, Gao T, Dong Z, Lu X. Histone chaperone FACT represses retrotransposon MERVL and MERVL-derived cryptic promoters. Nucleic Acids Res. 2020;48(18):10211-25.

232. Jeronimo C, Poitras C, Robert F. Histone Recycling by FACT and Spt6 during Transcription Prevents the Scrambling of Histone Modifications. Cell Rep. 2019;28(5):1206-18.e8.

233. Haberle V, Stark A. Eukaryotic core promoters and the functional basis of transcription initiation. Nat Rev Mol Cell Biol. 2018;19(10):621-37.

234. Compe E, Egly JM. The Long Road to Understanding RNAPII Transcription Initiation and Related Syndromes. Annu Rev Biochem. 2021;90:193-219.

235. Banerji J, Rusconi S, Schaffner W. Expression of a beta-globin gene is enhanced by remote SV40 DNA sequences. Cell. 1981;27(2 Pt 1):299-308.

236. Tuan D, Kong S, Hu K. Transcription of the hypersensitive site HS2 enhancer in erythroid cells. Proc Natl Acad Sci USA. 1992;89(23):11219-23.

237. Shlyueva D, Stampfel G, Stark A. Transcriptional enhancers: from properties to genome-wide predictions. Nat Rev Genet. 2014;15(4):272-86.

238. Grand RS, Pregnolato M, Baumgartner L, Hoerner L, Burger L, Schübeler D. Genome access is transcription factor-specific and defined by nucleosome position. Mol Cell. 2024;84(18):3455-68.e6.

239. Takahata S, Yu Y, Stillman DJ. FACT and Asf1 regulate nucleosome dynamics and coactivator binding at the HO promoter. Mol Cell. 2009;34(4):405-15.

240. Yu Y, Yarrington RM, Stillman DJ. FACT and Ash1 promote long-range and bidirectional nucleosome eviction at the HO promoter. Nucleic Acids Res. 2020;48(19):10877-89.

241. Schwabish MA, Struhl K. Evidence for eviction and rapid deposition of histones upon transcriptional elongation by RNA polymerase II. Mol Cell Biol. 2004;24(23):10111-

7.

242. Shakya A, Callister C, Goren A, Yosef N, Garg N, Khoddami V, et al. Pluripotency transcription factor Oct4 mediates stepwise nucleosome demethylation and depletion. Mol Cell Biol. 2015;35(6):1014-25.

243. Petrenko N, Jin Y, Dong L, Wong KH, Struhl K. Requirements for RNA polymerase II preinitiation complex formation in vivo. eLife. 2019;8:e43654.

244. Izban MG, Luse DS. Factor-stimulated RNA polymerase II transcribes at physiological elongation rates on naked DNA but very poorly on chromatin templates. J Biol Chem. 1992;267(19):13647-55.

245. Wind M, Reines D. Transcription elongation factor SII. Bioessays. 2000;22(4):327-36.

246. Krogan NJ, Kim M, Ahn SH, Zhong G, Kobor MS, Cagney G, et al. RNA Polymerase II Elongation Factors of Saccharomyces cerevisiae: a Targeted Proteomics Approach. Mol Cell Biol. 2002;22(20):6979-92.

247. Hartzog GA, Fu J. The Spt4-Spt5 complex: a multi-faceted regulator of transcription elongation. Biochim Biophys Acta. 2013;1829(1):105-15.

248. Ehara H, Yokoyama T, Shigematsu H, Yokoyama S, Shirouzu M, Sekine S-i. Structure of the complete elongation complex of RNA polymerase II with basal factors. Science. 2017;357(6354):921-4.

249. Ehara H, Kujirai T, Fujino Y, Shirouzu M, Kurumizaka H, Sekine S-i. Structural insight into nucleosome transcription by RNA polymerase II with elongation factors. Science. 2019;363(6428):744-7.

250. Filipovski M, Soffers JHM, Vos SM, Farnung L. Structural basis of nucleosome

retention during transcription elongation. Science. 2022;376(6599):1313-6.

251. Bondarenko VA, Steele LM, Újvári A, Gaykalova DA, Kulaeva OI, Polikanov YS, et al. Nucleosomes Can Form a Polar Barrier to Transcript Elongation by RNA Polymerase II. Mol Cell. 2006;24(3):469-79.

252. Kulaeva OI, Hsieh FK, Chang HW, Luse DS, Studitsky VM. Mechanism of transcription through a nucleosome by RNA polymerase II. Biochim Biophys Acta. 2013;1829(1):76-83.

253. Azmi IF, Watanabe S, Maloney MF, Kang S, Belsky JA, MacAlpine DM, et al. Nucleosomes influence multiple steps during replication initiation. eLife. 2017;6:e22512.

254. Budhavarapu VN, Chavez M, Tyler JK. How is epigenetic information maintained through DNA replication? Epigenetics Chromatin. 2013;6(1):32.

255. Stewart-Morgan KR, Petryk N, Groth A. Chromatin replication and epigenetic cell memory. Nat Cell Biol. 2020;22(4):361-71.

256. Shibahara K, Stillman B. Replication-dependent marking of DNA by PCNA facilitates CAF-1-coupled inheritance of chromatin. Cell. 1999;96(4):575-85.

257. Zhang K, Gao Y, Li J, Burgess R, Han J, Liang H, et al. A DNA binding winged helix domain in CAF-1 functions with PCNA to stabilize CAF-1 at replication forks. Nucleic Acids Res. 2016;44(11):5083-94.

258. Groth A, Corpet A, Cook AJ, Roche D, Bartek J, Lukas J, et al. Regulation of replication fork progression through histone supply and demand. Science. 2007;318(5858):1928-31.

259. Huang H, Strømme CB, Saredi G, Hödl M, Strandsby A, González-Aguilera C, et al. A unique binding mode enables MCM2 to chaperone histones H3–H4 at replication

forks. Nat Struct Mol Biol. 2015;22(8):618-26.

260. Richet N, Liu D, Legrand P, Velours C, Corpet A, Gaubert A, et al. Structural insight into how the human helicase subunit MCM2 may act as a histone chaperone together with ASF1 at the replication fork. Nucleic Acids Res. 2015;43(3):1905-17.

261. Zasadzińska E, Huang J, Bailey AO, Guo LY, Lee NS, Srivastava S, et al. Inheritance of CENP-A Nucleosomes during DNA Replication Requires HJURP. Dev Cell. 2018;47(3):348-62.e7.

262. Tan BC, Liu H, Lin CL, Lee SC. Functional cooperation between FACT and MCM is coordinated with cell cycle and differential complex formation. J Biomed Sci. 2010;17(1):11.

263. Prendergast L, Hong E, Safina A, Poe D, Gurova K. Histone chaperone FACT is essential to overcome replication stress in mammalian cells. Oncogene. 2020;39(28):5124-37.

264. VanDemark AP, Blanksma M, Ferris E, Heroux A, Hill CP, Formosa T. The structure of the yFACT Pob3-M domain, its interaction with the DNA replication factor RPA, and a potential role in nucleosome deposition. Mol Cell. 2006;22(3):363-74.

265. Liu S, Xu Z, Leng H, Zheng P, Yang J, Chen K, et al. RPA binds histone H3-H4 and functions in DNA replication-coupled nucleosome assembly. Science. 2017;355(6323):415-20.

266. Krohn NM, Stemmer C, Fojan P, Grimm R, Grasser KD. Protein kinase CK2 phosphorylates the high mobility group domain protein SSRP1, inducing the recognition of UV-damaged DNA. J Biol Chem. 2003;278(15):12710-5.

267. Kari V, Shchebet A, Neumann H, Johnsen SA. The H2B ubiquitin ligase RNF40

cooperates with SUPT16H to induce dynamic changes in chromatin structure during DNA double-strand break repair. Cell Cycle. 2011;10(20):3495-504.

268. Charles Richard JL, Shukla MS, Menoni H, Ouararhni K, Lone IN, Roulland Y, et al. FACT Assists Base Excision Repair by Boosting the Remodeling Activity of RSC. PLoS Genet. 2016;12(7):e1006221.

269. Dinant C, Ampatziadis-Michailidis G, Lans H, Tresini M, Lagarou A, Grosbart M, et al. Enhanced Chromatin Dynamics by FACT Promotes Transcriptional Restart after UV-Induced DNA Damage. Mol Cell. 2013;51(4):469-79.

270. Wienholz F, Zhou D, Turkyilmaz Y, Schwertman P, Tresini M, Pines A, et al. FACT subunit Spt16 controls UVSSA recruitment to lesion-stalled RNA Pol II and stimulates TC-NER. Nucleic Acids Res. 2019;47(8):4011-25.

271. Keller DM, Zeng X, Wang Y, Zhang QH, Kapoor M, Shu H, et al. A DNA Damage-Induced p53 Serine 392 Kinase Complex Contains CK2, hSpt16, and SSRP1. Mol Cell. 2001;7(2):283-92.

272. Li Y, Keller DM, Scott JD, Lu H. CK2 phosphorylates SSRP1 and inhibits its DNA-binding activity. J Biol Chem. 2005;280(12):11869-75.

273. Tsunaka Y, Toga J, Yamaguchi H, Tate S, Hirose S, Morikawa K. Phosphorylated intrinsically disordered region of FACT masks its nucleosomal DNA binding elements. J Biol Chem. 2009;284(36):24610-21.

274. Mah LJ, El-Osta A, Karagiannis TC. γH2AX: a sensitive molecular marker of DNA damage and repair. Leukemia. 2010;24(4):679-86.

275. Prabhu KS, Kuttikrishnan S, Ahmad N, Habeeba U, Mariyam Z, Suleman M, et al. H2AX: A key player in DNA damage response and a promising target for cancer therapy.

Biomed Pharmacother. 2024;175:116663.

276. Dejmek J, Iglehart JD, Lazaro JB. DNA-dependent protein kinase (DNA-PK)-dependent cisplatin-induced loss of nucleolar facilitator of chromatin transcription (FACT) and regulation of cisplatin sensitivity by DNA-PK and FACT. Mol Cancer Res. 2009;7(4):581-91.

277. Heo K, Kim H, Choi SH, Choi J, Kim K, Gu J, et al. FACT-Mediated Exchange of Histone Variant H2AX Regulated by Phosphorylation of H2AX and ADP-Ribosylation of Spt16. Mol Cell. 2008;30(1):86-97.

278. Kari V, Shchebet A, Neumann H, Johnsen SA. The H2B ubiquitin ligase RNF40 cooperates with SUPT16H to induce dynamic changes in chromatin structure during DNA double-strand break repair. Cell Cycle. 2011;10(20):3495-504.

279. Song H, Zeng J, Roychoudhury S, Biswas P, Mohapatra B, Ray S, et al. Targeting Histone Chaperone FACT Complex Overcomes 5-Fluorouracil Resistance in Colon Cancer. Mol Cancer Ther. 2020;19(1):258-69.

280. Gao Y, Li C, Wei L, Teng Y, Nakajima S, Chen X, et al. SSRP1 Cooperates with PARP and XRCC1 to Facilitate Single-Strand DNA Break Repair by Chromatin Priming. Cancer Res. 2017;77(10):2674-85.

281. Kumari A, Mazina OM, Shinde U, Mazin AV, Lu H. A role for SSRP1 in recombination-mediated DNA damage response. Journal of Cellular Biochemistry. 2009;108(2):508-18.

282. Rex EA, Seo D, Chappidi S, Pinkham C, Brito Oliveira S, Embry A, et al. FEAR antiviral response pathway is independent of interferons and countered by poxvirus proteins. Nat Microbiol. 2024;9(4):988-1006.

283. Huang H, Santoso N, Power D, Simpson S, Dieringer M, Miao H, et al. FACT Proteins, SUPT16H and SSRP1, Are Transcriptional Suppressors of HIV-1 and HTLV-1 That Facilitate Viral Latency. J Biol Chem. 2015;290(45):27297-310.

284. Lopez AP, Kugelman JR, Garcia-Rivera J, Urias E, Salinas SA, Fernandez-Zapico ME, et al. The Structure-Specific Recognition Protein 1 Associates with Lens Epithelium-Derived Growth Factor Proteins and Modulates HIV-1 Replication. J Mol Biol. 2016;428(14):2814-31.

285. Winans S, Larue RC, Abraham CM, Shkriabai N, Skopp A, Winkler D, et al. The FACT Complex Promotes Avian Leukosis Virus DNA Integration. J Virol. 2017;91(7):e00082-17.

286. Gasparian AV, Burkhart CA, Purmal AA, Brodsky L, Pal M, Saranadasa M, et al. Curaxins: anticancer compounds that simultaneously suppress NF-κB and activate p53 by targeting FACT. Sci Transl Med. 2011;3(95):95ra74.

287. Jin M-Z, Xia B-R, Xu Y, Jin W-L. Curaxin CBL0137 Exerts Anticancer Activity via Diverse Mechanisms. Front Oncol. 2018;8:1-6.

288. Zhou D, Wu Z, Park JG, Fiches GN, Li TW, Ma Q, et al. FACT subunit SUPT16H associates with BRD4 and contributes to silencing of interferon signaling. Nucleic Acids Res. 2022;50(15):8700-18.

289. O'Connor CM, Nukui M, Gurova KV, Murphy EA. Inhibition of the FACT Complex Reduces Transcription from the Human Cytomegalovirus Major Immediate Early Promoter in Models of Lytic and Latent Replication. J Virol. 2016;90(8):4249-53.

290. Hu J, Liu E, Renne R. Involvement of SSRP1 in latent replication of Kaposi's sarcoma-associated herpesvirus. J Virol. 2009;83(21):11051-63.

291. Fox HL, Dembowski JA, DeLuca NA. A Herpesviral Immediate Early Protein Promotes Transcription Elongation of Viral Transcripts. MBio. 2017;8(3):e00745-17.

292. Liu S, Maruzuru Y, Takeshima K, Koyanagi N, Kato A, Kawaguchi Y. Impact of the interaction between herpes simplex virus 1 ICP22 and FACT on viral gene expression and pathogenesis. J Virol. 2024;98(8):e00737-24.

293. Hidalgo P, Torres A, Jean Beltran PM, López-Leal G, Bertzbach LD, Dobner T, et al. The protein composition of human adenovirus replication compartments. MBio. 2024:e0214424.

294. Luzhin A, Rajan P, Safina A, Leonova K, Stablewski A, Wang J, et al. Comparison of cell response to chromatin and DNA damage. Nucleic Acids Res. 2023;51(21):11836-55.

295. Kantidze OL, Luzhin AV, Nizovtseva EV, Safina A, Valieva ME, Golov AK, et al. The anti-cancer drugs curaxins target spatial genome organization. Nat Commun. 2019;10(1):1441.

296. Volokh OI, Sivkina AL, Moiseenko AV, Popinako AV, Karlova MG, Valieva ME, et al. Mechanism of curaxin-dependent nucleosome unfolding by FACT. Front Mol Biosci. 2022;9:1048117.

297. Chang HW, Valieva ME, Safina A, Chereji RV, Wang J, Kulaeva OI, et al. Mechanism of FACT removal from transcribed genes by anticancer drugs curaxins. Sci Adv. 2018;4(11):eaav2131.

298. Safina A, Cheney P, Pal M, Brodsky L, Ivanov A, Kirsanov K, et al. FACT is a sensor of DNA torsional stress in eukaryotic cells. Nucleic Acids Res. 2017;45(4):1925-45.

299. Espinoza JA, Kanellis DC, Saproo S, Leal K, Martinez Johana F, Bartek J, et al. Chromatin damage generated by DNA intercalators leads to degradation of RNA Polymerase II. Nucleic Acids Res. 2024;52(8):4151–66.

300. Carter DR, Murray J, Cheung BB, Gamble L, Koach J, Tsang J, et al. Therapeutic targeting of the MYC signal by inhibition of histone chaperone FACT in neuroblastoma. Sci Transl Med. 2015;7(312):312ra176.

301. Dermawan JK, Hitomi M, Silver DJ, Wu Q, Sandlesh P, Sloan AE, et al. Pharmacological Targeting of the Histone Chaperone Complex FACT Preferentially Eliminates Glioblastoma Stem Cells and Prolongs Survival in Preclinical Models. Cancer Res. 2016;76(8):2432-42.

302. Kim M, Neznanov N, Wilfong CD, Fleyshman DI, Purmal AA, Haderski G, et al. Preclinical Validation of a Single-Treatment Infusion Modality That Can Eradicate Extremity Melanomas. Cancer Res. 2016;76(22):6620-30.

303. Barone TA, Burkhart CA, Safina A, Haderski G, Gurova KV, Purmal AA, et al. Anticancer drug candidate CBL0137, which inhibits histone chaperone FACT, is efficacious in preclinical orthotopic models of temozolomide-responsive and -resistant glioblastoma. Neuro-Oncol. 2017;19(2):186-96.

304. De S, Lindner DJ, Coleman CJ, Wildey G, Dowlati A, Stark GR. The FACT inhibitor CBL0137 Synergizes with Cisplatin in Small-Cell Lung Cancer by Increasing NOTCH1 Expression and Targeting Tumor-Initiating Cells. Cancer Res. 2018;78(9):2396-406.

305. Yang C, Wang Z-Q, Zhang Z-C, Lou G, Jin W-L. CBL0137 activates ROS/BAX signaling to promote caspase-3/GSDME-dependent pyroptosis in ovarian cancer cells.

Biomed Pharmacother. 2023;161:114529.

306. Fetisov TI, Borunova AA, Antipova AS, Antoshina EE, Trukhanova LS, Gorkova TG, et al. Targeting Features of Curaxin CBL0137 on Hematological Malignancies In Vitro and In Vivo. Biomedicines. 2023;11(1):230.

307. Pearson S, Blance R, Yan F, Hsieh YC, Geary B, Amaral FMR, et al. Identification of curaxin as a potential new therapeutic for JAK2 V617F mutant patients. PLoS One. 2023;18(5):e0286412.

308. Jean MJ, Hayashi T, Huang H, Brennan J, Simpson S, Purmal A, et al. Curaxin CBL0100 Blocks HIV-1 Replication and Reactivation through Inhibition of Viral Transcriptional Elongation. Front Microbiol. 2017;8:2007.

309. Jean MJ, Zhou D, Fiches G, Kong W, Huang H, Purmal A, et al. Curaxin CBL0137 has the potential to reverse HIV-1 latency. J Med Virol. 2019;91(8):1571-6.

310. Carlos-Reyes Á, López-González JS, Meneses-Flores M, Gallardo-Rincón D, Ruíz-García E, Marchat LA, et al. Dietary Compounds as Epigenetic Modulating Agents in Cancer. Front Genet. 2019;10.

311. El Omari N, Bakrim S, Bakha M, Lorenzo JM, Rebezov M, Shariati MA, et al. Natural Bioactive Compounds Targeting Epigenetic Pathways in Cancer: A Review on Alkaloids, Terpenoids, Quinones, and Isothiocyanates. Nutrients. 2021;13(11):3714.

312. Hassan F-u, Rehman MS-u, Khan MS, Ali MA, Javed A, Nawaz A, et al. Curcumin as an Alternative Epigenetic Modulator: Mechanism of Action and Potential Effects. Front Genet. 2019;10(514).

313. Wang Y-J, Pan M-H, Cheng A-L, Lin L-I, Ho Y-S, Hsieh C-Y, et al. Stability of curcumin in buffer solutions and characterization of its degradation products. J Pharm

Biomed Anal. 1997;15(12):1867-76.

314. Lee W-H, Loo C-Y, Bebawy M, Luk F, Mason RS, Rohanizadeh R. Curcumin and its derivatives: their application in neuropharmacology and neuroscience in the 21st century. Curr Neuropharmacol. 2013;11(4):338-78.

315. Kotha RR, Luthria DL. Curcumin: Biological, Pharmaceutical, Nutraceutical, and Analytical Aspects. Molecules. 2019;24(16):2930.

316. Kocaadam B, Şanlier N. Curcumin, an active component of turmeric (Curcuma longa), and its effects on health. Crit Rev Food Sci Nutr. 2017;57(13):2889-95.

317. Sidhu GS, Singh AK, Thaloor D, Banaudha KK, Patnaik GK, Srimal RC, et al. Enhancement of wound healing by curcumin in animals. Wound Repair Regen. 1998;6(2):167-77.

318. Wilken R, Veena MS, Wang MB, Srivatsan ES. Curcumin: A review of anti-cancer properties and therapeutic activity in head and neck squamous cell carcinoma. Mol Cancer. 2011;10:12.

319. Kunnumakkara AB, Bordoloi D, Padmavathi G, Monisha J, Roy NK, Prasad S, et al. Curcumin, the golden nutraceutical: multitargeting for multiple chronic diseases. Br J Pharmacol. 2017;174(11):1325-48.

320. Yang Y, Wu X, Wei Z, Dou Y, Zhao D, Wang T, et al. Oral curcumin has anti-arthritic efficacy through somatostatin generation via cAMP/PKA and Ca2+/CaMKII signaling pathways in the small intestine. Pharmacol Res. 2015;95-96:71-81.

321. Jin H, Qiao F, Wang Y, Xu Y, Shang Y. Curcumin inhibits cell proliferation and induces apoptosis of human non-small cell lung cancer cells through the upregulation of miR-192-5p and suppression of PI3K/Akt signaling pathway. Oncol Rep.

2015;34(5):2782-9.

322. Chen C, Johnston TD, Jeon H, Gedaly R, McHugh PP, Burke TG, et al. An in vitro study of liposomal curcumin: Stability, toxicity and biological activity in human lymphocytes and Epstein-Barr virus-transformed human B-cells. Int J Pharm. 2009;366(1):133-9.

323. Gandapu U, Chaitanya RK, Kishore G, Reddy RC, Kondapi AK. Curcumin-loaded apotransferrin nanoparticles provide efficient cellular uptake and effectively inhibit HIV-1 replication in vitro. PLoS One. 2011;6(8):e23388-e.

324. Bhullar KS, Jha A, Youssef D, Rupasinghe HPV. Curcumin and its carbocyclic analogs: structure-activity in relation to antioxidant and selected biological properties. Molecules. 2013;18(5):5389-404.

325. Kumari N, Kulkarni AA, Lin X, McLean C, Ammosova T, Ivanov A, et al. Inhibition of HIV-1 by curcumin A, a novel curcumin analog. Drug Des Devel Ther. 2015;9:5051-60.

326. Mirani A, Kundaikar H, Velhal S, Patel V, Bandivdekar A, Degani M, et al. Tetrahydrocurcumin-loaded vaginal nanomicrobicide for prophylaxis of HIV/AIDS: in silico study, formulation development, and in vitro evaluation. Drug Deliv Transl Res. 2019;9(4):828-47.

327. Hegde M, Girisa S, BharathwajChetty B, Vishwa R, Kunnumakkara AB. Curcumin Formulations for Better Bioavailability: What We Learned from Clinical Trials Thus Far? ACS Omega. 2023;8(12):10713-46.

328. Patel SS, Acharya A, Ray RS, Agrawal R, Raghuwanshi R, Jain P. Cellular and molecular mechanisms of curcumin in prevention and treatment of disease. Crit Rev Food

Sci Nutr. 2020;60(6):887-939.

329. Sadeghi M, Dehnavi S, Asadirad A, Xu S, Majeed M, Jamialahmadi T, et al. Curcumin and chemokines: mechanism of action and therapeutic potential in inflammatory diseases. Inflammopharmacology. 2023;31(3):1069-93.

330. Wang W, Li M, Wang L, Chen L, Goh B-C. Curcumin in cancer therapy: Exploring molecular mechanisms and overcoming clinical challenges. Cancer Lett. 2023;570:216332.

331. Borges GA, Elias ST, Amorim B, de Lima CL, Coletta RD, Castilho RM, et al. Curcumin downregulates the PI3K–AKT–mTOR pathway and inhibits growth and progression in head and neck cancer cells. Phytother Res. 2020;34(12):3311-24.

332. Wang Z, Liu F, Liao W, Yu L, Hu Z, Li M, et al. Curcumin suppresses glioblastoma cell proliferation by p-AKT/mTOR pathway and increases the PTEN expression. Archives of Biochemistry and Biophysics. 2020;689:108412.

333. Gonzales AM, Orlando RA. Curcumin and resveratrol inhibit nuclear factor-kappaB-mediated cytokine expression in adipocytes. Nutrition & Metabolism. 2008;5(1):17.

334. Dai J, Gu L, Su Y, Wang Q, Zhao Y, Chen X, et al. Inhibition of curcumin on influenza A virus infection and influenzal pneumonia via oxidative stress, TLR2/4, p38/JNK MAPK and NF-κB pathways. Int Immunopharmacol. 2018;54:177-87.

335. Ghasemi F, Shafiee M, Banikazemi Z, Pourhanifeh MH, Khanbabaei H, Shamshirian A, et al. Curcumin inhibits NF-kB and Wnt/β-catenin pathways in cervical cancer cells. Path Res Pract. 2019;215(10):152556.

336. Gogada R, Amadori M, Zhang H, Jones A, Verone A, Pitarresi J, et al. Curcumin

induces Apaf-1-dependent, p21-mediated caspase activation and apoptosis. Cell Cycle. 2011;10(23):4128-37.

337. Ferguson BS, Nam H, Morrison RF. Curcumin Inhibits 3T3-L1 Preadipocyte Proliferation by Mechanisms Involving Post-transcriptional p27 Regulation. Biochem Biophys Rep. 2016;5:16-21.

338. Hu A, Huang JJ, Zhang JF, Dai WJ, Li RL, Lu ZY, et al. Curcumin induces G2/M cell cycle arrest and apoptosis of head and neck squamous cell carcinoma in vitro and in vivo through ATM/Chk2/p53-dependent pathway. Oncotarget. 2017;8(31):50747-60.

339. Patiño-Morales CC, Soto-Reyes E, Arechaga-Ocampo E, Ortiz-Sánchez E, Antonio-Véjar V, Pedraza-Chaverri J, et al. Curcumin stabilizes p53 by interaction with NAD(P)H:quinone oxidoreductase 1 in tumor-derived cell lines. Redox Biol. 2020;28:101320.

340. Ming T, Tao Q, Tang S, Zhao H, Yang H, Liu M, et al. Curcumin: An epigenetic regulator and its application in cancer. Biomed Pharmacother. 2022;156:113956.

341. Liu H-l, Chen Y, Cui G-h, Zhou J-f. Curcumin, a potent anti-tumor reagent, is a novel histone deacetylase inhibitor regulating B-NHL cell line Raji proliferation. Acta Pharmacol Sin. 2005;26(5):603-9.

342. Wu Q, Chen Y, Li X. HDAC1 expression and effect of curcumin on proliferation of Raji cells. J Huazhong Univ Sci Technolog Med Sci. 2006;26(2):199-201, 10.

343. Chen Y, Shu W, Chen W, Wu Q, Liu H, Cui G. Curcumin, both Histone Deacetylase and p300/CBP-Specific Inhibitor, Represses the Activity of Nuclear Factor Kappa B and Notch 1 in Raji Cells. Basic Clin Pharmacol Toxicol. 2007;101(6):427-33.

344. Lee SJ, Krauthauser C, Maduskuie V, Fawcett PT, Olson JM, Rajasekaran SA.

Curcumin-induced HDAC inhibition and attenuation of medulloblastoma growth in vitro and in vivo. BMC cancer. 2011;11:144.

345. Roy M, Mukherjee S, Sarkar R, Biswas J. Curcumin Sensitizes Chemotherapeutic Drugs Via Modulation of PKC, telomerase, NF-κB and HDAC in Breast Cancer. Ther Deliv. 2011;2(10):1275-93.

346. Shu L, Khor TO, Lee JH, Boyanapalli SS, Huang Y, Wu TY, et al. Epigenetic CpG demethylation of the promoter and reactivation of the expression of Neurog1 by curcumin in prostate LNCaP cells. AAPS J. 2011;13(4):606-14.

347. Chen CQ, Yu K, Yan QX, Xing CY, Chen Y, Yan Z, et al. Pure curcumin increases the expression of SOCS1 and SOCS3 in myeloproliferative neoplasms through suppressing class I histone deacetylases. Carcinogenesis. 2013;34(7):1442-9.

348. Bhullar KS, Jha A, Rupasinghe HP. Novel carbocyclic curcumin analog CUR3d modulates genes involved in multiple apoptosis pathways in human hepatocellular carcinoma cells. Chem Biol Interact. 2015;242:107-22.

349. Guo Y, Shu L, Zhang C, Su ZY, Kong AN. Curcumin inhibits anchorage-independent growth of HT29 human colon cancer cells by targeting epigenetic restoration of the tumor suppressor gene DLEC1. Biochem Pharmacol. 2015;94(2):69-78.

350. Somsakeesit L-o, Senawong T, Kumboonma P, Saenglee S, Samankul A, Senawong G, et al. Influence of side-chain changes on histone deacetylase inhibitory and cytotoxicity activities of curcuminoid derivatives. Bioorg Med Chem Lett. 2020;30(11):127171.

351. Meja KK, Rajendrasozhan S, Adenuga D, Biswas SK, Sundar IK, Spooner G, et al. Curcumin restores corticosteroid function in monocytes exposed to oxidants by maintaining HDAC2. Am J Respir Cell Mol Biol. 2008;39(3):312-23.

352. Yun JM, Jialal I, Devaraj S. Epigenetic regulation of high glucose-induced proinflammatory cytokine production in monocytes by curcumin. J Nutr Biochem. 2011;22(5):450-8.

353. Balasubramanyam K, Varier RA, Altaf M, Swaminathan V, Siddappa NB, Ranga U, et al. Curcumin, a Novel p300/CREB-binding Protein-specific Inhibitor of Acetyltransferase, Represses the Acetylation of Histone/Nonhistone Proteins and Histone Acetyltransferase-dependent Chromatin Transcription. J Biol Chem. 2004;279(49):51163-71.

354. Sharma N, Nyborg JK. The coactivators CBP/p300 and the histone chaperone NAP1 promote transcription-independent nucleosome eviction at the HTLV-1 promoter. Proc Natl Acad Sci USA. 2008;105(23):7959-63.

355. Ogiwara H, Ui A, Otsuka A, Satoh H, Yokomi I, Nakajima S, et al. Histone acetylation by CBP and p300 at double-strand break sites facilitates SWI/SNF chromatin remodeling and the recruitment of non-homologous end joining factors. Oncogene. 2011;30(18):2135-46.

356. Ardebili A, Pouriayevali MH, Aleshikh S, Zahani M, Ajorloo M, Izanloo A, et al. Antiviral Therapeutic Potential of Curcumin: An Update. Molecules. 2021;26(22):6994.

357. Azarkar S, Abedi M, Lavasani ASO, Ammameh AH, Goharipanah F, Baloochi K, et al. Curcumin as a natural potential drug candidate against important zoonotic viruses and prions: A narrative review. Phytother Res. 2024;38(6):3080-121.

358. Sui Z, Salto R, Li J, Craik C, Ortiz de Montellano PR. Inhibition of the HIV-1 and HIV-2 proteases by curcumin and curcumin boron complexes. Bioorg Med Chem. 1993;1(6):415-22.

359. Ferreira VH, Nazli A, Dizzell SE, Mueller K, Kaushic C. The anti-inflammatory activity of curcumin protects the genital mucosal epithelial barrier from disruption and blocks replication of HIV-1 and HSV-2. PLoS One. 2015;10(4):e0124903-e.

360. Ali A, Banerjea AC. Curcumin inhibits HIV-1 by promoting Tat protein degradation. Sci Rep. 2016;6:27539.

361. Chen D-Y, Shien J-H, Tiley L, Chiou S-S, Wang S-Y, Chang T-J, et al. Curcumin inhibits influenza virus infection and haemagglutination activity. Food Chem. 2010;119(4):1346-51.

362. Richart SM, Li YL, Mizushina Y, Chang YY, Chung TY, Chen GH, et al. Synergic effect of curcumin and its structural analogue (Monoacetylcurcumin) on anti-influenza virus infection. J Food Drug Anal. 2018;26(3):1015-23.

363. Balasubramanian A, Pilankatta R, Teramoto T, Sajith AM, Nwulia E, Kulkarni A, et al. Inhibition of dengue virus by curcuminoids. Antivir Res. 2019;162:71-8.

364. Goc A, Sumera W, Rath M, Niedzwiecki A. Phenolic compounds disrupt spike-mediated receptor-binding and entry of SARS-CoV-2 pseudo-virions. PLoS One. 2021;16(6):e0253489.

365. Sharma VK, Prateeksha, Singh SP, Singh BN, Rao CV, Barik SK. Nanocurcumin Potently Inhibits SARS-CoV-2 Spike Protein-Induced Cytokine Storm by Deactivation of MAPK/NF-κB Signaling in Epithelial Cells. ACS Appl Bio Mater. 2022;5(2):483-91.

366. Emam MH, Mahmoud MI, El-Guendy N, Loutfy SA. Establishment of in-house assay for screening of anti-SARS-CoV-2 protein inhibitors. AMB Express. 2024;14(1):104.

367. Bormann M, Alt M, Schipper L, van de Sand L, Le-Trilling VTK, Rink L, et al.

Turmeric Root and Its Bioactive Ingredient Curcumin Effectively Neutralize SARS-CoV-2 In Vitro. Viruses. 2021;13(10):1914.

368. Kandeil A, Mostafa A, Kutkat O, Moatasim Y, Al-Karmalawy AA, Rashad AA, et al. Bioactive Polyphenolic Compounds Showing Strong Antiviral Activities against Severe Acute Respiratory Syndrome Coronavirus 2. Pathogens. 2021;10(6):758.

369. Marín-Palma D, Tabares-Guevara JH, Zapata-Cardona MI, Flórez-Álvarez L, Yepes LM, Rugeles MT, et al. Curcumin Inhibits In Vitro SARS-CoV-2 Infection In Vero E6 Cells through Multiple Antiviral Mechanisms. Molecules. 2021;26(22):6900.

370. Nicoliche T, Bartolomeo CS, Lemes RMR, Pereira GC, Nunes TA, Oliveira RB, et al. Antiviral, anti-inflammatory and antioxidant effects of curcumin and curcuminoids in SH-SY5Y cells infected by SARS-CoV-2. Sci Rep. 2024;14(1):10696.

371. Teli DM, Shah MB, Chhabria MT. In silico Screening of Natural Compounds as Potential Inhibitors of SARS-CoV-2 Main Protease and Spike RBD: Targets for COVID-19. Front Mol Biosci. 2020;7:599079.

372. Bahun M, Jukić M, Oblak D, Kranjc L, Bajc G, Butala M, et al. Inhibition of the SARS-CoV-2 3CL(pro) main protease by plant polyphenols. Food Chem. 2022;373(Part B):131594.

373. Naderi Beni R, Elyasi-Ebli P, Gharaghani S, Seyedarabi A. In silico studies of anti-oxidative and hot temperament-based phytochemicals as natural inhibitors of SARS-CoV-2 Mpro. PLoS One. 2023;18(11):e0295014.

374. Thongsri P, Pewkliang Y, Borwornpinyo S, Wongkajornsilp A, Hongeng S, Sa-Ngiamsuntorn K. Curcumin inhibited hepatitis B viral entry through NTCP binding. Sci Rep. 2021;11(1):19125.

375. Bourne KZ, Bourne N, Reising SF, Stanberry LR. Plant products as topical microbicide candidates: assessment of in vitro and in vivo activity against herpes simplex virus type 2. Antivir Res. 1999;42(3):219-26.

376. Kutluay SB, Doroghazi J, Roemer ME, Triezenberg SJ. Curcumin inhibits herpes simplex virus immediate-early gene expression by a mechanism independent of p300/CBP histone acetyltransferase activity. Virology. 2008;373(2):239-47.

377. Li H, Zhong C, Wang Q, Chen W, Yuan Y. Curcumin is an APE1 redox inhibitor and exhibits an antiviral activity against KSHV replication and pathogenesis. Antivir Res. 2019;167:98-103.

378. Lv Y, An Z, Chen H, Wang Z, Liu L. Mechanism of curcumin resistance to human cytomegalovirus in HELF cells. BMC Complement Med Ther. 2014;14:284.

379. Lv Y, Gong L, Wang Z, Han F, Liu H, Lu X, et al. Curcumin inhibits human cytomegalovirus by downregulating heat shock protein 90. Mol Med Rep. 2015;12(3):4789-93.

380. Butt AL, Chodosh J. Adenoviral Keratoconjunctivitis in a Tertiary Care Eye Clinic. Cornea. 2006;25(2):199-202.

381. Dhingra A, Hage E, Ganzenmueller T, Böttcher S, Hofmann J, Hamprecht K, et al. Molecular Evolution of Human Adenovirus (HAdV) Species C. Sci Rep. 2019;9.

382. Lenaerts L, De Clercq E, Naesens L. Clinical features and treatment of adenovirus infections. Rev Med Virol. 2008;18(6):357-74.

383. Izzedine H, Launay-Vacher V, Deray G. Antiviral Drug-Induced Nephrotoxicity. Am J Kidney Dis. 2005;45(5):804-17.

384. Nagafuji K, Aoki K, Henzan H, Kato K, Miyamoto T, Eto T, et al. Cidofovir for

treating adenoviral hemorrhagic cystitis in hematopoietic stem cell transplant recipients. Bone Marrow Transplant. 2004;34(10):909-14.

385. Sudhindra P, Knoll B, Nog R, Singh N, Dhand A. Brincidofovir (CMX001) for the Treatment of Severe Adenoviral Pneumonia in Kidney Transplant Recipient. Cureus. 2019;11(8):e5296-e.

386. Lopez SMC, Michaels MG, Green M. Adenovirus infection in pediatric transplant recipients: are effective antiviral agents coming our way? Curr Opin Organ Transplant. 2018;23(4):395-9.

387. Florescu DF, Schaenman JM, Practice obotAIDCo. Adenovirus in solid organ transplant recipients: Guidelines from the American Society of Transplantation Infectious Diseases Community of Practice. Clin Transplant. 2019;33(9):e13527.

388. Sanchez-Cespedes J, Moyer CL, Whitby LR, Boger DL, Nemerow GR. Inhibition of adenovirus replication by a trisubstituted piperazin-2-one derivative. Antivir Res. 2014;108:65-73.

389. Hartline CB, Keith KA, Eagar J, Harden EA, Bowlin TL, Prichard MN. A standardized approach to the evaluation of antivirals against DNA viruses: Orthopox-, adeno-, and herpesviruses. Antivir Res. 2018;159:104-12.

390. Saha B, Varette O, Stanford WL, Diallo J-S, Parks RJ. Development of a novel screening platform for the identification of small molecule inhibitors of human adenovirus. Virology. 2019;538:24-34.

391. Hussein ITM, Brooks J, Bowlin TL. The discovery and development of filociclovir for the prevention and treatment of human cytomegalovirus-related disease. Antivir Res. 2020;176:104710.

392. Liczbiński P, Michałowicz J, Bukowska B. Molecular mechanism of curcumin action in signaling pathways: Review of the latest research. Phytother Res. 2020:1992-2005.

393. Ismail NI, Othman I, Abas F, H Lajis N, Naidu R. Mechanism of Apoptosis Induced by Curcumin in Colorectal Cancer. Int J Mol Sci. 2019;20(10):2454.

394. Kim S-R, Park H-J, Bae Y-H, Ahn S-C, Wee H-J, Yun I, et al. Curcumin Down-Regulates Visfatin Expression and Inhibits Breast Cancer Cell Invasion. Endocrinology. 2012;153(2):554-63.

395. Clark CA, McEachern MD, Shah SH, Rong Y, Rong X, Smelley CL, et al. Curcumin Inhibits Carcinogen and Nicotine-Induced Mammalian Target of Rapamycin Pathway Activation in Head and Neck Squamous Cell Carcinoma. Cancer Prev. 2010;3(12):1586-95.

396. Tyagi P, Singh M, Kumari H, Kumari A, Mukhopadhyay K. Bactericidal activity of curcumin I is associated with damaging of bacterial membrane. PLoS One. 2015;10(3):e0121313-e.

397. Praditya D, Kirchhoff L, Brüning J, Rachmawati H, Steinmann J, Steinmann E. Anti-infective Properties of the Golden Spice Curcumin. Front Microbiol. 2019;10:912.

398. Mazumder A, Raghavan K, Weinstein J, Kohn KW, Pommier Y. Inhibition of human immunodeficiency virus type-1 integrase by curcumin. Biochem Pharmacol. 1995;49(8):1165-70.

399. Crisostomo L, Soriano AM, Frost JR, Olanubi O, Mendez M, Pelka P. The Influence of E1A C-Terminus on Adenovirus Replicative Cycle. Viruses. 2017;9(12):387.

400. Yang M, Lee G, Si J, Lee S-J, You HJ, Ko G. Curcumin Shows Antiviral Properties

against Norovirus. Molecules. 2016;21(10):1401.

401. Mounce BC, Cesaro T, Carrau L, Vallet T, Vignuzzi M. Curcumin inhibits Zika and chikungunya virus infection by inhibiting cell binding. Antivir Res. 2017;142:148-57.

402. Wen-Tsai J, Hung JL. PI3K-Akt Signaling and Viral Infection. Recent Pat Biotechnol. 2008;2(3):218-26.

403. Li E, Stupack D, Klemke R, Cheresh DA, Nemerow GR. Adenovirus endocytosis via alpha(v) integrins requires phosphoinositide-3-OH kinase. J Virol. 1998;72(3):2055-61.

404. Saha B, Parks RJ. Human adenovirus type 5 vectors deleted of early region 1 (E1) undergo limited expression of early replicative E2 proteins and DNA replication in non-permissive cells. PLoS One. 2017;12(7):e0181012.

405. Binder AM, Biggs HM, Haynes AK, Chommanard C, Lu X, Erdman DD, et al. Human Adenovirus Surveillance - United States, 2003-2016. MMWR Morb Mortal Wkly Rep. 2017;66(39):1039-42.

406. Adamson CS, Nevels MM. Bright and Early: Inhibiting Human Cytomegalovirus by Targeting Major Immediate-Early Gene Expression or Protein Function. Viruses. 2020;12(1):110.

407. Ramachandran C, Rodriguez S, Ramachandran R, Raveendran Nair PK, Fonseca H, Khatib Z, et al. Expression profiles of apoptotic genes induced by curcumin in human breast cancer and mammary epithelial cell lines. Anticancer Res. 2005;25(5):3293-302.

408. Radhakrishna Pillai G, Srivastava AS, Hassanein TI, Chauhan DP, Carrier E. Induction of apoptosis in human lung cancer cells by curcumin. Cancer Lett. 2004;208(2):163-70.

409. Lestari MLAD, Indrayanto G. Chapter Three - Curcumin. In: Brittain HG, editor. Profiles of Drug Substances, Excipients and Related Methodology. 39: Academic Press; 2014. p. 113-204.

410. Alves TF, Chaud MV, Grotto D, Jozala AF, Pandit R, Rai M, et al. Association of Silver Nanoparticles and Curcumin Solid Dispersion: Antimicrobial and Antioxidant Properties. AAPS PharmSciTech. 2018;19(1):225-31.

411. Yang XX, Li CM, Huang CZ. Curcumin modified silver nanoparticles for highly efficient inhibition of respiratory syncytial virus infection. Nanoscale. 2016;8(5):3040-8.

412. Lin C-J, Chang L, Chu H-W, Lin H-J, Chang P-C, Wang RYL, et al. High Amplification of the Antiviral Activity of Curcumin through Transformation into Carbon Quantum Dots. Small. 2019;15(41):1902641.

413. Shieh WJ. Human adenovirus infections in pediatric population - An update on clinico-pathologic correlation. Biomed J. 2022;45(1):38-49.

414. Totapally BR, Totapalli S, Sendi P, Martinez PA. Epidemiology of Adenovirus Infection in Hospitalized Children in the United States From 1997 to 2019. Pediatr Infect Dis J. 2024;43(8):748-55.

415. Martínez-Aguado P, Serna-Gallego A, Marrugal-Lorenzo JA, Gómez-Marín I, Sánchez-Céspedes J. Antiadenovirus drug discovery: potential targets and evaluation methodologies. Drug Discov Today. 2015;20(10):1235-42.

416. Graham FL, Smiley J, Russell WC, Nairn R. Characteristics of a human cell line transformed by DNA from human adenovirus type 5. J Gen Virol. 1977;36(1):59-74.

417. Graham FL. Growth of 293 cells in suspension culture. J Gen Virol. 1987;68(3):937-40.

418. Ross PJ, Parks RJ. Construction and characterization of adenovirus vectors. Cold Spring Harb Protoc. 2009;4(5):1-12.

419. Sargent KL, Ng P, Evelegh C, Graham FL, Parks RJ. Development of a size-restricted pIX-deleted helper virus for amplification of helper-dependent adenovirus vectors. Gene Ther. 2004;11(6):504-11.

420. Schindelin J, Arganda-Carreras I, Frise E, Kaynig V, Longair M, Pietzsch T, et al. Fiji: an open-source platform for biological-image analysis. Nat Methods. 2012;9(7):676-82.

421. Biological evaluation of medical devices—Part 5: Tests for in vitro cytotoxicity. ISO. 2009.

422. Berk AJ. Functions of adenovirus E1A. Cancer Surv. 1986;5(2):367-87.

423. Young CSH. The Structure and Function of the Adenovirus Major Late Promoter. In: Doerfler W, Böhm P, editors. Adenoviruses: Model and Vectors in Virus-Host Interactions: Virion-Structure, Viral Replication and Host-Cell Interactions. Berlin, Heidelberg: Springer Berlin Heidelberg; 2003. p. 213-49.

424. Wilson MD, Harreman M, Svejstrup JQ. Ubiquitylation and degradation of elongating RNA polymerase II: the last resort. Biochim Biophys Acta - Gene Regul Mech. 2013;1829(1):151-7.

425. Gao F, Fan Y, Zhou B, Guo W, Jiang X, Shi J, et al. The functions and properties of cullin-5, a potential therapeutic target for cancers. Am J Transl Res. 2020;12(2):618-32.

426. Muñoz JC, Beckerman I, Choudhary R, Bouvier LA, Muñoz MJ. DNA Damage-Induced RNAPII Degradation and Its Consequences in Gene Expression. Genes. 2022;13(11):1951-64.

427. Price R, Penman S. Transcription of the adenovirus genome by an -amanitine-sensitive ribonucleic acid polymerase in HeLa cells. J Virol. 1972;9(4):621-6.

428. Tufegdzic Vidakovic A, Harreman M, Dirac-Svejstrup AB, Boeing S, Roy A, Encheva V, et al. Analysis of RNA polymerase II ubiquitylation and proteasomal degradation. Methods. 2019;159-160:146-56.

429. Lock R, Carol H, Maris JM, Kolb EA, Gorlick R, Reynolds CP, et al. Initial testing (stage 1) of the curaxin CBL0137 by the pediatric preclinical testing program. Pediatr Blood Cancer. 2017;64(4):e26263.

430. Sarantopoulos J, Mahalingam D, Sharma N, Iyer RV, Ma WW, Ahluwalia MS, et al. Results of a completed phase I trial of CBL0137 administered intravenously (IV) to patients (Pts) with advanced solid tumors. J Clin Oncol. 2020;38(15_suppl):3583.

431. Sargent KL, Meulenbroek RA, Parks RJ. Activation of adenoviral gene expression by protein IX is not required for efficient virus replication. J Virol. 2004;78(10):5032-7.

432. Karakasili E, Burkert-Kautzsch C, Kieser A, Sträßer K. Degradation of DNA damage-independently stalled RNA polymerase II is independent of the E3 ligase Elc1. Nucleic Acids Res. 2014;42(16):10503-15.

433. Harada JN, Shevchenko A, Shevchenko A, Pallas DC, Berk AJ. Analysis of the adenovirus E1B-55K-anchored proteome reveals its link to ubiquitination machinery. J Virol. 2002;76(18):9194-206.

434. Al-Heeti OM, Cathro HP, Ison MG. Adenovirus Infection and Transplantation. Transplant. 2022;106(5):920-7.

435. Dotan M, Zion E, Bilavsky E, Nahum E, Ben-Zvi H, Zalcman J, et al. Adenovirus can be a serious, life-threatening disease, even in previously healthy children. Acta

Paediatr. 2021;111(3):614-9.

436. Lu K, Liu C, Liu Y, Luo A, Chen J, Lei Z, et al. Curaxin-Induced DNA Topology Alterations Trigger the Distinct Binding Response of CTCF and FACT at the Single-Molecule Level. Biochemistry. 2021;60(7):494-9.

437. Somers K, Kosciolek A, Bongers A, El-Ayoubi A, Karsa M, Mayoh C, et al. Potent antileukemic activity of curaxin CBL0137 against MLL-rearranged leukemia. Int J Cancer. 2020;146(7):1902-16.

438. Bensaude O. Inhibiting eukaryotic transcription: Which compound to choose? How to evaluate its activity? Transcription. 2011;2(3):103-8.

439. Wold WSM, Tollefson AE, Ying B, Spencer JF, Toth K. Drug development against human adenoviruses and its advancement by Syrian hamster models. FEMS Microbiol Rev. 2019;43(4):380-8.

440. Bertzbach LD, Ip WH, Dobner T. Animal Models in Human Adenovirus Research. Biology. 2021;10(12):1253-69.

441. Liang Y, Quenelle D, Vogel JL, Mascaro C, Ortega A, Kristie TM. A novel selective LSD1/KDM1A inhibitor epigenetically blocks herpes simplex virus lytic replication and reactivation from latency. MBio. 2013;4(1):e00558-12.

442. Wang J, Li GL, Ming SL, Wang CF, Shi LJ, Su BQ, et al. BRD4 inhibition exerts anti-viral activity through DNA damage-dependent innate immune responses. PLoS Pathog. 2020;16(3):e1008429.

443. Pedrotti S, Busà R, Compagnucci C, Sette C. The RNA recognition motif protein RBM11 is a novel tissue-specific splicing regulator. Nucleic Acids Res. 2012;40(3):1021-32.

444. Frisch SM, Mymryk JS. Adenovirus-5 E1A: paradox and paradigm. Nat Rev Mol Cell Biol. 2002;3(6):441-52.

445. Berk AJ. Recent lessons in gene expression, cell cycle control, and cell biology from adenovirus. Oncogene. 2005;24(52):7673-85.

446. Horwitz GA, Zhang K, McBrian MA, Grunstein M, Kurdistani SK, Berk AJ. Adenovirus Small e1a Alters Global Patterns of Histone Modification. Science. 2008;321(5892):1084-5.

447. Lawrence FJ, McStay B, Matthews DA. Nucleolar protein upstream binding factor is sequestered into adenovirus DNA replication centres during infection without affecting RNA polymerase I location or ablating rRNA synthesis. J Cell Sci. 2006;119(12):2621-31.

448. Charman M, Herrmann C, Weitzman MD. Viral and Cellular Interactions During Adenovirus DNA Replication. FEBS Lett. 2019;593(24):3531-50.

449. Lam YW, Evans VC, Heesom KJ, Lamond AI, Matthews DA. Proteomics Analysis of the Nucleolus in Adenovirus-infected Cells. Mol Cell Proteom. 2010;9(1):117-30.

450. Matthews DA. Adenovirus protein V induces redistribution of nucleolin and B23 from nucleolus to cytoplasm. J Virol. 2001;75(2):1031-8.

451. Hidalgo P, Anzures L, Hernández-Mendoza A, Guerrero A, Wood CD, Valdés M, et al. Morphological, Biochemical, and Functional Study of Viral Replication Compartments Isolated from Adenovirus-Infected Cells. J Virol. 2016;90(7):3411-27.

452. Luger K. Dynamic nucleosomes. Chromosome Res. 2006;14(1):5-16.

453. Brahma S, Henikoff S. Epigenome Regulation by Dynamic Nucleosome Unwrapping. Trends Biochem Sci. 2020;45(1):13-26.

454. Kouzarides T. Chromatin modifications and their function. Cell. 2007;128(4):693-

705.

455. Pelka P, Ablack JNG, Torchia J, Turnell AS, Grand RJA, Mymryk JS. Transcriptional control by adenovirus E1A conserved region 3 via p300/CBP. Nucleic Acids Res. 2009;37(4):1095-106.

456. Sung MT, Cao TM, Coleman RT, Budelier KA. Gene and protein sequences of adenovirus protein VII, a hybrid basic chromosomal protein. Proc Natl Acad Sci USA. 1983;80(10):2902-6.

457. Yoshida K, Higashino F, Fujinaga K. Transcriptional Regulation of the Adenovirus E1A Gene. In: Doerfler W, Böhm P, editors. The Molecular Repertoire of Adenoviruses III: Biology and Pathogenesis. Berlin, Heidelberg: Springer Berlin Heidelberg; 1995. p. 113-30.

458. Lundblad JR, Kwok RP, Laurance ME, Harter ML, Goodman RH. Adenoviral E1A-associated protein p300 as a functional homologue of the transcriptional co-activator CBP. Nature. 1995;374(6517):85-8.

459. Fuchs M, Gerber J, Drapkin R, Sif S, Ikura T, Ogryzko V, et al. The p400 Complex Is an Essential E1A Transformation Target. Cell. 2001;106(3):297-307.

460. Reid JL, Bannister AJ, Zegerman P, Martínez-Balbás MA, Kouzarides T. E1A directly binds and regulates the P/CAF acetyltransferase. EMBO J. 1998;17(15):4469-77.

461. Boyer J, Rohleder K, Ketner G. Adenovirus E4 34k and E4 11k inhibit double strand break repair and are physically associated with the cellular DNA-dependent protein kinase. Virology. 1999;263(2):307-12.

462. Stracker TH, Lee DV, Carson CT, Araujo FD, Ornelles DA, Weitzman MD. Serotype-specific reorganization of the Mre11 complex by adenoviral E4orf3 proteins. J

Virol. 2005;79(11):6664-73.

463. Engeland K. Cell cycle regulation: p53-p21-RB signaling. Cell Death Differ. 2022;29(5):946-60.

464. Giommarelli C, Zuco V, Favini E, Pisano C, Dal Piaz F, De Tommasi N, et al. The enhancement of antiproliferative and proapoptotic activity of HDAC inhibitors by curcumin is mediated by Hsp90 inhibition. Cell Mol Life Sci. 2010;67(6):995-1004.

465. Dalidowska I, Gazi O, Sulejczak D, Przybylski M, Bieganowski P. Heat Shock Protein 90 Chaperones E1A Early Protein of Adenovirus 5 and Is Essential for Replication of the Virus. Int J Mol Sci. 2021;22(4):2020.

Contributions of Collaborators

Dr. Robin J. Parks assisted in the generation of the plasmids pMJ100 in figures 2.3, 3.2, and 4.6, pMJ111 in figures 3.3 and 4.2, and pMJ102 in figure 4.5. Plasmids pRP3512 and pRP3516 used in figure 3.5 were generated entirely by Dr. Parks. Dr. Parks also provided editorial comments on this work.

Dr. Panayiotis O. Vacratsis performed mass-spectroscopy analysis of samples obtained by Morgan R. Jennings, generating data that was important in informing the direction of the project in chapter 4. This data was not presented.

Morgan R. Jennings generated all other data presented in this thesis.

Appendix 1: Authorizations

Figure 1.1 Schematic representation of the HAdV-5 genome.

- This figure was obtained from an open access article by Lee *et al*. published in Genes and Diseases (an Elsevier journal). It is subject to the Creative Commons Attributions License (CC-BY 4.0). As stated by Elsevier, reuse of its content for inclusion in a thesis or dissertation (provided that this is not to be published commercially) is permitted. No written permission from Elsevier is necessary.
- Citation: Lee CS, Bishop ES, Zhang R, Yu X, Farina EM, Yan S, et al. Adenovirus-mediated gene delivery: Potential applications for gene and cell-based therapies in the new era of personalized medicine. Genes Dis. 2017;4(2):43-63.
- Additional information: https://www.elsevier.com/about/policies/copyright/permissions

Figure 1.2 Schematic of the HAdV-5 virion

- This figure was obtained from an open access review article (provided in Appendix 2) published in Viruses (an MDPI journal), on which I am the primary author. Since the authors retain copyright and the article falls under the CC-BY, permissions are not required.
- Citation: Jennings MR, Parks RJ. Human Adenovirus Gene Expression and Replication Is Regulated through Dynamic Changes in Nucleoprotein Structure throughout Infection. Viruses. 2023;15(1):161.
- Additional information: https://www.mdpi.com/authors/rights

Figure 1.3 HAdV DNA strand displacement replication

- This figure was obtained from ViralZone, which is hosted by the Swiss Institute of Bioinformatics. It is also licensed under the CC-BY and use for non-commercial purposes is permitted. Citation and a link to the license is required (see below).
- Citation: Bioinformatics SSIo. DNA Strand Displacement Replication - ViralZone. https://viralzone.expasy.org/1940. Accessed October 15.
- CC-BY license: https://creativecommons.org/licenses/by-nc-nd/4.0/
- Additional information: https://viralzone.expasy.org

Figure 1.4 Schematic of the FACT complex

- This figure was obtained from an open access article by Jeronimo et al. published in Transcription (a Taylor and Francis journal). It is subject to the Creative Commons Attributions License (CC-BY 4.0). As stated by Taylor and Francis, reuse of its content for a thesis or dissertation is free of charge contingent on resubmission of permission request if work is published.
- Citation: Jeronimo C, Robert F. The histone chaperone FACT: a guardian of chromatin structure integrity. Transcription. 2022;13(1-3):16-38.
- Additional information: https://taylorandfrancis.com/contact/rights-and-permissions/journals/

Figure 1.6 Chemical structure of curcuminoids

- This figure was obtained from an open access review article (provided in Appendix 3) published in Viruses (an MDPI journal), on which I am the primary author. Since

the authors retain copyright and the article falls under the CC-BY, permissions are not required.

- Citation: Jennings MR, Parks RJ. Curcumin as an Antiviral Agent. Viruses. 2020;12(11):1242.
- Additional information: https://www.mdpi.com/authors/rights

Chapter 2: Antiviral Effects of Curcumin on Adenovirus Replication

- This article, on which I am the primary author, was published in Microorganisms, an MDPI journal. Since the authors retain copyright and the article falls under the CC-BY, permissions are not required.
- Citation: Jennings MR, Parks RJ. Antiviral Effects of Curcumin on Adenovirus Replication. Microorganisms. 2020;8(10):1524-40.
- Additional information: https://www.mdpi.com/authors/rights

Appendix 2: Human Adenovirus Gene Expression and Replication is Regulated through Dynamic Changes in Nucleoprotein Structure throughout Infection

- This article, on which I am the primary author, was published in Viruses, an MDPI journal. Since the authors retain copyright and the article falls under the CC-BY, permissions are not required.
- Citation: Jennings MR, Parks RJ. Human Adenovirus Gene Expression and Replication Is Regulated through Dynamic Changes in Nucleoprotein Structure throughout Infection. Viruses. 2023;15(1):161.
- Additional information: https://www.mdpi.com/authors/rights

Appendix 3: Curcumin as an Antiviral Agent

- This article, on which I am the primary author, was published in Viruses, an MDPI journal. Since the authors retain copyright and the article falls under the CC-BY, permissions are not required.
- Citation: Jennings MR, Parks RJ. Curcumin as an Antiviral Agent. Viruses. 2020;12(11):1242.
- Additional information: https://www.mdpi.com/authors/rights

Appendix 2:

Human Adenovirus Gene Expression and Replication is Regulated through Dynamic Changes in Nucleoprotein Structure throughout Infection

Viruses **2023**, *15*, 161; doi: 10.3390/v15010161.

Review

Human Adenovirus Gene Expression and Replication Is Regulated through Dynamic Changes in Nucleoprotein Structure throughout Infection

Morgan R. Jennings [1, 2] and Robin J. Parks [1, 2, 3, 4, *]

1 Regenerative Medicine Program, Ottawa Hospital Research Institute, Ottawa, ON K1H 8L6, Canada
2 Department of Biochemistry, Microbiology and Immunology, University of Ottawa, Ottawa, ON K1N 6N5, Canada
3 Centre for Neuromuscular Disease, University of Ottawa, Ottawa, ON K1N 6N5, Canada
4 Department of Medicine, The Ottawa Hospital, Ottawa, ON K1H 8L6, Canada

***** Correspondence

Received: 10 December 2022; Revised: 31 December 2022; Accepted: 3 January 2023; Published: 5 January 2023

Abstract: Human adenovirus (HAdV) is extremely common and can rapidly spread in confined populations such as daycare centers, hospitals, and retirement homes. Although HAdV usually causes only minor illness in otherwise healthy patients, HAdV can cause significant morbidity and mortality in certain populations, such as the very young, very old, or immunocompromised individuals. During infection, the viral DNA undergoes dramatic changes in nucleoprotein structure that promote the rapid expression of viral genes, replication of the DNA, and generation of thousands of new infectious virions—each process requiring a distinct complement of virus and host-encoded proteins. In this review, we summarize our current understanding of the nucleoprotein structure of HAdV DNA during the various phases of infection, the cellular proteins implicated in mediating these changes, and the role of epigenetics in HAdV gene expression and replication.

Keywords: adenovirus; epigenetics; nucleoprotein; nucleoprotein remodeling; viral replication; epigenetic modulators

1. Introduction

Adenoviruses (AdV) are a diverse group of viruses that infect a large range of vertebrates, including humans [1]. Human AdV (HAdV) was first isolated from adenoid tissues (from which it derives its name) in the 1950s [2, 3]. Since its discovery, research into HAdV has contributed greatly to our general understanding of many aspects of molecular cell biology, largely due to the fact that viruses are exquisitely adept at identifying crucial pathways/processes within the cell and then modulating the activity of key proteins within those pathways to facilitate optimal viral replication. For HAdV, examples include gene splicing, which was first identified as an aspect of HAdV gene expression [4, 5], but subsequently shown to be a fundamental process for almost all genes in eukaryotic cells. Studies of cellular proteins that interact with E1A proteins (early region 1A, the first viral proteins expressed following HAdV infection) contributed to the identification and/or functional characterization of many key cellular proteins, such as the histone acetyltransferase E1A-associated protein p300 (EP300 [6, 7]), and the tumor suppressor Rb and its family members [8–10]. In many ways, studying virus biology is synonymous with studying host molecular cell biology.

Within the cell, eukaryotic genomic DNA is packaged into chromatin, a highly organized complex of DNA and proteins that encodes epigenetic information governing gene expression and cell identity [11–13]. The basic unit of chromatin is the nucleosome, 147 base pairs of DNA wrapped around two molecules each of H2A, H2B, H3, and H4. Histones play an active role in gene regulation, through post-translational modification (PTM) of their N-termini, which are subsequently recognized by many cellular regulatory proteins [12, 14]. As a nuclear virus, it is within this environment that HAdV must express its genes and replicate its DNA, suggesting that the virus has likely evolved an ability to manipulate cellular epigenetic pathways to effectively accomplish these tasks. The purpose of this review is to summarize our current knowledge of viral and host proteins that establish and remodel the HAdV nucleoprotein structure.

2. Adenovirus Biology

The AdV virion (Figure 1) is comprised of a non-enveloped icosahedral capsid with

a diameter of ~80–90 nm, with each spike-like fiber protein protruding an additional ~12–35 nm, depending on the specific subtype [15]. HAdV contains a linear double-stranded DNA (dsDNA) genome of ~30–40 kb [15], with over 100 distinct types grouped into species A-G [16]. HAdV types 2 (HAdV-2) and 5 (HAdV-5), which both belong to species C, are perhaps the most extensively characterized and are very similar in biology and DNA sequence (i.e., most findings utilizing HAdV-2 are directly applicable to HAdV-5 and vice versa). If not otherwise stated, we refer here primarily to the situation in HAdV-2 and HAdV-5. The HAdV-5 genome is approximately 36 kb and encodes over 40 proteins. Adenoviral coding regions are designated early or late depending on when they are expressed (i.e., before or after DNA replication) [17]. The E1 region encodes the E1A proteins, which induce mitogenic activity in the host cell and stimulate expression of other viral genes [18, 19], and E1B proteins, which serve to prevent apoptosis induced by the activities of E1A [20, 21]. E1B-55K also associates with E4-encoded proteins and other cellular proteins to form a ubiquitin ligase complex that promotes degradation of specific proteins, such as the cellular Mre11-Rad50-Nbs1 (MRN) DNA repair complex [22]. The E2 region encodes proteins involved directly in viral DNA replication [23]. The E3 region encodes proteins that primarily have immunomodulatory functions [24], but also encodes the adenovirus death protein (ADP), which assists with cell lysis at the end of the infection cycle [25]. The E4 region encodes proteins with numerous functions, such as alteration of cellular protein stability, reorganization of cellular structures within the nucleus, regulation of late viral RNA splicing, and inhibition of the cellular DNA damage response (DDR), with several of these proteins having redundant activity [26, 27]. The onset of viral DNA replication leads to the activation of the major late promoter (MLP) [28], which gives rise to a long transcript that is alternatively spliced into the late transcription units, L1–L5. Indeed, during infection, HAdV uses high levels of alternative splicing, generating over 11,000 differently spliced transcripts, likely as a mechanism driving evolutionary change and possibly compensating for the reduced inherent spontaneous mutation rate during genome replication of this DNA virus relative to many RNA viruses [29, 30]. The regions encoding the L4-22K and L4-33K proteins are initially expressed at low levels from a promoter located within the L4 region [31], and these proteins contribute to full activation

of the MLP [32]. Additional transcripts are produced at intermediate/late times of infection, including the structural protein IX (pIX) and the IVa2 protein, which is involved in packing the viral DNA into immature virions [33]. The U exon protein (UXP) is expressed late in infection and likely has a role in DNA replication or RNA transcription, but it is largely uncharacterized [32, 34]. HAdV also encodes two virus-associated (VA) RNAs (VA RNAI and RNAII) which improve the translation of early and late viral genes, inhibit activation of the interferon response, and may alter the expression of host genes [35–37]. Given the large number of transcripts produced during infection [30], there are likely other as-yet uncharacterized proteins generated during normal HAdV infection. Located on both ends of the genome are the inverted terminal repeats (ITRs), which vary in length based on type (e.g., ~100 bp for HAdV-C5), and act as the origin of DNA replication, with the ~200 bp viral DNA packaging sequence positioned adjacent to the left ITR.

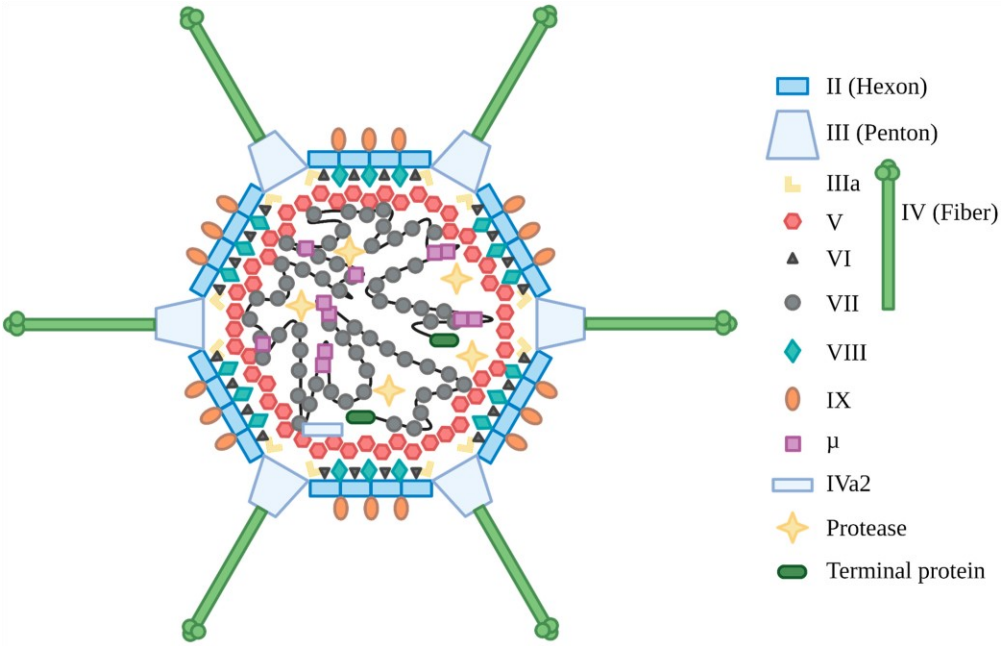

Figure 1. Schematic of the HAdV-5 virion. Adapted from [38], with modifications based on [33, 39–41]. Created with BioRender.com.

The mature HAdV-5 capsid is composed of proteins encoded within the late region. There are three major (II, III, and IV) and five minor (IIIa, IVa2, VI, VIII, and IX) proteins

that make up the viral capsid [33, 38–40, 42], reviewed in [15]. Trimers of protein II (more commonly known as hexon) form each facet of the icosahedron, with vertices being capped by pentamers of protein III (also known as penton). Extending from the penton bases are trimers of protein IV, the fiber protein. In large part, the minor polypeptides function to stabilize the major proteins and solidify the virion structure [43, 44]. HAdV DNA within the mature capsid associates with three highly basic proteins, VII, V, and μ (Mu) [42, 45–49].

The actual architecture of the HAdV DNA core within the virion is currently unknown [15]. Protein VII is the main protein responsible for wrapping and condensing the viral DNA [50]. Digestion of the viral nucleoprotein core with micrococcal nuclease (MNase) produces protected fragments of 90–150 bp [51, 52], somewhat analogous to what is observed for cellular chromatin. The protein VII-DNA nucleoprotein complex is believed to be organized into a central dense core with 12 large spherical nucleoprotein projections, termed adenosomes, which extend into each vertex of the capsid [53, 54]. Recent work using atomic force microscopy revealed that protein VII condenses the viral genome by both direct clustering and by promoting bridging of different regions through protein Mu [41]. Virions formed in the absence of protein VII are non-infectious due to an inability to escape the endosome as a result of a failure to process pre-protein VI [55], which normally facilitates endosomal escape during infection [56]. Protein V forms a shell around the protein VII-DNA complex within the virion [53, 57, 58] and tethers it to the capsid [47, 57–60]. Virions formed in the absence of protein V are recoverable but less infectious due to premature capsid degradation, which leads to early release of the viral DNA into the cytoplasm [61, 62]. Inappropriate release of the viral DNA in the cytoplasm can activate antiviral innate immune signaling through engagement of the cytoplasmic DNA sensor cGAS [62], clearly illustrating the crucial nature of the virion-stabilizing function of protein V.

The HAdV genomic DNA may also contribute indirectly to virion stability, as virions with genomes less than ~80% of the wildtype genome length are relatively unstable and rapidly disintegrate upon heating [63, 64]. Indeed, HAdV strongly selects for appropriate genome size: vectors with genome sizes greater than 105% [65] or less than

75% [66] undergo spontaneous genome rearrangement to attain a size closer to wildtype virus. This phenomenon has been observed for other viruses with icosahedral capsids [49, 64]. For HAdV, the mechanism by which the genome size influences virion stability has not been elucidated. In the HAdV virion, the nucleoprotein core extends into the vertex regions of the inner capsid and makes direct contact with penton and peripentonal hexon [59]. This region appears to be preferentially destabilized upon heating of HAdV vectors with sub-wildtype genomes [63]. Tight packaging of wildtype-length DNA into the capsid may force the DNA in the vertex regions into the proper position to achieve the required linkage between the DNA and the peripentonal hexons, bridged by proteins V and VI. For virions containing sub-wildtype length genomes, loose packing of the nucleoprotein core may prevent these interactions, leading to destabilization of the capsid.

While the receptors used by HAdVs for cell entry vary by type, for HAdV-5, the fiber protein binds to the Coxsackie adenovirus receptor (CAR), the primary receptor for HAdV5 and Coxsackie B virus [67, 68]. HAdV-5 can also utilize heparin sulfate proteoglycans located on the cell surface as an alternative receptor, either through direct binding to the fiber shaft of HAdV [69] or bridged through the interaction of HAdV-5 with various factors in the blood [70–73]. After the initial binding to CAR, the HAdV-5 penton protein interacts with a secondary receptor composed of αvβ3 or αvβ5 integrins, which triggers internalization of HAdV and occurs through clathrin-mediated endocytosis [74]. Acidification of the endosome alters the HAdV capsid structure, allowing for the release of protein VI from the inner capsid. Protein VI possesses membrane lytic activity [56] and mediates rupture of the endosome and release of the virus [75]. As the capsid is transported to the nucleus along the microtubule network [76], it is progressively dismantled [77–79]. Upon reaching the nuclear pore, protein V is released from the viral genome following ubiquitination by the E3 ligase Mind bomb 1 [62, 78], which allows release of the protein-VII-wrapped HAdV DNA and subsequent import into the nucleus [62, 77–82]. Both viral DNA replication and progeny formation occur within the nucleus, and one infectious cycle takes 24–36 h in immortalized cells, although the time for completion of the lifecycle is slightly extended in primary cells.

3. The Role of Protein VII in Early Infection

Protein VII is the only viral protein that accompanies the viral DNA into the nucleus and appears to have several functions during early infection. Protein VII is thought to protect the incoming HAdV DNA from detection by the DDR [83]. Inadvertent activation of the DDR can lead to concatemerization of the viral DNA, which presumably is too large to be efficiently packaged into capsids [22, 84]. Although protein VII is important for protecting the viral DNA during the very early stages of virus infection, some studies have suggested that prolonged association could negatively impact early viral gene expression. When injected into Xenopus laevis eggs, protein VII condenses the Xenopus chromatin and inhibits transcription [85]. Cell-free systems developed to study HAdV DNA replication have shown that protein-VII-wrapped viral DNA allows for only limited transcription and DNA replication [86–88]. Conversely, other studies have suggested that protein VII may be important for actually promoting transcription of viral genes. Transfection of plasmid DNA complexed to protein VII actually enhanced reporter gene expression compared to naked DNA alone [89]. The N-terminus of E1A is capable of associating with protein VII, which might allow protein VII to recruit E1A and other E1A-associated proteins, such as components of the cellular transcriptional machinery, to the protein-VII-wrapped DNA to facilitate initiation of transcription [85, 90]. Thus, dynamic regulation of protein VII is likely necessary for optimal viral growth; sufficient protein VII must be removed or remodeled to decondense the viral DNA–nucleoprotein complex to allow access to the transcription machinery, but some protein VII may need to be retained to stimulate transcription.

Protein VII can undergo PTM, which influences its subcellular localization [91, 92]. For example, mature protein VII can be acetylated on lysine 2 or lysine 3, and the mutation of either of these residues to alanine changes the localization of protein VII from being dispersed throughout the chromatin to localized in the nucleolus [92], while the same change on pre-protein VII has the opposite effect [91]. In the case of cellular histones, acetylation of histones “loosens” the cellular chromatin structure and promotes transcription [14], but whether such modification is required to loosen the viral nucleoprotein structure or as a prelude to protein VII removal is unknown.

The conflicting data on the importance of protein VII for early transcription are mirrored by conflicting data on the timing of protein VII removal from the viral DNA. Protein VII can be cross-linked to the viral DNA at all stages of infection [47], and chromatin immunoprecipitation (ChIP) studies have shown that protein VII can be found bound to the viral DNA up to at least ~10 hpi [85, 89, 93–96]. However, some studies found that protein VII association does not change during the early stage of infection [47, 90, 94], while others instead suggest a decline in protein VII association with the viral DNA [89, 93, 95, 97]. Compounding this issue is the observation that protein VII association may vary depending on the region of the genome being analysed. For example, between 1 and 10 hpi, protein VII appeared to remain stably associated with the late-gene hexon coding region but showed declining association over time with the major late promoter [89]. Protein VII also showed reduced association with the late hexon region when comparing early (4 hpi) versus late (18 hpi) time points of infection [96].

Another aspect of protein VII biology with contradictory data is whether transcription of the HAdV DNA template is required for removal of protein VII. Some studies showed that inhibiting transcription prolongs the retention of protein VII on the HAdV genome [90, 97], while others saw no such effect [89, 95, 96]. Recruitment of E1A to the protein-VII-wrapped genome may stimulate early transcription, which could subsequently strip protein VII from the viral DNA [85, 90]. However, protein VII is still removed in the absence of E1A [89, 95], suggesting that this function of E1A is not essential for expression of virus-encoded genes. If E1A was absolutely required for transcription initiation on HAdV DNA, HAdV-based vectors that are deleted of the E1 region would not function well, which is not the case. Transgene expression from E1-deleted vectors appears quite efficient and can be detected as early as 2 hpi [95]. However, there may be host-encoded proteins that can compensate for the loss of E1A. Indeed, E1-deleted HAdV can complete a full replication cycle in certain cell types, although the time required to complete the replication cycle is extended [98, 99], suggesting that compensating proteins may exist.

Based on studies in cell-free systems, three cellular proteins have been implicated in remodeling the protein-VII-wrapped viral DNA. Transcription activating factor (TAF)-

Iβ (also known as SET) is perhaps the best characterized [87]. TAF-Iβ can form a tertiary complex with the protein-VII-wrapped DNA [93, 94, 100], which improved accessibility to restriction enzymes [88], which would presumably also increase accessibility to transcriptional activators. Fluorescently labeled TAF-Iβ co-localizes with protein VII on incoming viral genomes in the nucleus, which can be used to track the virus in live cells [101]. siRNA mediated knockdown of TAF-Iβ had a modest effect on viral replication [102] but did not affect the binding level of protein VII on viral DNA as assessed by ChIP [89], suggesting that other proteins are responsible for the removal of protein VII or can compensate for the lack of TAF-Iβ. TAF-II (NAP-1 [103]) and TAF-III (B23/nucleophosmin [104]) were also identified as potential remodelers of the protein-VII-wrapped viral DNA in cell free systems, and both can stimulate replication from the HAdV core, while TAF-II can also enhance transcription.

Protein VII can also associate with host chromatin, where it contributes to suppressing immune danger signals [92]. Protein VII was shown to interact with the high-mobility group B (HMGB) family of proteins and cause their retention on chromatin [92]. Since free HMGB functions as a danger signal to activate an immune response [105], these data suggest that protein VII is acting to blunt the cells' response to infection. Protein VII also causes a depletion of histone H1 isoforms from cellular chromatin [106]. This imbalance of HMGB and H1 caused by protein VII prevents cell cycle progression, which the authors speculated could be a mechanism normally employed by HAdV to ensure that the cell cycle progression induced by E1 proteins stops in S phase [106], as progression beyond this phase may be deleterious to viral replication. Indeed, in the absence of protein VII, HAdV-infected cells express markers of G2 and mitosis [106]. Thus, protein VII released from the incoming virion, or newly synthesized within the infected cell, may help shape the microenvironment for optimal viral replication.

4. HAdV DNA Associates with Nucleosome-like Structures Early in Infection

Though there was initially debate over whether cellular histones were found on HAdV DNA [107–111], more recent studies have clearly shown that histones are detectable on the HAdV DNA as early as 1 h post-infection [89, 95, 96, 112]. Within the host cell,

histone variant H3.1 is expressed exclusively during S phase and is deposited on newly replicated cellular DNA by the Chromatin Assembly Factor I (CAF1) complex [113, 114]. Thus, deposition of H3.1 is intimately tied to host DNA replication. In contrast, the histone variant H3.3 is expressed throughout the cell cycle and is deposited on DNA independent of DNA replication [115]. The histone chaperone involved in deposition of H3.3 varies by chromosome region; H3.3 is deposited on active promoters and enhancers by EP400 [116], within actively transcribed genes or on incoming male pro-nuclear DNA by the histone cell cycle regulator A (HIRA) complex [117, 118], and on telomeres and pericentric DNA repeats by death-associated protein 6 (DAXX) [117, 119, 120]. Thus, the identity of the H3 variant contained in nucleosomes can provide some insight into the mechanism of deposition. During normal viral transmission, HAdV primarily infects non-dividing cells, inducing cell cycle progression only after E1A gene expression has already occurred, suggesting that HAdV DNA is likely to be chromatinized by exploiting a mechanism independent of host cell or viral DNA replication. ChIP experiments showed that DNA from replication-defective HAdV-based vectors [95] and wildtype HAdV [89, 96, 112] preferentially associates with H3.3 beginning as early as 1 hpi. Although the H3.1 chaperone CAF-1 appears to localize to viral replication centers in the nucleus of infected cells [112], H3.1 does not associate with HAdV DNA at any point during infection [95, 96, 112]. Herpes Simplex Virus 1 (HSV1) DNA also associates preferentially with H3.3 during the early phase of infection, although HSV1 switches to association with H3.1 late in infection [121]. Knockdown of HIRA decreased association of H3 with the HAdV-based vectors [95] and HSV1 DNA [121] and subsequently reduced expression of genes encoded by the viruses. However, knockdown of HIRA did not decrease association of H3.3 on wildtype HAdV-5 DNA [96], suggesting that either HIRA is not responsible for depositing H3.3 on wildtype HAdV DNA or that there are other proteins that can compensate for the loss of HIRA for wildtype virus but not for HAdV-based vectors. DAXX is likely not used by HAdV as a histone chaperone, as it is actively degraded during infection [122]. HAdVs that are unable to degrade DAXX ultimately associate with unacetylated histones, resulting in repression of viral transcription [122–124], indicating that DAXX functions as an innate factor to limit gene expression on incoming viral DNA. Despite TAF-Iβ demonstrating

histone chaperone activity [88], it does not appear to act as a histone chaperone for incoming HAdV genomes [89]. Knockdown of the histone chaperone CHD1, which binds to trimethylated lysine 4 on H3 (H3K4me3), a mark associated with active genes [125], did not lower viral yield in HAdV-5-infected cells [126], suggesting it is not used by HAdV to remodel its DNA.

Work by Komatsu et al. [89] demonstrated that HAdV DNA associates with all members of the nucleosome, H2A–H2B and H3–H4. While H4 would be deposited as a heterodimer with H3.3, the chaperone responsible for deposition of H2A/H2B is unknown. Upon MNase digestion, HAdV DNA in the nucleus displays a repeating ~200 bp structure similar to cellular chromatin, suggesting that much of the DNA is indeed wrapped in physiologically spaced, nucleosome-like structures, at least during the early phase of infection [95, 107–110, 127]. All regions of the genome are represented in the MNase-protected fractions [107]. The observation that both protein VII and histones can be found bound to the same viral DNA molecule at the same time suggests that the viral chromatin likely does not completely resemble that of the host cell [89]. At late times of infection (16–18 hpi), viral genomes no longer appear to be wrapped in the repeating nucleosome-like structure [96], instead showing irregularly spaced nucleosome-like structures at approximately one-tenth the density of cellular chromatin (three versus twenty-six nucleosomes per μm of DNA, respectively [109]). HSV1 also shows viral DNA associating with regularly spaced nucleosomes during latent infection, while the spacing becomes 'unstable' during a lytic infection [128]. For HAdV, the decreased nucleosome density at late times of infection could be merely a result of decreased histone expression [129, 130] coupled with increased amounts of viral DNA, thereby reducing the pool of histones available for binding to the viral DNA.

5. Nucleoprotein Structure of HAdV during Active DNA Replication

HAdV has evolved a unique mechanism to maintain genome length and replicate the ends of its linear dsDNA genome. Proteins directly involved in viral DNA replication are encoded within the E2 transcription unit, which consists of two regions, E2A and E2B, which have separate polyadenylation sites [23]. E2A encodes the 72 kDa DNA-binding

protein (DBP), whereas the E2B region codes for the 80 kDa precursor terminal protein (pTP) and the 140 kDa HAdV DNA polymerase (Pol). Replication initiates through a protein priming mechanism (reviewed in [131]); Pol covalently attaches a dCMP residue to pTP, the pTP/dCMP molecule then binds to the viral ITR, and the 30-OH group of the dCMP serves as a primer for elongation by Pol. Thus, the dCMP moiety becomes the first nucleotide of the newly synthesized genome. Pol replicates one entire strand of the genome in a continuous manner, while the second strand is displaced. pTP remains covalently bound to the ends of the viral DNA at all stages of infection and in the virion but is cleaved by the HAdV-encoded protease to produce the mature 55 kDa terminal protein (TP) during virion maturation. DBP aids in unwinding the dsDNA genome during replication [132, 133] and promotes DNA replication elongation [134]. DBP also coats and protects the displaced single-stranded DNA (ssDNA), thus preventing immune and DNA damage responses that can be induced in the cell against naked DNA [135, 136]. The displaced ssDNA can then form a "pan-handle" structure (by annealing the complementary ssDNA ITR at each end of the molecule), which functionally resembles the native ITR and can serve as a template for initiation of replication of the ssDNA in a manner similar to the dsDNA genome [137]. DBP also binds dsDNA but with lower affinity [134]. It is unlikely that newly replicated HAdV DNA is "naked" within the nucleus at any point in the lifecycle; naked DNA is not well tolerated in the nucleus of a cell [138] and can contribute to genome instability and susceptibility to mutation. Since there is a dramatic decline in cellular histone synthesis late in HAdV infection [129, 130], DBP may be the major protein associating with viral replicative intermediates and newly replicated genomes within the cell at late times of infection. However, DBP-wrapped viral DNA is probably not the template for late gene expression [139, 140], as cellular RNA polymerase likely cannot contend with such a radically different nucleoprotein structure compared to cellular chromatin. A small fraction of the viral DNA does remain associated with H3.3 at 18 hpi [96], and it is perhaps this subpopulation that acts as the transcription template. Indeed, each genome in a replication center may associate with different proteins depending on its assigned task—histones for gene expression, DBP for genome replication, and pVII for packaging into capsids, as discussed below.

6. The Switch from Histones to Protein VII

Prior to encapsidation, the histones or DBP must be displaced from the HAdV DNA and replaced with pre-protein VII. However, the mechanism by which this occurs is unknown. Given that histone production is reduced late in HAdV infection [129, 130], as the levels of cellular histones decline and the quantity of pre-protein VII within the cell increases, the viral genome may be predisposed to associate with pre-protein VII rather than histones [108, 110, 141]. During late infection, newly replicated viral dsDNA accumulates within the center of "virally induced post-replicative" (ViPR) bodies along with pre-protein VII, and these regions actively exclude cellular histones, indicating another potential mechanism for this switch [142]. Additionally, as discussed above, PTM of both pre-protein VII and protein VII may influence their localization within the nucleus [91, 92] and may therefore be another mechanism used by HAdV to mediate the switch of histones to pre-protein VII on viral DNA.

Mixing HAdV DNA and purified pre-protein VII leads to the formation of an insoluble complex [143], suggesting that a specific cellular chaperone(s) is required for deposition of pre-protein VII on HAdV DNA. TAF-III, identified using a cell-free system as a HAdV core remodeler, has a greater affinity for pre-protein VII than the mature protein VII and will transfer pre-protein VII onto HAdV DNA in cell-free systems [144]. Consistent with this, depletion of TAF-III caused histones to be retained longer on the viral DNA [145]. Pre-protein VII also interacts with chromatin remodeling proteins CHD3 and BAZ1A, suggesting these proteins could also be involved in late viral chromatin remodeling [146], although this has not been confirmed experimentally. Once wrapped in pre-protein VII, the viral DNA is available for packaging into capsids. Based on current evidence, HAdV capsids appear to form around nascent viral cores, as opposed to viral DNA being inserted into partially assembled capsids (the concerted vs. sequential models, respectively) [147].

7. Epigenetic Regulation of Viral and Cellular Chromatin during HAdV Infection

The observation that HAdV DNA is wrapped in physiologically spaced nucleosome-like structures, at least at earlier times of infection, suggests that HAdV may

make use of epigenetic regulation to help modulate viral gene expression. HAdV certainly induces global changes in the epigenetic landscape of the host cell in order to modulate the microenvironment for optimal viral replication. E1A interaction with CBP and p300 causes a global reduction in histone H3 lysine 18 acetylation (H3K18ac, a histone mark for active genes) [148] but maintains H3K18ac marks on the promoters for genes involved in the cell cycle [149]. Kulej et al. [150] also observed large-scale global changes in histone PTMs over the course of infection, but these changes were not mapped to any specific regions or genes in their study. Epigenetic changes are also observed on the HAdV chromatin, with an increase in the association of acetylated H3 at all HAdV promoters tested [89]. Since acetylated histones are commonly associated with actively transcribed genes, it suggests that as these promoters become active, they adopt an epigenetic status similar to cellular genes, which may aid in recruiting appropriate co-factors for optimal gene expression.

Several studies have demonstrated that compounds that modulate the activity of cellular epigenetic regulatory proteins are capable of impacting HAdV replication (reviewed in [151]). Histone deacetylase (HDAC) inhibitors, such as valproic acid [152], suberoylanilide hydroxamic acid (SAHA, also known as vorinostat), and trichostatin A [153], can inhibit HAdV infection. Indeed, HDAC inhibitors appear effective against multiple HAdV types, including HAdV-B7, HAdV-C5, and HAdV-E4 [153]. A screen of small molecules that modulate the activity of epigenetic regulatory proteins identified numerous pan-HDAC inhibitors with anti-HAdV properties [154]. However, HDAC inhibitors were also shown to reactivate latent viruses in tonsillectomy specimens [155], suggesting a varied mechanism of gene regulation during lytic and latent infection. Histone methyltransferases (HMTs) also appear to be required for HAdV replication, as inhibition of EZH2/1 (an H3K27 HMT [156]) or treatment of cells with chaetocin (an inhibitor of H3K9 HMT G9/G9a and SUV39H1/2 [154]) negatively impacted HAdV replication. These H3K9 methylation marks are typically associated with gene repression [157], and it is not clear if these compounds are primarily impacting viral or cellular chromatin (or both). In the case of the EZH2/1 HMT, inhibition appears to be affecting cellular chromatin and promotes the expression of cellular genes that establish an antiviral state within the cell that is hostile to virus replication [156].

8. Conclusions

As we have shown throughout this review, the HAdV nucleoprotein structure undergoes dynamic changes throughout viral replication (summarized in Figure 2). Understanding the mechanisms by which HAdV accomplishes viral gene expression and replication in the host cell is important for several reasons. First, while typically self-limiting in healthy adults, HAdV can induce severe disease in certain populations, such as pediatric, geriatric, and immunocompromised individuals (including those on immunosuppressants) [158–161]. For example, recently, HAdV has received significant notoriety for its potential involvement in a mysterious outbreak of severe acute hepatitis of unknown origin that has been diagnosed in over 650 children from 33 countries around the world (reviewed in [162, 163]). Despite the potential for significant HAdV-induced disease in infected patients, there are still no approved therapeutics for HAdV [151]. Use of some broad-spectrum antivirals shows some success against HAdV [164], but there are often secondary toxicities associated with these treatments [165]. Epigenetic modulator compounds, such as HDACs, are already being explored for use against other diseases such as cancer; thus, if they are proven safe, they could easily be used to treat HAdV infection [151]. Second, a better understanding of the dynamics of the epigenetic regulation of HAdV may help improve the safety and efficacy of HAdV-based vectors for gene therapy, such as improving tissue-specific transgene expression to avoid effects in non-target cells [166, 167]. Finally, given that HAdV is adept at identifying and hijacking key cellular processes, exploration of HAdV biology can lead to greater knowledge of host molecular cell biology, knowledge that could ultimately lead to new treatments and therapies for human disease. Undoubtedly, continued studies of HAdV-mediated epigenetic regulation of viral and cellular gene expression should provide novel insight in all of these areas.

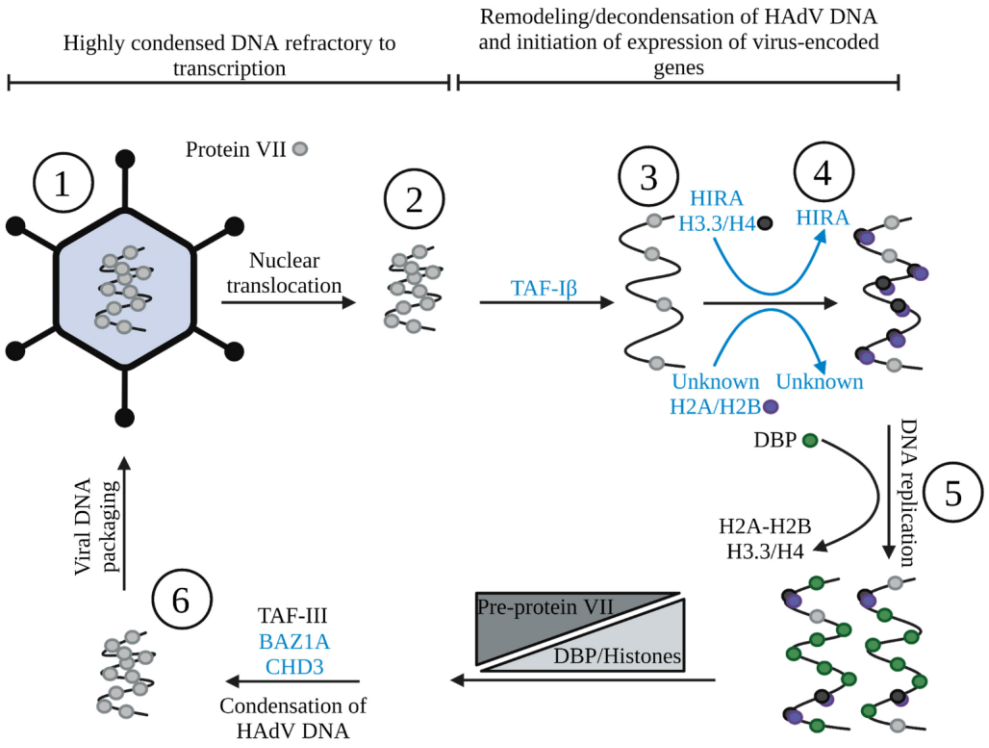

Figure 2. The structure of HAdV DNA throughout the replicative cycle. Black represents events/processes we know, while blue represents speculation based on the literature. Within the viral capsid, condensed viral DNA is wrapped in protein VII [50] (1). After entry into the cell, the protein-VII-wrapped DNA is translocated into the nucleus [77–82] (2) and is subsequently remodeled, possibly involving TAF-Iβ [87], removing some protein VII from viral DNA and decondensing the genome (3). Cellular histones are deposited onto viral DNA [89, 95, 96, 112], possibly by HIRA [95] and other histone chaperones (4), allowing for more efficient early gene expression. The nucleosome-like structures present on the viral DNA contain H2A-H2B, H3.3, and H4 [89, 96]. Following DNA replication, the viral DBP is deposited onto replicating genomes [134, 135], while some histones are present for late gene expression [96], possibly on two distinct DNA populations (5). As late infection progresses, histone pools decrease and are gradually replaced on viral DNA by pre-protein VII by TAFIII [145], recondensing the genome (6). The condensed viral core is subsequently encapsidated [147] and the virion released following lysis of the cell (1). Created with BioRender.com.

Author Contributions: Conceptualization, M.R.J.; literature search, M.R.J. and R.J.P.; resources, R.J.P.; writing—original draft, M.R.J. and R.J.P.; writing—review and editing, R.J.P. and M.R.J.; supervision, R.J.P.; funding acquisition, R.J.P.; project administration, R.J.P. All authors have read and agreed to the published version of the manuscript.

Funding: Research in the Parks lab is supported by grants to R.J.P from the Canadian Institutes of Health Research (MOP-142316, PJT-178120) and the Natural Sciences and Engineering Research Council (RGPIN-2019-04786). M.R.J is supported by a Queen Elizabeth II Graduate Scholarship in Science and Technology from the Ontario Provincial Government (Canada).

Institutional Review Board Statement: Not applicable.

Informed Consent Statement: Not applicable.

Conflicts of Interest: The authors declare no conflict of interest.

References

1. Benkő, M.; Aoki, K.; Arnberg, N.; Davison, A.J.; Echavarría, M.; Hess, M.; Jones, M.S.; Kaján, G.L.; Kajon, A.E.; Mittal, S.K.; et al. ICTV Virus Taxonomy Profile: Adenoviridae 2022. *J. Gen. Virol.* **2022**, *103*, 001721.
2. Rowe, W.P.; Huebner, R.J.; Gilmore, L.K.; Parrott, R.H.; Ward, T.G. Isolation of a Cytopathogenic Agent from Human Adenoids Undergoing Spontaneous Degeneration in Tissue Culture. *Proc. Soc. Exp. Biol. Med.* **1953**, *84*, 570–573.
3. Hilleman, M.R.; Werner, J.H. Recovery of new agent from patients with acute respiratory illness. *Proc. Soc. Exp. Biol. Med.* **1954**, *85*, 183–188.
4. Berget, S.M.; Moore, C.; Sharp, P.A. Spliced segments at the 5' terminus of adenovirus 2 late mRNA. *Proc. Natl. Acad. Sci. USA* **1977**, *74*, 3171–3175.
5. Chow, L.T.; Gelinas, R.E.; Broker, T.R.; Roberts, R.J. An amazing sequence arrangement at the 5' ends of adenovirus 2 messenger RNA. *Cell* **1977**, *12*, 1–8.
6. Whyte, P.; Williamson, N.M.; Harlow, E. Cellular targets for transformation by the adenovirus E1A proteins. *Cell* **1989**, *56*, 67–75.
7. Eckner, R.; Arany, Z.; Ewen, M.; Sellers, W.; Livingston, D.M. The adenovirus E1A-associated 300-kD protein exhibits properties of a transcriptional coactivator and

belongs to an evolutionarily conserved family. *Cold Spring Harb. Symp. Quant. Biol.* **1994**, *59*, 85–95.
8. Whyte, P.; Buchkovich, K.J.; Horowitz, J.M.; Friend, S.H.; Raybuck, M.; Weinberg, R.A.; Harlow, E. Association between an oncogene and an anti-oncogene: The adenovirus E1A proteins bind to the retinoblastoma gene product. *Nature* **1988**, *334*, 124–129.
9. Li, Y.; Graham, C.; Lacy, S.; Duncan, A.M.; Whyte, P. The adenovirus E1A-associated 130-kD protein is encoded by a member of the retinoblastoma gene family and physically interacts with cyclins A and E. *Genes Dev.* **1993**, *7*, 2366–2377.
10. Ewen, M.E.; Xing, Y.G.; Lawrence, J.B.; Livingston, D.M. Molecular cloning, chromosomal mapping, and expression of the cDNA for p107, a retinoblastoma gene product-related protein. *Cell* **1991**, *66*, 1155–1164.
11. Luger, K. Dynamic nucleosomes. *Chromosome Res.* **2006**, *14*, 5–16.
12. Allis, C.D.; Jenuwein, T. The molecular hallmarks of epigenetic control. *Nat. Rev. Genet.* **2016**, *17*, 487–500.
13. Brahma, S.; Henikoff, S. Epigenome Regulation by Dynamic Nucleosome Unwrapping. *Trends Biochem. Sci.* **2020**, *45*, 13–26.
14. Kouzarides, T. Chromatin modifications and their function. *Cell* **2007**, *128*, 693–705.
15. Gallardo, J.; Pérez-Illana, M.; Martín-González, N.; San Martín, C. Adenovirus Structure: What Is New? *Int. J. Mol. Sci.* **2021**, *22*, 5240.
16. Human Adenovirus Working Group. Available online: http://hadvwg.gmu.edu/ (accessed on 18 October 2022).
17. Davison, A.J.; Benko″, M.; Harrach, B. Genetic content and evolution of adenoviruses. *J. Gen. Virol.* **2003**, *84*, 2895–2908.
18. Berk, A.J. Recent lessons in gene expression, cell cycle control, and cell biology from adenovirus. *Oncogene* **2005**, *24*, 7673–7685.
19. King, C.R.; Zhang, A.; Tessier, T.M.; Gameiro, S.F.; Mymryk, J.S. Hacking the Cell: Network Intrusion and Exploitation by Adenovirus E1A. *MBio* **2018**, *9*, e00390-18.
20. Martin, M.E.D.; Berk, A.J. Adenovirus E1B 55K Represses p53 Activation In Vitro. *J. Virol.* **1998**, *72*, 3146–3154.
21. Querido, E.; Blanchette, P.; Yan, Q.; Kamura, T.; Morrison, M.; Boivin, D.; Kaelin, W.G.; Conaway, R.C.; Conaway, J.W.; Branton, P.E. Degradation of p53 by adenovirus E4orf6 and E1B55K proteins occurs via a novel mechanism involving a Cullin-containing complex. *Genes Dev.* **2001**, *15*, 3104–3117.
22. Stracker, T.H.; Carson, C.T.; Weitzman, M.D. Adenovirus oncoproteins inactivate the Mre11-Rad50-NBS1 DNA repair complex. *Nature* **2002**, *418*, 348–352.
23. Caravokyri, C.; Leppard, K.N. Human adenovirus type 5 variants with sequence alterations flanking the E2A gene: Effects on E2 expression and DNA replication. *Virus Genes* **1996**, *12*, 65–75.

24. Horwitz, M.S. Function of adenovirus E3 proteins and their interactions with immunoregulatory cell proteins. *J. Gene Med.* **2004**, *6*, S172–S183.
25. Georgi, F.; Greber, U.F. The Adenovirus Death Protein-A small membrane protein controls cell lysis and disease. *FEBS Lett.* **2020**, *594*, 1861–1878.
26. Weitzman, M.D. Functions of the adenovirus E4 proteins and their impact on viral vectors. *Front. Biosci.* **2005**, *10*, 1106–1117.
27. Dybas, J.M.; Lum, K.K.; Kulej, K.; Reyes, E.D.; Lauman, R.; Charman, M.; Purman, C.E.; Steinbock, R.T.; Grams, N.; Price, A.M.; et al. Adenovirus Remodeling of the Host Proteome and Host Factors Associated with Viral Genomes. *mSystems* **2021**, *6*, e00468-21.
28. Thomas, G.P.; Mathews, M.B. DNA replication and the early to late transition in adenovirus infection. *Cell* **1980**, *22*, 523–533.
29. Zhao, H.; Chen, M.; Pettersson, U. A new look at adenovirus splicing. *Virology* **2014**, *456–457*, 329–341.
30. Donovan-Banfield, I.a.; Turnell, A.S.; Hiscox, J.A.; Leppard, K.N.; Matthews, D.A. Deep splicing plasticity of the human adenovirus type 5 transcriptome drives virus evolution. *Commun. Biol.* **2020**, *3*, 124.
31. Morris, S.J.; Scott, G.E.; Leppard, K.N. Adenovirus late-phase infection is controlled by a novel L4 promoter. *J. Virol.* **2010**, *84*, 7096–7104.
32. Ying, B.; Tollefson, A.E.; Wold, W.S. Identification of a previously unrecognized promoter that drives expression of the UXP transcription unit in the human adenovirus type 5 genome. *J. Virol.* **2010**, *84*, 11470–11478.
33. Christensen, J.B.; Byrd, S.A.; Walker, A.K.; Strahler, J.R.; Andrews, P.C.; Imperiale, M.J. Presence of the adenovirus IVa2 protein at a single vertex of the mature virion. *J. Virol.* **2008**, *82*, 9086–9093.
34. Tollefson, A.E.; Ying, B.; Doronin, K.; Sidor, P.D.; Wold, W.S. Identification of a new human adenovirus protein encoded by a novel late l-strand transcription unit. *J. Virol.* **2007**, *81*, 12918–12926.
35. Svensson, C.; Akusjärvi, G. Adenovirus VA RNAI: A positive regulator of mRNA translation. *Mol. Cell. Biol.* **1984**, *4*, 736–742.
36. O'Malley, R.P.; Mariano, T.M.; Siekierka, J.; Mathews, M.B. A mechanism for the control of protein synthesis by adenovirus VA RNAI. *Cell* **1986**, *44*, 391–400.
37. Aparicio, O.; Razquin, N.; Zaratiegui, M.; Narvaiza, I.; Fortes, P. Adenovirus virus-associated RNA is processed to functional interfering RNAs involved in virus production. *J. Virol.* **2006**, *80*, 1376–1384.
38. Russell, W.C. Adenoviruses: Update on structure and function. *J. Gen. Virol.* **2009**, *90*, 1–20.
39. Liu, H.; Jin, L.; Koh, S.B.; Atanasov, I.; Schein, S.; Wu, L.; Zhou, Z.H. Atomic structure of human adenovirus by cryo-EM reveals interactions among protein networks. *Science* **2010**, *329*, 1038–1043.

40. Reddy, V.S.; Natchiar, S.K.; Stewart, P.L.; Nemerow, G.R. Crystal structure of human adenovirus at 3.5 A resolution. *Science* **2010**, *329*, 1071–1075.
41. Martín-González, N.; Hernando-Pérez, M.; Condezo, G.N.; Pérez-Illana, M.; Šiber, A.; Reguera, D.; Ostapchuk, P.; Hearing, P.; San Martín, C.; de Pablo, P.J. Adenovirus major core protein condenses DNA in clusters and bundles, modulating genome release and capsid internal pressure. *Nucleic Acids Res.* **2019**, *47*, 9231–9242.
42. Dai, X.; Wu, L.; Sun, R.; Zhou, Z.H. Atomic Structures of Minor Proteins VI and VII in the Human Adenovirus. *J. Virol.* **2017**, *91*, e00850-00817.
43. Vellinga, J.; Van der Heijdt, S.; Hoeben, R.C. The adenovirus capsid: Major progress in minor proteins. *J. Gen. Virol.* **2005**, *86*, 1581–1588.
44. Parks, R.J. Adenovirus protein IX: A new look at an old protein. *Mol. Ther.* **2005**, *11*, 19–25.
45. Maizel, J.V., Jr.; White, D.O.; Scharff, M.D. The polypeptides of adenovirus. I. Evidence for multiple protein components in the virion and a comparison of types 2, 7A, and 12. *Virology* **1968**, *36*, 115–125.
46. Russell, W.C.; Laver, W.G.; Sanderson, P.J. Internal components of adenovirus. *Nature* **1968**, *219*, 1127–1130.
47. Chatterjee, P.K.; Vayda, M.E.; Flint, S.J. Adenoviral protein VII packages intracellular viral DNA throughout the early phase of infection. *EMBO J.* **1986**, *5*, 1633–1644.
48. Fabry, C.M.; Rosa-Calatrava, M.; Conway, J.F.; Zubieta, C.; Cusack, S.; Ruigrok, R.W.; Schoehn, G. A quasi-atomic model of human adenovirus type 5 capsid. *EMBO J.* **2005**, *24*, 1645–1654.
49. Saha, B.; Wong, C.M.; Parks, R.J. The adenovirus genome contributes to the structural stability of the virion. *Viruses* **2014**, *6*, 3563.
50. Mirza, M.A.; Weber, J. Structure of adenovirus chromatin. *Biochim. Biophys. Acta* **1982**, *696*, 76–86.
51. Vayda, M.E.; Rogers, A.E.; Flint, S.J. The structure of nucleoprotein cores released from adenovirions. *Nucleic Acids Res.* **1983**, *11*, 441–460.
52. Vayda, M.E.; Flint, S.J. Isolation and characterization of adenovirus core nucleoprotein subunits. *J. Virol.* **1987**, *61*, 3335–3339.
53. Brown, D.T.; Westphal, M.; Burlingham, B.T.; Winterhoff, U.; Doerfler, W. Structure and composition of the adenovirus type 2 core. *J. Virol.* **1975**, *16*, 366–387.
54. Newcomb, W.W.; Boring, J.W.; Brown, J.C. Ion etching of human adenovirus 2: Structure of the core. *J. Virol.* **1984**, *51*, 52–56.
55. Ostapchuk, P.; Suomalainen, M.; Zheng, Y.; Boucke, K.; Greber, U.F.; Hearing, P. The adenovirus major core protein VII is dispensable for virion assembly but is essential for lytic infection. *PLoS Pathog.* **2017**, *13*, e1006455.
56. Wiethoff, C.M.; Wodrich, H.; Gerace, L.; Nemerow, G.R. Adenovirus protein VI mediates membrane disruption following capsid disassembly. *J. Virol.* **2005**, *79*, 1992–2000.

57. Everitt, E.; Sundquist, B.; Pettersson, U.; Philipson, L. Structural proteins of adenoviruses: X. Isolation and topography of low molecular weight antigens from the virion of adenovirus type 2. *Virology* **1973**, *52*, 130–147.
58. Pérez-Vargas, J.; Vaughan, R.C.; Houser, C.; Hastie, K.M.; Kao, C.C.; Nemerow, G.R. Isolation and characterization of the DNA and protein binding activities of adenovirus core protein V. *J. Virol.* **2014**, *88*, 9287–9296.
59. Stewart, P.L.; Fuller, S.D.; Burnett, R.M. Difference imaging of adenovirus: Bridging the resolution gap between X-ray crystallography and electron microscopy. *EMBO J.* **1993**, *12*, 2589–2599.
60. Matthews, D.A.; Russell, W.C. Adenovirus core protein V is delivered by the invading virus to the nucleus of the infected cell and later in infection is associated with nucleoli. *J. Gen. Virol.* **1998**, *79*, 1671–1675.
61. Ugai, H.; Borovjagin, A.V.; Le, L.P.; Wang, M.; Curiel, D.T. Thermostability/infectivity defect caused by deletion of the core protein V gene in human adenovirus type 5 is rescued by thermo-selectable mutations in the core protein X precursor. *J. Mol. Biol.* **2007**, *366*, 1142–1160.
62. Bauer, M.; Gomez-Gonzalez, A.; Suomalainen, M.; Schilling, N.; Hemmi, S.; Greber, U.F. A viral ubiquitination switch attenuates innate immunity and triggers nuclear import of virion DNA and infection. *Sci. Adv.* **2021**, *7*, eabl7150.
63. Smith, A.C.; Poulin, K.L.; Parks, R.J. DNA Genome Size Affects the Stability of the Adenovirus Virion. *J. Virol.* **2009**, *83*, 2025–2028.
64. Kennedy, M.A.; Parks, R.J. Adenovirus virion stability and the viral genome: Size matters. *Mol. Ther.* **2009**, *17*, 1664–1666.
65. Bett, A.J.; Prevec, L.; Graham, F.L. Packaging capacity and stability of human adenovirus type 5 vectors. *J. Virol.* **1993**, *67*, 5911–5921.
66. Parks, R.J.; Graham, F.L. A helper-dependent system for adenovirus vector production helps define a lower limit for efficient DNA packaging. *J. Virol.* **1997**, *71*, 3293–3298.
67. Bergelson, J.M.; Cunningham, J.A.; Droguett, G.; Kurt-Jones, E.A.; Krithivas, A.; Hong, J.S.; Horwitz, M.S.; Crowell, R.L.; Finberg, R.W. Isolation of a common receptor for Coxsackie B viruses and adenoviruses 2 and 5. *Science* **1997**, *275*, 1320–1323.
68. Tomko, R.P.; Xu, R.; Philipson, L. HCAR and MCAR: The human and mouse cellular receptors for subgroup C adenoviruses and group B coxsackieviruses. *Proc. Natl. Acad. Sci. USA* **1997**, *94*, 3352–3356.
69. Smith, T.A.; Idamakanti, N.; Rollence, M.L.; Marshall-Neff, J.; Kim, J.; Mulgrew, K.; Nemerow, G.R.; Kaleko, M.; Stevenson, S.C. Adenovirus serotype 5 fiber shaft influences in vivo gene transfer in mice. *Hum. Gene Ther.* **2003**, *14*, 777–787.
70. Shayakhmetov, D.M.; Gaggar, A.; Ni, S.; Li, Z.Y.; Lieber, A. Adenovirus binding to blood factors results in liver cell infection and hepatotoxicity. *J. Virol.* **2005**, *79*, 7478–7491.

71. Waddington, S.N.; McVey, J.H.; Bhella, D.; Parker, A.L.; Barker, K.; Atoda, H.; Pink, R.; Buckley, S.M.; Greig, J.A.; Denby, L.; et al. Adenovirus serotype 5 hexon mediates liver gene transfer. *Cell* **2008**, *132*, 397–409.
72. Kalyuzhniy, O.; Di Paolo, N.C.; Silvestry, M.; Hofherr, S.E.; Barry, M.A.; Stewart, P.L.; Shayakhmetov, D.M. Adenovirus serotype 5 hexon is critical for virus infection of hepatocytes in vivo. *Proc. Natl. Acad. Sci. USA* **2008**, *105*, 5483–5488.
73. Tian, J.; Xu, Z.; Moitra, R.; Palmer, D.J.; Ng, P.; Byrnes, A.P. Binding of adenovirus species C hexon to prothrombin and the influence of hexon on vector properties in vitro and in vivo. *PLoS Pathog.* **2022**, *18*, e1010859.
74. Wickham, T.J.; Mathias, P.; Cheresh, D.A.; Nemerow, G.R. Integrins alpha v beta 3 and alpha v beta 5 promote adenovirus internalization but not virus attachment. *Cell* **1993**, *73*, 309–319.
75. Wiethoff, C.M.; Nemerow, G.R. Adenovirus membrane penetration: Tickling the tail of a sleeping dragon. *Virology* **2015**, *479–480*, 591–599.
76. Leopold, P.L.; Ferris, B.; Grinberg, I.; Worgall, S.; Hackett, N.R.; Crystal, R.G. Fluorescent virions: Dynamic tracking of the pathway of adenoviral gene transfer vectors in living cells. *Hum. Gene Ther.* **1998**, *9*, 367–378.
77. Greber, U.F.; Willetts, M.; Webster, P.; Helenius, A. Stepwise dismantling of adenovirus 2 during entry into cells. *Cell* **1993**, *75*, 477–486.
78. Bauer, M.; Flatt, J.W.; Seiler, D.; Cardel, B.; Emmenlauer, M.; Boucke, K.; Suomalainen, M.; Hemmi, S.; Greber, U.F. The E3 Ubiquitin Ligase Mind Bomb 1 Controls Adenovirus Genome Release at the Nuclear Pore Complex. *Cell Rep.* **2019**, *29*, 3785–3795.e3788.
79. Greber, U.F.; Suomalainen, M. Adenovirus entry: Stability, uncoating, and nuclear import. *Mol. Microbiol.* **2022**, *118*, 309–320.
80. Chatterjee, P.K.; Vayda, M.E.; Flint, S.J. Identification of proteins and protein domains that contact DNA within adenovirus nucleoprotein cores by ultraviolet light crosslinking of oligonucleotides 32P-labelled in vivo. *J. Mol. Biol.* **1986**, *188*, 23–37.
81. Strunze, S.; Engelke, M.F.; Wang, I.H.; Puntener, D.; Boucke, K.; Schleich, S.; Way, M.; Schoenenberger, P.; Burckhardt, C.J.; Greber, U.F. Kinesin-1-Mediated Capsid Disassembly and Disruption of the Nuclear Pore Complex Promote Virus Infection. *Cell Host Microbe* **2011**, *10*, 210–223.
82. Cassany, A.; Ragues, J.; Guan, T.; Bégu, D.; Wodrich, H.; Kann, M.; Nemerow, G.R.; Gerace, L.; Imperiale, M.J. Nuclear Import of Adenovirus DNA Involves Direct Interaction of Hexon with an N-Terminal Domain of the Nucleoporin Nup214. *J. Virol.* **2015**, *89*, 1719–1730.
83. Avgousti, D.C.; Della Fera, A.N.; Otter, C.J.; Herrmann, C.; Pancholi, N.J.; Weitzman, M.D. Adenovirus Core Protein VII Downregulates the DNA Damage Response on the Host Genome. *J. Virol.* **2017**, *91*, e01089-17.

84. Carson, C.T.; Schwartz, R.A.; Stracker, T.H.; Lilley, C.E.; Lee, D.V.; Weitzman, M.D. The Mre11 complex is required for ATM activation and the G2/M checkpoint. *EMBO J.* **2003**, *22*, 6610–6620.
85. Johnson, J.S.; Osheim, Y.N.; Xue, Y.; Emanuel, M.R.; Lewis, P.W.; Bankovich, A.; Beyer, A.L.; Engel, D.A. Adenovirus protein VII condenses DNA, represses transcription, and associates with transcriptional activator E1A. *J. Virol.* **2004**, *78*, 6459–6468.
86. Vayda, M.E.; Leong, K.; Flint, S.J. Transcription of adenovirus cores in vitro. *Virology* **1984**, *139*, 152–163.
87. Matsumoto, K.; Nagata, K.; Ui, M.; Hanaoka, F. Template activating factor I, a novel host factor required to stimulate the adenovirus core DNA replication. *J. Bio. Chem.* **1993**, *268*, 10582–10587.
88. Okuwaki, M.; Nagata, K. Template Activating Factor-I Remodels the Chromatin Structure and Stimulates Transcription from the Chromatin Template *. *J. Bio. Chem.* **1998**, *273*, 34511–34518.
89. Komatsu, T.; Haruki, H.; Nagata, K. Cellular and viral chromatin proteins are positive factors in the regulation of adenovirus gene expression. *Nucleic Acids Res.* **2011**, *39*, 889–901.
90. Chen, J.; Morral, N.; Engel, D.A. Transcription releases protein VII from adenovirus chromatin. *Virology* **2007**, *369*, 411–422.
91. Inturi, R.; Thaduri, S.; Punga, T. Adenovirus precursor pVII protein stability is regulated by its propeptide sequence. *PLoS ONE* **2013**, *8*, e80617.
92. Avgousti, D.C.; Herrmann, C.; Kulej, K.; Pancholi, N.J.; Sekulic, N.; Petrescu, J.; Molden, R.C.; Blumenthal, D.; Paris, A.J.; Reyes, E.D.; et al. A core viral protein binds host nucleosomes to sequester immune danger signals. *Nature* **2016**, *535*, 173–177.
93. Haruki, H.; Gyurcsik, B.; Okuwaki, M.; Nagata, K. Ternary complex formation between DNA-adenovirus core protein VII and TAF-Ibeta/SET, an acidic molecular chaperone. *FEBS Lett.* **2003**, *555*, 521–527.
94. Xue, Y.; Johnson, J.S.; Ornelles, D.A.; Lieberman, J.; Engel, D.A. Adenovirus protein VII functions throughout early phase and interacts with cellular proteins SET and pp32. *J. Virol.* **2005**, *79*, 2474–2483.
95. Ross, P.J.; Kennedy, M.A.; Christou, C.; Risco Quiroz, M.; Poulin, K.L.; Parks, R.J. Assembly of helper-dependent adenovirus DNA into chromatin promotes efficient gene expression. *J. Virol.* **2011**, *85*, 3950–3958.
96. Giberson, A.N.; Saha, B.; Campbell, K.; Christou, C.; Poulin, K.L.; Parks, R.J. Human adenoviral DNA association with nucleosomes containing histone variant H3.3 during the early phase of infection is not dependent on viral transcription or replication. *Biochem. Cell Biol.* **2018**, *96*, 797–807.
97. Karen, K.A.; Hearing, P. Adenovirus core protein VII protects the viral genome from a DNA damage response at early times after infection. *J. Virol.* **2011**, *85*, 4135–4142.

98. Nelson, J.E.; Kay, M.A. Persistence of recombinant adenovirus in vivo is not dependent on vector DNA replication. *J. Virol.* **1997**, *71*, 8902–8907.
99. Saha, B.; Parks, R.J. Human adenovirus type 5 vectors deleted of early region 1 (E1) undergo limited expression of early replicative E2 proteins and DNA replication in non-permissive cells. *PLoS ONE* **2017**, *12*, e0181012.
100. Gyurcsik, B.; Haruki, H.; Takahashi, T.; Mihara, H.; Nagata, K. Binding Modes of the Precursor of Adenovirus Major Core Protein VII to DNA and Template Activating Factor I: Implication for the Mechanism of Remodeling of the Adenovirus Chromatin. *Biochemistry* **2006**, *45*, 303–313.
101. Komatsu, T.; Dacheux, D.; Kreppel, F.; Nagata, K.; Wodrich, H. A Method for Visualization of Incoming Adenovirus Chromatin Complexes in Fixed and Living Cells. *PLoS ONE* **2015**, *10*, e0137102.
102. Haruki, H.; Okuwaki, M.; Miyagishi, M.; Taira, K.; Nagata, K. Involvement of template-activating factor I/SET in transcription of adenovirus early genes as a positive-acting factor. *J. Virol.* **2006**, *80*, 794–801.
103. Kawase, H.; Okuwaki, M.; Miyaji, M.; Ohba, R.; Handa, H.; Ishimi, Y.; Fujii-Nakata, T.; Kikuchi, A.; Nagata, K. NAP-I is a functional homologue of TAF-I that is required for replication and transcription of the adenovirus genome in a chromatin-like structure. *Genes Cells* **1996**, *1*, 1045–1056.
104. Okuwaki, M.; Iwamatsu, A.; Tsujimoto, M.; Nagata, K. Identification of nucleophosmin/B23, an acidic nucleolar protein, as a stimulatory factor for in vitro replication of adenovirus DNA complexed with viral basic core proteins. *J. Mol. Biol.* **2001**, *311*, 41–55.
105. Lotze, M.T.; Tracey, K.J. High-mobility group box 1 protein (HMGB1): Nuclear weapon in the immune arsenal. *Nat. Rev. Immunol.* **2005**, *5*, 331–342.
106. Lynch, K.L.; Dillon, M.R.; Bat-Erdene, M.; Lewis, H.C.; Kaai, R.J.; Arnold, E.A.; Avgousti, D.C. A viral histone-like protein exploits antagonism between linker histones and HMGB proteins to obstruct the cell cycle. *Curr. Biol.* **2021**, *31*, 5227–5237.e5227.
107. Sergeant, A.; Tigges, M.A.; Raskas, H.J. Nucleosome-like structural subunits of intranuclear parental adenovirus type 2 DNA. *J. Virol.* **1979**, *29*, 888–898.
108. Daniell, E.; Groff, D.E.; Fedor, M.J. Adenovirus chromatin structure at different stages of infection. *Mol. Cell. Biol.* **1981**, *1*, 1094–1105.
109. Beyer, A.L.; Bouton, A.H.; Hodge, L.D.; Miller, O.L., Jr. Visualization of the major late R strand transcription unit of adenovirus serotype 2. *J. Mol. Biol.* **1981**, *147*, 269–295.
110. Déry, C.V.; Toth, M.; Brown, M.; Horvath, J.; Allaire, S.; Weber, J.M. The structure of adenovirus chromatin in infected cells. *J. Gen. Virol.* **1985**, *66*, 2671–2684.
111. Wong, M.L.; Hsu, M.T. Psoralen-cross-linking study of the organization of intracellular adenovirus nucleoprotein complexes. *J. Virol.* **1988**, *62*, 1227–1234.

112. Komatsu, T.; Nagata, K. Replication-uncoupled histone deposition during adenovirus DNA replication. *J. Virol.* **2012**, *86*, 6701–6711.
113. Smith, S.; Stillman, B. Purification and characterization of CAF-I, a human cell factor required for chromatin assembly during DNA replication in vitro. *Cell* **1989**, *58*, 15–25.
114. Talbert, P.B.; Henikoff, S. Histone variants at a glance. *J. Cell Sci.* **2021**, *134*, jcs244749.
115. Tagami, H.; Ray-Gallet, D.; Almouzni, G.; Nakatani, Y. Histone H3.1 and H3.3 complexes mediate nucleosome assembly pathways dependent or independent of DNA synthesis. *Cell* **2004**, *116*, 51–61.
116. Pradhan, S.K.; Su, T.; Yen, L.; Jacquet, K.; Huang, C.; Côté, J.; Kurdistani, S.K.; Carey, M.F. EP400 Deposits H3.3 into Promoters and Enhancers during Gene Activation. *Mol. Cell* **2016**, *61*, 27–38.
117. Goldberg, A.D.; Banaszynski, L.A.; Noh, K.M.; Lewis, P.W.; Elsaesser, S.J.; Stadler, S.; Dewell, S.; Law, M.; Guo, X.; Li, X.; et al. Distinct factors control histone variant H3.3 localization at specific genomic regions. *Cell* **2010**, *140*, 678–691.
118. Loppin, B.; Bonnefoy, E.; Anselme, C.; Laurençon, A.; Karr, T.L.; Couble, P. The histone H3.3 chaperone HIRA is essential for chromatin assembly in the male pronucleus. *Nature* **2005**, *437*, 1386–1390.
119. Drané, P.; Ouararhni, K.; Depaux, A.; Shuaib, M.; Hamiche, A. The death-associated protein DAXX is a novel histone chaperone involved in the replication-independent deposition of H3.3. *Genes Dev.* **2010**, *24*, 1253–1265.
120. Lewis, P.W.; Elsaesser, S.J.; Noh, K.M.; Stadler, S.C.; Allis, C.D. Daxx is an H3.3-specific histone chaperone and cooperates with ATRX in replication-independent chromatin assembly at telomeres. *Proc. Natl. Acad. Sci. USA* **2010**, *107*, 14075–14080.
121. Placek, B.J.; Huang, J.; Kent, J.R.; Dorsey, J.; Rice, L.; Fraser, N.W.; Berger, S.L. The histone variant H3.3 regulates gene expression during lytic infection with herpes simplex virus type 1. *J. Virol.* **2009**, *83*, 1416–1421.
122. Schreiner, S.; Wimmer, P.; Sirma, H.; Everett, R.D.; Blanchette, P.; Groitl, P.; Dobner, T. Proteasome-dependent degradation of Daxx by the viral E1B-55K protein in human adenovirus-infected cells. *J. Virol.* **2010**, *84*, 7029–7038.
123. Ullman, A.J.; Hearing, P. Cellular proteins PML and Daxx mediate an innate antiviral defense antagonized by the adenovirus E4 ORF3 protein. *J. Virol.* **2008**, *82*, 7325–7335.
124. Schreiner, S.; Bürck, C.; Glass, M.; Groitl, P.; Wimmer, P.; Kinkley, S.; Mund, A.; Everett, R.D.; Dobner, T. Control of human adenovirus type 5 gene expression by cellular Daxx/ATRX chromatin-associated complexes. *Nucleic Acids Res.* **2013**, *41*, 3532–3550.

125. Lin, J.J.; Lehmann, L.W.; Bonora, G.; Sridharan, R.; Vashisht, A.A.; Tran, N.; Plath, K.; Wohlschlegel, J.A.; Carey, M. Mediator coordinates PIC assembly with recruitment of CHD1. *Genes Dev.* **2011**, *25*, 2198–2209.
126. Marcos-Villar, L.; Pazo, A.; Nieto, A. Influenza Virus and Chromatin: Role of the CHD1 Chromatin Remodeler in the Virus Life Cycle. *J. Virol.* **2016**, *90*, 3694–3707.
127. Tate, V.E.; Philipson, L. Parental adenovirus DNA accumulates in nucleosome-like structures in infected cells. *Nucleic Acids Res.* **1979**, *6*, 2769–2785.
128. Lacasse, J.J.; Schang, L.M. During Lytic Infections, Herpes Simplex Virus Type 1 DNA Is in Complexes with the Properties of Unstable Nucleosomes. *J. Virol.* **2010**, *84*, 1920–1933.
129. Hodge, L.D.; Scharff, M.D. Effect of adenovirus on host cell DNA synthesis in synchronized cells. *Virology* **1969**, *37*, 554–564.
130. Tallman, G.; Akers, J.E.; Burlingham, B.T.; Reeck, G.R. Histone synthesis is not coupled to the replication of adenovirus DNA. *Biochem. Biophys. Res. Commun.* **1977**, *79*, 815–822.
131. Hoeben, R.C.; Uil, T.G. Adenovirus DNA Replication. *Cold Spring Harb. Perspect. Biol.* **2013**, *5*, a013003.
132. Zijderveld, D.C.; van der Vliet, P.C. Helix-destabilizing properties of the adenovirus DNA-binding protein. *J. Virol.* **1994**, *68*, 1158–1164.
133. Dekker, J.; Kanellopoulos, P.N.; Loonstra, A.K.; van Oosterhout, J.A.; Leonard, K.; Tucker, P.A.; van der Vliet, P.C. Multimerization of the adenovirus DNA-binding protein is the driving force for ATP-independent DNA unwinding during strand displacement synthesis. *EMBO J.* **1997**, *16*, 1455–1463.
134. Stuiver, M.H.; Bergsma, W.G.; Arnberg, A.C.; van Amerongen, H.; van Grondelle, R.; van der Vliet, P.C. Structural alterations of double-stranded DNA in complex with the adenovirus DNA-binding protein. Implications for its function in DNA replication. *J. Mol. Biol.* **1992**, *225*, 999–1011.
135. van der Vliet, P.C.; Keegstra, W.; Jansz, H.S. Complex Formation between the Adenovirus Type 5 DNA-Binding Protein and Single-Stranded DNA. *Eur. J. Biochem.* **1978**, *86*, 389–398.
136. Nagata, K.; Guggenheimer, R.A.; Hurwitz, J. Adenovirus DNA replication in vitro: Synthesis of full-length DNA with purified proteins. *Proc. Natl. Acad. Sci. USA* **1983**, *80*, 4266–4270.
137. Leegwater, P.A.J.; Rombouts, R.F.A.; van der Vliet, P.C. Adenovirus DNA replication in vitro: Duplication of single-stranded DNA containing a panhandle structure. *Biochim. Biophys. Acta Gene Struct. Expr.* **1988**, *951*, 403–410.
138. Ray-Gallet, D.; Woolfe, A.; Vassias, I.; Pellentz, C.; Lacoste, N.; Puri, A.; Schultz, D.C.; Pchelintsev, N.A.; Adams, P.D.; Jansen, L.E.; et al. Dynamics of histone H3 deposition in vivo reveal a nucleosome gap-filling mechanism for H3.3 to maintain chromatin integrity. *Mol. Cell* **2011**, *44*, 928–941.

139. Pombo, A.; Ferreira, J.; Bridge, E.; Carmo-Fonseca, M. Adenovirus replication and transcription sites are spatially separated in the nucleus of infected cells. *EMBO J.* **1994**, *13*, 5075–5085.
140. Brison, O.; Kédinger, C.; Chambon, P. Adenovirus DNA template for late transcription is not a replicative intermediate. *J. Virol.* **1979**, *32*, 91–97.
141. Brown, M.; Weber, J. Virion core-like organization of intranuclear adenovirus chromatin late in infection. *Virology* **1980**, *107*, 306–310.
142. Komatsu, T.; Robinson, D.R.; Hisaoka, M.; Ueshima, S.; Okuwaki, M.; Nagata, K.; Wodrich, H. Tracking adenovirus genomes identifies morphologically distinct late DNA replication compartments. *Traffic* **2016**, *17*, 1168–1180.
143. Burg, J.L.; Schweitzer, J.; Daniell, E. Introduction of superhelical turns into DNA by adenoviral core proteins and chromatin assembly factors. *J. Virol.* **1983**, *46*, 749–755.
144. Samad, M.A.; Okuwaki, M.; Haruki, H.; Nagata, K. Physical and functional interaction between a nucleolar protein nucleophosmin/B23 and adenovirus basic core proteins. *FEBS Lett.* **2007**, *581*, 3283–3288.
145. Samad, M.A.; Komatsu, T.; Okuwaki, M.; Nagata, K. B23/nucleophosmin is involved in regulation of adenovirus chromatin structure at late infection stages, but not in virus replication and transcription. *J. Gen. Virol.* **2012**, *93*, 1328–1338.
146. Inturi, R.; Mun, K.; Singethan, K.; Schreiner, S.; Punga, T. Human Adenovirus Infection Causes Cellular E3 Ubiquitin Ligase MKRN1 Degradation Involving the Viral Core Protein pVII. *J. Virol.* **2018**, *92*, e01154-17.
147. Condezo, G.N.; San Martín, C. Localization of adenovirus morphogenesis players, together with visualization of assembly intermediates and failed products, favor a model where assembly and packaging occur concurrently at the periphery of the replication center. *PLoS Pathog.* **2017**, *13*, e1006320.
148. Horwitz, G.A.; Zhang, K.; McBrian, M.A.; Grunstein, M.; Kurdistani, S.K.; Berk, A.J. Adenovirus Small e1a Alters Global Patterns of Histone Modification. *Science* **2008**, *321*, 1084–1085.
149. Ferrari, R.; Pellegrini, M.; Horwitz, G.A.; Xie, W.; Berk, A.J.; Kurdistani, S.K. Epigenetic reprogramming by adenovirus e1a. *Science (New York, N.Y.)* **2008**, *321*, 1086–1088.
150. Kulej, K.; Avgousti, D.C.; Weitzman, M.D.; Garcia, B.A. Characterization of histone post-translational modifications during virus infection using mass spectrometry-based proteomics. *Methods* **2015**, *90*, 8–20.
151. Saha, B.; Parks, R.J. Recent Advances in Novel Antiviral Therapies against Human Adenovirus. *Microorganisms* **2020**, *8*, 1284.
152. Höti, N.; Chowdhury, W.; Hsieh, J.-T.; Sachs, M.D.; Lupold, S.E.; Rodriguez, R. Valproic Acid, a Histone Deacetylase Inhibitor, Is an Antagonist for Oncolytic Adenoviral Gene Therapy. *Mol. Ther.* **2006**, *14*, 768–778.

153. Saha, B.; Parks, R.J. Histone Deacetylase Inhibitor Suberoylanilide Hydroxamic Acid Suppresses Human Adenovirus Gene Expression and Replication. *J. Virol.* **2019**, *93*, e00088-19.
154. Saha, B.; Parks, R.J. Identification of human adenovirus replication inhibitors from a library of small molecules targeting cellular epigenetic regulators. *Virology* **2021**, *555*, 102–110.
155. Wang, L.; Zhang, M.; Li, J.; Yang, G.; Huang, Q.; Li, J.; Wang, H.; He, S.; Li, E. HDAC inhibitors promote latent adenovirus reactivation from tonsillectomy specimens. *J. Virol.* **2020**, *94*, e00100-20.
156. Arbuckle, J.H.; Gardina, P.J.; Gordon, D.N.; Hickman, H.D.; Yewdell, J.W.; Pierson, T.C.; Myers, T.G.; Kristie, T.M. Inhibitors of the Histone Methyltransferases EZH2/1 Induce a Potent Antiviral State and Suppress Infection by Diverse Viral Pathogens. *MBio* **2017**, *8*, e01141-17.
157. Zhao, Y.; Garcia, B.A. Comprehensive Catalog of Currently Documented Histone Modifications. *Cold Spring Harb. Perspect. Biol.* **2015**, *7*, a025064.
158. Lion, T. Adenovirus infections in immunocompetent and immunocompromised patients. *Clin. Microbiol. Rev.* **2014**, *27*, 441–462.
159. Bhatti, Z.; Dhamoon, A. Fatal adenovirus infection in an immunocompetent host. *Am. J. Emerg. Med.* **2017**, *35*, 1034.e1031–1034.e1032.
160. Al-Heeti, O.M.; Cathro, H.P.; Ison, M.G. Adenovirus Infection and Transplantation. *Transplantation* **2022**, *106*, 920–927.
161. Dotan, M.; Zion, E.; Bilavsky, E.; Nahum, E.; Ben-Zvi, H.; Zalcman, J.; Yarden-Bilavsky, H.; Kadmon, G. Adenovirus can be a serious, life-threatening disease, even in previously healthy children. *Acta Paediatr.* **2021**, *111*, 614–619.
162. Pérez-Gracia, M.T.; Tarín-Pelló, A.; Suay-García, B. Severe Acute Hepatitis of Unknown Origin in Children: What Do We Know Today? *J. Clin. Transl. Hepatol.* **2022**, *10*, 711–717.
163. Uwishema, O.; Mahmoud, A.; Wellington, J.; Mohammed, S.M.; Yadav, T.; Derbieh, M.; Arab, S.; Kolawole, B. A review on acute, severe hepatitis of unknown origin in children: A call for concern. *Ann. Med. Surg.* **2022**, *81*, 104457.
164. Chamberlain, J.M.; Sortino, K.; Sethna, P.; Bae, A.; Lanier, R.; Bambara, R.A.; Dewhurst, S. Cidofovir Diphosphate Inhibits Adenovirus 5 DNA Polymerase via both Nonobligate Chain Termination and Direct Inhibition, and Polymerase Mutations Confer Cidofovir Resistance on Intact Virus. *Antimicrob. Agents Chemother.* **2018**, *63*, e01925-18.
165. Takamatsu, A.; Tagashira, Y.; Hasegawa, S.; Honda, H. Disseminated adenovirus infection in a patient with a hematologic malignancy: A case report and literature review. *Future Sci. OA* **2019**, *5*, FSO412.

166. Amalfitano, A.; Parks, R.J. Separating fact from fiction: Assessing the potential of modified adenovirus vectors for use in human gene therapy. *Curr. Gene Ther.* **2002**, *2*, 111–133.
167. Watanabe, M.; Nishikawaji, Y.; Kawakami, H.; Kosai, K.I. Adenovirus Biology, Recombinant Adenovirus, and Adenovirus Usage in Gene Therapy. *Viruses* **2021**, *13*, 2502.

Appendix 3:

Curcumin as an Antiviral Agent

Viruses **2020**, *12*, 1242; doi: 10.3390/v12111242.

Review

Curcumin as an Antiviral Agent

Morgan R. Jennings [1, 2] and Robin J. Parks [1, 2, 3, 4, *]

[1] Regenerative Medicine Program, Ottawa Hospital Research Institute, Ottawa, ON K1H 8L6, Canada
[2] Department of Biochemistry, Microbiology and Immunology, University of Ottawa, Ottawa, ON K1N 6N5, Canada
[3] Centre for Neuromuscular Disease, University of Ottawa, Ottawa, ON K1N 6N5, Canada
[4] Department of Medicine, The Ottawa Hospital, Ottawa, ON K1H 8L6, Canada

***** Correspondence

Received: 01 October 2020; Accepted: 29 October 2020; Published: 31 October 2020

Abstract: Curcumin, the primary curcuminoid compound found in turmeric spice, has shown broad activity as an antimicrobial agent, limiting the replication of many different fungi, bacteria and viruses. In this review, we summarize recent studies supporting the development of curcumin and its derivatives as broad-spectrum antiviral agents.

Keywords: curcumin; antiviral; broad-spectrum; phytochemical

1. Introduction

Curcumin (diferuloylmethane) is the primary curcuminoid derived from the rhizome of Curcuma longa plant [1, 2], and is typically used both as a strong food dye and consumed as a spice in the form of turmeric [1]. In addition, curcumin has seen wide use in traditional medicine throughout Asia, due to its anti-inflammatory and wound-healing properties [3, 4]. Modern research has also demonstrated that curcumin has diverse biological functions, with reported anti-cancer, antioxidant and anti-microbial properties [3, 5, 6]. Curcumin can act not only as an anti-fungal and anti-bacterial compound, but also as an anti-viral compound, inhibiting replication in a wide-range of viruses [7], as summarized in Table 1. In this review, recent research into the antiviral properties of curcumin, its derivatives, and formulations will be discussed.

Table 1. Pathways/processes impacted by curcumin and analogues, and their effect on viruses.

Pathway/Process	Antiviral Activity	Virus	References
Actin filament organization	Viral entry	Dengue virus Viral hemorrhagic septicemia virus	[8] [9]
	Replication	Dengue virus	[8]
Anti-inflammation	Replication	Human immunodeficiency virus	[10]
Antioxidation	Replication	Human immunodeficiency virus	[11]
APE1 redox reactions	Replication	Kaposi's sarcoma-associated herpesvirus	[12]
Cell lipogenesis	Replication	Dengue virus	[8]
Cleavage of eIF4G	Protein expression	Enterovirus 71	[13]
Conformation of viral/cellular surface proteins	Viral attachment	Zika virus Chikungunya virus Vesicular stomatitis virus	[14–16]
		Human respiratory syncytial virus	[17, 18]
HSC71 expression	Viral entry	Viral hemorrhagic septicemia virus	[9]
NF-κB signalling	Replication Viral egress	Influenza A virus Herpes simplex virus 2	[19] [10]
PKCδ phosphorylation	Protein expression?	Enterovirus 71	[20]
ROS production	Viricidal	Norovirus	[21, 22]
Lipid raft formation		Bovine herpes virus 1	[23]
Viral enzymes	Viral egress Viral protease	Influenza A virus Dengue virus	[24] [8]
Viral proteins	Viral entry	Influenza A virus Porcine reproductive and respiratory syndrome virus	[24] [25]
	Viral protein degradation	Human immunodeficiency virus	[26]
	Viricidal	Norovirus	[21]

2. Curcumin

Approximately 3–5% of ground and dried turmeric are the curcuminoids [27]. The curcuminoids are comprised of curcumin (77%), demethoxycurcumin (17%) and bisdemethoxycurcumin (6%) (Figure 1). For the purpose of this review, we will refer to the purified products by name, and curcuminoid will refer to two or more of these compounds together. Curcumin is "generally recognized as safe" by the Food and Drug Administration (FDA) [28], with consumption of doses up to 5 g/kg reported to have no toxic effects in rats [29]. For comparison, the median lethal dose (LD50) of table salt in rats is approximately 3 g/kg [30].

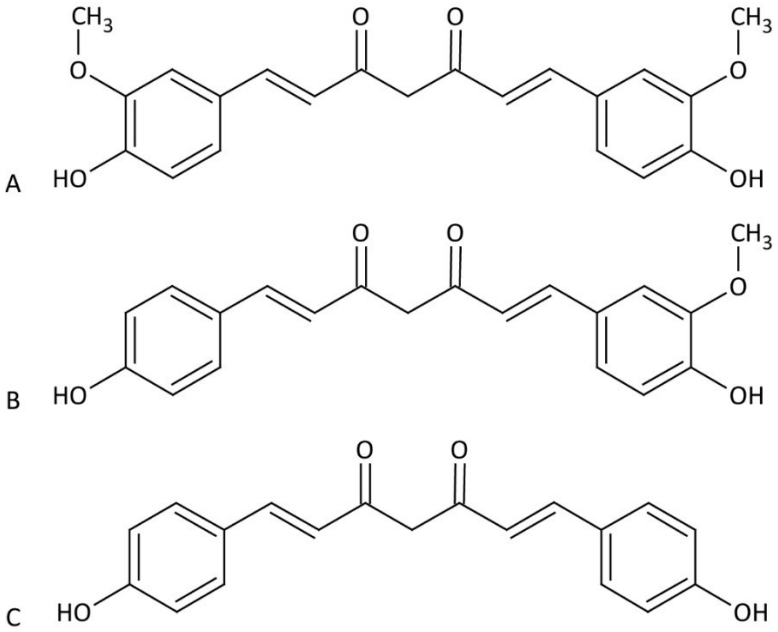

Figure1. Chemical structure of curcuminoids. Chemical structure of curcumin (A), demethoxycurcumin (B) and bisdemethoxycurcumin (C).

The first suggestion that curcumin had antiviral properties came in the 1990s with the discovery that curcumin could inhibit the human immunodeficiency virus (HIV) viral protease in vitro, with a median inhibitory concentration (IC50) of 100 μM [31]. Since then, numerous studies have reported on the antiviral properties of curcumin against a diverse set of viruses, including those with RNA and DNA genomes, both enveloped and

non-enveloped, as discussed in greater detail below.

Despite promise as an antimicrobial agent, curcumin has several limitations. Curcumin is practically insoluble in water, with low *in vivo* bioavailability. As little as 1% of administered curcumin is absorbed by the body, and it remains virtually undetectable in target tissues [32, 33]. For example, ingestion of 12 g of curcumin resulted in a concentration of 29.7 ng/mL (~81 nM) of curcumin in human blood serum one-hour (h) post-ingestion [34], which is far below any effective concentration reported in many *in vitro* studies. For example, curcumin is needed at an IC50 of 40 μM to inhibit the HIV-1 integrase [35], while the effective dose against influenza A virus (IAV) is ~10 μM [36]. In addition, curcumin is unstable at physiological pH, with a half-life in growth medium containing serum of approximately 8 h, and rapidly degrades into several ineffective products [1]. Such limitations have prevented translation of the many very promising in vitro findings with curcumin into clinical benefit. To overcome these obstacles, researchers have explored the use of curcumin derivatives. These compounds include the other curcuminoids present in turmeric besides curcumin, as well as synthetic curcumin analogues. Typically, these compounds maintain a particular chemical moiety of curcumin that is responsible for biological efficacy, but are designed to improve biological activity, solubility and/or stability. One such example includes the synthesis of novel carbocyclic curcumin derivatives (addition of a carbon ring to one of curcumin's ketone groups), which led to improved HIV-1 protease inhibition [37]. Many research groups have sought to improve delivery of curcumin through the use of various formulations such as nanoemulsions and nanoparticles. Examples include liposome-encapsulated curcumin, which improved stability in phosphate-buffered saline (PBS) and reduced toxicity compared to free curcumin [38], and curcumin-loaded apotransferrin nanoparticles, which improved cellular uptake [39]. Further examples of chemical derivatives and alternative formulations for delivery and stability are provided throughout this review.

3. RNA Viruses

3.1. Human Immunodeficiency Virus

Perhaps the largest body of work on the anti-viral properties of curcumin pertain to

its efficacy against HIV. Indeed, curcumin can impact HIV function at several different stages of the virus lifecycle. Given the anti-inflammatory properties of curcumin, Ferreira et al. [10] evaluated whether curcumin could reduce inflammation in the female genital tract (FGT), which is known to facilitate HIV acquisition. Epithelial cells lining the FGT play a key role in forming a primary barrier to HIV entry, yet exposure of genital epithelial cells (GECs) to intact virus or HIV-1 glycoprotein 120 (gp120) induces an inflammatory response that results in downregulation of tight junction (TJ) proteins [40]. This loss of barrier integrity may allow HIV-1 to traverse the genital epithelium and establish an infection. Pre-treatment of primary GECs with 5 μM of curcumin prevented the down-regulation of TJ proteins, thus potentially reducing HIV infection rates [10]. Treatment of chronically infected T-cells (H9 T-cells) with at least 5 μM curcumin significantly reduced expression of p24, a marker of virus replication, at 24 hpi compared to untreated cells [10]. This inhibition could be maintained for several days if the curcumin in the medium was replaced every 24 h [10]. Curcumin can inhibit HIV replication through impacting the function of several viral proteins including the viral integrase, protease, as well as the trans-activator of transcription (Tat) protein [31, 35, 41]. Curcumin may inhibit the viral integrase through direct interaction with the catalytic core of the protein [35]. Similarly, computer modeling suggests that curcumin may also bind the active site of the HIV-1 protease [31, 42]. In the case of Tat, treatment with curcumin induces Tat degradation in a dose- (20 to 120 μM) and time-dependent manner, which appears to be mediated through a proteasomal pathway independent of ubiquitination [26]. Five μM of curcumin can also inhibit HIV-LTR activation by inflammatory cytokines induced through infection of other STI, such as HSV-1, HSV-2 and N. gonorrhoeae [10, 43].

Hypothesizing that the β-diketone moiety of curcumin may be responsible for its decomposition at physiological pH, Kumari et al. [11] evaluated the anti-HIV-1 properties of a synthetic curcumin analogue lacking the β-diketone moiety, termed curcumin A. Curcumin A exhibited improved stability relative to curcumin in PBS and in serum in vitro, but similar stability in complete tissue culture medium [11]. Using an HIV reporter virus encoding luciferase, curcumin A reduced luciferase activity to a similar extent as curcumin in human T-cell leukemia (CEM) cells (IC50 of 0.8 and 0.7 μM, respectively) and with

greater potency in primary peripheral blood mononuclear cells (PMBCs) (IC50 of 2 and 12 μM, respectively). Although both curcumin and curcumin A could inhibit early reverse transcription of the virus, only curcumin A lowered late viral genome copy levels. At least part of the therapeutic efficacy of curcumin and curcumin A appears to be due to their ability to activate heme oxygenase-1 (HO-1), since activation of HO-1 by heme inhibits HIV-1 [44]. Curcumin A was moderately less toxic than curcumin to both cell lines (median cytotoxic concentration (CC50) of 2.4 vs 1.26 μM, and 35 vs. 22 μM, respectively), suggesting that curcumin A has an improved therapeutic potential compared to native curcumin [11].

Curcumin-stabilized silver nanoparticles (Cur-AgNP) have also been investigated for their efficacy against HIV [45]. Treatment of ACH-2 cells with Cur-AgNP was more effective at lowering HIV-LTR expression compared to curcumin alone [45]. However, Cur-AgNP did not completely abolish HIV-1 p24 expression, as the levels of this protein continued to increase throughout the course of infection, albeit with significantly reduced kinetics relative to vehicle-treated cells. Cur-AgNP also showed greater immunomodulatory effects than curcumin, lowering expression of TNF-α, IL-6, IL-1β, and NF-κB [45]. These results suggest that stabilized nanoparticles may hold promise for improving the efficacy of curcumin for treating HIV, and possibly other viruses.

Mirani et al. [46] studied the efficacy of tetrahydrocurcumin, a colourless metabolite of curcumin, either alone or formulated as a microemulsion (designated TME), as a potential vaginal microbicide for topical application as a prophylactic approach to prevent HIV infection. In a reporter cell line, TME showed greater HIV-1 inhibition than the drug alone (IC50 of 0.9357 μM and 3.639 μM, respectively). In a p24 antigen assay, 1 μM of TME also showed a greater ability to lower p24 levels over a 10-day time course of infection compared to 5 μM of tetrahydrocurcumin [46]. To further validate the potential of TME as a vaginal microbicide, the effect of TME on *Lactobacillus* species was evaluated, as these bacteria form part of the natural microbiota and are important for maintaining the acidic environment of the FGT [47]. No change in viability was observed at any concentration for *L. casie and L. acidophilus* [46]. Finally, the authors showed that both TME and tetrahydrocurcumin were efficacious when formulated into suspension gels,

which would be easy to apply, with no loss of anti-HIV-1 efficacy. Collectively, these studies show curcumin's potential against HIV-1, both through direct inhibition and as a prophylactic strategy.

3.2. Zika Virus

Mounce et al. [14] compared the efficacy of curcumin and several curcumin analogues against Zika (ZIKV), chikungunya virus (CHIKV) and vesicular stomatitis virus (VSV), all enveloped viruses, as well as Coxsackie B3 virus (CVB3), a non-enveloped virus. Direct incubation of ZIKV in 10 μM to 1 mM of curcumin, bisdemethoxycurcumin, demethoxycurcumin or the synthetic curcumin structural analogue EF-24 and derivative FLLL31 (originally synthesized by Adams et al. [48] and Lin et al. [49], respectively), resulted in a dose- and time-dependent decrease in subsequent virus infection, suggesting these drugs have a direct ability to inactivate virus or inhibit cell attachment. EF-24 and FLLL31 were less effective than the curcuminoids, and only the curcuminoids had a lower IC50 relative to their CC50 in HeLa cells [14]. In several time-of-addition assays, only cells treated prior to or during infection reduced ZIKV recovery, indicating that curcumin acts against ZIKV exclusively during cell-attachment or entry and not at later stages of infection [14]. Incubation with curcumin was shown to reduce virus binding to the cell, but it did not lower the total number of virus particles, indicating that curcumin and its analogues are not viricidal compounds per se but rather prevent ZIKV attachment to cells. The authors speculated that, since curcumin has been reported to alter the membrane fluidity of the hepatitis C virus (HCV) envelope [50], it may work by a similar mechanism to prevent ZIKV cell attachment.

Gao et al. [15] evaluated a natural product library for phytochemicals, including curcumin, for compounds with anti-ZIKV activity. In their initial screen in Vero E6 cells, curcumin (amongst other compounds) had a lower IC50 (~5–14 μM) relative to CC50 (~53 μM) against several strains of ZIKV as determined by plaque assay. Time-of-addition assays again suggested that curcumin exerts anti-ZIKV activity through an ability to interfere with cell attachment [15]. Taken together, these studies demonstrate curcumin's potential against ZIKV.

3.3. Dengue Virus

In addition to evaluating curcumin against ZIKV, Gao et al. [15] also investigated the same selection of compounds against dengue virus (DENV). Curcumin reduced plaque formation of all four strains (DENV-1-4, IC50 of 9.37, 3.07, 2.09, and 4.83 μM, respectively) examined in LLC-MK2 cells while showing limited toxicity (CC50 of 59.42 μM) [15]. Though the mechanism of inhibition was not addressed, an earlier study demonstrated that curcumin likely inhibits DENV-2 indirectly through impact on cellular systems rather than directly on viral functions [51].

Balasubramanian et al. [8] evaluated the anti-DENV properties of curcumin, bisdemethoxycurcumin and three other synthesized analogues. In an in vitro activity assay, curcumin and the four analogues modestly inhibited viral protease activity (IC50 of ~36–66 μM). Similarly, these compounds only modestly inhibited replication of a DENV2 reporter replicon construct, with the acyclic and cyclohexanone analogues of curcumin performing slightly better than the natural curcuminoids (50% effective concentration (EC50) of 8.61 and 8.07 μM versus 13.91 μM) [8]. However, the compounds showed greater activity in a plaque assay, with all analogues demonstrating greater inhibition than curcumin (EC50 of 2.34–6.49 μM versus 13.95 μM, respectively). The mechanism by which curcumin inhibits DENV appeared to be due to effects on cellular lipid metabolism. Curcumin and its derivatives downregulated acetyl-CoA carboxylase and fatty acid synthase, and lowered lipid droplet (LD) formation, processes that normally may function to enhance DENV infection [8]. Curcumin treatment also led to actin filament disorganization and defects in polymerization, another process that is naturally important for DENV entry and replication [8].

3.4. Chikungunya Virus

Pre-incubation of lentiviral vectors pseudotyped with chikungunya virus (CHIKV) envelop proteins E2 and E1 with curcumin prevented infection of HEK 293T cells (IC50 of 10.79 μM) [16]. Time-of-addition assays with CHIKV encoding an mCherry-tagged viral replicase showed that treatment with curcumin lowered the number of mCherry positive cells when added up to 2 hpi, but it had no effect thereafter. Immunofluorescence

analysis revealed that curcumin treatment did not alter the intensity or pattern of mCherry staining within the cells, but it did reduce the total amount of cells positive for mCherry. Taken together, this study suggests that, much like ZIKV, curcumin prevents cell-entry or attachment, but it has no effect on virus replication [16]. A similar conclusion was obtained by Mounce et al. [14], who postulated that curcumin may be altering the conformation of viral surface glycoproteins, thus preventing viral attachment. Thus, for CHIKV, curcumin may be an effective treatment to prevent initial infection but is likely ineffective at controlling a pre-existing infection.

3.5. Vesicular Stomatitis Virus

As in the case with ZIKV and CHIKV, VSV infection was inhibited when the virus was incubated directly with curcumin (IC50 of 4.5 μM) [14, 16]. Although these studies did not address the mechanism by which curcumin inhibited VSV, this effect can likely be attributed to inhibition of cell attachment [14].

3.6. Influenza A Virus

Curcumin is also a potent inhibitor of IAV, and likely exerts its effect at multiple different stages of the virus lifecycle. Incubation of IAV with curcumin results in reduced infectivity, possibly due to the ability of curcumin to interfere with viral haemagglutinin activity [19, 36]. Curcumin also inhibits NF-κB signalling, which is required for IAV replication [52]. Time-of-addition experiments showed that addition of curcumin as late as 5 hpi reduced plaque formation (EC50 of ~58 μM), suggesting curcumin interferes with an early stage of virus gene expression or replication [19]. Additionally, curcumin inhibited several IAV-induced toll-like receptor (TLR) signalling pathways and proteins, which are normally required for efficient virus internalization and/or replication, including TLR2/4/7, MyD88, TRIF, and TRAF6. Indeed, treatment of cells with agonists for TLR2/4, p38/JNK MAPK or NF-κB were able to circumvent the replication block imposed by curcumin [19]. Importantly, curcumin treatment by oral gavage (50 and 150 mg/kg) reduced IAV replication and lung injury in an in vivo animal model [19], clearly illustrating that curcumin can provide a therapeutic benefit to combat infection and virus-induced disease.

This latter observation was supported by a study by Han et al. [53], who demonstrated that mice infected with the IAV strain PR8 and fed 30 or 100 mg/kg of curcumin had increased survival, reduced bodyweight loss, and lower IAV burden in lung tissues as determined by immunohistochemistry. Bronchoalveolar lavage (BAL) fluid and lung tissues from infected, curcumin-treated mice had lower levels of monocyte chemoattractant protein-1 (MCP-1) and tumour necrosis factor-alpha (TNFα) compared to untreated mice, suggesting reduced inflammation. Similarly, bone marrow-derived macrophages (BMDM cells) isolated from mice and infected with PR8 produced lower levels of inflammatory cytokines IL-6, TNF-α and MCP-1 following treatment with curcumin [53]. These results indicate that curcumin is not only capable of inhibiting IAV replication, but also attenuates IAV-induced lung disease, likely through inhibition of NF-κB signaling leading to reduced secretion of inflammatory cytokines by resident macrophages [53].

The enone functional groups (α, β-unsaturated carbonyls) of curcumin appear to be at least partially responsible for the anti-IAV properties of curcumin [54]. These enone groups can form Michael adducts with sulfhydryl (SH) groups on other proteins, suggesting that curcumin may exert anti-IAV activity through the ability to conjugate with viral surface protein(s) and interfere with their function [54]. Richart et al. [24] compared the effectiveness of curcumin and monoacetylcurcumin (MAC), a curcumin analogue that maintains the enone groups and shows improved stability. As with curcumin, direct incubation of IAV with MAC inhibited subsequent plaque formation (IC50 of ~0.2 μM), and 30 μM of MAC was more effective in limiting virus replication in long-term cultures (up to 36 h, [24]). Addition of GSH, which can act as a competitive inhibitor during the Michael addition reaction, to MAC reduced its ability to prevent plaque formation, once again highlighting the importance of the enone groups on MAC efficacy. Although both MAC and curcumin were capable of mildly reducing IAV neuraminidase (NA) activity (which is vital for viral egress) at high drug concentrations (200 μM), only MAC was effective at lower concentrations (25 μM) [24]. However, unlike curcumin, MAC was unable to reduce haemagglutinin (HA) activity at any concentration tested, indicating MAC cannot prevent cell attachment [24]. Compared to curcumin, MAC was a stronger suppressor of the PI3K/Akt signalling pathway, which is required for IAV membrane

fusion, suggesting at least part of the anti-IAV efficacy of MAC may be due to its effects on membrane fusion and virus internalization. Given that curcumin and MAC appear to inhibit IAV via different mechanisms, the authors also showed that combined treatment with both compounds was more effective than either compound alone.

Combining several aspects of the studies described above, Lai et al. [55] analyzed curcumin and several analogues for anti-IAV activity. In MDCK cells, treatment with the maximum non-toxic dose of each compound significantly reduced mRNA levels of the IAV M gene in infected cells, with curcumin showing the greatest reduction. Using immunohistochemistry, only curcumin and tetramethylcurcumin inhibited the nuclear export of the IAV nucleoprotein, thus preventing viral assembly. All compounds reduced neuraminidase activity. Consistent with the previous studies, in vivo treatment of mice with 25–100 mg/kg of curcumin reduced lung pathology compared to untreated controls [55]. Additionally, both pre- and post-infection treatment with curcumin improved average survival time of infected mice [55].

Taken together, treatment with curcumin or curcumin analogues can inhibit IAV through several means, including preventing entry [24, 55], inhibiting replication [19, 55], and preventing exit [24, 55]. Additionally, oral treatment with curcumin improved the survival of IAV-infected mice [19, 53, 55], indicating the potential of curcumin and its analogues against IAV infection.

3.7. Enterovirus 71

Though previous research has demonstrated that curcumin can inhibit human enterovirus 71 (EV71) replication in vitro [56], those studies were performed using Vero cells, which are non-human kidney epithelial cells. To better approximate the *in vivo* conditions of EV71 infection, Huang et al. [20] evaluated curcumin against EV71 in HT29 human intestinal epithelial cells. Treatment with 10 μM of curcumin significantly reduced viral protein expression, genome replication and titer, and prevented EV71-induced cell death. Time-of-addition assays revealed that curcumin did not affect viral attachment and entry, but it effectively inhibited protein expression during early stages of infection [20]. These effects appear to be at least partly due to the ability of curcumin to inhibit protein

kinase C-δ (PKCδ). Infection of a cell with EV71 induces phosphorylation of a key activating residue of PKCδ, Tyr311, which is reduced in curcumin-treated cells. Knockdown of PKCδ using siRNA or administration of the PKCδ inhibitor rottlerin also drastically reduced viral protein expression, indicating the importance of PKCδ activation for optimal EV71 gene expression [20]. Treatment with 10–20 μM of curcumin also reduced viral protein expression in C2BBe1 cells that had been differentiated into mature intestinal epithelial cells [20].

Lin et al. evaluated several curcumin-derived carbon quantum dot (Cur-CQD) formulations against EV71 [13]. These quantum dot formulations improve curcumin's solubility in water, which may explain its increased antiviral activity [13]. In human rhabdomyosarcoma (RD) cells, all Cur-CQD formulations had superior CC50 and EC50 scores compared to curcumin, with Cur-CQD-180 (named for the heat applied during synthesis, i.e., 180 ◦C) having the highest selectivity index (SI, <0.07 vs. 2261.0, respectively) inhibiting EV71-induced cytopathic effect (CPE) and virus recovery [13]. Cur-CQD-180 lowered expression of several viral proteins when added post-infection, such as the structural protein VP1 and non-structural proteins 3CDpro and 3Dpol, in a dose-dependent manner [13]. Additionally, Cur-CQD-180 reduced the cleavage of eukaryotic translation initiation factor 4G (eIF4G), which the virus utilizes to inhibit host protein synthesis while encouraging its own [13, 57]. In vivo, treatment of EV71-infected mice with Cur-CQD-180 improved survival, lowered pathology scores and prevented virus-induced weight loss compared to untreated and curcumin-treated mice [13]. Cur-CQD-180 treatment also reduced the quantity of viral mRNA and protein that were detected in brain and limb muscle tissue [13]. These results demonstrate the potential of curcumin formulations in bypassing the limitations of native curcumin for in vivo treatment against EV71.

3.8. Human Respiratory Syncytial Virus

Incubation of Human Respiratory Syncytial Virus (HRSV) with curcumin-stabilized silver nanoparticles (Cur-AgNP) produced particles of ~200 nm, which is larger than either Cur-AgNP or HRSV particles alone, suggesting Cur-AgNP binds directly to

HRSV, and this binding appeared to inhibit virus infection [17]. Treatment of cells with Cur-AgNP post-infection was not as effective as the pre-treatment at reducing virus recovery [17]. A derivate of curcumin in which the drug was loaded into β-cyclodextrin and attached to sulfonated graphene oxide sheets (termed GSCC) was also evaluated against HRSV [18]. This formulation inhibited HRSV primarily by preventing viral attachment, but it also inhibited HRSV when applied to cells after infection [18]. Given the presence of sulfonic acid in the formulation and that HRSV can utilise heparin sulfate for entry [58, 59], the authors suggest the GSCC sheets prevent infection by acting as a competitive inhibitor to sequester viruses away from the cell. Additionally, both pre- and post-treatment with the GSCC sheets reduced viral G protein expression, which is responsible for viral attachment, indicating the GSCC sheets also can directly affect viral gene expression [18]. Taken together, these results clearly show that encapsulation can be used to improve the efficacy of curcumin against HRSV.

3.9. Norovirus

For enveloped viruses, direct incubation of curcumin frequently reduces the ability of the virus to infect cells, which is thought to be due to the ability of curcumin to bind to and inhibit the action of surface glycoproteins on the virus [14–16]. Somewhat surprisingly, incubation of murine norovirus (MuNoV) with ~679 μM curcumin also significantly lowered plaque formation, despite the fact that noroviruses are non-enveloped [60]. This effect was time- and dose-dependent, suggesting the reduction in plaque formation was due to direct neutralization of viral particles as opposed to preventing infection [60]. However, in human norovirus (HuNoV) replicon-bearing HG23 cells, curcumin had no effect on HuNoV replication [60], suggesting curcumin only affects virus particle integrity and does not alter other aspects of the virus lifecycle.

Curcumin has also been investigated against norovirus in the context of a photodynamic therapy (PDT), in which the compound in question (termed the sensitizer) is “activated” by exposure to specific wavelengths of light, leading to the production of reactive oxygen species (ROS). Treatment with 5 μM of curcumin photodynamically activated (PDAC) by blue light radiation reduced MuNoV titers with greater effect than

curcumin or blue light alone [21]. The morphology of the virions were examined using TEM, and samples treated with PDAC had visible viral debris suggesting PDAC treatment is capable of physically disrupting MuNoV particles [21]. For an in vivo test of this therapy, live oysters, which are known to bio-accumulate norovirus, were exposed to MuNoV and curcumin for 6 h, the intestines of the oysters were then removed and exposed to blue light. Titration of virus from these tissues showed that, while the viral titer was reduced in a dose-dependent manner, curcumin was less effective in oyster tissues compared to virus in solution, which was attributed to lower final concentration of curcumin in the oysters and possible absorption of light by oyster tissues, reducing the fraction of energy reaching the curcumin [21].

Randazzo et al. [22] also evaluated PDAC against norovirus, using MuNoV and feline calicivirus (FCV) as HuNoV surrogates. PDAC treatment using up to 13.6 μM of curcumin reduced the 50% tissue culture infective dose (TCID50) of both FCV and MuNoV, but appeared more effective against FCV [22]. Increasing the concentration of viruses reduced the effect of PDAC, which the authors attributed to the limited quantity of ROS produced being spread over a greater quantity of virus—each particle receives less damage from the available ROS [22]. The strategy of using PDAC against norovirus in oysters represents a potentially simple solution to combat norovirus accumulation, given curcumin is already viewed as safe for use in the food industry.

3.10. Viral Hemorrhagic Septicemia Virus

Viral Hemorrhagic Septicemia Virus (VHSV) affects numerous species of fish throughout the world, with mortality as high as 90% [61]. Pre-treatment of fathead minnow (FHM) cells with 0–240 μM curcumin reduced CPE and improved cell viability in a dose-dependent manner [9]. VHSV infection significantly increases ROS production compared to uninfected cells, and pre-treatment with curcumin lowered ROS production to baseline levels, which could have contributed to the lower CPE observed in the curcumin pre-treated cells [9]. Additionally, 120 μM curcumin reduced viral genome copy numbers within infected cells, indicating curcumin can inhibit virus replication [9]. Based on protein network analysis, the authors speculated that curcumin reduced VHSV infection by

downregulating heat shock cognate 71 kDa protein (HSC71), which is naturally upregulated by PNV during early infection. Consistent with this mechanism, treatment with heat shock protein inhibitor KNK437 reduced virus-induced CPE and lowered viral genome copy numbers within the cell [9].

3.11. Porcine Reproductive and Respiratory Syndrome Virus

Porcine reproductive and respiratory syndrome virus (PRSSV) causes large economic losses in the swine industry [62]. Although a vaccine exists against PRSSV, adverse effects from vaccine treatments have led researchers to look for antiviral compounds [63]. Incubation of 15 μM of curcumin directly with several strains of PRRSV prevented infection of Marc-145 cells (permissive to PRRSV infection) [25]. While curcumin did not lower expression of surface receptors or prevent viral attachment, curcumin appeared to inhibit PRRSV cell membrane fusion and internalization. Similar results were obtained in primary porcine alveolar macrophage [25].

3.12. Transmissible Gastroenteritis Virus

Another virus that causes significant livestock and economic loss in the pork industry is transmissible gastroenteritis virus (TGV), a porcine coronavirus [64]. Noting curcumin's activity against other enveloped viruses, Li et al. [65] evaluated curcumin against TGV. Direct incubation with at least 20 μM of curcumin prior to infection reduced viral yield. Furthermore, treatment with curcumin caused a dose-dependant decrease in viral absorption, and a reduction in both viral yield (IC50 of 8.6 μM) and protein levels at concentrations that are non-toxic to porcine kidney (PD-15) cells [65].

3.13. Severe Acute Respiratory Syndrome Coronavirus 2

While there have been no published research articles at the time of writing on any antiviral effect of curcumin on severe acute respiratory syndrome coronavirus 2 (SARS-CoV-2), the causative agent in the worldwide COVID-19 pandemic, it has been speculated that curcumin could inhibit SARS-CoV-2 replication. Curcumin has already been demonstrated to inhibit SARS-CoV-1 replication (EC50 of >10 μM), the coronavirus

which caused the 2003 epidemic [66]. Additionally, several molecular docking studies have been performed that suggest curcumin would be effective at inhibiting SARS-CoV-2 replication [67], through interacting with the spike glycoprotein and inhibiting angiotensin-converting enzyme 2 (ACE2) [68], inhibiting the viral non-structural protein Nsp15 [69], or inhibiting the main viral protease [70].

4. DNA Viruses

4.1. Herpes Simplex Virus 2

Herpes Simplex Virus 2 (HSV-2) infection is associated with increased susceptibility to HIV infection and control of HSV-2 replication lowers HIV replication [71]. As part of their study investigating the efficacy of curcumin against HIV, Ferreira et al. [10] also examined the effect of curcumin on HSV-2 replication. In primary human GECs, pre-treatment of cells with 5 μM curcumin reduced HSV-2 shedding by 1000-fold, and 50 μM completely prevented production of virus [10]. Investigation of the cellular pathways known to be impacted by curcumin implicated NF-κB was responsible for the effects on HSV-2 [10]. Vitali et al. [72] evaluated the efficacy of curcumin encapsulated by Poly-(Lactic-Co-Glycolic Acid) (PLGA, Cur-PLGA), which can enhance curcumin bioavailability 9-fold [73] against HSV-2 infection in vivo. In mice, although intravaginal (IVAG) delivery of Cur-PLGA (containing 0.5 mg of curcumin) reduced CpG-oligodeoxynucleotides (ODN)-induced acute inflammation, Cur-PLGA had no effect on mice survival following a low- or lethal-dose of HSV-2 [72]. The authors next examined the use of crude curcumin extract in conjunction with polymers that increase curcumin solubility in water [74, 75]. Compared to 1 mg of crude curcumin, mice treated with 100 μg of curcumin with PVP-K30 or Soluplus® had increased survival and lower pathology scores [72]. The authors commented that it is difficult to determine if an effective dose is reached when using nanoparticles, whereas it is easier to control the dosage using crude extracts in combination with compounds to improve solubility [72].

4.2. Kaposi's Sarcoma-Associated Herpesvirus

Li et al. [12] noted while reviewing the genes and pathways impacted by curcumin

that there was overlap with pathways controlling the redox reaction of apurinic/apyrimidinic endonuclease 1 (APE1), suggesting curcumin could inhibit APE1 redox reactions. Since Kaposi's sarcoma-associated herpesvirus (KSHV) replication requires the redox function of APE1 [76], the authors investigated whether curcumin could inhibit KSHV replication. Primary effusive lymphoma (PEL) BCBL-1 cells that were latently infected with KSHV were treated with TPA to induce activation of KSHV and subsequently treated with curcumin. Treatment with 30 μM of curcumin effectively blocked reactivation of KSHV by lowering expression of the switch gene replication and transcription activator (RTA), and the delayed-early gene K8 [12]. Curcumin treatment reduced both the intra- and extracellular KSHV genomic DNA levels (IC50 of 8.76 μM and EC50 of 6.68 μM, respectively) [12], indicating that curcumin is an effective treatment for KSHV infection.

4.3. Bovine Herpesvirus 1

Bovine herpesvirus 1 (BoHV-1) incubated directly with 10 μM of curcumin caused a significant reduction in viral titer as analyzed by TCID50 [23]. However, curcumin did not reduce BoHV-1 titer during a binding assay, suggesting curcumin does not prevent viral attachment but, rather, may be affecting internalization. In Madin-Darby Bovine Kidney (MDBK) cells, 10 μM of curcumin significantly reduced viral titer when applied at the time of infection, but it had no significant effect when added immediately after the one h incubation of cells with the virus inoculum. The authors speculate that curcumin may be inhibiting BoHV-1 infection by upregulating lipid raft formation, a process they previously reported to be disrupted during BoHV-1 infection [23, 77]. Reolon et al. [78] evaluated the co-encapsulation of acyclovir, an approved pro-drug that inhibits HSV replication [79], and curcumin into three microparticle (MP) formulations composed of the polymers hydroxypropyl methylcellulose, Eudragit® RS100, or both for efficacy against BoHV-1. In MDBK cells, all three MP formulations significantly reduced plaque formation of BoHV-1 to a greater extent than each antiviral test compound individually at all concentrations (2.7–203.6 μM).

4.4. Human Adenovirus

Our group evaluated curcumin against human adenovirus (HAdV). In A549 human lung adenocarcinoma cells infected with HAdV types 4, 5 or 7, curcumin (0–100 μM) caused a dose-dependent decrease in expression of the viral early 1A (E1A) proteins, which are vital for the virus to complete its replicative cycle [80, 81], indicating curcumin is effective against multiple types of HAdV. Treatment with curcumin also decreased HAdV-5 viral genome copy numbers, as well as reduced virus recovery as determined by plaque assay [81]. However, the most effective concentrations of curcumin were only slightly lower than the CC50 (~68 μM) of curcumin in this cell line, indicating that curcumin may have only a very narrow therapeutic window against HAdV [81].

5. Conclusions

Curcumin and its analogues are capable of inhibiting the replication of a diverse group of viruses through numerous mechanisms (summarized in Table 1). However, curcumin has low bioavailability and is rapidly metabolized (reviewed in [82]), compromising curcumin's effectiveness as an antiviral compound, and likely contributing to the limited success observed in human clinical trials [83]. Additionally, though consumption of curcumin in high doses in humans appears to be safe, numerous studies report in vitro CC50 concentrations in tens of micromolars, leading to a relatively low SI, further reducing its potential effectiveness. Nevertheless, research into curcumin formulation technology has shown promise, due to improved solubility, stability and uptake of curcumin and its derivatives [84]. Continued research into such formulations as well as synthesis of novel curcumin-derivates that show greater antiviral activity with reduced toxicity may lead to development of curcumin as a broad-spectrum antiviral for human clinical use.

Author Contributions: Conceptualization, M.R.J.; literature search, M.R.J.; resources, R.J.P.; writing—original draft, M.R.J.; writing—review and editing, M.R.J., R.J.P.; supervision, R.J.P.; funding acquisition, R.J.P.; project administration, R.J.P. All authors have read and agreed to the published version of the manuscript.

Funding: This research was supported by grants to R.J.P. from the Canadian Institutes of Health Research (MOP-136898, MOP-142316) and the Natural Sciences and Engineering Research Council (RGPIN-2014-04810, RGPIN-2019-04786).

Conflicts of Interest: The authors declare no conflict of interest.

References

1. Wang, Y.-J.; Pan, M.-H.; Cheng, A.-L.; Lin, L.-I.; Ho, Y.-S.; Hsieh, C.-Y.; Lin, J.-K. Stability of curcumin in buffer solutions and characterization of its degradation products. *J. Pharm. Biomed. Anal.* **1997**, *15*, 1867–1876.
2. Lee, W.-H.; Loo, C.-Y.; Bebawy, M.; Luk, F.; Mason, R.S.; Rohanizadeh, R. Curcumin and its derivatives: Their application in neuropharmacology and neuroscience in the 21st century. *Curr. Neuropharmacol.* **2013**, *11*, 338–378.
3. Kocaadam, B.; Şanlier, N. Curcumin, an active component of turmeric (Curcuma longa), and its effects on health. *Crit. Rev. Food Sci. Nutr.* **2017**, *57*, 2889–2895.
4. Sidhu, G.S.; Singh, A.K.; Thaloor, D.; Banaudha, K.K.; Patnaik, G.K.; Srimal, R.C.; Maheshwari, R.K. Enhancement of wound healing by curcumin in animals. *Wound Repair Regen.* **1998**, *6*, 167–177.
5. Wilken, R.; Veena, M.S.; Wang, M.B.; Srivatsan, E.S. Curcumin: A review of anti-cancer properties and therapeutic activity in head and neck squamous cell carcinoma. *Mol. Cancer* **2011**, *10*, 12.
6. Kunnumakkara, A.B.; Bordoloi, D.; Padmavathi, G.; Monisha, J.; Roy, N.K.; Prasad, S.; Aggarwal, B.B. Curcumin, the golden nutraceutical: Multitargeting for multiple chronic diseases. *Br. J. Pharm.* **2017**, *174*, 1325–1348.
7. Praditya, D.; Kirchhoff, L.; Brüning, J.; Rachmawati, H.; Steinmann, J.; Steinmann, E. Anti-infective Properties of the Golden Spice Curcumin. *Front. Microbiol.* **2019**, *10*, 912.
8. Balasubramanian, A.; Pilankatta, R.; Teramoto, T.; Sajith, A.M.; Nwulia, E.; Kulkarni, A.; Padmanabhan, R. Inhibition of dengue virus by curcuminoids. *Antivir. Res.* **2019**, *162*, 71–78.
9. Jeong, E.-H.; Vaidya, B.; Cho, S.-Y.; Park, M.-A.; Kaewintajuk, K.; Kim, S.R.; Oh, M.-J.; Choi, J.-S.; Kwon, J.; Kim, D. Identification of regulators of the early stage of viral hemorrhagic septicemia virus infection during curcumin treatment. *Fish Shellfish Immunol.* **2015**, *45*, 184–193.

10. Ferreira, V.H.; Nazli, A.; Dizzell, S.E.; Mueller, K.; Kaushic, C. The anti-inflammatory activity of curcumin protects the genital mucosal epithelial barrier from disruption and blocks replication of HIV-1 and HSV-2. *PLoS ONE* **2015**, *10*, e0124903.
11. Kumari, N.; Kulkarni, A.A.; Lin, X.; McLean, C.; Ammosova, T.; Ivanov, A.; Hipolito, M.; Nekhai, S.; Nwulia, E. Inhibition of HIV-1 by curcumin A, a novel curcumin analog. *Drug Des. Dev.* **2015**, *9*, 5051–5060.
12. Li, H.; Zhong, C.; Wang, Q.; Chen, W.; Yuan, Y. Curcumin is an APE1 redox inhibitor and exhibits an antiviral activity against KSHV replication and pathogenesis. *Antivir. Res.* **2019**, *167*, 98–103.
13. Lin, C.-J.; Chang, L.; Chu, H.-W.; Lin, H.-J.; Chang, P.-C.; Wang, R.Y.L.; Unnikrishnan, B.; Mao, J.-Y.; Chen, S.-Y.; Huang, C.-C. High Amplification of the Antiviral Activity of Curcumin through Transformation into Carbon Quantum Dots. *Small* **2019**, *15*, 1902641.
14. Mounce, B.C.; Cesaro, T.; Carrau, L.; Vallet, T.; Vignuzzi, M. Curcumin inhibits Zika and chikungunya virus infection by inhibiting cell binding. *Antivir. Res* **2017**, *142*, 148–157.
15. Gao, Y.; Tai, W.; Wang, N.; Li, X.; Jiang, S.; Debnath, A.K.; Du, L.; Chen, S. Identification of Novel Natural Products as Effective and Broad-Spectrum Anti-Zika Virus Inhibitors. *Viruses* **2019**, *11*, 1019.
16. Von Rhein, C.; Weidner, T.; Henß, L.; Martin, J.; Weber, C.; Sliva, K.; Schnierle, B.S. Curcumin and Boswellia serrata gum resin extract inhibit chikungunya and vesicular stomatitis virus infections in vitro. *Antivir. Res* **2016**, *125*, 51–57.
17. Yang, X.X.; Li, C.M.; Huang, C.Z. Curcumin modified silver nanoparticles for highly efficient inhibition of respiratory syncytial virus infection. *Nanoscale* **2016**, *8*, 3040–3048.
18. Yang, X.X.; Li, C.M.; Li, Y.F.; Wang, J.; Huang, C.Z. Synergistic antiviral effect of curcumin functionalized graphene oxide against respiratory syncytial virus infection. *Nanoscale* **2017**, *9*, 16086–16092.
19. Dai, J.; Gu, L.; Su, Y.; Wang, Q.; Zhao, Y.; Chen, X.; Deng, H.; Li, W.; Wang, G.; Li, K. Inhibition of curcumin on influenza A virus infection and influenzal pneumonia via oxidative stress, TLR2/4, p38/JNK MAPK and NF-κB pathways. *Int. Immunopharmacol.* **2018**, *54*, 177–187.
20. Huang, H.I.; Chio, C.C.; Lin, J.Y. Inhibition of EV71 by curcumin in intestinal epithelial cells. *PLoS ONE* **2018**, *13*, e0191617.

21. Wu, J.; Hou, W.; Cao, B.; Zuo, T.; Xue, C.; Leung, A.W.; Xu, C.; Tang, Q.J. Virucidal efficacy of treatment with photodynamically activated curcumin on murine norovirus bio-accumulated in oysters. *Photodiagnosis Photodyn. Ther.* **2015**, *12*, 385–392.
22. Randazzo, W.; Aznar, R.; Sánchez, G. Curcumin-Mediated Photodynamic Inactivation of Norovirus Surrogates. *Food Environ. Virol.* **2016**, *8*, 244–250.
23. Zhu, L.; Ding, X.; Zhang, D.; Yuan, C.; Wang, J.; Ndegwa, E.; Zhu, G. Curcumin inhibits bovine herpesvirus type 1 entry into MDBK cells. *Acta Virol.* **2015**, *59*, 221–227.
24. Richart, S.M.; Li, Y.L.; Mizushina, Y.; Chang, Y.Y.; Chung, T.Y.; Chen, G.H.; Tzen, J.T.; Shia, K.S.; Hsu, W.L. Synergic effect of curcumin and its structural analogue (Monoacetylcurcumin) on anti-influenza virus infection. *J. Food Drug Anal.* **2018**, *26*, 1015–1023.
25. Du, T.; Shi, Y.; Xiao, S.; Li, N.; Zhao, Q.; Zhang, A.; Nan, Y.; Mu, Y.; Sun, Y.; Wu, C.; et al. Curcumin is a promising inhibitor of genotype 2 porcine reproductive and respiratory syndrome virus infection. *BMC Vet. Res.* **2017**, *13*, 298.
26. Ali, A.; Banerjea, A.C. Curcumin inhibits HIV-1 by promoting Tat protein degradation. *Sci. Rep.* **2016**, *6*, 27539.
27. Kotha, R.R.; Luthria, D.L. Curcumin: Biological, Pharmaceutical, Nutraceutical, and Analytical Aspects. *Molecules* **2019**, *24*, 2930.
28. GRN No. 822 Curcumin. Available online: https://www.cfsanappsexternal.fda.gov/scripts/fdcc/?set= GRASNotices&id=822 (accessed on 1 October 2020).
29. Wahlström, B.; Blennow, G. A study on the fate of curcumin in the rat. *Acta Pharmacol. Toxicol.* **1978**, *43*, 86–92.
30. *Sodium Chloride*; MSDS No. 21105 [Online]; Fisher Scientific: Fairview, NJ, USA, 12 July 1999; Available online: https://fscimage.fishersci.com/msds/21105.htm (accessed on 3 June 2020).
31. Sui, Z.; Salto, R.; Li, J.; Craik, C.; Ortiz de Montellano, P.R. Inhibition of the HIV-1 and HIV-2 proteases by curcumin and curcumin boron complexes. *Bioorg. Med. Chem.* **1993**, *1*, 415–422.
32. Yang, Y.; Wu, X.; Wei, Z.; Dou, Y.; Zhao, D.; Wang, T.; Bian, D.; Tong, B.; Xia, Y.; Xia, Y.; et al. Oral curcumin has anti-arthritic efficacy through somatostatin generation via cAMP/PKA and Ca2+/CaMKII signaling pathways in the small intestine. *Pharmacol. Res.* **2015**, *95–96*, 71–81.
33. Jin, H.; Qiao, F.; Wang, Y.; Xu, Y.; Shang, Y. Curcumin inhibits cell proliferation and induces apoptosis of human non-small cell lung cancer cells through the upregulation

of miR-192-5p and suppression of PI3K/Akt signaling pathway. *Oncol. Rep.* **2015**, *34*, 2782–2789.

34. Lao, C.D.; Ruffin, M.T.; Normolle, D.; Heath, D.D.; Murray, S.I.; Bailey, J.M.; Boggs, M.E.; Crowell, J.; Rock, C.L.; Brenner, D.E. Dose escalation of a curcuminoid formulation. *BMC Complement. Altern. Med.* **2006**, *6*, 10.
35. Mazumder, A.; Raghavan, K.; Weinstein, J.; Kohn, K.W.; Pommier, Y. Inhibition of human immunodeficiency virus type-1 integrase by curcumin. *Biochem. Pharmacol.* **1995**, *49*, 1165–1170.
36. Chen, D.-Y.; Shien, J.-H.; Tiley, L.; Chiou, S.-S.; Wang, S.-Y.; Chang, T.-J.; Lee, Y.-J.; Chan, K.-W.; Hsu, W.-L. Curcumin inhibits influenza virus infection and haemagglutination activity. *Food Chem.* **2010**, *119*, 1346–1351.
37. Bhullar, K.S.; Jha, A.; Youssef, D.; Rupasinghe, H.P.V. Curcumin and its carbocyclic analogs: Structure-activity in relation to antioxidant and selected biological properties. *Molecules* **2013**, *18*, 5389–5404.
38. Chen, C.; Johnston, T.D.; Jeon, H.; Gedaly, R.; McHugh, P.P.; Burke, T.G.; Ranjan, D. An in vitro study of liposomal curcumin: Stability, toxicity and biological activity in human lymphocytes and Epstein-Barr virus-transformed human B-cells. *Int. J. Pharm.* **2009**, *366*, 133–139.
39. Gandapu, U.; Chaitanya, R.K.; Kishore, G.; Reddy, R.C.; Kondapi, A.K. Curcumin-loaded apotransferrin nanoparticles provide efficient cellular uptake and effectively inhibit HIV-1 replication in vitro. *PLoS ONE.* **2011**, *6*, e23388.
40. Nazli, A.; Chan, O.; Dobson-Belaire, W.N.; Ouellet, M.; Tremblay, M.J.; Gray-Owen, S.D.; Arsenault, A.L.; Kaushic, C. Exposure to HIV-1 directly impairs mucosal epithelial barrier integrity allowing microbial translocation. *PLoS Pathog.* **2010**, *6*, e1000852.
41. Zhang, H.-S.; Ruan, Z.; Sang, W.-W. HDAC1/NFκB pathway is involved in curcumin inhibiting of Tat-mediated long terminal repeat transactivation. *J. Cell. Physiol.* **2011**, *226*, 3385–3391.
42. Vajragupta, O.; Boonchoong, P.; Morris, G.M.; Olson, A.J. Active site binding modes of curcumin in HIV-1 protease and integrase. *Bioorg. Med. Chem. Lett.* **2005**, *15*, 3364–3368.
43. Ferreira, V.H.; Nazli, A.; Khan, G.; Mian, M.F.; Ashkar, A.A.; Gray-Owen, S.; Kaul, R.; Kaushic, C. Endometrial epithelial cell responses to coinfecting viral and bacterial pathogens in the genital tract can activate the HIV-1 LTR in an NFκB-and AP-1-dependent manner. *J. Infect. Dis.* **2011**, *204*, 299–308.

44. Devadas, K.; Hewlett, I.K.; Dhawan, S. Lipopolysaccharide suppresses HIV-1 replication in human monocytes by protein kinase C-dependent heme oxygenase-1 induction. *J. Leukoc. Biol.* **2010**, *87*, 915–924.
45. Sharma, R.K.; Cwiklinski, K.; Aalinkeel, R.; Reynolds, J.L.; Sykes, D.E.; Quaye, E.; Oh, J.; Mahajan, S.D.; Schwartz, S.A. Immunomodulatory activities of curcumin-stabilized silver nanoparticles: Efficacy as an antiretroviral therapeutic. *Immunol. Investig.* **2017**, *46*, 833–846.
46. Mirani, A.; Kundaikar, H.; Velhal, S.; Patel, V.; Bandivdekar, A.; Degani, M.; Patravale, V. Tetrahydrocurcumin-loaded vaginal nanomicrobicide for prophylaxis of HIV/AIDS: In silico study, formulation development, and in vitro evaluation. *Drug Deliv. Transl. Res.* **2019**, *9*, 828–847.
47. Lackman-Smith, C.; Osterling, C.; Luckenbaugh, K.; Mankowski, M.; Snyder, B.; Lewis, G.; Paull, J.; Profy, A.; Ptak, R.G.; Buckheit, R.W.; et al. Development of a Comprehensive Human Immunodeficiency Virus Type 1 Screening Algorithm for Discovery and Preclinical Testing of Topical Microbicides. *Antimicrob. Agents Chemother.* **2008**, *52*, 1768–1781.
48. Adams, B.K.; Ferstl, E.M.; Davis, M.C.; Herold, M.; Kurtkaya, S.; Camalier, R.F.; Hollingshead, M.G.; Kaur, G.; Sausville, E.A.; Rickles, F.R.; et al. Synthesis and biological evaluation of novel curcumin analogs as anti-cancer and anti-angiogenesis agents. *Bioorg. Med. Chem.* **2004**, *12*, 3871–3883.
49. Lin, L.; Hutzen, B.; Zuo, M.; Ball, S.; Deangelis, S.; Foust, E.; Pandit, B.; Ihnat, M.A.; Shenoy, S.S.; Kulp, S.; et al. Novel STAT3 Phosphorylation Inhibitors Exhibit Potent Growth-Suppressive Activity in Pancreatic and Breast Cancer Cells. *Cancer Res.* **2010**, *70*, 2445–2454.
50. Colpitts, C.C.; Schang, L.M.; Rachmawati, H.; Frentzen, A.; Pfaender, S.; Behrendt, P.; Brown, R.J.; Bankwitz, D.; Steinmann, J.; Ott, M.; et al. Turmeric curcumin inhibits entry of all hepatitis C virus genotypes into human liver cells. *Gut* **2014**, *63*, 1137–1149.
51. Padilla, S.L.; Rodríguez, A.; Gonzales, M.M.; Gallego, G.J.; Castaño, O.J. Inhibitory effects of curcumin on dengue virus type 2-infected cells in vitro. *Arch. Virol.* **2014**, *159*, 573–579.
52. Nimmerjahn, F.; Dudziak, D.; Dirmeier, U.; Hobom, G.; Riedel, A.; Schlee, M.; Staudt, L.M.; Rosenwald, A.; Behrends, U.; Bornkamm, G.W.; et al. Active NF-kappaB signalling is a prerequisite for influenza virus infection. *J. Gen. Virol.* **2004**, *85*, 2347–2356.

53. Han, S.; Xu, J.; Guo, X.; Huang, M. Curcumin ameliorates severe influenza pneumonia via attenuating lung injury and regulating macrophage cytokines production. *Clin. Exp. Pharmacol. Physiol.* **2018**, *45*, 84–93.
54. Ou, J.L.; Mizushina, Y.; Wang, S.Y.; Chuang, D.Y.; Nadar, M.; Hsu, W.L. Structure-activity relationship analysis of curcumin analogues on anti-influenza virus activity. *FEBS J.* **2013**, *280*, 5829–5840.
55. Lai, Y.; Yan, Y.; Liao, S.; Li, Y.; Ye, Y.; Liu, N.; Zhao, F.; Xu, P. 3D-quantitative structure-activity relationship and antiviral effects of curcumin derivatives as potent inhibitors of influenza H1N1 neuraminidase. *Arch. Pharm. Res.* **2020**.
56. Qin, Y.; Lin, L.; Chen, Y.; Wu, S.; Si, X.; Wu, H.; Zhai, X.; Wang, Y.; Tong, L.; Pan, B.; et al. Curcumin inhibits the replication of enterovirus 71 in vitro. *Acta Pharm. Sin. B* **2014**, *4*, 284–294.
57. Thompson, S.R.; Sarnow, P. Enterovirus 71 contains a type I IRES element that functions when eukaryotic initiation factor eIF4G is cleaved. *Virology* **2003**, *315*, 259–266.
58. Feldman, S.A.; Audet, S.; Beeler, J.A. The fusion glycoprotein of human respiratory syncytial virus facilitates virus attachment and infectivity via an interaction with cellular heparan sulfate. *J. Virol.* **2000**, *74*, 6442–6447.
59. Sametband, M.; Kalt, I.; Gedanken, A.; Sarid, R. Herpes Simplex Virus Type-1 Attachment Inhibition by Functionalized Graphene Oxide. *ACS Appl. Mater. Interfaces* **2014**, *6*, 1228–1235.
60. Yang, M.; Lee, G.; Si, J.; Lee, S.-J.; You, H.J.; Ko, G. Curcumin Shows Antiviral Properties against Norovirus. *Molecules* **2016**, *21*, 1401.
61. Einer-Jensen, K.; Harmache, A.; Biacchesi, S.; Bremont, M.; Stegmann, A.; Lorenzen, N. High virulence differences among phylogenetically distinct isolates of the fish rhabdovirus viral hemorrhagic septicaemia virus are not explained by variability of the surface glycoprotein G or the non-virion protein Nv. *J. Gen. Virol.* **2014**, *95*, 307–316.
62. Montaner-Tarbes, S.; del Portillo, H.A.; Montoya, M.; Fraile, L. Key Gaps in the Knowledge of the Porcine Respiratory Reproductive Syndrome Virus (PRRSV). *Front. Vet. Sci.* **2019**, 6.
63. Khatun, A.; Shabir, N.; Seo, B.-J.; Kim, B.-S.; Yoon, K.-J.; Kim, W.-I. The Attenuation Phenotype of a Ribavirin-Resistant Porcine Reproductive and Respiratory Syndrome Virus Is Maintained during Sequential Passages in Pigs. *J. Virol.* **2016**, *90*, 4454–4468.
64. Xia, L.; Yang, Y.; Wang, J.; Jing, Y.; Yang, Q. Impact of TGEV infection on the pig small intestine. *Virol. J.* **2018**, *15*, 102.

65. Li, Y.; Wang, J.; Liu, Y.; Luo, X.; Lei, W.; Xie, L. Antiviral and virucidal effects of curcumin on transmissible gastroenteritis virus in vitro. *J. Gen. Virol.* **2020**.
66. Wen, C.-C.; Kuo, Y.-H.; Jan, J.-T.; Liang, P.-H.; Wang, S.-Y.; Liu, H.-G.; Lee, C.-K.; Chang, S.-T.; Kuo, C.-J.; Lee, S.-S.; et al. Specific Plant Terpenoids and Lignoids Possess Potent Antiviral Activities against Severe Acute Respiratory Syndrome Coronavirus. *J. Med. Chem.* **2007**, *50*, 4087–4095.
67. Zahedipour, F.; Hosseini, S.A.; Sathyapalan, T.; Majeed, M.; Jamialahmadi, T.; Al-Rasadi, K.; Banach, M.; Sahebkar, A. Potential effects of curcumin in the treatment of COVID-19 infection. *Phytother. Res.* **2020**.
68. Maurya, V.K.; Kumar, S.; Prasad, A.K.; Bhatt, M.L.B.; Saxena, S.K. Structure-based drug designing for potential antiviral activity of selected natural products from Ayurveda against SARS-CoV-2 spike glycoprotein and its cellular receptor. *Virus disease* **2020**, *31*, 179–193.
69. Kumar, S.; Kashyap, P.; Chowdhury, S.; Kumar, S.; Panwar, A.; Kumar, A. Identification of phytochemicals as potential therapeutic agents that binds to Nsp15 protein target of coronavirus (SARS-CoV-2) that are capable of inhibiting virus replication. *Phytomedicine Int. J. Phytother. Phytopharm.* **2020**.
70. Rajagopal, K.; Varakumar, P.; Baliwada, A.; Byran, G. Activity of phytochemical constituents of Curcuma longa (turmeric) and Andrographis paniculata against coronavirus (COVID-19): An *in silico* approach. *Future J. Pharm. Sci.* **2020**, *6*, 104.
71. Celum, C.; Wald, A.; Lingappa, J.R.; Magaret, A.S.; Wang, R.S.; Mugo, N.; Mujugira, A.; Baeten, J.M.; Mullins, J.I.; Hughes, J.P.; et al. Acyclovir and transmission of HIV-1 from persons infected with HIV-1 and HSV-2. *N. Engl. J. Med.* **2010**, *362*, 427–439.
72. Vitali, D.; Bagri, P.; Wessels, J.M.; Arora, M.; Ganugula, R.; Parikh, A.; Mandur, T.; Felker, A.; Garg, S.; Kumar, M.; et al. Curcumin Can Decrease Tissue Inflammation and the Severity of HSV-2 Infection in the Female Reproductive Mucosa. *Int. J. Mol. Sci.* **2020**, *21*, 337.
73. Shaikh, J.; Ankola, D.D.; Beniwal, V.; Singh, D.; Kumar, M.N. Nanoparticle encapsulation improves oral bioavailability of curcumin by at least 9-fold when compared to curcumin administered with piperine as absorption enhancer. *Eur. J. Pharm. Sci.* **2009**, *37*, 223–230.
74. Parikh, A.; Kathawala, K.; Song, Y.; Zhou, X.-F.; Garg, S. Curcumin-loaded self-nanomicellizing solid dispersion system: Part I: Development, optimization, characterization, and oral bioavailability. *Drug Deliv. Transl. Res.* **2018**, *8*, 1389–1405.

75. Shamma, R.N.; Basha, M. Soluplus®: A novel polymeric solubilizer for optimization of Carvedilol solid dispersions: Formulation design and effect of method of preparation. *Powder Technol.* **2013**, *237*, 406–414.
76. Zhong, C.; Xu, M.; Wang, Y.; Xu, J.; Yuan, Y. An APE1 inhibitor reveals critical roles of the redox function of APE1 in KSHV replication and pathogenic phenotypes. *PLoS Pathog.* **2017**, *13*, e1006289.
77. Zhu, L.; Ding, X.; Tao, J.; Wang, J.; Zhao, X.; Zhu, G. Critical role of cholesterol in bovine herpesvirus type 1 infection of MDBK cells. *Vet. Microbiol.* **2010**, *144*, 51–57.
78. Reolon, J.B.; Brustolin, M.; Accarini, T.; Viçozzi, G.P.; Sari, M.H.M.; Bender, E.A.; Haas, S.E.; Brum, M.C.S.; Gündel, A.; Colomé, L.M. Co-encapsulation of acyclovir and curcumin into microparticles improves the physicochemical characteristics and potentiates in vitro antiviral action: Influence of the polymeric composition. *Eur. J. Pharm. Sci.* **2019**, *131*, 167–176.
79. Park, N.-H.; Pavao-Langston, D.; McLean, S.L. Acyclovir in Oral and Ganglionic Herpes Simplex Virus Infections. *J. Infect. Dis.* **1979**, *140*, 802–806.
80. Berk, A.J. Functions of adenovirus E1A. *Cancer Surv.* **1986**, *5*, 367–387.
81. Jennings, M.R.; Parks, R.J. Antiviral Effects of Curcumin on Adenovirus Replication. *Microorganisms* **2020**, *8*, 1524.
82. Metzler, M.; Pfeiffer, E.; Schulz, S.I.; Dempe, J.S. Curcumin uptake and metabolism. *BioFactors* **2013**, *39*, 14–20.
83. Nelson, K.M.; Dahlin, J.L.; Bisson, J.; Graham, J.; Pauli, G.F.; Walters, M.A. The Essential Medicinal Chemistry of Curcumin. *J. Med. Chem.* **2017**, *60*, 1620–1637.
84. Stohs, S.J.; Chen, O.; Ray, S.D.; Ji, J.; Bucci, L.R.; Preuss, H.G. Highly Bioavailable Forms of Curcumin and Promising Avenues for Curcumin-Based Research and Application: A Review. *Molecules* **2020**, *25*, 1397.

Appendix 4:

Curriculum Vitae

Morgan R. Jennings

EDUCATION

2019-2025 **Doctor of Philosophy, Microbiology and Immunology,** University of Ottawa

Transferred from MSc program

Thesis: *Targeting viral epigenetics for the control of human adenovirus replication.*

Supervisor: Dr. Robin Parks

2014-2018 **Bachelor of Science with Distinction, Honours Specialization, Biology**, Nipissing University

HONOURS

2022-2023 Queen Elizabeth II Graduate Scholarship in Science and Technology, University of Ottawa (merit-based scholarship)

2021-2022 Queen Elizabeth II Graduate Scholarship in Science and Technology, University of Ottawa (merit-based scholarship)

2019-2025 Graduate Admissions Scholarship, University of Ottawa (entrance scholarship)

2015-2018 Carl Sanders Award, Nipissing University (for high academic standing)

2014 Schulich School of Education Scholarship, Nipissing University (entrance scholarship)

RESEARCH EXPERIENCE

2019-2025 **PhD Student**, University of Ottawa/Ottawa Hospital Research Institute

Research project evaluating the effect of epigenetic modulating compounds on human adenovirus type 5 (HAdV-5) replication. Techniques used include basic tissue and viral culture, molecular cloning including generation of plasmids and recombinant viruses, immunoblot and qRT-PCR, immunoprecipitation, and immunofluorescence microscopy.

2017-2018 **Undergraduate Student**, Nipissing University

Honours thesis project on the antibacterial properties of Northern Ontario Chaga extracts. Using the disc diffusion method, the antibacterial properties of various Chaga extracts derived from a Soxhlet extractor were analyzed on four species of bacteria.

TRAINING

2024 Tri-Council Policy Statement: Ethical Conduct for Research Involving Humans (TCPS 2: CORE 2022)

2021 Canadian Bioinformatics Workshops: Epigenetic Analysis

2019 CIHR Online Training Modules: Integrating Sex & Gender in Health Research

PUBLICATIONS

2025 **Jennings, M. R.**, Vacratsis P.O., Parks R. J., The FACT complex is Required for Optimal Human Adenoviral Replication. Submitted

2024 **Jennings, M. R.**, Parks R. J., Inhibition of Human Adenovirus Replication by the Small Molecule Curaxin. Submitted, in revision.

2023 **Jennings, M. R.**, Parks R. J., Human Adenovirus Gene Expression and Replication Is Regulated through Dynamic Changes in Nucleoprotein Structure throughout Infection, *Viruses*, 2023, 15, 161

2020 **Jennings, M. R**., Parks, R. J., Antiviral Effects of Curcumin on Adenovirus Replication, *Microorganisms* 2020, 8, 1524.

2020 J**ennings, M. R.**, Parks, R. J., Curcumin as an Antiviral Agent, *Viruses* 2020, 12, 1242.

CONFERENCES ATTENDED

Platform Presentations

2023 **Jennings, M. R.**, Parks, R. J., The Facilitates Chromatin Transactions (FACT) Complex is Required for Human Adenovirus Replication, 15th International Adenovirus Meeting, Ruđer Bošković Institute, Brach Island, Croatia, September 2023

2023 **Jennings, M. R.**, Parks, R. J., The Facilitates Chromatin Transactions (FACT) Complex is Required for Human Adenovirus Replication, Montreal DNA Tumour Virus Meeting, McGill University, Montreal, QB, CA, July 2023

2023 **Jennings, M. R.**, Parks, R. J., The Facilitates Chromatin Transactions (FACT) Complex is Required for Human Adenovirus Replication, 66th annual CSMB meeting, University of Ottawa, Ottawa, ON, CA, May 2023

2022 **Jennings, M. R.**, Parks, R. J., The Facilitates Chromatin Transactions (FACT) Complex is Required for Human Adenovirus Replication, Biochemistry, Microbiology, and Immunology Seminar Day, University of Ottawa, Ottawa, ON, CA, April 2022

2021 **Jennings, M. R.**, Parks, R. J., Histone Methyltransferase SUV39H1 is Required for Optimal Human Adenovirus Replication, Biochemistry, Microbiology, and Immunology Seminar Day, University of Ottawa,

Ottawa, ON, CA, April 2021

Poster Presentations

2024 **Jennings, M. R.**, Parks, R. J., Inhibition of Human Adenovirus Replication by the Small Molecule Curaxin, Ottawa Hospital Research Institute's Annual Research Day 2024, Ottawa, ON, CA, November 2024

2024 **Jennings, M. R.**, Parks, R. J., Curaxin Inhibits Human Adenovirus Replication, Biochemistry, Microbiology, and Immunology Poster Day, University of Ottawa, Ottawa, ON, CA, April 2024

2023 **Jennings, M. R.**, Parks, R. J., The Facilitates Chromatin Transactions (FACT) Complex is Required for Human Adenovirus Replication, Ottawa Hospital Research Institute's Annual Research Day 2023, Ottawa, ON, CA, November 2023

2023 **Jennings, M. R.**, Parks, R. J., The Facilitates Chromatin Transactions (FACT) complex is required for efficient expression of adenovirus vector-encoded transgenes, 6th Ottawa International Conference on Neuromuscular Disease & Biology, Ottawa, ON, CA

2022 **Jennings, M. R.**, Parks, R. J., The Facilitates Chromatin Transactions (FACT) Complex is Required for Human Adenovirus Replication, Ottawa Hospital Research Institute's Annual Research Day 2022, Ottawa, ON, CA, November 2022

2022 **Jennings, M. R.**, Parks, R. J., The Facilitates Chromatin Transactions (FACT) Complex is Required for Human Adenovirus Replication, Chromatin Control of Viral Infection 2022, Bethesda, MD, USA, September 2022

2022 **Jennings, M. R.**, Parks, R. J., The Facilitates Chromatin Transactions (FACT) Complex is Required for Human Adenovirus Replication, BMI Symposium 2022, Montebello, QC, CA, May 2022

2021 **Jennings, M. R.**, Parks, R. J., Histone Methyltransferase SUV39H1 is Required for Optimal Human Adenovirus Replication, Faculty of Medicine Research Day 2021, Ottawa, ON, CA, April 2021

2020 **Jennings, M. R.**, Parks, R. J., Antiviral Effects of Curcumin on Adenovirus Replication, Ottawa Hospital Research Institute's Annual Research Day 2020, Ottawa, ON, CA, November 2020.

2020 **Jennings, M. R.**, Parks, R. J., Inhibition of Human Adenovirus Replication by Curcumin, Biochemistry, Microbiology, and Immunology Poster/Seminar Day, University of Ottawa, Ottawa, ON, CA, May 2020

2019 **Jennings, M. R.**, Parks, R. J., Inhibition of Human Adenovirus Replication by Curcumin, Ottawa Hospital Research Institute's Annual Research Day 2019, Ottawa, ON, CA, October 2019.

2018 **Jennings, M. R.**, Rossi, L., Jha, M., Antibacterial Properties of Northern

	Ontario Yellow Birch Chaga (*Inonotus obliquus*) Extracts, 31st Annual Ontario Biology Day 2018, Waterloo, ON, CA, March 2018.
Attendee	
2019	5th Ottawa International Conference on Neuromuscular Disease & Biology, Ottawa, ON, CA
2019	1st Annual Faculty of Medicine Research Day 2019, University of Ottawa, ON, CA

REFERENCES

References available upon request